Alfred-Wegener-Institut, Helmholtz-Zentrum für Polar- und Meeresforschung

Helmholtz-Zentrum Potsdam Deutsches GeoForschungsZentrum

Methane distribution and oxidation across aquatic interfaces: case studies from Arctic water bodies and the Elbe estuary

---

Kumulative Dissertation

zur Erlangung des Grades eines Doktors der Naturwissenschaften

„doctor rerum naturalium“

-Dr. rer. Nat.-

in der Wissenschaftsdisziplin „Mikrobiologie“

Eingereicht an der

Mathematisch-Naturwissenschaftlichen Fakultät

der Universität Potsdam

Von Roman Osudar

Potsdam, Mai 2016

Published online at the
Institutional Repository of the University of Potsdam:
URN urn:nbn:de:kobv:517-opus4-96799
http://nbn-resolving.de/urn:nbn:de:kobv:517-opus4-96799

Preface

This work represents a joint project between Helgoland and Potsdam units of The Alfred Wegener Institute, Helmholtz Centre for Polar and Marine Research and also between The GFZ German Research Centre for Geosciences, Helmholtz Centre Potsdam. The work was supervised by Prof. Dr. Dirk Wagner (GFZ, section 5.3: Geomicrobiology) and Dr. Ingeborg Bussmann (AWI, Helgoland, section: Shelf Sea System Ecology). The aim of the project was to extent our knowledge about environmental controls of methane distribution and aerobic methane oxidation in aquatic ecosystems which are subject to pronounced interaction with bordering environments. Arctic water bodies and estuaries were chosen as study sites which exemplify these aquatic interfaces.

The field sampling campaigns took place in the Elbe estuary from 2011 to 2013 and in the Lena Delta in July 2012 (expedition LENA 2012), with a personal participation. The laboratory work was performed at the three mentioned institutes (AWI Helgoland, AWI Potsdam and GFZ) and also partly in the Winogradsky Institute of Microbiology, Russian Academy of Science, Moscow, Russia with the support of Prof. Dr. Nikolay Pimenov. Sampling campaign in the Lena Delta was financially supported by the European cooperation for long-term monitoring (PERGAMON) [COST STSM Reference Number: ECOST-STSM-ES0902-290811-008783]. The workshop and conference attendances were supported by the Helmholtz Graduate School for Polar and Marine Research (POLMAR) and the Association for General and Applied Microbiology (VAAM).

This thesis is written in English and submitted as a cumulative dissertation to the Faculty of Mathematics and Natural Science at the University of Potsdam. The main body of the thesis consists of: (1) general introduction to the research topic with the particular objectives of the study and the description of the study area; (2) manuscripts, which describe the carried out research; and (3) synthesis, which summarizes the obtained results. The “Manuscripts” section is composed of three manuscripts with first authorship, two of which are published or accepted for publication in peer-reviewed scientific journals and one is presented as a final draft.

Acknowledgments

I am happy to acknowledge everybody who contributed to the success of my work.

I wish to particularly thank…

… my supervisors: Prof. Dr. Dirk Wagner and Dr. Ingeborg Bussmann for the invaluable help, support and patience generously granted to me during the whole period of my study.

... heads of the AWI Helgoland, AWI Potsdam and GFZ: Prof. Dr. Karen Helen Wiltshire, Prof. Dr. H.-W. Hubberten, and Prof. Dr. Dr. h.c. R. Hüttl and Dr. S. Schwartze, respectively for the opportunity to work in a great scientific and collegial atmosphere.

... all my colleagues at all three Institutes, Geomicrobiology section and especially: Dr. Mashal Alawi, Prof. Dr. Susanne Liebner, Andrea Kiss, Janine Heise, Dr. Felizitas Bajerski, Dr. Paloma Serrano, Dr. Sizhong Yang, Julia Magritz and Steffi Genderjahn for the scientific contribution and simply for always "being there for me".

… Günther 'Molo' Stoof, Waldemar Schneider and all the others involved in the expedition LENA 2012 for a wonderful Arctic summer.

… my family and my friends for believing in me.

TABLE OF CONTENTS

Summary

The increase in atmospheric methane concentration, which is determined by an imbalance between its sources and sinks, has led to investigations of the methane cycle in various environments. Aquatic environments are of an exceptional interest due to their active involvement in methane cycling worldwide and in particular in areas sensitive to climate change. Furthermore, being connected with each other aquatic environments form networks that can be spread on vast areas involving marine, freshwater and terrestrial ecosystems. Thus, aquatic systems have a high potential to translate local or regional environmental and subsequently ecosystem changes to a bigger scale. Many studies neglect this connectivity and focus on individual aquatic or terrestrial ecosystems.

The current study focuses on environmental controls of the distribution and aerobic oxidation of methane at the example of two aquatic ecosystems. These ecosystems are Arctic fresh water bodies and the Elbe estuary which represent interfaces between freshwater-terrestrial and freshwater-marine environments, respectively.

Arctic water bodies are significant atmospheric sources of methane. At the same time the methane cycle in Arctic water bodies is strongly affected by the surrounding permafrost environment, which is characterized by high amounts of organic carbon. The results of this thesis indicate that the methane concentrations in Arctic lakes and streams substantially vary between each other being regulated by local landscape features (e.g. floodplain area) and the morphology of the water bodies (lakes, streams and river). The highest methane concentrations were detected in the lake outlets and in a floodplain lake complex. In contrast, the methane concentrations measured at different sites of the Lena River did not vary substantially. The lake complexes in comparison to the Lena River, thus, appear as more individual and heterogeneous systems with a pronounced imprint of the surrounding soil environment. Furthermore, connected with each other Arctic aquatic environments have a large potential to transport methane from methane-rich water bodies such as streams and floodplain lakes to aquatic environments relatively poor in methane such as the Lena River.

Estuaries represent hot spots of oceanic methane emissions. Also, estuaries are intermediate zones between methane-rich river water and methane depleted marine water. Substantiated through this thesis at the example of the Elbe estuary, the methane distribution in estuaries, however, cannot entirely be described by the conservative mixing model i.e. gradual decrease from the freshwater end-member to the marine water end-member. In addition to the methane-rich water from the Elbe River mouth substantial methane input occurs from tidal flats, areas of significant interaction between aquatic and terrestrial environments. Thus, this study demonstrates the complex interactions and their consequences for the methane distribution within estuaries. Also it reveals how important it is to investigate estuaries at larger spatial scales.

Methane oxidation (MOX) rates are commonly correlated with methane concentrations. This was shown in previous research studies and was substantiated by the present thesis. In detail, the highest MOX rates in the Arctic water bodies were detected in methane-rich streams and in the floodplain area while in the Elbe estuary the highest MOX rates were observed at the coastal stations. However, in these bordering environments, MOX rates are affected not only via the regulation through methane concentrations. The MOX rates in the Arctic lakes were shown to be also dependent on the abundance and community composition of methane-oxidising bacteria (MOB), that in turn are controlled by local landscape features (regardless of the methane concentrations) and by the transport of MOB between neighbouring environments. In the Elbe estuary, the MOX rates in addition to the methane concentrations are largely affected by the salinity, which is in turn regulated by the mixing of fresh- and marine waters. The magnitude of the salinity impact on MOX rates thereby depends on the MOB community composition and on the rate of the salinity change.

This study extends our knowledge of environmental controls of methane distribution and aerobic methane oxidation in aquatic environments. It also illustrates how important it is to investigate complex ecosystems rather than individual ecosystems to better understand the functioning of whole biomes.

Zusammenfassung

Aufgrund des Anstiegs der Methankonzentration in der Atmosphäre, der durch ein Ungleichgewicht zwischen Quellen und Senken hervorgerufen wird, steht der Methankreislauf im Fokus der Forschung. Aquatische Ökosysteme, und im Speziellen solche, die vom Klimawechsel besonders betroffen sind, spielen eine wichtige Rolle im globalen Methankreislauf. Darüber hinaus können sie über große Areale miteinander verknüpft sein und terrestrische mit marinen Ökosystemen verbinden. In aquatischen Systemen können sich daher lokale und regionale Umweltänderungen auf sehr große räumliche Skalen auswirken. Viele Untersuchungen berücksichtigen diesen Zusammenhang nicht und betrachten aquatische unabhängig von den sich angrenzenden Ökosystemen.

Die vorliegende Arbeit untersucht den Einfluss von Umweltfaktoren auf die Methankonzentration und die mikrobielle aerobe Methanoxidation. Der Schwerpunkt liegt dabei auf zwei aquatischen Ökosystemen, arktische Süßwassertransekte und Ästuare, und auf deren mikrobieller Ökologie. Diese beiden Ökosysteme beschreiben typische terrestrisch-limnische und limnisch-marine Übergangsbereiche.

Arktische Gewässer stellen eine wichtige Quelle für atmosphärisches Methan dar. Sie werden außerdem stark durch den umgebenden Permafrost, der reich an organischer Substanz ist, beeinflusst. Die Ergebnisse der vorliegenden Arbeit zeigen am Beispiel des Lena-Deltas, dass sich die Methankonzentrationen in arktischen Seen und Fließgewässern wesentlich voneinander unterscheiden. Besonderen Einfluss üben hierbei das örtliche Landschaftsbild (z.B. Überflutungsbereiche) und die Charakteristika der Wasserkörper (Seen, Wasserläufe und Flüsse) aus. Die höchsten Methankonzentrationen wurden in Seeabläufen und in Seen einer Überflutungsebene (Seekomplex) gemessen. Im Gegensatz dazu unterschieden sich die Methankonzentrationen an verschiedenen Messpunkten der Lena nur unwesentlich. Der Seekomplex erscheint daher im Vergleich zur Lena heterogener und stark vom umgebenden Bodenökosystem beeinflusst. Die miteinander vernetzten arktischen aquatischen Ökosysteme haben darüber hinaus ein hohes Potential, Methan von methan-reichen Gewässern, wie Wasserläufen und Überflutungsgebieten, zu relativ methan-armen Gewässern wie der Lena zur transportieren.

Ästuare sind „hot spots“ der Methanemission von marin beeinflussten Systemen. Sie stellen Übergangszonen zwischen methan-reichem Flusswasser und methan-armem Meerwasser dar. Wie die Untersuchungen am Elbe Ästuar zeigen, kann die Methanverteilung jedoch nicht immer hinreichend durch das konservative Durchmischungs-Model (graduelle Abnahme vom Süß- zum Meerwasser hin) beschrieben werden. Zusätzlich zum methan-reichen Wasser der Elbemündung konnte der Eintrag von Methan in Wattbereichen, Gegenden starker aquatischer und terrestrischer

Interaktion, gezeigt werden. Diese Studie verdeutlicht demnach die Komplexität von Ästuarsystemen hinsichtlich der Methanverteilung und die Notwendigkeit, diese in größeren Maßstäben zu untersuchen.

Methanoxidationsraten (MOX-Raten) korrelieren gewöhnlich mit den Methankonzentrationen. Dies zeigen die hier vorliegenden Daten aber auch vorherige Studien. Die höchsten MOX-Raten der arktischen Gewässer wurden im Rahmen dieser Arbeit in methan-reichen Fließgewässern sowie einer Überflutungsebene gemessen. Im Elbeästuar wurden die höchsten Werte an den Küstenstationen aufgezeichnet. In den jeweils untersuchten Übergangszonen werden die MOX-Raten jedoch nicht nur durch die Methankonzentrationen gekennzeichnet. In den arktischen Seen werden sie zusätzlich durch die Zellzahl und Populationsstruktur von Methan oxidierenden Bakterien (MOB) bestimmt, welche wiederum durch lokale Umweltfaktoren (unabhängig von der Methankonzentration) und den Transport von MOB zwischen benachbarten Ökosystemen beeinflusst werden. Im Elbeästuar hingegen werden die MOX-Raten neben den Methankonzentrationen größtenteils von der Salinität, die durch die Vermischung von Süß- und Salzwasser reguliert wird, bedingt. Die Ergebnisse dieser Arbeit zeigen auch, dass im Elbeästuar die Salinität, die durch die Vermischung von Süß- und Salzwasser reguliert wird, einen großen Einfluss auf die MOX-Raten hat. Das Ausmaß dieses Einflusses hängt dabei von der Populationsstruktur der MOB und der Geschwindigkeit des Salinitätswechsels ab.

Zusammenfassend trägt die vorliegende Arbeit dazu bei, Zusammenhänge zwischen Methankonzentration, dem Prozess und Mikrobiom der aeroben Methanoxidation und bestimmten Umweltfaktoren wie beispielsweise der Salinität in aquatischen Systemen besser zu verstehen. Sie verdeutlicht außerdem, wie bedeutsam es ist, aquatische Ökosysteme in ihrer räumlichen Komplexität und nicht entkoppelt zu betrachten.

I. INTRODUCTION

1.1 Methane cycle

Methane is the most abundant organic trace gas in the atmosphere (Wuebbles & Hayhoe, 2000). It plays a key-role in the microbial carbon cycling and thus is very important for the functioning of small and large-scale ecosystems. Furthermore, methane is an important greenhouse gas. After carbon dioxide, methane has the largest radiative forcing of the long-lived greenhouse gases (Ramaswamy *et al.*, 2001) and it accounts for up to 20–30% of global warming effect. The contribution of methane to global warming is attenuated by comparatively low concentrations and short lifetime in the atmosphere. However, atmospheric concentration of methane is constantly increasing, and has doubled over the last 50 years. This increase is likely the result of anthropogenic activity (IPCC, 2014). In the beginning of the century the methane concentration stabilized but from approximately 2007 its increase continued. The current concentration of methane in the atmosphere is around 1.8 ppm, which is unprecedented in at least the last 800,000 years (Stocker *et al.*, 2013).

The increase in concentration of atmospheric methane is determined by the imbalance between methane sources and sinks. Most sources and sinks of methane have been identified, but their relative contributions to atmospheric methane levels are highly uncertain (Kirschke *et al.*, 2013). Methane sources can be divided into three categories: thermogenic, pyrogenic and biogenic (Kirschke *et al.*, 2013). Thermogenic methane represents fossil fuel, which was formed through geological processes. Thermogenic methane is vented to the atmosphere through terrestrial seeps, marine seeps and mud volcanoes. Additionally, it reaches the atmosphere through the exploitation of fossil fuels such as coal, oil and natural gas (Kirschke *et al.*, 2013). Pyrogenic methane is produced by the incomplete combustion of biomass, soil carbon, biofuels and fossil fuels (Kirschke *et al.*, 2013). Biogenic methane production, also referred to as methanogenesis, is the largest methane source and contributes approximately 70% to the total methane emission (Conrad, 2009). Methanogenesis is mediated by phylogenetically diverse group of archaea, called methanogens. These archaea are classified into three classes, six orders, 12 families and 35 genera (Nazaries *et al.*, 2013). These orders are: *Methanobacteriales, Methanococcales, Methanomicrobiales, Methanosarcinales, Methanopyrales* and *Methanocellales.* There are several pathways of methanogenesis. Aceticlastic and carbon dioxide reduction pathways are considered as the main pathways that account for majority of methane production (Conrad, 2005, Wagner & Liebner, 2009). The contribution of each of these two pathways can vary significantly depending on the environment (Galand *et al.*, 2005). Additionally, minor but ecologically important amounts of methane are produced by the conversion of methylotrophic substrates like methanol, methylamines and methyl sulfides (Ferry, 2010). Methane production is the terminal phase of the degradation of organic material. Methanogens

cannot use complex organic compounds and thus have to rely on trophic chains with other bacteria, which first degrade organic compounds into simple sugars and fatty acids and then ferment them into acetate, formate, hydrogen and carbon dioxide (Cicerone & Oremland, 1988).

It is generally considered that methanogenesis occurs under strictly anoxic conditions. However, there is also evidence of methanogenesis in oxic zones in the water column, which is linked to algal dynamics and driven by acetoclastic production (Bogard et al., 2014). Most methanogens are mesophiles; however some of them can be found in extreme environments (Nazaries *et al.*, 2013). Anoxic sediments and soil are the main environments were methane production takes place.

In anoxic marine and freshwater sediments methane production is balanced by anaerobic methane oxidation (AOM). AOM is coupled with the reduction of sulphate (Boetius *et al.*, 2000), nitrite (Ettwig *et al.*, 2010), nitrate (Haroon *et al.*, 2013), iron (Beal *et al.*, 2009) or manganese (Beal *et al.*, 2009). Conventional AOM is mediated by a syntrophic consortium of methanotrophic archaea (ANME) and bacteria, however, there are studies suggesting that AOM can also be performed independently by ANME (Haroon *et al.*, 2013) or syntrophic bacteria (Ettwig *et al.*, 2010). AOM has been studied mainly in marine and freshwater sediments, however, there are also studies of AOM in soil (Pozdnyakov *et al.*, 2011). About 90% of methane produced through methanogenesis is oxidized through AOM before it reaches oxic environments (Reeburgh, 2007). Some methane, however, reaches oxic environments where its fate is largely dependent on aerobic bacterial methane oxidation (MOX). In total, up to 90% of methane in oxic soil and aquatic environments can be oxidized before it reaches the atmosphere (King *et al.*, 1990, Guérin & Abril, 2007, Bastviken *et al.*, 2008). Methane is oxidized according the following reaction:

$$CH_4 + 2O_2 \rightarrow CO_2 + 2H_2O \qquad (1)$$

Aerobic methane oxidation preferentially occurs at oxic-anoxic interfaces. The main factors controlling MOX rates are methane and oxygen availability (Hanson & Hanson, 1996). Other factors which effect MOX are temperature (Lofton *et al.*, 2014), salinity (de Angelis & Scranton, 1993), suspended particulate matter (Middelburg *et al.*, 2002, Abril *et al.*, 2007) and light (van der Nat & Middelburg, 1998, Murase & Sugimoto, 2005). Aerobic methanotrophic bacteria (MOB), which are responsible for methane oxidation will be discussed in more details in the next chapters. The principal mechanism of methane cycling is given in the Figure 1.

Methane, which was not oxidized, reaches the atmosphere. About 4% of it is oxidized by high-affinity methanotrophs in upland soils. Another 3% are oxidized by chlorine radicals from sea salt in the marine boundary layer. The rest methane is oxidized by hydroxyl radicals in the troposphere (90%) and by chlorine radicals and atomic oxygen radicals in the stratosphere (3%) (Kirschke *et al.*, 2013).

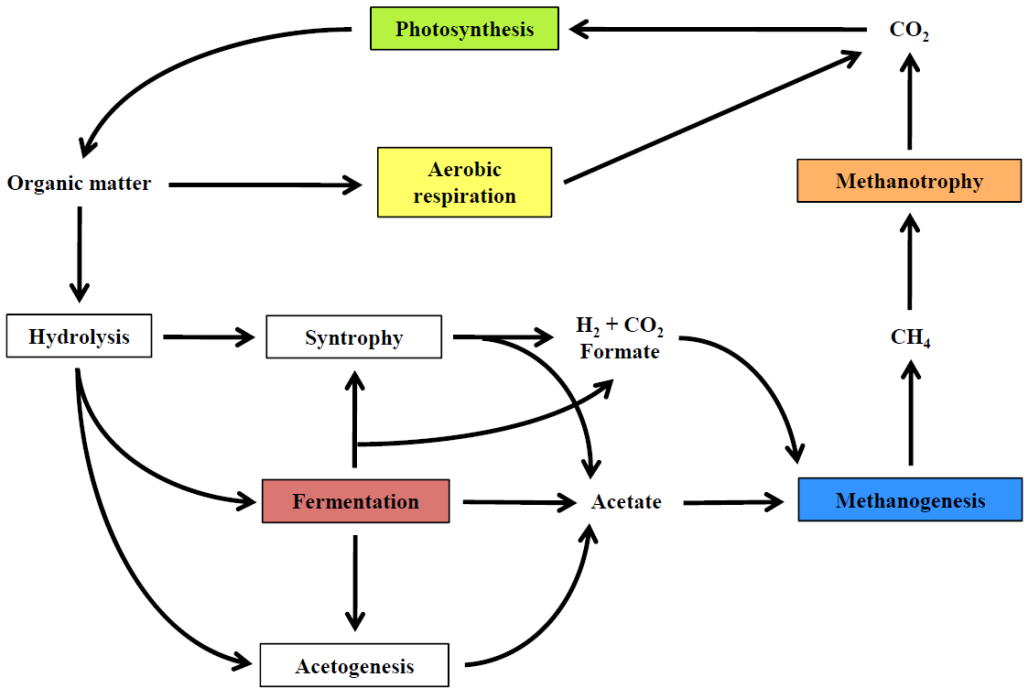

Figure 1. Global methane cycle in nature and its linkage with carbon cycle. The five main compartments of carbon processing are indicated by the colored boxes. Arrows indicate the substrates either produced by a process or for which other process intermediates are produced (Nazaries et al., 2011).

It should be noted that due to methane oxidation, methane emission rates are not proportional to the rates of initial methane production. So, for example, due to anaerobic methane oxidation in the marine sediments, which accounts for 70–300 Tg methane per year (Reeburgh, 2007), only minor amounts of methane (5–6 Tg methane per year) are release to the atmosphere through the gas hydrates (Conrad, 2009). About 50–60% of the methane released to the atmosphere is connected to anthropogenic activity (Kirschke *et al.*, 2013). Main anthropogenic sources of methane emission are agriculture and waste, biomass burning, and fossil fuels. The main natural methane sources are wetlands, geological sources (including oceans), and fresh water bodies (lakes and rivers) (Kirschke *et al.*, 2013). According to bottom-up approach estimation they contribute to the atmosphere 217, 54 and 40 Tg of methane per year, respectively, which altogether constitute approximately 90% of methane released from natural sources. At the same time, these methane sources have the largest absolute uncertainty, with a min–max range of 107, 42 and 65 Tg of methane per year respectively. Uncertainties in estimations can be explained by the low numbers of studies, inconsistency in methods applied, and heterogeneity of sampling sites on both regional and global scales.

Aquatic environments are important sources of methane emission. Additionally, aquatic environments are of an exceptional interest due to their ability to translate local environmental changes to regional or even global scales. Lakes, streams, rivers, and seas, as well as the surrounding terrestrial environments, represent individual ecosystems, that being connected with each other, form continuous biomes. The interfaces between aquatic and terrestrial environments, and also between adjacent aquatic compartments, represent areas, that are among the first to face environmental transformations and can be used as indicators of the sustainability of the overall regional or global ecosystems. Studying of these systems exposed to multifunctional regulation of methane cycling helps to reduce uncertainties in understanding of methane cycling and to predict consequences of global climate change.

Arctic regions, which host large numbers of wetlands, water bodies and are water-rich in general (Vonk *et al.*, 2015), play an exceptional role in methane cycling due to their current significant contribution to global methane emission and their high potential to increase this contribution in future. The importance of Arctic environments as a methane source is attributed to the large amounts of organic carbon stored in permafrost soils, coupled with the sensitivity of these regions to climate change. With the predicted temperature increase, more organic carbon is expected to become available for mineralization into methane, giving, thus, a positive feedback to global climate change. Water bodies are playing a key role in these processes (Wik *et al.*, 2016).

Estuaries are other aquatic interface areas which on the one hand appear to be “hot spots” of methane emission and on the other hand represent complex ecosystems, which connect different environments. High rates of methane emission result from the input of methane and organic carbon from draining rivers and also from *in situ* methane production. At the same time fresh river water and marine water represent two diverse environments regarding methane-related processes. Finally, estuaries, being interfaces between coastal waters and terrestrial aquatic systems, have a high potential to convey changes which might occur in any of these environments. So, for example, change in the physical or chemical parameters of the marine or river water as well as change in the river discharge and sea level rise with the subsequent relocation of the estuarine area is likely to disturb established ecosystems.

This study focuses on the methane-related processes in water bodies in Arctic region and estuaries as two key interface areas between aquatic and terrestrial environments, with a special regard to the aerobic methane oxidation and methanotrophic bacteria, controlling it. The principal mechanisms for methane cycling in these interface areas are discussed in detail in the following chapters and are given in Figure 2.

1.2 Methane distribution and cycling in bordering aquatic and terrestrial environments

1.2.1 Arctic water bodies

Water bodies are abundant in Arctic regions and occupy up to 30% of the land surface (Schneider *et al.*, 2009, Muster *et al.*, 2012). There is growing evidence that Arctic lakes and ponds play a significant role in methane emission (Walter *et al.*, 2006, Bastviken *et al.*, 2011, Boike *et al.*, 2012, Langer *et al.*, 2014). For a long time their importance was overshadowed by wetlands; however, recent investigation, which summarized observations made in the last decades, suggests that lakes and ponds are a **dominant** methane source at high northern latitudes, with an emission rate of 16.5 Tg per year (Wik *et al.*, 2016). Methane distribution and cycling in Arctic water bodies is strongly affected by the surrounding soil environments and this influence has multiple aspects. Most of the Arctic soil is permanently frozen (permafrost), except for its uppermost layer (the active layer), which undergoes seasonal freezing-thawing cycles. The active layer thickness varies from several centimetres to meters (Shiklomanov *et al.*, 2010). Permafrost is extremely rich in organic carbon (about 1330–1580 Pg) (Schuur *et al.*, 2015), and accounts for approximately 50% of global below-ground carbon storage (Tarnocai *et al.*, 2009). High amounts of organic carbon result from the accumulation and inhibited decomposition of organic matter due to low temperatures and water logging (Davidson & Janssens, 2006). Thawing of permafrost leads to the remobilisation of nutrients and organic carbon and introduction them into aquatic systems. Permafrost coverage, landscape topography, ground ice content, thawing type and soil type determine the delivery of organic carbon and nutrients into aquatic environments (Vonk *et al.*, 2015). The form of organic carbon (dissolved or particulate), its abundance and its composition determine the fate of organic carbon; i.e., conversion to methane, storage in sediments, or transportation with further possible metabolization (Vonk *et al.*, 2015). Permafrost regions are quite heterogeneous in all these parameters, which results in a large range in methane concentrations in water bodies, and complicates assessments of the methane budget.

Methane produced in sediments can reach the atmosphere by diffusion throughout the water column, ebullition (bubbling) or plant-mediated transport. The contribution of these pathways to methane emission varies between and within water bodies depending on the size of the water body (Bastviken *et al.*, 2004), presence and composition of vegetation (Knoblauch *et al.*, 2015) and likely by other yet unknown factors. Knoblauch *et al.* (2015) investigated methane cycling in the Siberian Lena Delta, and concluded that plant-mediated transport accounted for most (70–90%) of total methane fluxes above emerged vegetation. For most *open water* sites methane transport was dominated by diffusion (Knoblauch *et al.*, 2015). Ebullitive fluxes were substantial but sparse (Knoblauch *et al.*, 2015). Diffusion of methane is characterized by elevated residence times of

dissolved methane, allowing time for methane oxidation. Methane bubbles reach the surface without substantial diffusion of methane into the water. However, in winter when methane bubbles are trapped under the ice, they can also contribute to the dissolved methane budget (Greene et al., 2014), where it is accessible for bacterial methane oxidation (Ricão Canelhas *et al.*, 2016). Crevecoeur *et al.* (2015) showed that methanotrophic bacteria account for up to 27% of the total bacterial sequences in the permafrost thaw ponds, indicating the importance of methane oxidation in the functioning of these ecosystems.

In addition to organic carbon delivery, the interaction between terrestrial and aquatic environments can also affect methane cycling through alterations in physical, chemical, and optical properties of the water bodies (Vonk *et al.*, 2015). These parameters control respiration, primary production, and the food web structure, which likely reflects on the functioning of the whole ecosystem, including methanogenic and methanotrophic microorganisms. For example, primary production enhanced by the nutrients release from thawing permafrost (Anthony *et al.*, 2014) can substantially supplement the labile organic carbon budget in lake sediments (Heslop *et al.*, 2015). Additionally, Arctic plants and mosses have symbiotic relationships with both methanogenic and methanotrophic microorganisms (Liebner *et al.*, 2011, Knoblauch *et al.*, 2015). MOB also are a potentially important part of the zooplankton diet (Borrel *et al.*, 2011). Finally, the transfer of microorganisms from terrestrial environments may substantially shape the structure of microbial communities (Crump *et al.*, 2012).

Although methane oxidation may be a significant sink for methane in aquatic environments, **there are very few studies dedicated to measurements of MOX rates and evaluating factors that affect MOX**. **Even less is known about methanotrophic bacterial communities and the factors that determine their abundance and community structure**.

Finally, permafrost thawing creates new aquatic bodies and changes the morphology of the existing bodies, thus, contributing to the formation of new aquatic networks and the redistribution of carbon, methane and supposedly methane-related microorganisms (Vonk *et al.*, 2015).

1.2.2 Estuaries

Estuaries are the interface between rivers and the adjacent seas and oceans and therefore represent very dynamic and complex systems. This complexity is also reflected in the methane distribution and cycling. Methane concentrations at the mouths of rivers and in the coastal waters are often orders of magnitude higher than those in the adjacent seas (Middelburg *et al.*, 2002). Thus, river input represents a methane source for estuaries in most cases. Other methane sources include: methane production in sediments, ground water input, and lateral transport (outwelling) from tidal flats and

marshes (Abril & Borges, 2005). Estuaries are often characterized by high concentrations of suspended particulate matter (SPM). In such zones riverine phytoplankton receives insufficient light and dies, which results in a considerable increase in the amount of organic matter (Cole *et al.*, 1992). This material is subsequently decomposed and re-mineralized by heterotrophic bacteria, resulting in elevated levels of methane production (Harley *et al.*, 2015). Methane production in tidal flats and marshes is enhanced by the large input of organic matter at anoxic depths from plants rooted in the sediments (Abril & Borges, 2005).

The primary sinks of methane in estuaries are dilution with methane-depleted marine water, bacterial methane oxidation, and emission from the water surface. All these parameters are subject to substantial spatial and temporal fluctuations. Spatial fluctuations are determined by the water dynamics, which in turn is controlled by the river discharge and tidal surge. Many rivers are subject to seasonal and non-seasonal discharge fluctuations. The magnitude of tidal surges is also variable and depends on the morphology of the coastal area and geographically dependent tidal constituents. Methane production, being largely dependent on input of organic matter, varies seasonally following the growing, maturing and dying cycle of plants (Kelley *et al.*, 1995). Additionally, the activity of methanogenic and methanotrophic microorganisms depends on temperature (Duc *et al.*, 2010, Lofton *et al.*, 2014, Martinez-Cruz *et al.*, 2015). Methane oxidation is further dependent on methane concentration and salinity (de Angelis & Scranton, 1993); whereby the ratio of marine- and freshwater controls salinity. Finally, estuaries are characterized by the enhanced gas exchange due to tidal currents and exposure to wind (Abril & Borges, 2005).

The variety of factors that control methane distribution and cycling in estuaries creates the necessity for a more detailed investigation of individual estuaries. **Many research projects** to date **lack seasonal and spatial coverage** which leads to uncertainty in global estimations of methane fluxes. Furthermore, **direct measurements of MOX rates in estuaries are still scarce** and are often substituted by extrapolations or interpolations. Finally, **an improved understanding of the environmental factors controlling bacterial methane oxidation and the physiological properties of these organisms is needed** (Valentine, 2011, Mau *et al.*, 2013).

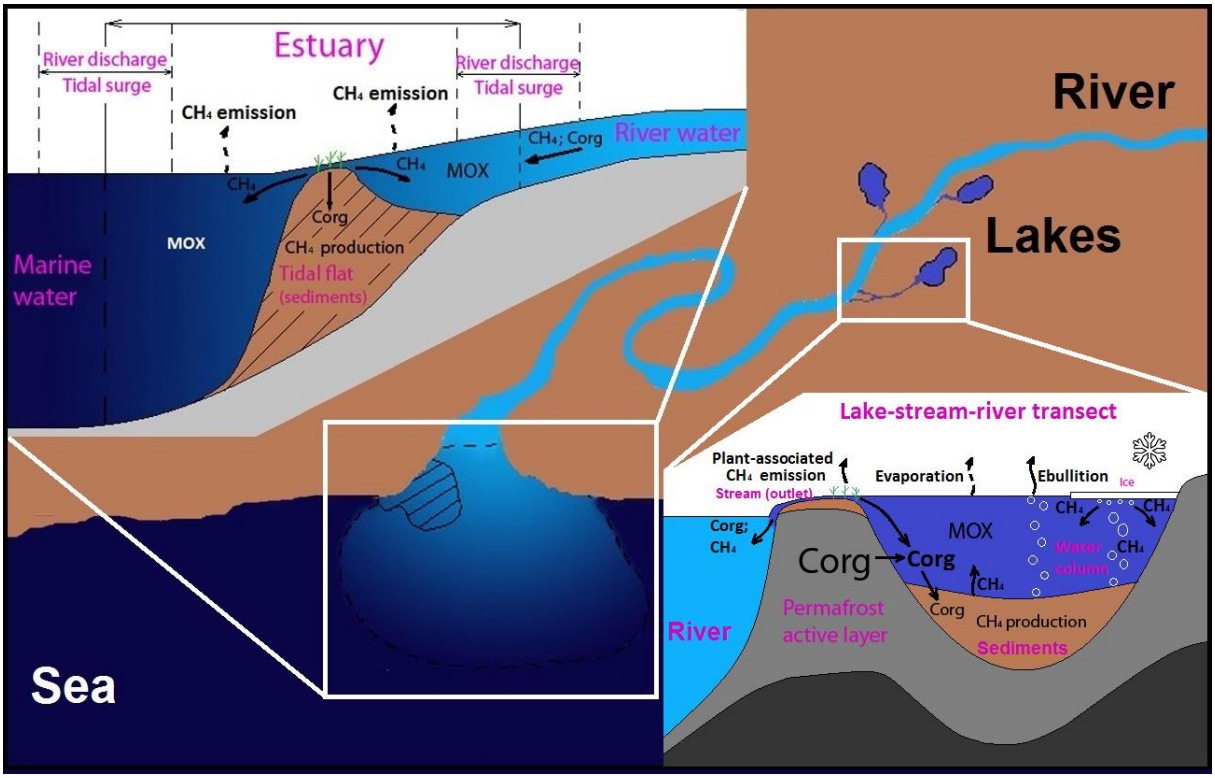

Figure 2. Principal mechanisms for methane cycling in the Arctic water bodies (bottom-right) and estuary (top-left). Indigo-blue, light-blue and dark-blue display lake, river and sea waters, respectively. Thawing of permafrost and primary production result in delivery of organic carbon (Corg) into the anoxic lake sediments where it gets metabolised to methane (CH_4) by methanogens. Produced methane reaches the atmosphere via plant-associated methane emission, ebullition, and diffusion through the water column with subsequent evaporation. Methane dissolved in the water (diffused from the sediments and partly from the bubbles trapped under the ice during winter) is subject to aerobic methane oxidation (MOX), which, thus, partly reduces general methane emission from the lake. Organic carbon and methane from the lake is transported to the adjacent river via lake outlets. To the estuary methane is delivered with the methane-rich river water (in contrast to the methane-depleted marine water) as well as from the tidal flats, which are characterised by the enhanced methane production due to organic carbon input (plants rooted in the sediments). Methane dissolved in the water gets oxidised by the marine and freshwater MOB, which, thus, reduce methane emission from the estuary. River discharge fluctuations and tidal surge control the water dynamics and the area of mixed marine and freshwater.

1.3 Aerobic methanotrophic bacteria (MOB)

1.3.1 Classification of MOB

Aerobic methanotrophic bacteria (methanotrophs, MOB) are a subset of methylotrophic bacteria, specialized to utilize methane or methanol as their sole source of carbon and energy (Hanson & Hanson, 1996). The ability to utilize methane is ensured by the activity of the key enzyme methane monooxygenase (MMO), which can exist in a soluble or particulate form. Despite their similar functions, these two forms have different evolutionary origins and mechanisms. The particulate form

is almost ubiquitous within the phylogeny, while the soluble form is rarer. Currently all cultivated MOB belong to three phyla: *Alphaproteobacteria*, *Gammaproteobacteria* and recently discovered *Verrucomicrobia*. The methanotrophic *Alphaproteobacteria* are further divided into two families: *Beijerinckiaceae* and *Methylocystaceae*, which contain together five genera. The methanotrophic *Gammaproteobacteria* are represented by two families: *Methylothermaceae* and *Methylococcaceae*, which are further classified into 18 genera. The methanotrophic *Verrucomicrobia* are represented by one family, *Methylacidiphilaceae*, which has two genera. There are around 70 different cultivated MOB species in total. *Beijerinckiaceae* and *Methylocystaceae* are the only families that also contain non-methanotrophic bacteria. Phylogenetic trees showing the taxonomic relation of methanotrophic type strains based on 16S rRNA gene and commonly used functional gene *pmoA* are presented in the Figure 3. It should be noted that though these two approaches generally give congruent results some discrepancies also exist. For example in the *pmoA*-based phylogenetic tree *Methylobacter* and *Methylomicrobium* species do not form monophyletic cluster but are highly divergent instead.

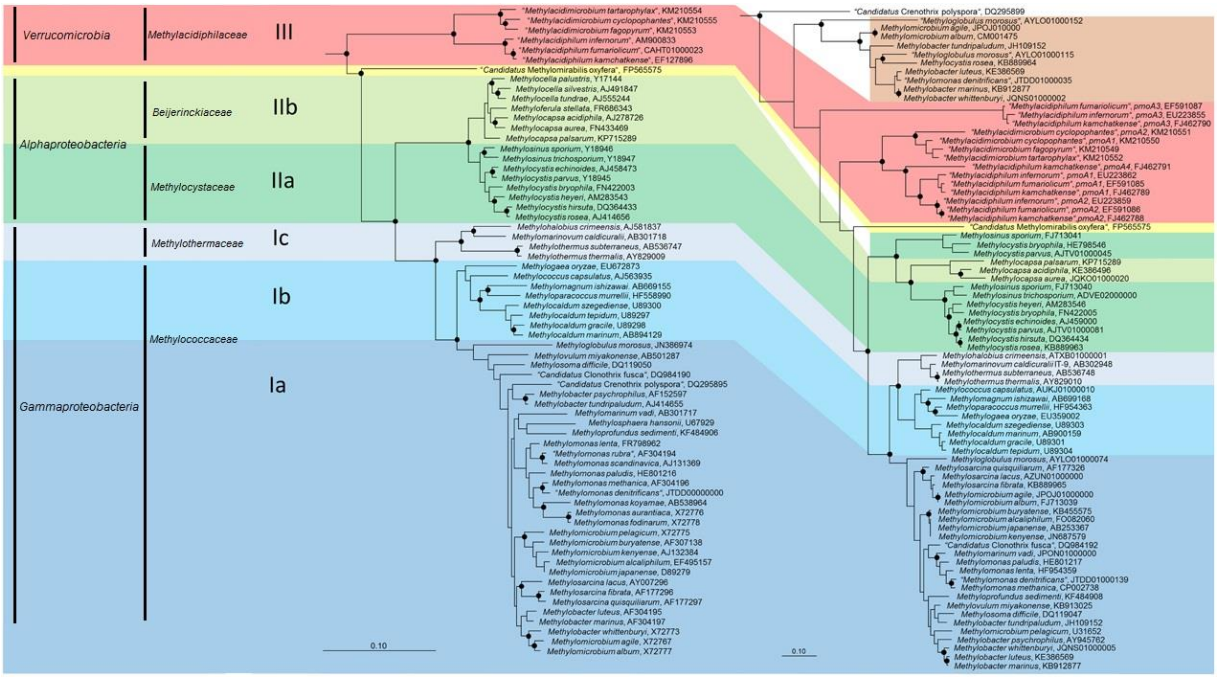

Figure 3. Phylogenetic trees showing the phylogeny of methanotrophic type strains based on 16S rRNA gene sequences (left tree) and *pmoA* sequences (right tree). Modified from Knief (2015).

The methanotrophic *Verrucomicrobia* are the most phylogenetically distant from the rest MOB which is likely the result of ancient divergence from methanotrophic *Proteobacteria* rather than a recent horizontal gene transfer of methanotrophic ability (Dunfield *et al.*, 2007). This group is also referred to as type III MOB. Methanotrophs from this cluster were shown to be thermophilic or mesophilic, and initially were detected in acidic geothermal environments (Sharp *et al.*, 2014). However, recent

investigations also detected them in ponds in northeastern Canadian sub-Arctic (Crevecoeur *et al.*, 2015). Their physiology, metabolism and cell structure stay largely unknown, however intensively investigated. Khadem *et al.* (2011) showed that *Methylacidiphilum fumariolicum* strain uses the Calvin-Benson-Bassham cycle for carbon dioxide fixation. So far *Verrucomicrobia* MOB were not proven to be functionally important in natural and anthropogenic environments, thus the main focus of the current study is on conventional MOB from the *Proteobacteria* phylum.

Methanotrophic *Alphaproteobacteria* and *Gammaproteobacteria* are also rather divergent and traditionally referred to as type II and type I MOB, respectively. Apart from phylogeny, differentiation between these two clusters includes internal membrane arrangement and the carbon assimilation pathway employed. Type I methanotrophs have disc-shaped membrane bundles distributed throughout the cytoplasm and assimilate carbon as formaldehyde via the RuMP pathway. Type II methanotrophs possess paired internal membrane structures aligned with the periphery of the cell and assimilate formaldehyde via the serine pathway (Hanson & Hanson, 1996). Other traits which were previously thought to be exclusive for one or another type, such as nitrogen fixation, phospholipid fatty acid profile, or formation of resting stages, are now discovered to be more widespread throughout methanotrophic *Proteobacteria* (Knief, 2015). Types I and II are further divided into subtypes: Ia, Ib, Ic, IIa and IIb (Knief, 2015) (Fig. 3).

1.3.2 Environmental controls and biogeography of MOB

Most methanotrophic bacteria are mesophilic and neutrophilic, however some are adapted to extreme environments for pH, temperature, salt, or oxygen (Trotsenko & Khmelenina, 2002). Methane concentration is thought to be the main environmental control of MOX (Sundh *et al.*, 2005, Lofton *et al.*, 2014). MOB can be categorized into two groups according to affinity for methane. High-affinity oxidation occurs at methane concentrations close to atmospheric (≈2 ppm), while low-affinity oxidation occurs at methane concentrations generally higher than 40 ppm (Chowdhury & Dick, 2013). High-affinity MOB are found mainly in aerobic upland soils and represent a minor group regarding their relative abundance in overall bacterial community (Maxfield *et al.*, 2008). This MOB group is suggested to consist primarily of type II MOB (Lau *et al.*, 2007) as well as of distinct, uncultivated clades distant from known type I and type II MOB (Horz *et al.*, 2005). Despite the low capacity, high-affinity MOB contribute approximately 4% to the total methane sink (Kirschke *et al.*, 2013). Low-affinity methanotrophs are more widespread and characterized by a higher methanotrophic capacity. MOX rates were shown to be positively correlated to methane concentrations in various environments. Oxygen is another important factor controlling MOB. Aerobic methane oxidation preferentially occurs at oxic-anoxic interfaces (Hanson & Hanson, 1996, Lee et al., 2015). At the same time MOX rates were shown to be positively correlated to oxygen in

the range from 0.1 to 10 mg L^{-1} (Martinez-Cruz et al., 2015). Vice versa, MOB were found in high abundance at the anoxic bottom waters (Crevecoeur et al., 2015) and in the anoxic littoral sediments (Rahalkar et al., 2009). Temperature seems to have a weak impact on MOX, though this effect is getting more pronounced at higher methane concentrations (Duc et al., 2010, Lofton et al., 2014). In other words, MOX rates are regulated primarily by substrate availability and secondarily by temperature (Lofton *et al.*, 2014). However, results of Martinez-Cruz *et al.* (2015) suggest temperature to be an important (if not the main) control of MOX in the Arctic lakes. Salinity is thought to be a critical environmental control for freshwater MOB. It is considered that microbial methane oxidation is significantly reduced already at salinities < 10 (Abril & Borges (2005) and references therein). However, effect of salinity on MOX rates was usually studied on environmental samples, where salinity is co-correlated with other variables such as temperature or methane concentration. **Further investigation on the specific impact of salinity on methane oxidation is needed**. Furthermore, **it is not clear how marine MOB react to a decrease in salinity**. Light was shown to have either an inhibitory effect on methane oxidation (Dumestre *et al.*, 1999, Murase & Sugimoto, 2005) or no effect at all (van der Nat & Middelburg, 1998); thus **revision of this environmental control of MOX should also be considered**.

Diversity-distribution patterns of MOB in different habitats were studied on different taxonomic levels. Initial attempts focused on habitat preferences of type I and type II MOB, which appears to be reasonable due to physiological differentiation of these two groups. It appears that presence or absence of a certain MOB type is common for extreme environments, such as peat bogs or acidic forest soils, rather than for moderate environments, where both types are represented, but in different abundances. It is reasonable to assume that dominance of a certain MOB cluster, in most cases, results from its competitive characteristics rather than from physiological limitations. This statement is supported by the successful retrieval of type II MOB in enrichment cultures from environments, which are dominated by type I MOB (Rockne & Strand, 2003, Bussmann *et al.*, 2004). It is generally assumed that type II MOB are prone to dominate environments with high methane, low oxygen, and limited combined nitrogen and copper concentrations. Type I methanotrophs, on the contrary, are dominant in environments in which methane is limited and combined nitrogen and copper levels are relatively high (Hanson & Hanson, 1996). Further research, however, showed that methane concentration is not the only controlling factor of MOB dominance. Thus type I MOB (*Methylobacter*) were shown to be indicative for high methane source strength in rice field soil microcosms (Krause *et al.*, 2012) and Arctic tundra soil (Liebner *et al.*, 2009). Furthermore, in the tropical Lake Kivu type II MOB were shown to be dominant in the methane- and oxygen-rich, yet depleted in nutrients, water layers (Zigah *et al.*, 2015). Temperature, which was already mentioned as an important factor affecting MOB, seems to have selective impact on different MOB types. Low

temperatures were shown to favor the development of type I over type II MOB in various soil (Gebert *et al.*, 2003, Börjesson *et al.*, 2004) and aquatic environments (Sundh *et al.*, 2005, He *et al.*, 2012b). However, the opposite results were also shown when winter conditions did not increase type I MOB abundance, but in contrast, increased the relative abundance of type II (Siljanen, 2012). Effect of salinity on the different MOB types can also vary (Bissett *et al.*, 2012).

It is suggested that type I and type II MOB, having distinct traits, also apply different life strategies. Some authors suggest characterizing methanotrophs according to r/K selective theory, where type I and type II MOB are r- and K-strategists, respectively (Siljanen *et al.*, 2011). Type I MOB seem to be less tolerant, but more responsive to environmental conditions than type II. For example, type I MOB thrive in favorable conditions, but quickly reduce their cell numbers when conditions are limited. Type II MOB can tolerate harsh conditions, but stay in a dormant state (Ho *et al.*, 2013). This can be explained by the higher efficiency of RuMP pathway (type I), ability to utilize alternative substrates (type II: *Methylocystis spp*., *Methylocapsa*), and capability of the formation of resting stages (mainly type II). An even more specific ecological classification was proposed by Ho *et al.* (2013). According to the universal adaptive strategy theory he suggested to classify type I MOB as competitor-ruderal organisms and type II MOB as stress tolerators.

Representatives of both: type I and type II MOB were detected in all the main aquatic and terrestrial environments and were not restricted to a single phylogenetic cluster (Fig. 4) (Knief, 2015). At the same time, some clusters can be found exclusively in a certain environment, such as marine MOB clusters, and some are spread over a large number of different soil and aquatic environments, such as *Methylocystis* genus (Knief, 2015). It is remarkable that individual species or even strains within *Methylocystis* genus are, however, very habitat-specific (Knief, 2015). Ecophysiological characteristics were also shown to differ among members of the genus *Methylobacter* (Tsutsumi *et al*., 2011). This brings to question how strongly dominance of type I or type II MOB representatives in a certain environment is connected with general type characteristics vs individual traits of the species/strain. Thus, **to better understand habitat specificity of MOB and its affecting factors it is necessary to perform an investigation at higher taxonomic resolution** (Tsutsumi *et al.*, 2011, Knief, 2015). Additionally, it should be noted that environments classified in one group can substantially vary between each other and also have distinct micro-niches, which can also be reflected on MOB distribution (Knief, 2015). So, for example, in acidic soils USCα MOB cluster was found to be more preferential, while in pH-neutral upland soil it was USCγ MOB cluster (Knief *et al.*, 2003). Finally, MOB presence in a certain environment can result from transport of these microorganisms from the bordering environments (Crump *et al.*, 2012).

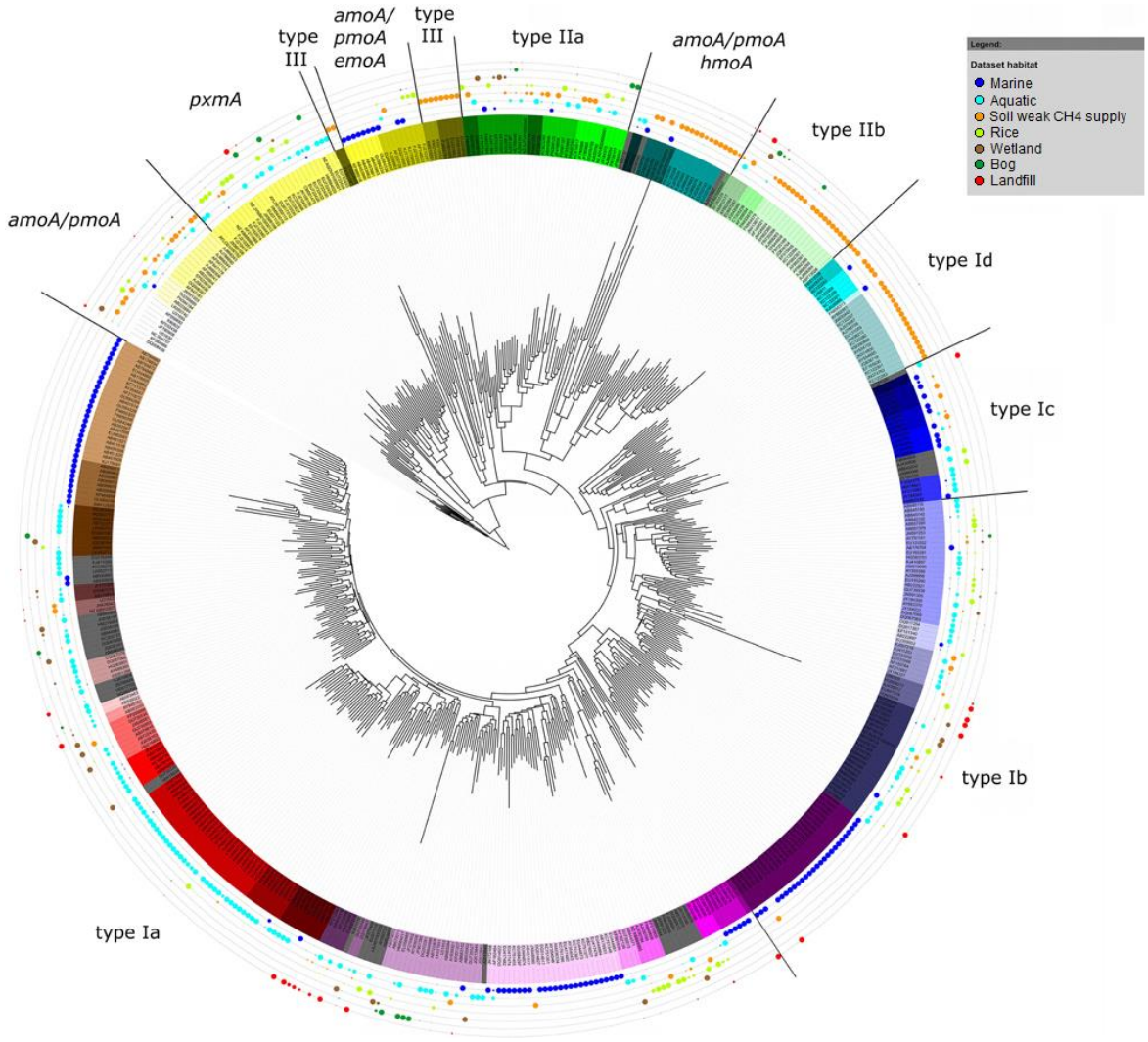

Figure 4. Neighbor joining tree showing the phylogeny of representative *pmoA* sequences and the habitats in which they were detected. The dots on the rings around the tree display detection in different habitat types. Colors of the ring display MOB clusters. Modified from Knief (2015).

1.3.3 Taxon-specific activity of MOB

It is a challenging task to connect MOB diversity and abundance with methanotrophic activity. Correlating the relative abundance of type I and type II MOB with MOX rates reveals that type I MOB are generally more active (Sundh *et al.*, 2005, Jugnia *et al.*, 2006, Siljanen, 2012). Stable isotope probing experiments performed with samples from various environments showed a higher level of activity for type I than type II MOB even when the type I MOB were less numerous (Ho *et al.*, 2013 and references therein). However, few other studies have reported the opposite finding, where type II MOB being outnumbered were more active than type I MOB (Lin *et al.*, 2005, Yun *et al.*, 2012). In several studies it was shown that diversity of MOB is positively correlated with methanotrophic activity (Singh *et al.*, 2007, Degelmann *et al.*, 2010, Levine *et al.*, 2011), however it is not clear if this activity is related to a certain MOB cluster, which is more likely to be present when diversity is high,

or if it is related to the combined activities of the species present (Levine *et al.*, 2011). Furthermore, increased methanotrophic activity was shown to be correlated with the richness of the heterotrophic bacterial community in general (Ho *et al.*, 2014). Finally, MOX rates are positively correlated with methanotrophic abundance which in turn increases in favorable conditions such as increased substrate availability (Sundh *et al.*, 2005, Rahalkar *et al.*, 2009, Steinle *et al.*, 2015). However, MOX rates can also be controlled by the changing activity per cell (Rahalkar *et al.*, 2009). Theoretically, high MOX rates can also result from optimization of cytoarchitectural components relevant for substrate metabolism (Mau *et al.*, 2013).

1.3.4 Aquatic MOB

In marine and freshwater environments in low and middle latitudes type I MOB are found to be dominant and also more active in comparison with type II MOB (Holmes *et al.*, 1996, Costello *et al.*, 2002, Eller *et al.*, 2005, Sundh *et al.*, 2005, Chen *et al.*, 2008, Rahalkar *et al.*, 2009, Reed *et al.*, 2009, Tsutsumi *et al.*, 2011). There are only few exceptions reported from the tropics when type II MOB were dominant (Dumestre *et al.*, 2002, Zigah *et al.*, 2015). The relative abundance of type I MOB in freshwater environments usually varies from 90 to 100% of the total MOB abundance. Type I MOB are mainly represented by such genera like *Methylobacter*, *Methylomonas*, *Methylomicrobium*, *Methylosarcina* and *Methyloferula*, while type II MOB are represented with *Methylocystis* and *Methylosinus* (Borrel et al., 2011).

Substantially less is known about MOB community composition in Arctic aquatic environments. He *et al.* (2012a) studied MOB in Arctic and sub-Arctic lakes using enrichment cultures (water column) and SIP microcosms (sediments) and showed high heterogeneity of MOB throughout lakes, as well as sampling locations within the same lake, and also in the water column vs sediments, and different sediments depths. Enrichment cultures from the water column were dominated (up to 75% of total bacterial reads) by type II MOB (*Methylocystis*). Active MOB in the upper sediments were dominated by type I (*Methylobacter*, *Methylomonas* or *Methylosoma* depending on the sampling site), while the deep sediments (15–20 cm) were dominated by either type I (*Methylobacter*) or type II (*Methylocystis*). It should be noted that dominance of one MOB type over another varied from overwhelming (99%) to minor (70%). Relative abundance of MOB to total reads varied from 5 to 70%. While it is possible that enrichment cultures and SIP microcosms may favor the proliferation of some MOB clusters and diverge their relative abundance from the *in situ* measurements, the obtained results were in agreement with direct sequencing performed in previous studies (He *et al.*, 2012c). Another research study on methanotrophic community composition in sediments of three sub-Arctic lakes in the Canadian taiga (Jugnia *et al.*, 2006) showed the predominance of *Methylomonas* (type I) in one of the lakes while the two others were dominated by *Methylocystis* (type II). In contrast

Crevecoeur *et al.* (2015) observed dominance of type I MOB and particularly *Methylobacter* in shallow lakes in the Nunavik sub-Arctic region (northern Québec, Canada). However, the presence of type II MOB (*Methylocystis*) was also found in previous investigations of these ponds (Rossi *et al.*, 2013). Furthermore, these authors observed high diversity of bacterial communities in neighboring ponds in general linking it with the "potentially complex response of thaw pond systems to climate change".

Arctic soil and wetland environments are preferably dominated by type I MOB (Wartiainen *et al.*, 2003, Liebner *et al.*, 2009, Martineau *et al.*, 2010, Graef *et al.*, 2011), though predominance of type II MOB was also shown (Barbier *et al.*, 2012). Diversity of MOB in these environments is restricted to only several genera, mainly *Methylobacter* and to a lesser extent *Methylosarcina* (type I MOB), and *Methylocystis* and *Methylosinus* (type II MOB).

1.4 Molecular tools for the study of MOB

Phylogeny of methanotrophs, presence of the specific enzymes, and membrane molecular structures (phospholipid fatty acids; PLFAs), provide the possibility for quantitative and qualitative analyses of this group using molecular tools. The availability of large datasets made the 16S rRNA gene one of the main markers used to characterize methanotrophs. Alternative markers are functional genes which encode the methane monooxygenase (MMO). In many cases these genes are more preferable targets, providing higher specificity and giving clues on the physiology of methanotrophs (McDonald *et al.*, 2008). However, both approaches give comparable results and are used to supplement each other (McDonald *et al.*, 2008). The most frequently targeted functional genes are *pmoA*, which encodes the β-subunit of the particulate monooxygenase, pMMO and *mmoX*, which encodes the α-subunit of the soluble monooxygenase, sMMO. Except for *Methylocella* and *Methyloferula* spp, the *pmoA* gene is found in all the known methanotrophs (Dedysh *et al.*, 2000, Vorobev *et al.*, 2011), which makes it a more preferable target than *mmoX,* which is typical for type II but rarely found among type I MOB. Other gene markers, which are not exclusive for methanotrophs but can be used to characterize them, are: *mxaF* (which encodes the α-subunit of the methanol dehydrogenase) (Neufeld *et al.*, 2007), *nifH* (which encodes dinitrogen reductase, a key component of the nitrogenase enzyme complex) (Dedysh *et al.*, 2004), and *fhcD* (which encodes the D subunit of the formyltransferase/hydrolase complex, part of the H_4MPT-linked C_1-transfer pathway) (Kalyuzhnaya *et al.*, 2004). Fingerprinting methods, such as DGGE (Lin *et al.*, 2005), T-RFLP (Bussmann *et al.*, 2004), and MISA (Tavormina *et al.*, 2010), were successfully adapted for the analysis of the diversity of methanotrophs. Another method, which allows identifying methanotrophs and provides data on their diversity at higher taxonomic resolution, is DNA microarray technology (Abell *et al.*, 2014, Martineau *et al.*, 2014). Nowadays *pmoA* microarrays are produced for all the known genera and in

some cases for separate species or groups of species (McDonald *et al.*, 2008). However, currently this method is losing its popularity and is not widespread anymore.

The main limitation of the aforementioned techniques is that they are applicable mainly for the known sequences of methanotrophs. Sequencing of multiplied genes, which allows for identification of novel species, is usually performed using next-generation sequencing methods (NGS), such as pyrosequencing. This method is based on "sequencing by synthesis" principle and uses a chemiluminescent enzymatic reaction.

Quantitative methods, which are used to analyze the abundance of MOB, can be divided into culture-dependent techniques such as most-probable-number (MPN) (Bussmann *et al.*, 2004) and gradient cultivation (Bussmann *et al.*, 2006), and culture-independent techniques such as fluorescence *in situ* hybridization (FISH) targeting the 16S rRNA gene (Rahalkar *et al.*, 2009), Southern hybridization with probes for the *pmoA* or the *mmoX* gene (Costello *et al.*, 2002), and real-time PCR targeting *pmoA* gene (Krause *et al.*, 2015, present research).

PLFAs patterns are another fingerprint used to identify methanotrophs and distinguish the different types from each other. The type I methanotrophs contain mainly 14C and 16C PLFAs, whereas the type II contain mainly 18C PLFA. Additionally, methanotrophs possess PLFAs which are exclusive to this group of microorganisms. For type I MOB these fatty acids are: C16:1ω8c and C16:1ω5t; for type II MOB – C18:1ω8c (Nichols *et al.*, 1985, Bowman *et al.*, 1993). It should be noted, however, that there are also exceptions (Dedysh *et al.*, 2007).

Stable isotope probing (SIP), which links identification of microorganisms to estimation of their activity, was also applied for methanotrophs. ^{13}C isotope, which in contrast to ^{12}C is minor in nature, is added as substrate to the targeted microbial community placed in microcosms simulating natural conditions. Metabolic activity and consequent proliferation of the targeted microorganisms lead to insertion of the tracer into DNA, mRNA, rRNA (Dumont *et al.*, 2011) or PLFA (Chen *et al.*, 2008) where it could be detected after sequencing or PLFA analysis.

Several techniques have been applied to qualify and quantify the microbial methane consumption. MOX can be measured by the decrease of methane concentration over time (calculated using gas chromatography (Abril *et al.*, 2007) or Infrared Tunable Diode Laser Absorption Spectroscopy (HE-TDLAS), (Martinez-Cruz *et al.*, 2015)), the change in isotopic composition (Bastviken *et al.*, 2002) or by a combination of stable isotope and conservative tracer measurements (Rehder *et al.*, 1999, Heeschen *et al.*, 2004). The most sensitive measurements, however, are obtained adding a radioactive tracer such as $^{3}H\text{-}CH_4$ (Valentine *et al.*, 2001, Mau *et al.*, 2013) or $^{14}C\text{-}CH_4$ (Pack *et al.*, 2011). Usage of $^{3}H\text{-}CH_4$ in comparison with $^{14}C\text{-}CH_4$ seems to be more advantageous due to generally higher simplicity of the corresponding method which is especially important when measurements are

conducted during sampling campaigns. Furthermore $^{3}H\text{-}CH_4$ has a higher specific activity (3.7–7.4 × 10^{11} Bq $mmol^{-1}$) than $^{14}C\text{-}CH_4$ with 3.7 – 18 ×10^{7} Bq $mmol^{-1}$ and thus can be used in lower amounts, which results in only minor alteration of *in situ* methane concentrations in the collected samples (Bussmann *et al.*, 2015 – Additional manuscript I).

1.5 Aims and objectives

Aquatic environments are of exceptional interest due to their active involvement in methane cycling. Furthermore, being connected with each other aquatic environments form networks which are spread on vast areas, and involve various marine, freshwater, and terrestrial ecosystems. Thus, aquatic systems have a high potential to translate local or regional environmental and subsequently ecosystem changes to a larger scale. Many studies neglect this connectivity and focus on individual aquatic or terrestrial biogeocenoses. Investigation of their interfaces is the next step in understanding the link between individual ecosystems and the encompassing biomes which is of a particular importance in the era of a rapidly changing world.

This thesis focuses on Arctic water bodies and on estuaries, which represent interfaces between permafrost soil and aquatic environments and between marine and freshwater environments, respectively. These interface areas are studied in the context of methane cycling with the main focus on methane distribution and aerobic methane oxidation as well as their environmental controls (primarily MOB). Considering these objectives more specific questions are to be answered:

1) What determines methane distribution in the interfaces between aquatic and terrestrial environments?
2) How does the interaction between bordering aquatic and terrestrial environments affect abundance and community composition of MOB and MOX rates?

1.6 Study area

The Arctic water bodies were investigated in the Lena Delta region (Fig. 5.) and more specifically on Samoylov Island. The Lena Delta is the largest Arctic delta, which became a center for various research campaigns since the late 20th century. Samoylov Island is representative of the currently active portion of the Lena Delta and is located in its central part. Estuaries were investigated at the example of the Elbe estuary (Fig. 6.), which is located in the south-east of the North Sea. Given that the Elbe River is one of the major rivers in Western Europe its estuary plays an important role in the ecology of the region.

1.6.1 The Lena Delta

The Lena River is one of the largest Siberian rivers with a catchment area of about 2,490,000 km^2 and discharge up to 16,000 $m^3 s^{-1}$ (Dai & Trenberth, 2002). It starts near Baikal Lake and flows northeast until it reaches the city of Yakutsk. Then it turns north until it finally discharges into the Laptev Sea. As it passes through its estuarine area, the main flow of the Lena River splits into numerous arms forming the most extensive delta in the Russian Arctic and one of the largest deltas in the world. It covers 29,000 km^2 and includes more than 1,000 islands and an enormous amount of lakes, ponds, and river channels, which altogether cover more than 30% of the area (Schneider *et al*., 2009). It extends 100 km into the Laptev Sea and is approximately 400 km wide. The entire delta is situated in the zone of continuous permafrost with a thickness of about 500–600 m (Romanovskii & Hubberten, 2001). The upper soil layer (30–50 cm), however, forms the active layer which thaws during summer. Field work was conducted on Samoylov Island, a typical island in the central part of the delta (72.37N, 126.47E) with an area of about 5 km^2. It belongs to the active and youngest part (8,000–9,000 years old) of the Lena Delta. Samoylov Island consists of a floodplain in the west and an elevated river terrace, dominated by active ice-wedge formation, low-centre polygons and small thermokarst ponds, in the east. The western coast of the island is characterized by modern accumulation processes of fluvial and aeolian sedimentation, while the eastern coast is dominated by erosion processes which form an abrasional coast (Hubberten *et al.*, 2006).

In the present study we analyzed five lakes, located along the coastline of Samoylov Island, and their outlets, which connect the lakes with the surrounding Lena River. We also sampled the river itself next to the lake outlet and in the middle, thus completing five lake – river transects. The sampling campaign took place from 13.07.2012 to 26.07.2012. A detailed description of sampling sites with their designations and locations is given in a chapter II (Manuscripts).

Fig. 5. The Lena Delta, northeast Siberia and Samoylov Island (red square).

1.6.2 The Elbe estuary

The Elbe River is one of the major rivers of central Europe, with a total catchment area of about 150,000 km^2. It starts in the northeast of the Czech Republic and reaches the North Sea in the northwest of Germany, near the city of Cuxhaven. This part of the North See is also known as the German Bight. The Elbe's mean annual discharge at the river mouth is 860 m^3 s^{-1}. The discharge regime is mainly controlled by rainfall and snowmelt; therefore it peaks in April/May (Simon, 2005). Another factor, which controls water dynamics near the mouth of the river, is high tidal current velocities (up to 1.8 m s^{-1}) (Bergemann & Gaumert, 2010).

The North Sea (including its estuaries and fjords) has a surface area of about 750,000 km^2 and a volume of approximately 94,000 km^3 (Commission, 2000). The non-tidal circulation of the North Sea is dominated by a cyclonic residual current. Water from the Atlantic (Fair Isle Current, Shetland Flow) flows southward along the British coast and returns northward, together with influxes from the English Channel and various rivers along the coasts of the Netherlands, Germany, and Denmark (Rehder *et al.*, 1998). The German Bight is bounded by the Netherlands and Germany to the south, and Denmark with Germany to the east (the Jutland peninsula). To the north and west, it is bounded by the Dogger Bank. The depth in this area varies mainly from 20 to 40 m (Czitrom *et al.*, 1988). The German Bight consists mainly of a mixture of the Central (southern) North Sea water masses and continental coastal waters (Becker *et al.*, 1992). The water column in the central (southern) North Sea can be stratified into two slightly different layers (Czitrom *et al.*, 1988, Becker *et al.*, 1992).

Inshore water did not show any stratification in either summer or winter. Freshwater discharge from the Elbe and Weser rivers causes a large salinity contrast near the shore (Czitrom *et al.*, 1988). Analysis of horizontal density gradients did not show a clear annual cycle either near the shore or offshore (Czitrom *et al.*, 1988). Surface sediments affected by tidal or residual current, wave action, and heavy bottom trawling are very mobile (ICES, 1988, Becker *et al.*, 1992). Strong tidal motions and consequent water exchange have a strong effect on the ecology of the German Bight and Elbe estuary.

Water samples analysed in the second publication were collected from the seven stations distributed along the 60 km transect stretching from the mouth of the Elbe River, near the city of Cuxhaven north-west towards Helgoland archipelago. Samples were collected for 2 years from 2010 to 2012 during eleven one-day sampling cruises. Samples used for the third publication were collected from the Elbe River near the city of Hamburg at Elbe kilometer EC 659 and from the North Sea near Helgoland archipelago in the period of time from 2011 to 2013. A detailed description of sampling sites with their designations and locations is given in a chapter II (Manuscripts).

Fig. 6. The Elbe estuary. The red square denotes the study area discussed in the second manuscript, while the yellow squares mark sampling sites used in the third manuscript.

1.7 Overview of the publications and manuscripts

Manuscript I (Published in *FEMS Microbiology Ecology*, 2016, fiw116,

DOI: http://dx.doi.org/10.1093/femsec/fiw116)

Methane turnover and methanotrophic communities in Arctic aquatic ecosystems of the Lena Delta, Northeast Siberia

Authors: Roman Osudar[1,2,3], Susanne Liebner[2], Mashal Alawi[2], Sizhong Yang[2], Ingeborg Bussmann[3], Dirk Wagner[2]

Aims: The aims of this study were to investigate methane distribution and variation of the MOX rates in the water bodies of Samoylov Island (Lena Delta) and the surrounding Lena River and to identify environmental factors affecting methane cycling. Furthermore, we investigated methanotrophic bacterial community structure (abundance and composition) and its environmental controls in the studied water bodies. We hypothesized that lakes, their outlets and river sites represent different patterns resulting from the heterogeneity of their morphology and terrestrial influence.

Summary: Our results showed that regarding methane distribution and methane cycling lakes and outlets, in contrast to the river, are strongly affected by the soil environment. The methane concentrations in the lakes and outlets varied significantly (170–24,000 nmol L^{-1}), being generally higher in the outlets except for the floodplain lake (23,000 nmol L^{-1}). The abundance of methane-oxidizing bacteria (< 10^2–10^5 cells L^{-1}) and MOX rates (0.2–480 nmol L^{-1} h^{-1}) in the lakes and outlets were correlated with methane concentrations but also showed individual patterns. Furthermore, MOB community composition differed in all the lakes and their outlets. In contrast, river sites did not show high variation in methane concentrations (140–200 nmol L^{-1}) except for one site, which had a strong input of methane from the outlet (6,400 nmol L^{-1}). Also MOX rates (on average 0.8 ± 0.4 nmol L^{-1} h^{-1}), the abundance of MOB (on average 6.2 ± (3.4)*10^3 cells L^{-1}) and their community composition through the river sites were very homogeneous. Remarkably, in all the water bodies we detected both type I and type II MOB in comparable ratios, which is unusual for Arctic permafrost environments and for freshwater systems in middle and low latitudes. We hypothesize that Arctic freshwater systems represent a developing ecosystem and also a less extreme habitat than the surrounding permafrost soils.

Contribution of the co-authors: *Susanne Liebner* participated in analysis of pyrosequencing data, phylogenetic analysis, gave valuable input throughout the writing of the manuscripts, participated in the interpretation of the results and provided valuable discussion. *Mashal Alawi* participated in library preparation, gave valuable input throughout the writing of the manuscripts, participated in the interpretation of the results and provided valuable discussion *Sizhong Yang* participated in the

analysis of the pyrosequencing data and provided useful comments. *Ingeborg Bussmann* and *Dirk Wagner* gave valuable input throughout the writing of the manuscripts, participated in the interpretation of the results and provided valuable discussion.

Manuscript II (Published in *Estuarine, Coastal and Shelf science*, 2015, 160, 10–21, DOI http://dx.doi.org/10.1016/j.ecss.2015.03.028)

Environmental factors affecting methane distribution and bacterial methane oxidation in the German Bight (North Sea)

Authors: Roman Osudar[1,2,3], Anna Matoušů[4,5], Mashal Alawi[2], Dirk Wagner[2] and Ingeborg Bussmann[3]

Aims: The objectives of this study were to describe the spatial and seasonal variations of methane in the German Bight, near the Elbe estuary and to bring the importance of bacterial methane oxidation as a significant methane sink into focus. The methane concentration, as well as several hydro-chemical parameters from the bottom and surface waters, such as salinity, temperature, the concentrations of inorganic nutrients (ammonium, nitrite, nitrate, phosphate, and silicate) and suspended particulate matter (SPM) were measured to determine the main environmental factors that control methane distribution and MOX rates.

Summary: Methane distribution in the German Bight was influenced by input of the methane-rich water in the mouth of the Elbe and gradual dilution by methane-depleted sea water. Methane concentrations near the coast were on average 30 ± 13 nmol L^{-1}, while in the open sea, they were 14 ± 6 nmol L^{-1}. Interestingly, the highest methane concentrations were repeatedly detected near Cuxhaven, not in the Elbe River freshwater end-member as previously reported. Though, we did not observe a clear seasonality we observed temporal methane variations, which depended on temperature and presumably on water discharge from the Elbe River. The highest MOX rates generally coincided with the highest methane concentrations, and varied from 2.6 ± 2.7 near the coast to 0.417 ± 0.529 nmol L^{-1} d^{-1} in the open sea. Turnover times varied from 3 to >1000 days. MOX rates were strongly affected by methane concentration, temperature and salinity. We ruled out the supposition that MOX is not an important methane sink in most of the Elbe estuary and the adjacent German Bight.

Contribution of the co-authors: *Anna Matoušů* participated in collecting and analyzing of the data and also provided useful comments. *Mashal Alawi* and *Dirk Wagner* gave valuable input throughout the writing of the manuscripts, participated in the interpretation of the results and provided valuable discussion. *Ingeborg Bussmann* participated in collecting and analyzing of the data, gave valuable input throughout the writing of the manuscripts, participated in the interpretation of the results and provided valuable discussion.

Manuscript III (In preparation for submission to *Aquatic Microbial Ecology*)

Effect of salinity and light on aerobic bacterial methane oxidation in the marine and freshwater

Authors: Roman Osudar[1,2,3], Karl-Walter Klings[3], Julia Warnstedt[6], Dirk Wagner[2], Ingeborg Bussmann[3]

Aims: The objectives of this research were to figure out how changing salinity and light affect methane oxidation rates in marine and freshwater environments.

Summary: According to our results *Methylomonas* sp. and *Methylosinus trichosporium* are resistant to salinity increase in contrast to *Methylovulum* sp. and *Methylobacter luteus*, which are sensitive to salinity increase. Natural MOB populations from the freshwater are more resistant to salinity increase than those from the marine water to salinity decrease. In both cases, however, response of the natural MOB populations to salinity stress appeared to be heterogeneous, which is likely attributed to variance in MOB community composition. Gradual salinity increase in contrast to immediate one can attenuate salinity effect. Light has a selective inhibitory effect on methanotrophic activity of MOB isolates and communities in natural environments.

Contribution of the co-authors: *Karl-Walter Klings* and *Julia Warnstedt* participated in experimental work and analysis of results. *Dirk Wagner* provided valuable discussion. *Ingeborg Bussmann* gave valuable input throughout the writing of the manuscripts, participated in the interpretation of the results and provided valuable discussion.

List of author's affiliations:

[1]Alfred Wegener Institute Helmholtz Centre for Polar and Marine Research, Research Unit Potsdam, Germany.

[2]GFZ German Research Centre for Geosciences, Helmholtz Centre Potsdam, Section 5.3: Geomicrobiology, Germany.

[3]Alfred Wegener Institute, Helmholtz Centre for Polar and Marine Research, Marine Station Helgoland, Germany.

[4]University of South Bohemia, Faculty of Science – Dept. of Ecosystem Biology, České Budějovice, Czech Republic.

[5]Biology Centre of the Czech Academy of Sciences, Institute of Hydrobiology, České Budějovice, Czech Republic.

[6]Carl-von-Ossietzky University Oldenburg, Department of Biology and Environmental Sciences, Germany.

II MANUSCRIPTS

Manuscript I

Methane turnover and methanotrophic communities in Arctic aquatic ecosystems of the Lena Delta, Northeast Siberia

Roman Osudar, Susanne Liebner, Mashal Alawi, Sizhong Yang, Ingeborg Bussmann, Dirk Wagner

Abstract

Large amounts of organic carbon are stored in Arctic permafrost environments, and microbial activity can potentially mineralize this carbon into methane, a potent greenhouse gas. In this study, we assessed the methane budget, the bacterial methane oxidation (MOX) and the underlying environmental controls of Arctic lake systems, which represent substantial sources of methane. Five lake systems located on Samoylov Island (Lena Delta, Siberia) and the connected river sites were analyzed using radiotracers to estimate the MOX rates, and molecular biology methods to characterize the abundance and the community composition of methane-oxidizing bacteria (MOB). In contrast to the river, the lake systems had high variation in the methane concentrations, the abundance and composition of the MOB communities, and consequently, the MOX rates. The highest methane concentrations and the highest MOX rates were detected in the lake outlets and in a lake complex in a floodplain area. Though, in all aquatic systems we detected both, Type I and II MOB, in lake systems we observed a higher diversity including MOB, typical of the soil environments. The inoculation of soil MOB into the aquatic systems, resulting from permafrost thawing, might be an additional factor controlling the MOB community composition and potentially methanotrophic capacity.

Introduction

Methane is an important radiatively active trace gas that is responsible for approximately 20% of the greenhouse effect (Cicerone & Oremland, 1988, IPCC, 2014). Large amounts of organic carbon, which can be mineralized to methane and carbon dioxide, are stored in the Arctic permafrost environments (Zimov *et al*., 2006, Tarnocai *et al*., 2009, Knoblauch *et al*., 2013, Hugelius *et al*., 2014). With the predicted global climate warming and the resultant thawing of the permafrost, more methane is expected to escape into the atmosphere, contributing positive feedback for climate warming (Wagner *et al*., 2009, Graham *et al*., 2012, IPCC, 2014). Water bodies, which are abundant in the Arctic Lena Delta (8900 km^2) (Schneider *et al*. (2009), represent a transition zone between the soil and the atmosphere and play a key role in methane emission and in the carbon cycle in general (Walter *et al*., 2007, Bastviken *et al*., 2011, Boike *et al*., 2012, Knoblauch *et al*., 2015). Additionally, water bodies act as transportation systems. The methane dissolved in the water can be carried away

by rivers until it reaches the open ocean (Shakhova *et al*., 2007, Bussmann, 2013, Crawford *et al*., 2014).

The process of microbial methane formation, termed methanogenesis, is mediated by methanogenic archaea and occurs under strictly anoxic conditions. There is also evidence of methanogenesis in the oxic zones of the water column, which is linked to algal dynamics and driven by acetoclastic production (Bogard *et al*., 2014); however, this process needs further investigation. In water bodies, methanogenesis takes place mostly in anoxic sediments (Bartlett *et al*., 1988) and depends mainly on the supply of organic matter, the availability of electron acceptors and the temperature (Duc *et al*., 2010, Lofton *et al*., 2014). Methane from the sediments and the water column reaches the atmosphere either by ebullition or by diffusion from a water surface. Additionally, methane flux can be associated with plant-mediated transport in the littoral zones (Knoblauch *et al*., 2015). The contribution of each pathway to the methane emission rates is uncertain due to their spatial and temporal variations. Ebullition, which acts as a methane transport pathway, was previously underestimated and is now considered to drive methane emissions from the Arctic lakes (Bastviken *et al*., 2004, Walter *et al*., 2007). Ebullition can also contribute to the budget of methane dissolved in the water column. According to the estimations of Greene *et al*. (2014), up to 80% of the methane in bubbles trapped under the ice during the winter can dissolve into the lake water. Thus, each pathway of methane transport, as well as the methane-related processes that affect this transport, are important for understanding the methane dynamics in the Arctic permafrost ecosystems.

The fate of the methane dissolved in water is largely dependent on bacterial methane oxidation (MOX). The main factors controlling the MOX rates are methane and oxygen availability (Hanson & Hanson, 1996). In the low- and mid-latitude freshwaters, up to 90% of the methane can be oxidized before reaching the atmosphere (Guérin & Abril, 2007, Bastviken *et al*., 2008). At the same time, very few MOX rate measurements have been conducted in the Arctic freshwater environments, especially in the water column (He *et al*., 2012a, Bussmann, 2013, Lofton *et al*., 2014, Martinez-Cruz *et al*., 2015). These studies reveal high spatial variability, which makes the assessment of the role of methane oxidation as a methane sink difficult. Additionally, very little is known about the abundance and the diversity of aerobic methanotrophic bacteria (MOB), which are responsible for MOX in oxic freshwater environments at high latitudes.

Methanotrophic bacteria are a subset of methylotrophic bacteria that are specialized to utilize methane or methanol as a sole source of carbon and energy (Hanson & Hanson, 1996). The ability to utilize methane is ensured by the activity of the key enzyme methane monooxygenase (MMO), which can exist in soluble and particulate forms. The particulate form is almost ubiquitous in MOB, while the soluble form is rare. Currently, all known cultivated MOB belong to three phyla:

Alphaproteobacteria (Type II MOB), *Gammaproteobacteria* (Type I MOB) and the recently discovered *Verrucomicrobia* (Dunfield *et al*., 2007, Pol *et al*., 2007, Islam *et al*., 2008). Apart from their phylogeny, the differences between Type I and II MOB include the internal membrane arrangement and the carbon assimilation pathway used. Type I methanotrophs have disc-shaped membrane bundles distributed throughout the cytoplasm and assimilate carbon as formaldehyde via the RuMP pathway. Type II methanotrophs have paired internal membrane structures aligned with the periphery of the cell and assimilate formaldehyde via the serine pathway (Hanson & Hanson, 1996). Other traits that were previously thought to be exclusive to one type or the other, such as nitrogen fixation, the phospholipid fatty acid profile or the formation of resting stages, have been found to be more widespread throughout methanotrophic *Proteobacteria* (Knief, 2015). Types I and II are further divided into the following subtypes: Ia, Ib, Ic, IIa and IIb. This categorization, however, is not consistent among different publications. In the current study, we will follow the classification proposed by Dumont *et al*. (2014). According to this classification, Type Ia has *pmoA* sequences affiliated with the classic Type I methanotrophs (i.e., not Type X). Type Ib, also referred to elsewhere as Type X) are those methanotrophs that belong to *Methylococcus* and closely related genera. Type Ic are all other Type I-related sequences with a more ambiguous affiliation. Type IIa was used to group the primary *pmoA* sequences of *Methylocystaceae*. Type IIb was used to group all other Type II-related (i.e., *Alphaproteobacteria*) sequences, including those from *Beijerinckiaceae* and the alternate pMMO2 identified in some *Methylocystis* species.

Large uncertainties are connected to the factors that determine the community structure of MOB in lake environments. Apart from the various environmental variables that favor the proliferation of certain groups of microorganisms, the microbial community composition can be largely affected by the physical transfer of microorganisms from neighboring terrestrial and aquatic environments (Crump *et al*., 2012).

In this study, we investigated the methane fluxes in the water bodies of Samoylov Island (Lena Delta, Northeast Siberia) and the surrounding Lena River. The main foci of this study were two questions: 1) How variable are the methane concentrations and MOX rate in different types of Arctic water bodies, and what are the controlling environmental factors, and 2) Are the methane concentrations and MOX rates related to the diversity and abundance of MOB in Arctic freshwater environments? To better understand the specific importance of the different types of water bodies as methane sources and to assess the methane transport along lake-river transects, our study included five lakes and their outlet streams, which connect these lakes with the surrounding Lena River and the river itself. We assumed that the land-water/water-water transfers of substances and MOB determine the characteristics of the methane flux. Furthermore, these results should help us understand to what

extent bacterial methane oxidation contributes as a methane sink in these systems. In addition to the methane concentrations, we measured the MOX rates using the radiotracer technique and performed quantitative and qualitative analyses of the methanotrophic bacterial communities by analyzing the *pmoA* gene using qPCR and pyrosequencing. Environmental factors, such as temperature, salinity, oxygen and suspended particulate matter (SPM), were included in the investigation to study their influence on methane turnover and the methanotrophic community.

Materials and methods

Study area and water sampling

With an area of 29,000 km^2, the Lena Delta is one of the largest deltas in the world (Schneider *et al*., 2009). It extends 100 km into the Laptev Sea and is approximately 400 km wide. Field work was conducted on Samoylov Island, which is representative of the currently active portion of the Lena Delta; the island is located in the central part of the Lena Delta (72.37N, 126.47E). The island hosts a research station that has been operated since the late 20^{th} century, which made it a center for various research campaigns. Samoylov Island consists of a floodplain in the west and an elevated river terrace in the east that is characterized by a polygonal tundra, which is a typical peatland of the Arctic zone (Minke *et al*., 2007). More details about Samoylov Island are given by Boike *et al*., 2012. Samples were collected from five lake-river transects (hereafter called lake complexes), and each included four sampling sites: a lake, its outlet, a river close to the outlet and a river in the middle (Fig. 1). All the lakes were located at the coastline of the island and were of thermokarst origin, with a surface area up to 0.03 km^2 and a depth up to 6 m. The North Lake complex was located at the floodplain area. The remaining lake complexes were located on the upper terrace. Outlets represented shallow streams (2–10 cm deep) varying from several meters to several tens of meters in length. The Lena River was approximately half a meter deep near the mouth of an outlet and up to 6 m deep in the middle. The geomorphological data of the water bodies investigated are summarized in Table 1.

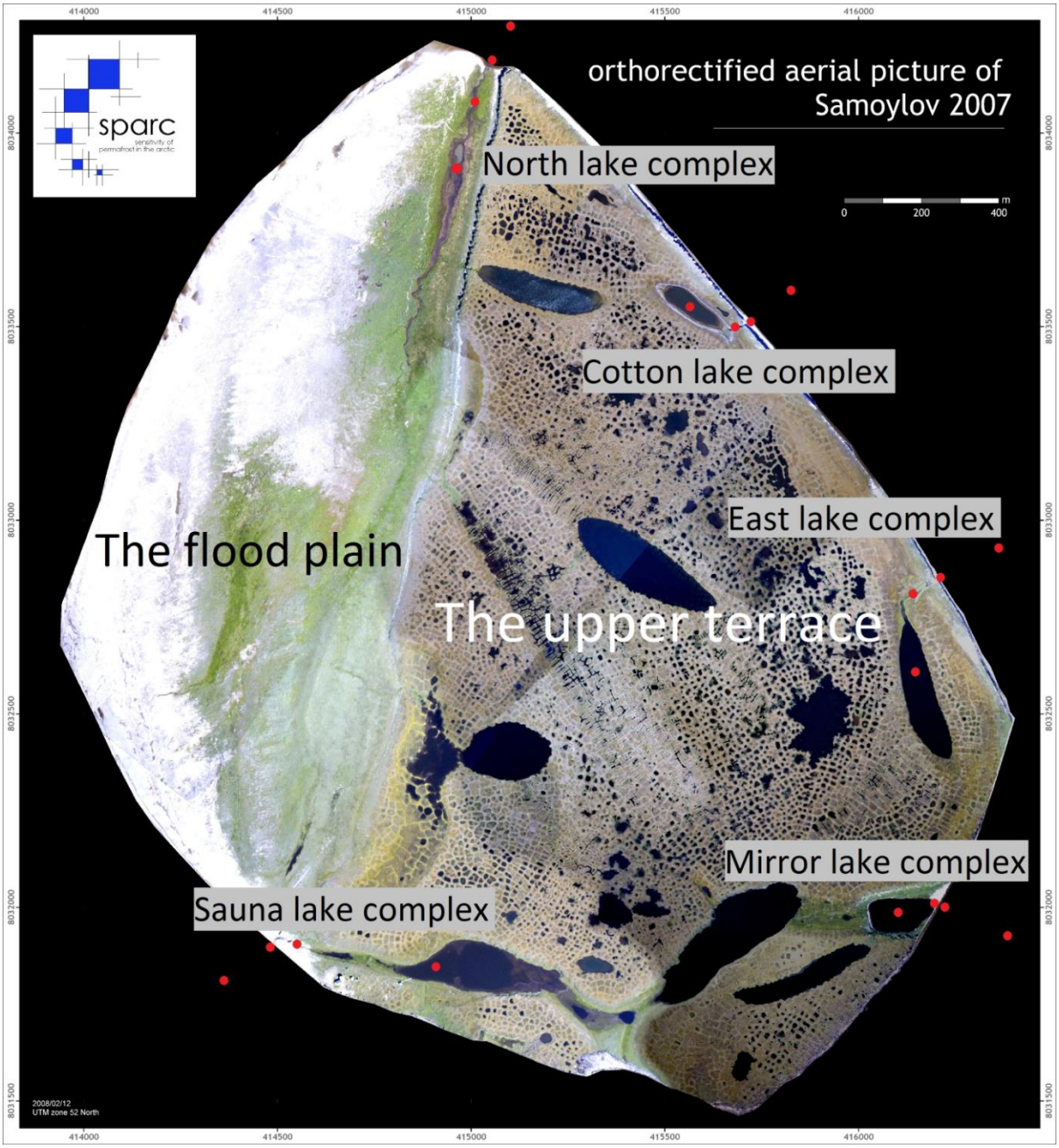

Fig. 1. Location of the studied lake complexes on Samoylov Island. Lake names are unofficial and were invented by the authors. The aerial image is provided by Boike *et al*. (2008).

The sampling campaign took place from 13-07-2012 to 26-07-2012. Water samples from the lakes and the middle of the river were collected from aboard a small rubber boat using a Niskin bottle. Due to the shallow depths, water samples from the other locations were collected using 60-mL plastic syringes.

Samples used for the methane concentration and MOX rate measurements, as well as for the molecular studies of MOB, were collected from the surface waters of all the lake complexes (Mirror, Cotton, Sauna, East, and North Lake complexes). The bottom water samples were taken for only the

methane concentration and MOX rate measurements from the Mirror and Cotton Lakes and from the mid-river sites of the Mirror, Cotton and Sauna Lake complexes. For the methane concentration and MOX rate measurements, the collected water was transferred bubble-free into 120 mL glass serum bottles that were flushed out with the sampled water several times, capped with black rubber stoppers, and sealed with an aluminum crimp according to Bussmann *et al*. (2015). To eliminate agents that inhibit methane oxidation (such as soap), the glass bottles and the stoppers received extensive chemical cleaning before being used, as suggested by Osudar *et al*. (2015). Samples used for the methane concentration and MOX measurements were collected in duplicate and triplicate, respectively. Samples for the molecular studies of MOB were collected without replicates.

Temperature, salinity, oxygen and SPM measurements

The temperature, salinity, and oxygen content of the water column were measured from the surface of all the sampling sites. In most of the lakes and the mid-river sites, the salinity, temperature and SPM were also measured at the bottom of the water column. The measurements were performed immediately after sampling using a Universal Pocket Meter (Multi 340i) with a precision of 1% for salinity, 0.1 °C for temperature, and 0.5% for oxygen content. The salinity was measured in µS cm^{-1} and converted according to the Practical Salinity Scale. To measure the SPM, the sampled water was filtered using pre-washed and pre-weighed GFC filters (Whatman^{TM}). After drying the filters for 48 hours at room temperature, they were weighed again. The SPM concentration was calculated as the difference between the filter weights before and after filtering divided by the water volume. The water volumes varied from 250 to 400 mL, depending on the turbidity. The measurements of pH at the sampling sites were not performed in the current study. However, it was previously shown that the pH values of the lakes on Samoylov Island vary over a relatively narrow range from 6.8 to 7.5 (Abnizova *et al*., 2012). The pH of the Lena River also does not substantially vary (7.8–7.9) (Semiletov *et al*. (2011)).

Methane concentration measurements

Immediately after filling, capping and sealing the bottles, 0.3 mL of 5 N NaOH was added to the samples to prevent methane oxidation. NaOH was added using a syringe with a second needle to allow for the displacement of water. The samples were stored in the dark at approximately +10 °C for 1–2 weeks before further processing. The methane concentrations were measured using the headspace technique; 10 mL of N_2 was added (McAuliffe, 1971). Three 1 mL headspace aliquots from each sample were analyzed using gas chromatography (Chromatec-Crystal 5000.1). Gas standards (Air Liquide) with concentrations of 10 and 100 ppm methane were used for calibration. The atmospheric equilibrium solubility of the methane in the water (the equilibrium concentrations of

the methane in the water column with respect to atmospheric concentrations) were calculated according to the formula proposed by Wiesenburg & Guinasso Jr. (1979). The data measuring the methane concentration of the atmosphere were obtained from the Tiksi Hydrometeorological Observatory in Russia (http://www.esrl.noaa.gov/gmd/dv/iadv/). The saturation rates were calculated as the ratio between the observed methane concentration in the water column and the equilibrium concentrations multiplied by 100%.

Methane oxidation (MOX) rate measurements

The MOX rates were measured using the radiotracer technique with tritiated methane (American Radiolabeled Chemicals, 20 Ci $mmol^{-1}$) according to a modified method from Bussmann *et al*. (2015). Immediately after filling the bottles, the diluted tracer (0.1 mL) was added to the samples (2 kBq mL^{-1}). The samples were vigorously shaken and incubated for 11–16 hours in the dark at near *in situ* temperatures (approximately +15 °C). After incubation, the methane oxidation was stopped by adding 0.3 mL of 5 N NaOH. The methane oxidation of the control samples was stopped before the addition of the tracer. The MOX rate estimation is the comparison of the total amount of radioactivity added to the water sample (C^*H_4) and the radioactive (tritiated) water ($^*H_2O$) that was produced due to the oxidation of the tritiated methane. The ambient MOX rate is the ratio between these values ($r = {}^*H_2O / C^*H_4$) multiplied by the ambient methane concentration ($[CH_4]$) corrected for the incubation time (t).

$$MOX = r \times [CH_4] / t \qquad (1)$$

Additionally, we calculated the turnover time, which is the time it would take to oxidize all the methane at a given MOX rate, assuming that methane oxidation is a first-order reaction. A detailed description of the calculation can be found in a publication by Osudar *et al*. (2015). To determine the total radioactivity of the sample and the radioactivity of the tritiated water, 4-mL aliquots of water were mixed with 10 mL of the scintillation cocktail (Ultima Gold LLT, Perkin Elmer) and analyzed using a liquid scintillation counter (Tri-Carb® 2800 TR, Perkin Elmer); decays per minute (dpm) were used as the units.

DNA extraction

The recovery of the DNA from water samples was conducted using 0.2 µm filters to filter 150 mL of water right after the sample was taken. Afterwards, the filters were stored at -20 °C before they were brought to the laboratory for further procedures. The DNA extraction was performed using the RapidWater® DNA Isolation Kit (MoBio Laboratories) according to the manufacturer's protocol. The total DNA concentration was calculated using a Qubit®2.0 fluorometer.

Polymerase chain reaction (PCR)

Due to the generally low concentrations of MOB DNA in the samples collected from the East and Cotton Lake complexes (section 3.4), sequencing was performed using only the samples from the North, Mirror and Sauna lake complexes. The detection of aerobic methanotrophs was performed by targeting the *pmoA* gene, which encodes a subunit of the methane monooxygenase particulate and is a functional marker for most of the representatives of this group. Amplification of the *pmoA* gene was performed using the A189f/mb661r primer pair (Holmes *et al.*, 1995, Costello & Lidstrom, 1999, McDonald *et al.*, 2008). The total PCR mixture, which had a volume of 25 µL, contained the following ingredients: HotStar Taq Plus DNA polymerase (Qiagen) (5 U μL^{-1}), 0.25 µL; forward and reverse primers (10 µM), 0.5 µL of each; dNTP mix (10 mM), 0.5 µL; BSA (0.2 µg μL^{-1}), 1 µL; CoralLoad PCR buffer (Qiagen), 2.5 µL; PCR water, 17.75 µL; and template, 2 µL. The total DNA concentration of the templates varied from 2 to 20 ng μL^{-1}. The PCR conditions were as follows: initial denaturation and polymerase activation at 95 °C for 5 min, 33 cycles of the denaturation temperature of 95 °C for 1 min and an annealing temperature of 57 °C for 1 min, elongation at 72 °C for 1 min, and a final elongation at 72 °C for 10 min. The PCR products were loaded onto a 1.5% agarose gel containing GelRed stain (Biotium). Amplicons of the expected size were excised from the gel and purified using the HiYield®PCR Clean-up/Gel Extraction Kit (SLG) according to the manufacturer's protocol.

A second round of PCR was performed using the purified amplicons as a template and primers containing the multiplex identifier (MID). Each sample was done in triplicate. The PCR conditions were the same as the first PCR but with 20 cycles. The PCR products were purified using the HiYield®PCR Clean-up/Gel Extraction Kit (SLG) according to the manufacturer's protocol for the purification of PCR products. Finally, 454 pyrosequencing was performed by Eurofins MWG Operon in Germany.

Pyrosequencing data analysis

MOTHUR software (Schloss *et al.*, 2009) was used for most of the sequence processing and the operational taxonomic unit (OTU) assignments. The sequences that did not pass the translation check using FrameBot (Wang *et al.*, 2013) were discarded from the whole dataset. Afterwards, the sequences with a quality score below 25 were considered to be poor quality and were removed from the dataset. In addition, the sequences that did not have the exact primer sequence, sequences that contained an ambiguous base, sequences with a homopolymer stretch longer than 8 bases, and sequences shorter than 350 bp were also removed from the datasets in MOTHUR. The remaining sequences were aligned against the pre-aligned *pmoA* nucleotide sequences, which were originally retrieved from the FunGene database (http://fungene.cme.msu.edu/). After preclustering, a chimera check was conducted in MOTHUR using the default settings. The valid sequences were binned into

different OTUs at a cutoff of 0.13, which corresponds to a 97% species cutoff value based on the 16S rRNA genes (Degelmann *et al*., 2010).

Construction of a phylogenetic tree

A phylogenetic tree was constructed to show the relationship of the *pmoA* gene sequences of aerobic methanotrophic bacteria from the investigated water bodies of Samoylov Island, Lena Delta, to the most closely branching *pmoA* gene sequences of the known methanotrophic isolates as references. The *pmoA* gene sequences shown were selected according to their affiliation with the 28 most abundant OTUs detected in this study.

A phylogenetic tree was built using the NJ (neighbor-joining) tree algorithm of the MEGA6 software with 500 bootstrap replications. The closest relatives were obtained by BLASTing the querying sequences against the NCBI database. The representative sequences for each OTU from our *pmoA* library were used to construct the tree.

Data deposition

The *pmoA* gene sequence data were deposited in the NCBI Sequence Read Archive (SRA) under the submission ID SRP062221.

Quantitative PCR (qPCR)

qPCR of the *pmoA* gene was performed using the same primer pair: A189f/mb661r. The total PCR mixture, which had a volume of 12.5 mL, contained the following ingredients: SYBR Green Master Mix (Bio-Rad), 6.25 µL; forward and reverse primers (10 µM), 0.5 µL of each; PCR-grade water, 0.25 µL; and template, 5 µL. The PCR conditions were as follows: the initial denaturation and polymerase activation at 95 °C for 10 min, 37 cycles of the denaturation temperature at 95 °C for 30 s and the annealing temperature at 62 °C for 30 s, elongation at 72 °C for 45 s, and the denaturation of the primer dimers at 80 °C for 3 s.

The cell numbers were estimated according to Kolb *et al*. (2003), assuming that each bacterial cell contains, on average, 2 copies of the *pmoA* gene. The detection limit, determined by the volume of the water samples collected and the DNA concentration, was 10^2 cells L^{-1}.

Statistical analysis

The methane concentrations and MOX rates for each sampling site are given as averages (arithmetic means) of the procedural triplicates and duplicates, respectively. The concentration of the MOB cells (MOB abundance) and the relative abundance of the OTUs are given as averages of the technical triplicates. When several sampling sites were combined as described, the average of all the replicate

measurements performed at the mentioned sampling sites is given with the standard deviation. The standard deviations of the measurements performed at the individual sampling sites are omitted in the main text but are given in Table 1 and Fig. 2. The standard deviation of the relative abundance of most of the OTUs did not exceed 3% of the total abundance of the OTUs at the sampling site; thus, these standard deviations are not shown. To investigate if the methane concentration, the MOX rate and the MOB abundance are correlated with each other and dependent on the temperature or the SPM, we performed simple linear regression analyses. When the linear correlation was not significant or the power of the performed test was less than desired due to the dispersion of the data, we performed a Spearman rank-order correlation analysis, which indicates whether the variables are monotonically related or not, i.e., if an increase in one variable causes an increase/decrease in the other variable.

Results

Most of the measurements (methane concentrations, MOX rates and MOB abundance) revealed that all the lake complexes could be divided into two different groups according to their location. The first group included the lake complexes on the upper terrace, while the second group included the North Lake complex, which was located in the floodplain area. Thus, these sampling sites will be described separately. All the measurements are summarized in Table 1 and are published on www. Pangea.de. The measurements of the methane concentrations, MOX rates and the MOB abundance are also presented in Figs. 2a, b and c, respectively.

Table 1. Freshwater characteristics (temperature, salinity, oxygen content and SPM), methane concentrations, MOX rates and MOB abundance in the studied lake complexes. In cases of replicate measurements (technical replicates), the average value with standard deviation is given.

Lake complex	Complex constituents	Coordinates (North latitude, East longitude)	Water surface area (lakes, m^2) and length (outlets, m^2)	Depth (m)	Methane concentration (nmol L^{-1})	MOX rate (nmol $L^{-1} h^{-1}$)	Abundance of MOB (cells L^{-1}) $*10^3$	Temperature (°C)	Salinity	Oxygen (mg L^{-1})	SPM (mg L^{-1})
North lake complex	Lake surf.	72.3867, 126.4826	9000	n.d.	22974 ± 1442	357 ± 24	41 ± 13	15	0.04	9.5	11.5
	Lake bot.		n.d.	n.d.	n.d.	n.d.	n.d.	n.d.	n.d.	n.d.	n.d.
	Outlet	72.3887, 126.4837	200	0.1	5409 ± 110	151 ± 31	18 ± 3	14	0.04	8.96	8.8
	River near the shore	72.3893, 126.4844	n.d.	0.5	6406 ± 626	109 ± 0.4	130 ± 30	14	0.04	9.77	43.72
	River middle surf.	72.3916, 126.4870	n.d.	n.d.	153 ± 1	1 ± 0.2	1.6 ± 0.4	17	0	9.68	27.85
	River middle bot.		n.d.	n.d.	n.d.	n.d.	n.d.	n.d.	n.d.	n.d.	n.d.
Mirror lake complex	Lake surf.	72.3701, 126.5185	11500	6	258 ± 7	8 ± 0.3	0.7 ± 0.2	11.3	0	9.82	7.02
	Lake bot.		n.d.	n.d.	240 ± 16	9 ± 1	n.d.	n.d.	0	9.92	29.55
	Outlet	72.3706, 126.5224	10	0.1	24343 ± 176	480 ± 19	24 ± 3	11.3	0.2	9.51	56.81
	River near the shore	72.3705, 126.5233	n.d.	0.5	140 ± 3	0.4 ± 0.03	11 ± 2	17	0	9.52	91.8
	River middle surf.	72.3700, 126.5265	n.d.	n.d.	146 ± 3	0.3 ± 0.01	6 ± 2	n.d.	0	9.54	22.05
	River middle bot.		n.d.	n.d.	146	0.4 ± 0.05	n.d.	n.d.	0	9.39	27.1
Sauna lake complex	Lake surf.	72.3684, 126.4832	27000	4	747	8.5 ± 0.7	1.8 ± 0.3	n.d.	0	10.02	9.42
	Lake bot.		n.d.	n.d.	n.d.	n.d.	n.d.	n.d.	0	n.d.	n.d.
	Outlet	72.3688, 126.4736	100	0.1	912 ± 8	13 ± 0.4	4.8 ± 0.1	n.d.	0	9.02	229.2
	River near the shore	72.3681, 126.4722	n.d.	0.5	150 ± 0.03	0.7 ± 0.03	2.8 ± 1	n.d.	0	8.64	12.27
	River middle surf.	72.3668, 126.4697	n.d.	n.d.	197	1 ± 0.1	1.2 ± 1.3	n.d.	0	8.82	8.37
	River middle bot.		n.d.	n.d.	171 ± 10	0.9 ± 0.01	n.d.	n.d.	n.d.	8.44	26.65
East lake complex	Lake surf.	72.3752, 126.5197	22000	n.d.	205 ± 6	0.2 ± 0.02	n.d.	15.7	0	9.16	3.55
	Lake bot.		n.d.	n.d.	n.d.	n.d.	n.d.	n.d.	0	n.d.	n.d.
	Outlet	72.3778, 126.5178	100	0.1	166 ± 0.5	0.6 ± 0.03	n.d.	n.d.	0	9.4	2.52
	River near the shore	72.3790, 126.5193	n.d.	0.5	193 ± 15	1.4 ± 0.2	8.5 ± 2.2	n.d.	0	9.61	32.75
	River middle surf.	72.3798, 126.5232	n.d.	n.d.	146 ± 2	0.7 ± 0.1	8	17	0	9.07	29.97
	River middle bot.		n.d.	n.d.	n.d.	n.d.	n.d.	n.d.	0	n.d.	n.d.
Cotton lake complex	Lake surf.	72.3839, 126.5010	8000	6	249 ± 7	0.3 ± 0.03	n.d.	13.4	0	8.3	1.1
	Lake bot.		n.d.	n.d.	308 ± 16	9.1 ± 1.9	n.d.	n.d.	0	8.3	n.d.
	Outlet	72.3835, 126.5045	100	0.1	12490 ± 293	151 ± 10	1 ± 0.1	13.4	0	8.13	9.95
	River near the shore	72.3837, 126.5061	n.d.	0.5	256 ± 2	1.1 ± 0.1	n.d.	16.5	0	8.11	29.55
	River middle surf.	72.3843, 126.5087	n.d.	n.d.	216 ± 7	1.2 ± 0.1	6 ± 4.7	16.5	0	7.96	25.05
	River middle bot.		n.d.	n.d.	216 ± 3	1.4 ± 0.2	n.d.	n.d.	0	7.95	50.5

n.d. – not determined

Freshwater characteristics: temperature, salinity, oxygen content and SPM

The water temperature of all the sampling sites varied from 11 to 17 °C and was 2-4 °C higher in the river than in the lakes and the outlets. The salinity varied from 0 to 0.2. The oxygen content varied relatively little, at a range from 8 to 10 mg L^{-1}. No difference between the surface and bottom water was detected for the oxygen content. The SPM varied from 1 to 230 mg L^{-1}. In the river sites, the SPM was generally higher (32 ± 20 mg L^{-1}) than in the lakes (10 ± 10 mg L^{-1}). The SPM in the outlets was the highest on average (60 ± 97 mg L^{-1}); however, it varied over a wide range of 3 to 230 mg L^{-1}. We did not find a correlation between any of these parameters and the methane concentration, the MOX rate or the MOB abundance.

Methane concentration in the water column

The calculated equilibrium methane concentration in the water column with respect to the methane concentration in the atmosphere was approximately 4 nmol L^{-1}. The methane concentrations of all the sampling sites varied over two orders of magnitude, from 140 nmol L^{-1} to 24,000 nmol L^{-1}. Thus, all the water bodies that were investigated were supersaturated with methane. The saturation rates varied from approximately 3,500 to 600,000%. The surface and bottom methane concentrations were comparable (the ratio between the average values did not exceed 1.3) for both the lakes (Mirror Lake and Cotton Lake) and the sites in the middle of the river (Mirror, Cotton and Sauna). Because our data set from the surface was more consistent, we will focus on the surface data in the following discussion.

The distribution of the methane concentrations along the lake complex of the upper terrace generally followed a specific trend: from the lake to the outlet, the concentration rose (up to 100 times – Mirror Lake) or stayed the same but dropped upon reaching the river sites. The methane concentrations of these lakes varied over a relatively narrow range, with an average of 370 ± 260 nmol L^{-1} and were slightly higher than those of the river sites, which had an average of 180 ± 40 nmol L^{-1}. The outlets varied over a wide range, from 210 nmol L^{-1} (East Lake complex) to 24,000 nmol L^{-1} (Mirror Lake complex). In comparison with the upper terrace lake complexes, the North Lake complex had substantially higher methane concentrations in the lake and in the river near the shore (23,000 and 6,400 nmol L^{-1}, respectively), while in the outlet and the middle of the river (5,400 and 150 nmol L^{-1}, respectively), the methane concentrations were comparable.

Methane oxidation (MOX) rates in the water column

The MOX rates of the surface and the bottom of Mirror Lake and of the three river sites were comparable (the ratio between the surface and bottom average values did not exceed 1.4), except in Cotton Lake, which had MOX rates 30 times higher at the bottom than at the surface. The MOX rates

were correlated with the methane concentrations (Spearman Rank Order Correlation, r_s = 0.84, n = 20, Fig. s2, supplementary materials). However, there were some deviations. Despite comparable methane concentrations, the MOX rates of the Mirror and Sauna Lakes (8 and 8.5 nmol L^{-1} h^{-1}, respectively) were higher than those of the East and Cotton Lakes (0.2 and 0.3 nmol L^{-1} h^{-1}, respectively) and higher than those of the corresponding river sites. The MOX rates were generally the highest in the outlets, where they varied over a wide range, from 0.6 nmol L^{-1} h^{-1} (East Lake complex) to 480 nmol L^{-1} h^{-1} (Mirror Lake complex). The MOX rates of the river sites of the upper terrace were comparable (average of 0.8 ± 0.4 nmol L^{-1} h^{-1}). In comparison with the upper terrace lake complexes, the North Lake complex had substantially higher MOX rates in the lake and in the river near the shore (360 and 8 nmol L^{-1} h^{-1}, respectively), while in the outlet and the middle of the river (150 and 1 nmol L^{-1} h^{-1}, respectively), the MOX rates were comparable with those of the other lake complexes.

Abundance of methane oxidizing bacteria (MOB)

The total amount of DNA calculated related to the volume of the filtered water varied from 1 to 14 ng mL^{-1}. The highest concentrations (8–14 ng mL^{-1}) were detected at the North Lake complex (except for the river in the middle site) and at the Mirror and Sauna streams. The concentration of the total DNA from most of the other sites did not exceed 4 ng mL^{-1}.

The MOB abundance was positively correlated with the methane concentrations, but only at the lake-outlet complexes (Spearman Rank Order Correlation, r_s = 0.75, n = 7, Fig. s3, supplementary materials). The deviations included the lakes of the upper terrace. Despite the comparable methane concentrations, the East and Cotton Lakes had a lower MOB abundance (< 10^2 cells L^{-1}) than the Mirror and Sauna Lakes (0.7 × 10^3 and 1.8 × 10^3 cells L^{-1}, respectively). The river sites of the upper terrace had a slightly higher MOB abundance (average of 6.2 (± 3.4) × 10^3 cells L^{-1}) than the Mirror and Sauna Lakes. The cell numbers were generally the highest in the outlets, varying from 4.8 × 10^3 cells L^{-1} (Sauna Lake complex) to 24.0 × 10^3 cells L^{-1} (Mirror Lake complex). The North Lake complex had substantially higher MOB abundance in the lake and in the river near the shore (41 × 10^3 and 130 × 10^3 cells L^{-1}, respectively), while in the outlet and the middle of the river, the MOB abundance was comparable to the rest of the complexes (18 × 10^3 and 1.6 × 10^3 cells L^{-1}, respectively).

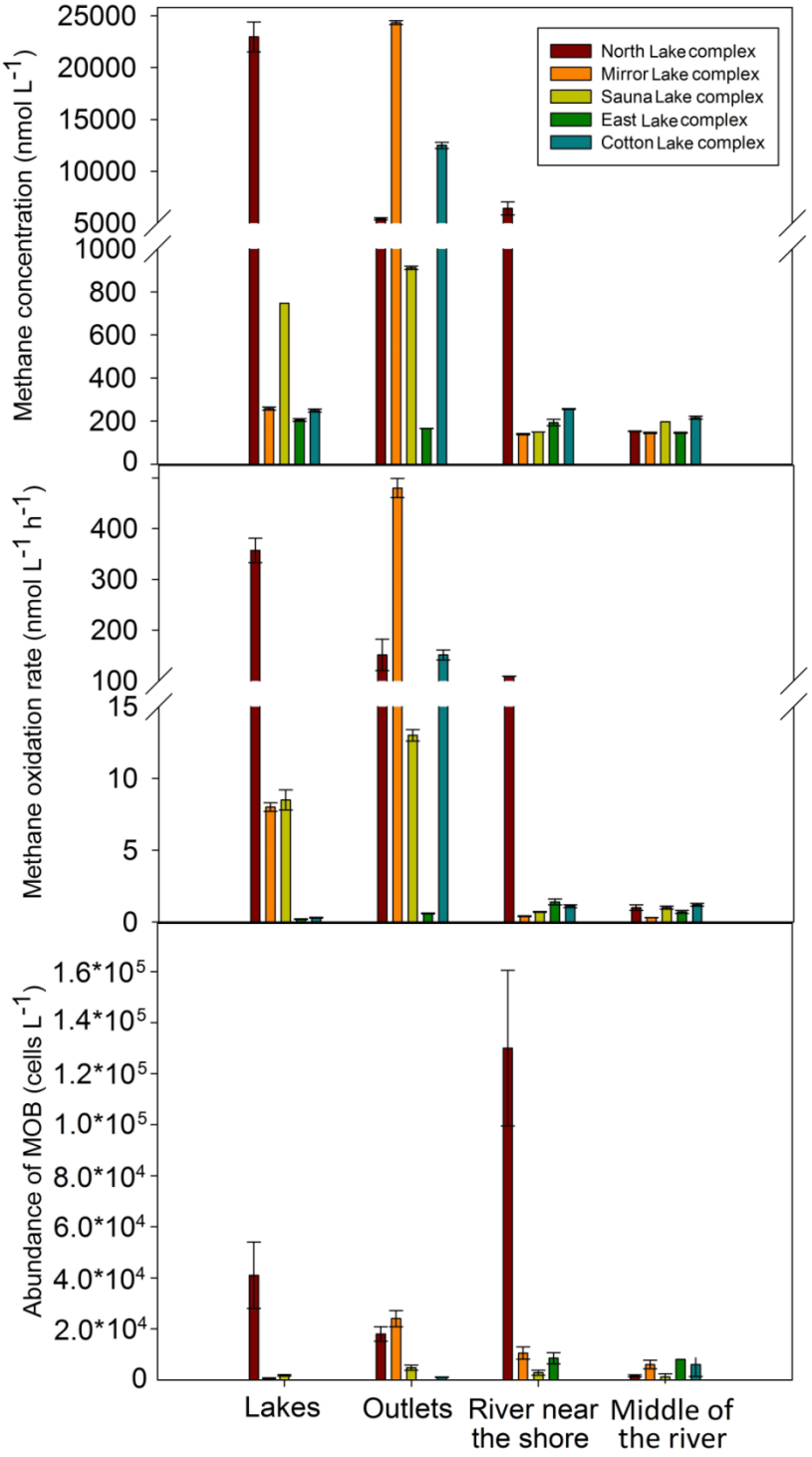

Fig. 2. Methane concentrations, methane oxidation rate and the abundance of methanotrophic bacteria in the surface water of the different lake complexes. Data represent the mean of technical replicates (± standard deviation, SD). Measurements of methane concentrations and abundance of methanotrophic bacteria are performed in triplicate, methane oxidation rates are performed in duplicate.

Diversity of MOB

The number of sequences analyzed per sampling site was approximately 5,000 on average (Fig. s1, supplementary materials). The total number of the OTUs with a cutoff of 0.13 (Degelmann *et al*., 2010) was 391. A total of 28 OTUs, each of which represented > 3% of the total abundance of at least one sampling site, were identified. The other OTUs represented minor groups (< 3% each) and together constituted approximately 13% of the total MOB abundance. The most relatively abundant OTUs (> 3%) were clustered into five groups: Types Ia, -b, and -c and Types IIa and -b. (Dumont *et al*., 2014). Their relation to the previously isolated MOB strains is demonstrated using the neighbor joining tree (Fig. 3). Type Ia was represented by a single OTU (OTU 14) related to *Methylobacter*. Type Ib was represented by 12 OTUs. According to the classification proposed by Dumont *et al*. (2014), we subclustered these OTUs into the following groups (typical habitats or origin are in brackets): FWs, LWs (freshwater lakes), RPCs, RPC-1, JRC-4 (rice field soil), and OSC-related (organic soil). Type Ic was represented by a single OTU (OTU 65), which belonged to the USC-g (upland soils) cluster (Dumont *et al*., 2014). Type IIa was represented by 13 OTUs from the genus *Methylocystis*. Type IIb was represented by a single OTU (OTU 31) that belongs to the genus *Methylocapsa*.

Fig. 3. A neighbor-joining tree of *pmoA* gene sequences, showing the relationship between the most abundant OTUs from this study (red color font) and strains from previous studies. Blue or black font indicates the strains isolated from the aquatic and terrestrial environments, respectively. A neighbor-joining tree was built with Mega6 software, NJ (neighbor- joining) tree algorithm, with bootstrap of 500 times. The close relatives were obtained by blasting the querying sequences against the NCBI database.

The relative abundance of the main clusters is summarized in Table s1, and together with the most relatively abundant OTUs is shown in Fig. 4. In all three investigated lakes, Type Ib was prevalent, constituting 60–70% of the total MOB abundance. At the North Lake complex, Type Ib was also

dominant in the outlet (77%) and in the river near the shore (76%). At the outlets and river sites of the East and Sauna Lake complexes, Type IIa MOB (46–68% of the total MOB abundance) was dominant. The remaining clusters were minor (≤ 5%). The Type Ia (*Methylobacter)* cluster was the only exception, constituting 6 and 14% of the total MOB abundance of the Mirror Lake and its outlet, respectively.

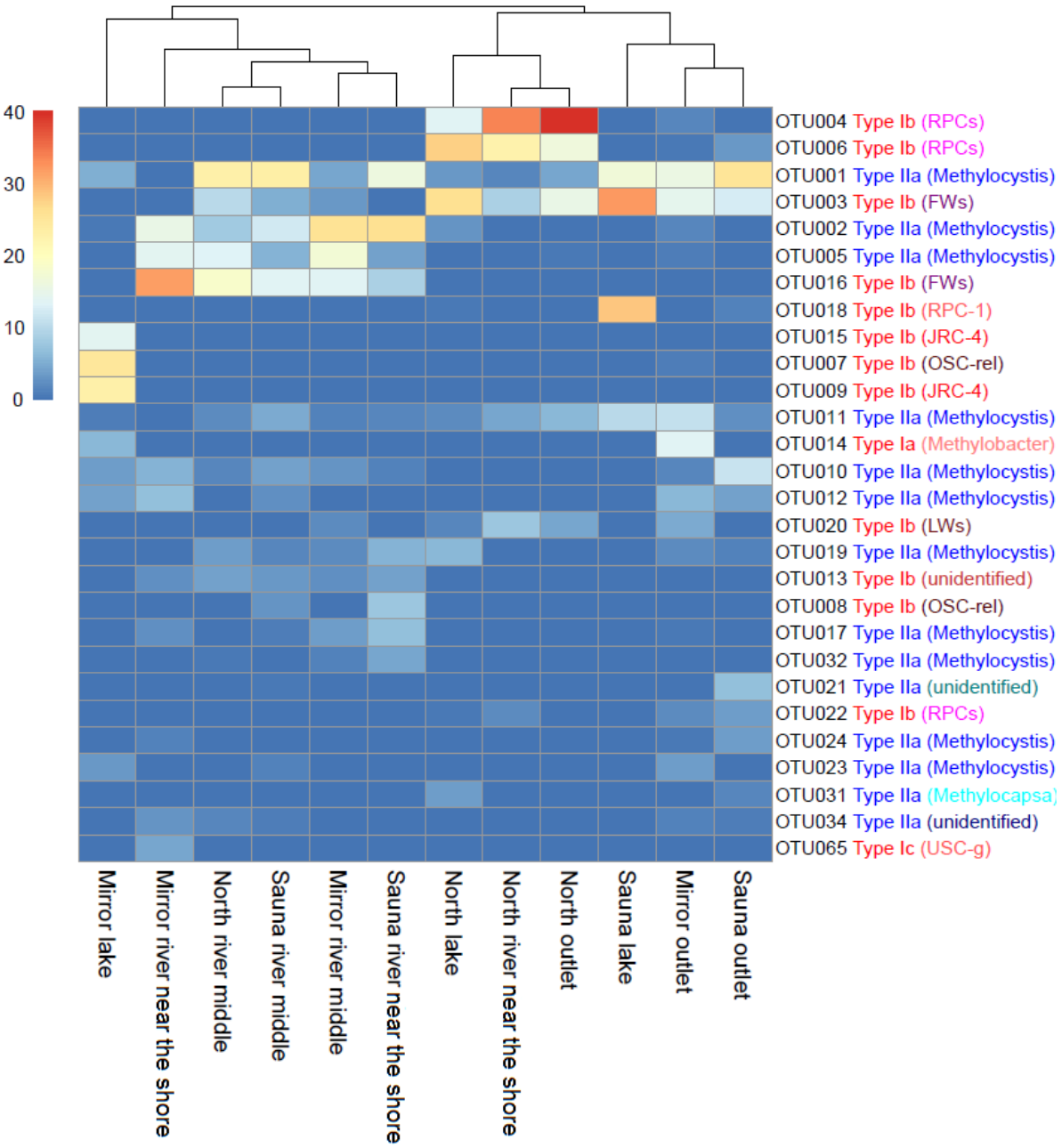

Fig. 4. Heat map showing the relative abundance (%) of the most prevalent OTUs with the dendrogram demonstrating the relationship between the MOB communities from the different sampling sites.

Cluster analysis based on the abundance of the dominant OTUs (Fig. 4) indicated that the sampling sites could be divided into river sites and lake-outlet complexes. The river sites (except for the North river near the shore site) were very similar to each other compared to the lake-outlet complexes, with the *Methylocystis* cluster (OTUs 1, 2, 5) and the FWs cluster (OTUs 3, 16) being dominant. The neighbor-joining tree (Fig. 3) also showed that the OTUs that were abundant in the river sites were related to previously identified MOB strains typical for water rather than for soil environments. The other group contained the lakes and outlets. The North Lake complex (the lake, the outlet and the river near the shore) was characterized by the high abundance of the RPCs cluster (42-59%), while at the rest of the sampling sites, the relative abundance of this cluster did not exceed 8%. Sauna Lake differed from the rest of the lakes in its high abundance of the RPC-1 cluster (29%). Mirror Lake differed from the other sampling sites because it was the only habitat where the JRC-4 and OSC-related clusters were relatively abundant (38 and 25%, respectively). On the contrary, the abundance of the FW clusters in Mirror Lake was minor in comparison with the other lake-outlet complexes. The outlets of the Mirror and Sauna Lakes were dominated by the *Methylocystis* cluster, but the OTUs within the cluster differed from those dominant in the river sites.

Discussion

The freshwater bodies in the Arctic permafrost environment are an important ecosystem involved in the global methane cycle. Our results show that the water bodies, which included lakes, their outlets and the Lena River, represent a heterogeneous system with large variations in methane distribution, MOX rates, and methanotrophic bacterial community structure and abundance.

All the water bodies investigated were supersaturated with methane in relation to the atmosphere; thus, they act as a methane source for the atmosphere (Middelburg *et al*., 2002, Bange, 2006). The methane distribution in all the lakes and outlets was highly variable, which is remarkable, given the small size of Samoylov Island (4.34 km^2). The methane concentrations in the lakes of the upper terrace varied over a relatively narrow range (365 ± 256 nmol L^{-1}) and were substantially lower than those of the North Lake (22,974 ± 1,442 nmol L^{-1}). All these values are in the range of previously reported methane concentrations of high-latitude lakes and ponds (Table 2). The uniqueness of North Lake is likely related to its location in the floodplain area of the island. All of the lakes investigated, except for Eastern Lake, are flooded in the spring at a different periodicity. This flooding, however, has a local, sporadic impact, while the floodplain area, which is flooded annually, forms a unique ecosystem also in regard to the vegetation (Boike *et al*., 2012). The production of methane, which takes place mainly in lake sediments, is strongly dependent upon carbon loading (Zimov *et al*., 1997). We expect that the substantial supply of organic matter brought by the river leads to higher methane concentrations. Flooding can also result in the input and transport of

nutrients and other substances. Indeed, the concentrations of many ions are higher in the North Lake (Abnizova *et al*., 2012, Chetverova *et al*., 2013). Additionally, high proportions of silt and clay material in the floodplain soil support the availability and uptake of substrates (Liebner & Wagner, 2007), which may result not only in enhanced methane oxidation but also in methane production.

Table 2. Methane concentrations and MOX rates in the water columns of high-latitude freshwater lakes and rivers.

Sampling area	Methane concentration (nmol L^{-1})	MOX rate (nmol L^{-1} h^{-1})	Reference
Lakes and ponds			
North Slope of Alaska (9 lakes)	80–16700, 165000*	n.d.	Kling *et al*.,1992
Canadian High Arctic (4 ponds)	100 –3400	n.d.	Negandhi *et al*., 2013
Western Siberia (3 lakes)	66–7800	n.d.	Repo *et al*., 2007
North Slope of Alaska (2 lakes)	780–1520	2–340	Lofton *et al*., 2014
North slope of Alaska and Alaska's interior (2 lakes)	n.d.	0–60000	He *et al*., 2012a
Alaska (30 lakes)	<600–940000	0–1400	Martinez-Cruz *et al*., 2015
Northeast Siberia (5 lakes)	200–23000	0.2–360	This study
Rivers			
North Siberia, Ob estuary	7–41	n.d.	Shakhova *et al*., 2007
North Siberia, Yenisei estuary	7–131	n.d.	Shakhova *et al*., 2007
Northeast Siberia, Lena estuary	62–651	n.d.	Shakhova *et al*., 2007
Northeast Siberia, Lena estuary	30–85	n.d.	Bussmann, 2013
Northeast Siberia, Lena estuary	150–200	0.3–1	This study

n.d. – not determined

*the only measurement, which substantially stood out of the rest

In most of the outlets of the upper terrace, the methane concentrations were higher (up to 100 times) than in the corresponding lakes. Shallow streams can accumulate organic carbon in sediments, which results in enhanced methane production (Sanders *et al*., 2007). Additionally, a higher saturation of methane diffusing from the outlet sediments is explained by the small volume of the outlets. Our findings corroborate the hypothesis that streams might be important sources of methane (Crawford *et al*., 2014).

Upon reaching the river, the methane-rich water from the outlet is diluted with the methane-poor river water. On the upper terrace, the methane concentrations of the river near the shore did not

substantially differ from those of the middle of the river. However, at the North Lake complex, the methane concentrations of the river near the shore remained high. This indicates that, at least in some cases, the input of methane from the streams into the river can be significant and can alter the concentrations of methane, at least in the near-shore area.

The MOX rates at all the sampling sites varied from 0.2 to 480 nmol L^{-1} h^{-1}, which is in the range previously reported in studies of high-latitude lakes and rivers (Table 2). The turnover time of methane varied from 1 to 43 days, at an average of 10 ± 11 days, indicating that methane oxidation can be an important methane sink in lakes, streams and rivers. The MOX rates generally coincided with the methane concentrations, especially when we compared the sites with low and high methane concentrations (Fig. s2). A positive correlation between the MOX rates and the methane concentrations was shown in many other studies (Gentz *et al*., 2013, Jakobs *et al*., 2013, Osudar *et al*., 2015). The abundance of MOB, in turn, was generally positively correlated to the methane concentration (Fig. s3). However, at our study sites, neither the methane concentration nor the MOB abundance could fully explain the observed differences in the MOX rates. According to Mau and colleagues (2013), the size of the MOB community is an important variable for methane flux, but we showed that the also community structure controls the effectiveness of methane oxidation. For instance, the Mirror and Sauna lakes had methane concentrations comparable with the river sites but had a lower abundance of MOB and higher MOX rates. Therefore, we assume that MOB in these lakes are more efficient in oxidizing methane. Indeed, the analysis of the MOB community structure revealed that the lakes, outlet streams and river showed individual patterns in terms of their MOB community structure. Though we did not find any correlation between the MOX rates and the relative abundance of any MOB cluster, the sites with the highest MOX rates were characterized by a higher diversity of the MOB clusters (Table s1). Thus, for example, the river sites were characterized by a rather homogeneous MOB community, with the dominance of three OTUs related to the genus *Methylocystis* and two OTUs related to the FWs cluster. The MOB composition of the lake-outlet complexes was more heterogeneous. Apart from the MOB clusters common for all the sampling sites, each lake and outlet had unique MOB clusters. Additionally, the dominant OTUs of the river sites were related to strains typical of water rather than of soil environments, while in the lakes and outlets, the trend was opposite. Therefore, it is reasonable to assume that the lakes and outlets are more affected by the input of MOB from the soil environment, which occurs due to erosion and flooding. In the outlets, the inoculation of MOB from the sediments additionally occurs due to high water velocity and sediment resuspension. The highest diversity of MOB in this study was observed in the outlets, which corroborates the observations of Crump *et al*. (2012). At the same time, presumably terrestrial MOB were not restricted to the Type I or Type II clusters. The lakes were dominated by Type I MOB, while the outlets and river sites were dominated by Type II MOB.

The high abundance of Type II MOB in all the water bodies, however, is remarkable, regardless of its origin. Most of the previous research showed that Type I MOB generally dominate over Type II, both in the freshwaters of the temperate zone (including sediments (Costello *et al*., 2002, Rahalkar *et al*., 2009) and the water column (Eller *et al*., 2005, Sundh *et al*., 2005, Tsutsumi *et al*., 2011)), as well as in the Arctic wetlands (Wartiainen *et al*., 2003, Graef *et al*., 2011). Methane and oxygen concentrations as the controlling factors (Hanson & Hanson, 1996) could not explain the abundance of Type II MOB in our study. Ho *et al*. (2013) suggested that according to the universal adaptive strategy theory, Type I MOB should be classified as competitor-ruderal organisms. This could explain the predominance of Type I MOB in the Arctic wetlands, which are exposed to freeze-thaw cycles. Consequently, the presence of the Type II MOB cluster in our study can be explained by the rather stable environmental conditions with lower disturbance. The thermal regimes of the permafrost-affected soil and the lakes and rivers are different. The lakes of this study, which were 4 to 6 meters deep, do not freeze to the bottom in the winter and are most likely underlain with layers of year-round unfrozen ground called taliks (Boike *et al*., 2015). The same is true for the Lena River (Costard & Gautier, 2007). An alternative hypothesis is that Type II methanotrophs become relatively abundant in the summer, due to the warming of the surface water layer. All the samples were collected from the surface during the summer when the water temperature varied between 11 and 15 °C in the lakes and was approximately 17 °C in the river. Type II MOB were shown to successfully compete with Type I MOB in low-latitude soils starting at 15 °C (Börjesson *et al*., 2004).

Conclusion

This study contributes to the understanding of methane fluxes in the Arctic water bodies of the Lena Delta area, including the lakes, the outlets and the river. Our results suggest that the MOX rates are determined by the methane distribution and the abundance and diversity of MOB. The lake-outlet complexes, in contrast to the Lena River, represent a more heterogeneous ecosystem, which is reflected in the high variation of the MOX rates and the controlling environmental factors. The lake complexes thus appear as more individual systems that have a pronounced interaction with the surrounding soil environment. The floodplain area, for example, facilitates the increased availability of substrates and represents a potential “hot spot” for methane emissions. The Lena River sites represent a connected and, consequently, more uniform environment with a weaker terrestrial imprint. With the expected climate change and consequent thawing of the permafrost, more terrestrial MOB will be transferred into the aquatic environments, most likely leading to a more pronounced terrestrial methanotrophic fingerprint.

Funding

This work was supported by the European cooperation for long-term monitoring (PERGAMON) [COST STSM Reference Number: ECOST-STSM-ES0902-290811-008783].

Acknowledgements

We are deeply grateful to Prof. Nikolay Pimenov and his group from the laboratory of relict microbial communities at the Winogradsky Institute of Microbiology, Russian Academy of Science (Moscow, Russia) who provided a working space and assisted in the processing of the collected samples. We would also like to thank AWI Logistics, especially W. Schneider, for the invaluable help and support during the sampling campaign.

Supplementary material

Tables

Table s1. Relative abundance (%) of the dominant clusters.

Sampling site	Type Ia	Type Ib							Type Ic	Type IIa	Type IIb	others
	Methylobacter	Unidentified (OTU13)	RPCs	FWs	RPC-1	JRC-4	OSC-rel	LWs	USC-g	Methylocystis	Methylocapsa	
North lake	0.00	0.00	41.92	26.20	0.63	0.00	0.05	1.75	0.00	15.04	3.93	10.48
North outlet	0.00	0.00	56.95	15.38	0.00	0.15	0.00	4.78	0.00	11.41	0.00	11.33
North river near the shore	0.03	0.00	58.83	9.24	0.06	0.00	0.00	7.87	0.00	7.11	0.00	16.86
North river middle	0.00	4.31	0.00	28.88	0.00	0.00	0.00	0.00	0.00	54.74	0.00	12.07
Mirror lake	6.28	0.01	0.01	0.00	0.00	37.55	25.14	0.14	0.00	18.15	0.00	12.73
Mirror outlet	13.93	0.02	4.77	14.56	0.00	0.00	1.29	4.97	0.00	46.23	0.00	14.23
Mirror river near the shore	0.00	2.60	0.00	31.90	0.00	0.06	0.06	0.00	4.67	49.85	0.00	10.87
Mirror river middle	0.00	2.43	0.09	17.01	0.00	0.26	0.35	2.08	0.00	60.76	0.00	17.01
Sauna lake	0.00	0.00	0.03	32.34	28.76	0.00	0.03	0.00	0.00	27.64	0.00	11.21
Sauna outlet	0.23	0.01	7.26	12.62	1.41	0.01	0.01	0.00	0.00	57.31	1.86	19.29
Sauna river near the shore	0.00	4.07	0.40	9.15	0.05	0.00	8.16	0.10	0.00	67.74	0.00	10.34
Sauna river middle	0.00	3.46	0.00	19.08	0.00	0.00	2.94	0.00	0.00	59.31	0.00	15.21

Figures

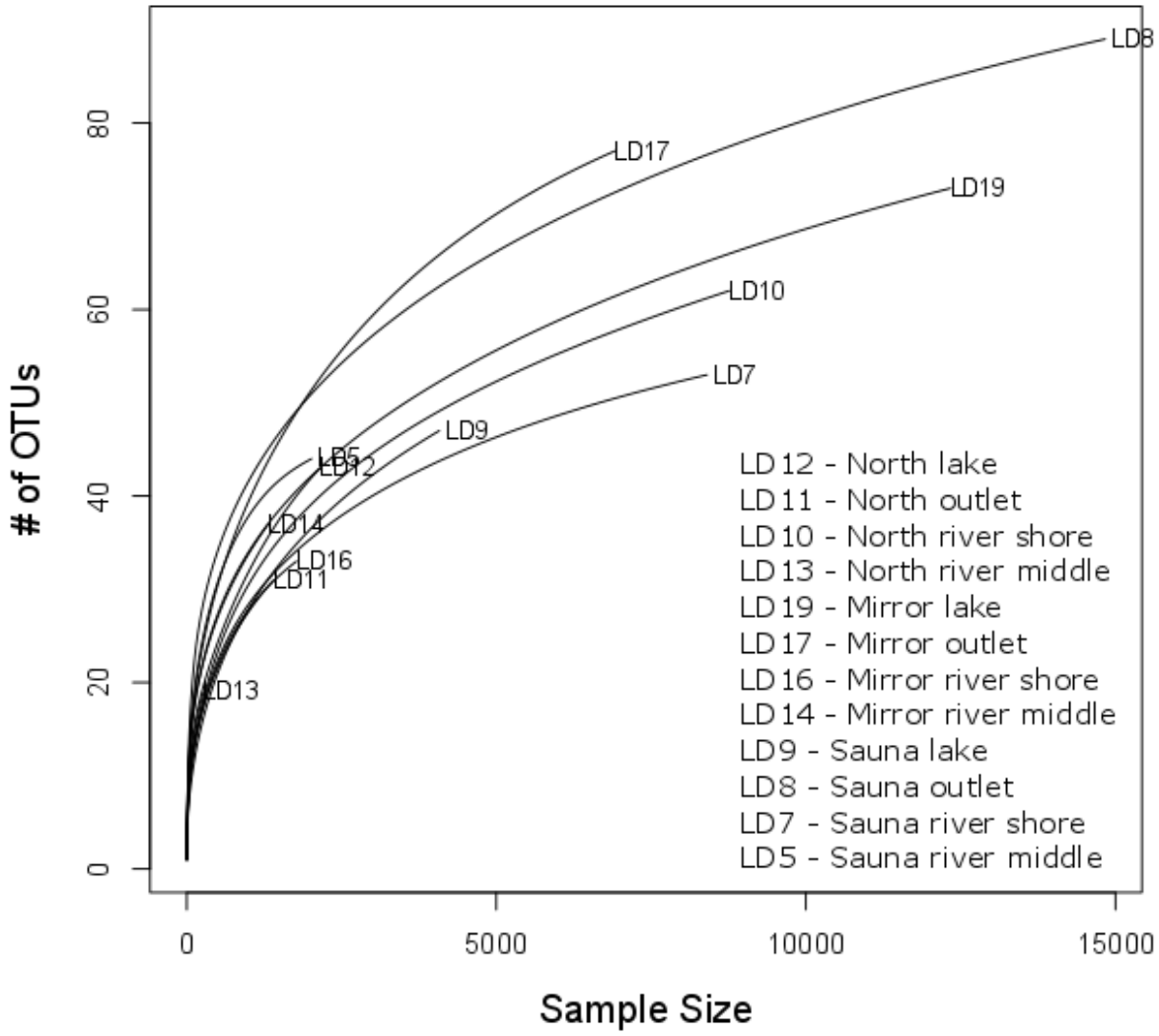

Fig. s1. Rarefaction analysis of *pmoA* gene sequences.

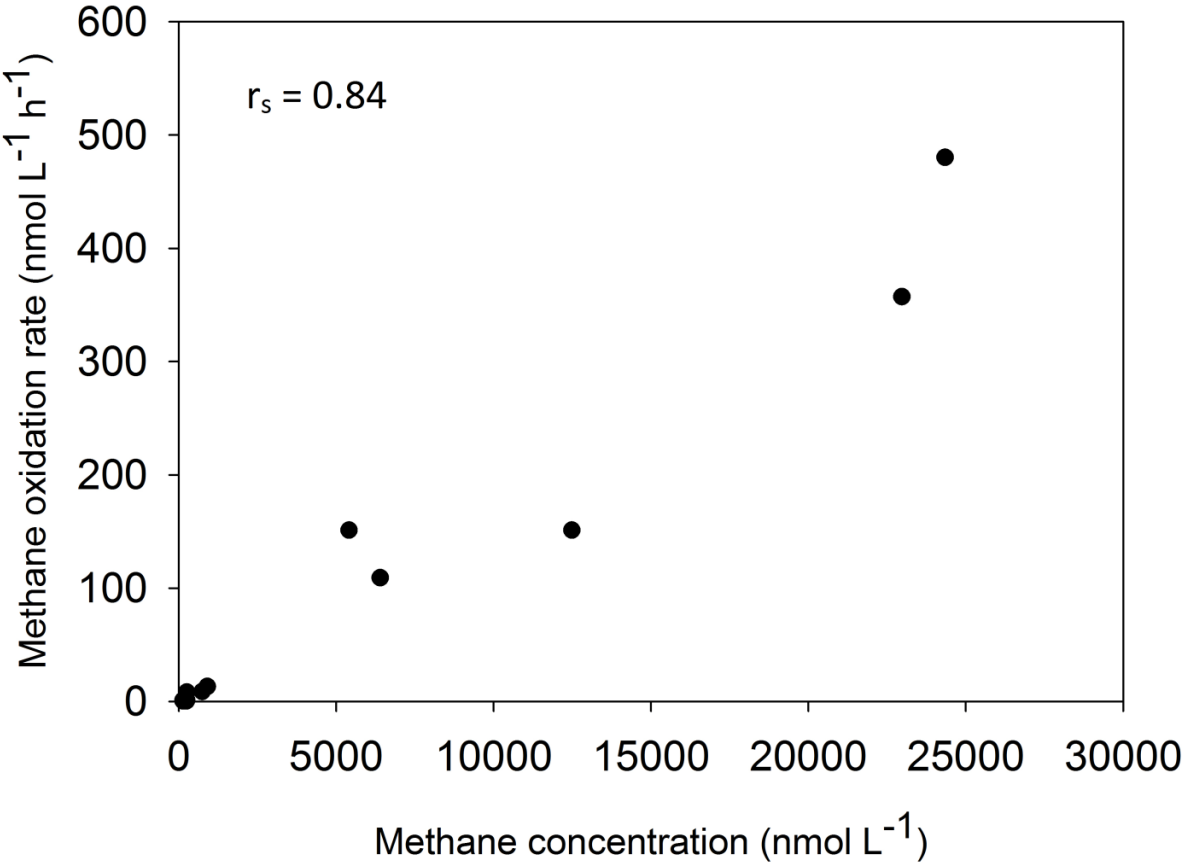

Fig. s2. Methane oxidation (MOX) rate as a function of methane concentration. The data shown here are from the surface water. r_s – Spearman Rank Order Correlation coefficient

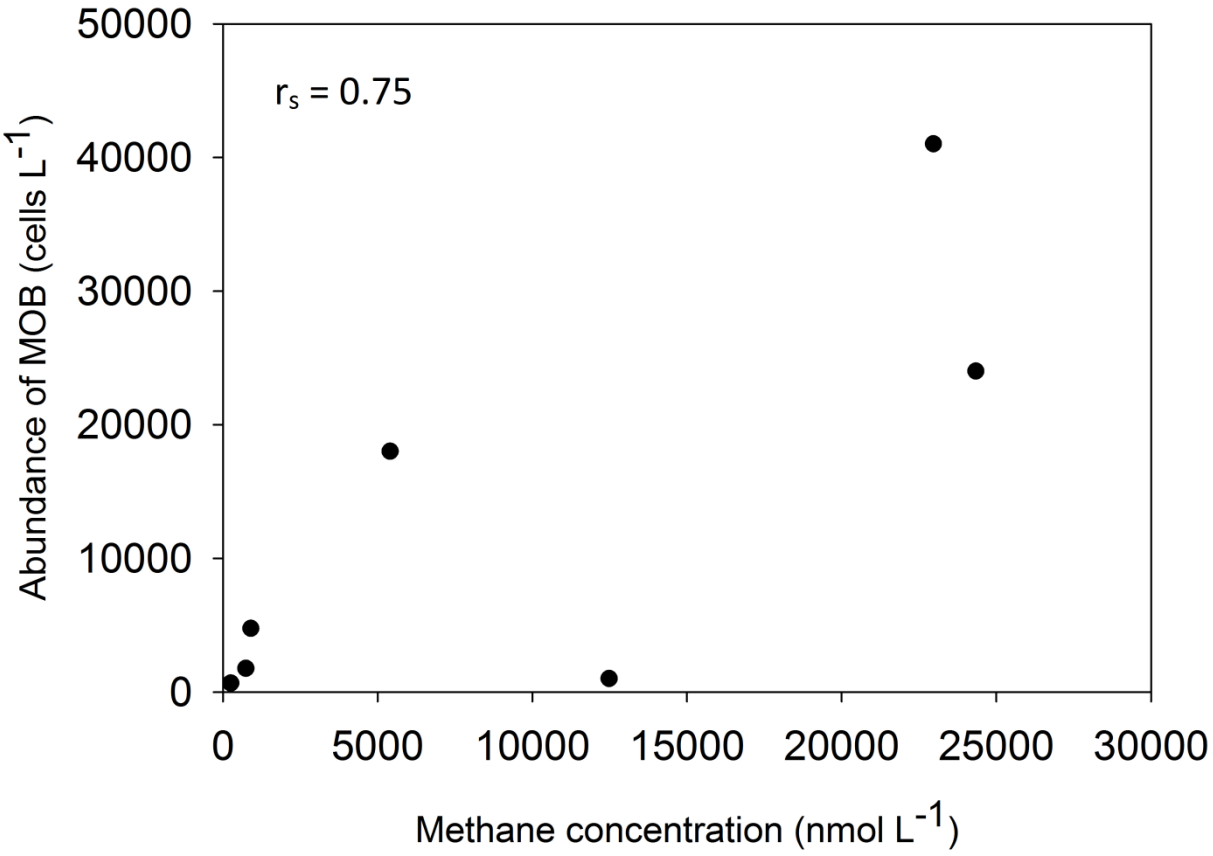

Fig. s3. Abundance of methane-oxidizing bacteria (MOB) as a function of methane concentration. The data shown here are from surface water., r_s – Spearman Rank Order Correlation coefficient

Manuscript II

Environmental factors affecting methane distribution and bacterial methane oxidation in the German Bight (North Sea)

Roman Osudar, Anna Matoušů, Mashal Alawi, Dirk Wagner and Ingeborg Bussmann

Abstract

River estuaries are responsible for high rates of methane emissions to the atmosphere. The complexity and diversity of estuaries require detailed investigation of methane sources and sinks, as well as of their spatial and seasonal variations. The Elbe river estuary and the adjacent North Sea were chosen as the study site for this survey, which was conducted from October 2010 to June 2012. Using gas chromatography and radiotracer techniques, we measured methane concentrations and methane oxidation (MOX) rates along a 60 km long transect from Cuxhaven to Helgoland. Methane distribution was influenced by input from the methane-rich mouth of the Elbe and gradual dilution by methane-depleted sea water. Methane concentrations near the coast were on average 30 ± 13 nmol L^{-1}, while in the open sea, they were 14 ± 6 nmol L^{-1}. Interestingly, the highest methane concentrations were repeatedly detected near Cuxhaven, not in the Elbe River freshwater end-member as previously reported. Though, we did not find clear seasonality we observed temporal methane variations, which depended on temperature and presumably on water discharge from the Elbe River. The highest MOX rates generally coincided with the highest methane concentrations, and varied from 2.6 ± 2.7 near the coast to 0.417 ± 0.529 nmol L^{-1} d^{-1} in the open sea. Turnover times varied from 3 to >1000 days. MOX rates were strongly affected by methane concentration, temperature and salinity. We ruled out the supposition that MOX is not an important methane sink in most of the Elbe estuary and adjacent German Bight.

1. Introduction

Methane is the most abundant organic gas in the atmosphere. Being a potent greenhouse gas, it plays an important role in warming the Earth's atmosphere (Kirschke et al., 2013). Its contribution to global warming is attenuated by comparatively low concentrations and short lifetime in the atmosphere. Methane has the second-largest radiative forcing of the long-lived greenhouse gases, after CO_2 (Ramaswamy et al., 2001). The atmospheric concentration of methane has increased to a level unprecedented in at least the last 800,000 years (Stocker et al., 2013). Its average concentration nowadays is around 1.8 ppm (Kirschke et al., 2013). Changes in methane concentration, which are defined by the balance between sources and sinks of methane, have led to investigations on the microbial-driven methane cycle in various environments.

About 60% of the methane released to the atmosphere is from anthropogenic sources such as agriculture, waste treatment, biomass burning, and fossil fuels. The remaining 40% originates from natural sources, mainly wetlands (Kirschke et al., 2013). Among these sources, the world's oceans contribute <0.1–10% of the methane emissions (Scranton and McShane, 1991, Bates et al., 1996, Middelburg et al., 2002 and Conrad, 2009). Digestive tracts of zooplankton (Bianchi et al., 1992 and De Angelis and Lee, 1994), and organic particulate matter (Karl and Tilbrook, 1994) are the main methane sources in the open ocean. However, about 75% of global oceanic methane emission occurs in shelf areas and estuaries (Bange et al., 1994 and Bange, 2006). The main sources of methane in these areas are sediments, adjacent rivers, tidal flats, and marshes (Bange et al., 1994, Bange, 2006, Abril et al., 2007, Grunwald et al., 2009 and Bussmann, 2013). Sedimentary release of methane which follows methanogenesis (Koch et al., 2009 and Bussmann, 2013) and abiotic methane production (Hovland et al., 1993) is supplemented with lateral methane transport. Water discharge from rivers, as well as tidal influence, are factors that greatly control methane distribution (Rehder et al., 1998 and Grunwald et al., 2009). Thus, these areas represent diverse and complex hydro-dynamic systems. Besides, estuarine systems are subject to significant seasonal changes (Sansone et al., 1998, Middelburg et al., 2002 and Abril and Borges, 2005), a factor which is not considered in many studies. Bacterial methane oxidation, along with degasing and dilution of methane-rich water, are also important factors controlling methane distribution in the water column (Grunwald et al., 2009). Up to 80–90% of the available methane can be metabolized and thereby disposed of by bacterial methane oxidation in the freshwater (Reeburgh et al., 1993 and Guérin and Abril, 2007). In the marine environment, however, methane oxidation (MOX) rates are in general lower (Valentine et al., 2001 and Mau et al., 2013). Though, knowledge on bacterial methane oxidation in the water column rapidly improves, MOX rates measurements in estuaries are still scarce. Additionally, an improved knowledge of the environmental factors controlling bacterial methane oxidation and the physiological properties of these organisms is crucial and this topic needs further investigation (Valentine, 2011 and Mau et al., 2013).

The objectives of this study were to describe the spatial and seasonal variations of methane in the German Bight, near the Elbe estuary. The methane concentration, as well as several hydro-chemical parameters from the bottom and surface waters, were measured over a period of two years along a 60 km long transect in the German Bight. Along with temperature, the concentrations of inorganic nutrients (ammonium, nitrite, nitrate, phosphate, and silicate) and suspended particulate matter (SPM) were measured. Salinity was an especially important parameter, as it is a direct indicator of the extent of water discharge of the Elbe River. The aim of this study was to bring the importance of bacterial methane oxidation as a significant methane sink into focus. Therefore, we made highly sensitive radiotracer measurements to estimate MOX rates in the water column (Valentine et al.,

2001). Only on the basis of these comprehensive examinations we were able to determine the main environmental factors that control methane distribution and MOX rates.

2. Materials and methods

2.1. Study area

The North Sea (including its estuaries and fjords) has a surface area of about 750,000 km^2 and a volume of about 94,000 km^3 (Commission, 2000). The non-tidal circulation of the North Sea is dominated by a cyclonic residual current. Water from the Atlantic (Fair Isle Current, Shetland Flow) flows southward along the British coast and returns northward, together with influxes from the English Channel and various rivers along the coasts of the Netherlands, Germany, and Denmark (Rehder et al., 1998). The German Bight is the south-eastern bight of the North Sea, bounded by the Netherlands and Germany to the south, and Denmark and Germany to the east (the Jutland peninsula). To the north and west, it is bounded by the Dogger Bank. The depths in this area vary mainly from 20 to 40 m (Czitrom et al., 1988). The German Bight consists mainly of a mixture of the Central (Southern) North Sea water masses and continental coastal waters (Becker et al., 1992). The water column in the central (southern) North Sea can be stratified into two slightly different layers (Czitrom et al., 1988 and Becker et al., 1992). Inshore water did not show any stratification in either summer or winter. Freshwater discharge from the Elbe and Weser rivers causes a large salinity contrast near the shore (Czitrom et al., 1988). Analysis of horizontal density gradients did not show a clear annual cycle either near the shore or offshore (Czitrom et al., 1988). Surface sediments affected by tidal or residual current, wave action, and heavy bottom trawling are very mobile (ICES, 1988 and Becker et al., 1992).

The Elbe is one of the major rivers of central Europe, with a total catchment area of about 150,000 km^2. It runs from the Czech Republic through Germany, and reaches the German Bight in its north-eastern region, near Cuxhaven. The Elbe's mean annual discharge at the river mouth is 860 $m^3 s^{-1}$. The discharge regime is mainly controlled by rainfall and snowmelt, therefore it peaks in April/May (Simon, 2005).

2.2. Water sampling

Samples were collected for 2 years from 2010 to 2012. Eleven one-day sampling cruises took place on the 7.10, 8.12 in 2010, 12.01, 2.03, 4.05, 6.07, 29.09 in 2011 and 11.01, 29.02, 28.03, 11.06 in 2012. All sampling procedures and some of the processing of the samples were done on board the research vessels ‘Uthörn’ and ‘Ludwig Prandtl’. Seven sampling stations were distributed along the Helgoland – Cuxhaven transect (Fig. 1). The names of the stations were determined by their distance from the northernmost coastal point near Cuxhaven, so the most south-eastern station was denoted

'Sea kilometre (Sk) 1', and the most north-western, near Helgoland, 'Sk 59'. We determined stations Sk 1, Sk 14, and Sk 20 to be 'coastal stations', and stations Sk 27, Sk 32, Sk 49, and Sk 59 to be 'marine stations'. Water samples were collected with Niskin bottles from the water surface (1 m below the surface) and from the bottom (1 m above the bottom).

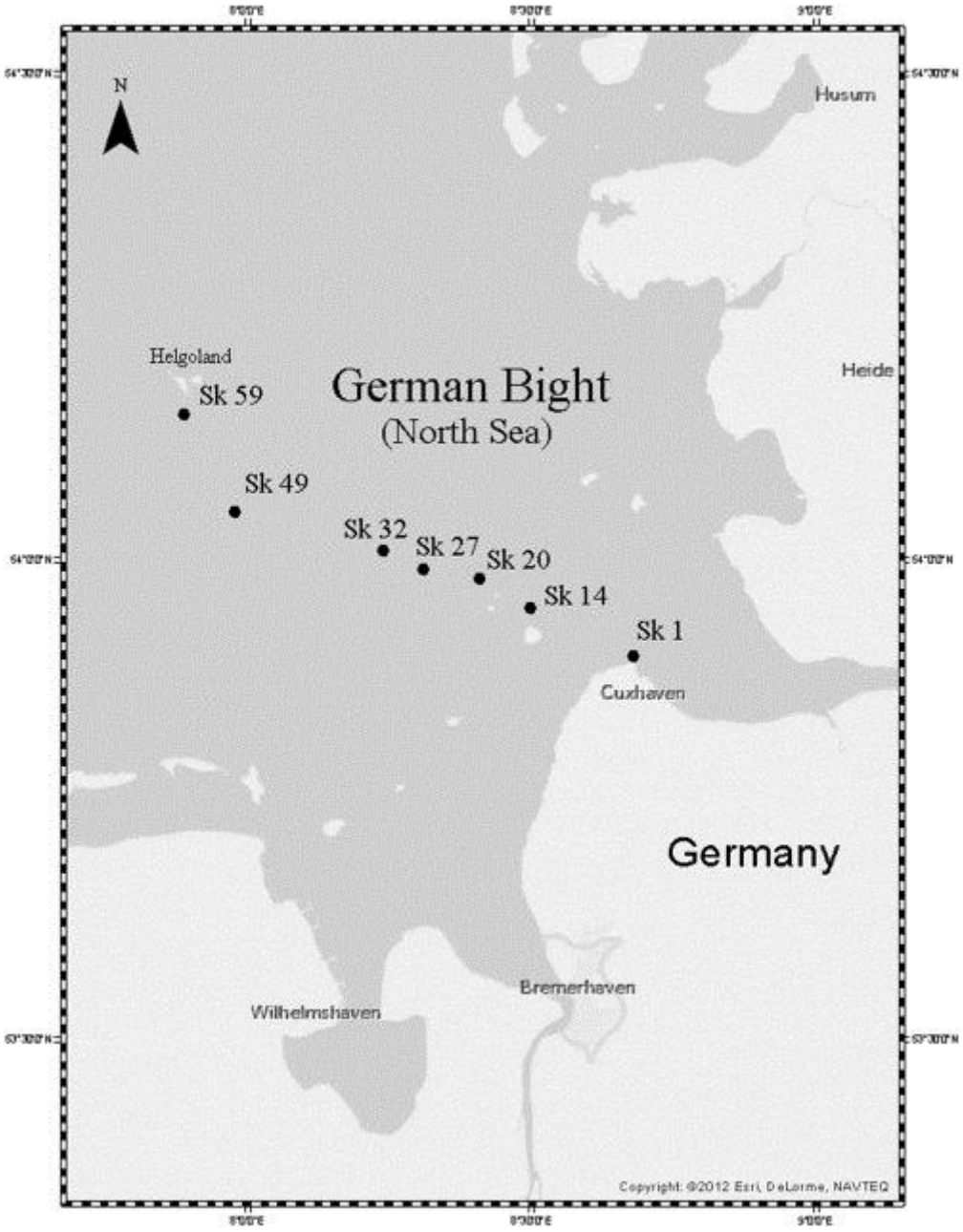

Fig. 1. Map of the German Bight with sampling stations along the Cuxhaven – Helgoland transect.

2.2.1. Oceanographic parameters

Water temperature was measured to monitor seasonality during the study period. Salinity was measured to account for the proportion of freshwater from the Elbe River in North Sea water. Oxygen concentration was measured to investigate its effect on MOX rate, and accordingly, on methane distribution. During the Prandtl cruises, temperature, salinity, and oxygen in the water

column were measured immediately after sampling on board using a Universal Pocket Meter (Multi 340i) with precisions of 1% for salinity, 0.1 °C for temperature, and 0.5% for oxygen. Salinity was measured in µS cm^{-1}, and then converted according to the Practical Salinity Scale. For the Uthörn cruises, a sea-bird CTD sensor was mounted to the water sampling rosette. In July 2011, temperature measurements were not made due to technical problems. Thus, we obtained temperature data from the database of the River Basin Community Elbe (RBC Elbe; in German, 'Flussgebietsgemeinschaft (RBC) Elbe; http://www.fgg-elbe.de/elbe-datenportal.html). These data were collected near Cuxhaven two days before our cruise. Comparisons of RBC measurements with ours for other months did not reveal any significant difference (±1 °C). These data from July were excluded from the comparison of temperatures on the surface and on the bottom, but were used for the correlation analysis between temperature and other factors.

2.2.2. Suspended particulate matter (SPM)

Sampled water was filtered using pre-washed and pre-weighed GFC filters (Whatman TM), which were afterwards dried for 24 hours at 60 °C and weighed again. Water volumes varied from 100 to 250 ml, depending on turbidity. Filtration was done on board right after collecting water samples. The other procedures were done in the laboratory.

2.2.3. Inorganic nutrient analysis

Samples for inorganic nutrients (NO_2, NO_3, NH_4, PO_4) and silicate concentrations were taken after sampling for methane and MOX rates. During the Prandtl cruises, sampled water was filtered with GFC filters (Whatman TM), transferred into 50 ml Falcon tubes, and frozen until further analysis in the laboratory. Sampling during the Uthörn cruises and analysis of all the samples was performed by Karen Wiltshire's group (Wiltshire, 2011 and Wiltshire, 2012) following the technique described by Grasshoff et al. (1983). Nutrient analysis was performed only for surface waters.

2.3. Methane concentration

We measured methane concentrations along the transect in different months to assess seasonal and spatial variations. Right after sampling collected water was transferred, bubble-free, into 120 ml glass serum bottles. The bottles were rinsed with approximately two volumes of sample water, capped with black rubber stoppers, and sealed with an aluminium crimp.

To eliminate agents (such as soap) that inhibit methane oxidation, the glass bottles had been washed and soaked in 3% HCl for 12 hours, and then soaked in distilled water overnight. The stoppers had been autoclaved for 20 min at 120 °C three times, and then rinsed with distilled water.

To determine methane concentrations, samples from each depth and each station were collected in single (March–September 2011) or duplicate bottles (October 2010–January 2011, January–June 2012).

Immediately after filling the bottles, samples were poisoned with 0.3 ml of 25% H_2SO_4 (samples from marine stations) or 0.3 ml of 5N NaOH (samples from coastal stations) to prevent methane oxidation. Poisoning agents were chosen according to the results of preliminary testing of the efficiency of both chemicals in marine and brackish water (Bussmann et al., 2015). Methane concentrations were measured using a headspace technique, by adding 10 ml of N_2 according to McAuliffe (1971). Three 0.1 ml headspace aliquots from each sample were analysed with a gas chromatograph (GC 2014; Shimadzu) equipped with a flame ionization detector and a molecular sieve column (Hay Sep N, 80/100, Alltech). The temperatures of the oven, the injector, and detector were 40, 120, and 160 °C, respectively. The carrier gas (N_2) flow was 20 ml min^{-1}. The gas flow of the FID was 40 ml min^{-1} for H_2 and 400 ml min^{-1} for synthetic air. Gas standards (Air Liquide) with concentrations of 10 and 100 ppm methane were used for calibration. The measurement error of the GC was less than 5%.

Equilibrium concentrations were calculated according the formula proposed by Wiesenburg and Guinasso Jr (1979). Data on the methane concentration in the atmosphere were obtained from the Mace Head Atmospheric Research Station, located on the west coast of Ireland (http://agage.eas.gatech.edu). Saturation rates were calculated as the ratio between observed methane concentrations in the water column and equilibrium concentrations with respect to the ambient methane concentrations in the atmosphere, multiplied with 100%.

2.4. Methane oxidation (MOX) rate

In addition to the chemical parameters, we also measured the microbial methane oxidation, as a possible important methane sink. Samples for MOX rates were collected from each depth and each station in triplicate bottles. According to Bussmann et al. (2015) the coefficient of variation in this case is about 23 ± 11% at low activities (<10 nmol $L^{-1}d^{-1}$) and 7 ± 5% at higher activities (>10 nmol $L^{-1}d^{-1}$). MOX rates were measured following radiotracer techniques using tritiated methane (American Radiolabeled Chemicals, 20 Ci $mmol^{-1}$) according to a method modified from Valentine et al. (2001). A diluted tracer (0.1 ml) was added to the samples (2 kBq ml^{-1}). Samples were vigorously shaken and incubated for 24 h in the dark at near *in situ* temperatures. After incubation, methane oxidation was stopped by adding 0.3 ml of 25% H_2SO_4 (for marine station samples) or 5N NaOH (for coastal station samples). Controls were stopped before the addition of the tracer.

Under oxic conditions methane is oxidized according the following reaction:

$$CH_4 + 2O_2 \rightarrow CO_2 + 2H_2O \quad (1)$$

The consumption of tritiated methane (C^*H_4) leads to the production of tritiated water ($^*H_2O$) and to the decrease of radioactive tracer in the gas phase:

$$C^*H_4 + 2O_2 \rightarrow CO_2 + 2^*H_2O \quad (2)$$

Then, the total radioactivity ($^3H–CH_4$ and $^3H–H_2O$) added to the sample, and the fraction of the labelled gas oxidized or produced water ($^3H–H_2O$) have to be measured. To determine the total radioactivity of the sample, the sample bottle is opened, and 2 ml of the subsample is mixed with a 5 ml scintillation cocktail. To determine the radioactivity of the tritiated water, the rest of the sample was sparged with air to expel all methane. Bottles were then half emptied, a long needle was inserted to the bottom of the bottle, and the sample was purged with air for 30 min. Two ml water aliquots after sparging were mixed with 5 ml of the scintillation cocktail (Ultima Gold LLT, Perkin Elmer) and analysed on a liquid scintillation counter (Tri-Carb® 2910 TR, Perkin Elmer) using decays per minute (dpm) values. The MOX rate in nmol L^{-1} d^{-1} was calculated by taking the ratio of the produced radioactive water to the amount of added tracer ($r = ^*H_2O/C^*H_4$, in dpm) and multiplying it with the ambient methane concentration ($[CH_4]$ in nmol L^{-1}) and correcting for the incubation time (t in d) (Valentine et al., 2001)

$$MOX=r\times[CH_4]/tMOX=r\times[CH4]/t \quad (3)$$

The turnover time (tt in days) is the time it would take to oxidize all the methane at a given MOX rate. It was calculated as the inverse of the ratio (r), corrected for the incubation time (t). Thus, this parameter is independent of the ambient methane concentration, and gives a good measure of the methanotrophic potential (Heintz et al., 2012).

However, there might be some $^*H_2O$ which was not the result of methane oxidation but was a contamination of the tracer. The $^*H_2O$ from the killed controls reveals this value. In marine waters, about 0.06% of the injected tracer was found to be ‘abiotic water’. In freshwater, the percentage increased to about 0.62%. The value of $^*H_2O$ were corrected for this ‘abiotic’ water.

2.5. Statistical analysis

For comparison of surface and bottom values and for comparison of values at different stations (spatial variation), we used a paired *t*-test in the case of a normal distribution, and a non-parametric Wilcoxon signed- rank test when a normality test (Shapiro – Wilk) failed. Marine and coastal stations were analysed separately. When no significant difference between data sets was found, the respective data were pooled. To investigate the dependence of methane concentration, turnover time, and MOX rate on hydrographical and chemical factors such as temperature, salinity, methane, phosphate, oxygen, and SPM, we performed simple linear regression analyses. If the linear correlation was not significant, we performed a Spearman rank order correlation analysis, which

shows if variables are related monotonically, i.e. an increase of one variable causes an increase/decrease of the other variable.

The Spearman correlation coefficient (r_s) is defined as the Pearson correlation coefficient between the ranked variables. For a sample of size n, the n raw scores X_i, Y_i are converted to ranks x_i, y_i, and r_s is computed as:

$$r_s = \frac{\sum_i (x_i - \bar{x})(y_i - \bar{y})}{\sqrt{\sum_i (x_i - \bar{x})^2 \sum_i (y_i - \bar{y})^2}}. \quad (4)$$

Calculations were performed using SigmaPlot for Windows Version 11.0 software.

3. Results

3.1. Oceanographic parameters

No significant difference between surface and bottom temperature was observed (paired *t*-test, $n = 39$, $p = 0.917$), so the data were pooled. The lowest temperatures were measured in January 2011, with an average of 2.6 ± 1.2 °C. The highest temperature (19.0 ± 1.4 °C) was observed in September 2011.

Surface water generally had a lower salinity than bottom water (paired *t*-test, $n = 49$, $p < 0.001$). The stratification of the water column was most pronounced from June to September. Due to the input of freshwater from the Elbe River, salinity increased with distance from the shore. This is well illustrated by two independent sampling campaigns in the summer (July 2011) and winter (February 2012) (Fig. 2). For all sampling dates, at marine station Sk 59, the average salinity was 32.2 ± 1.0, while coastal station Sk 1 had an average salinity of 16.3 ± 5.7. The lowest salinity at this station (7.8) was detected in September 2011, and the highest salinity at this station (24.7) was detected in June 2012.

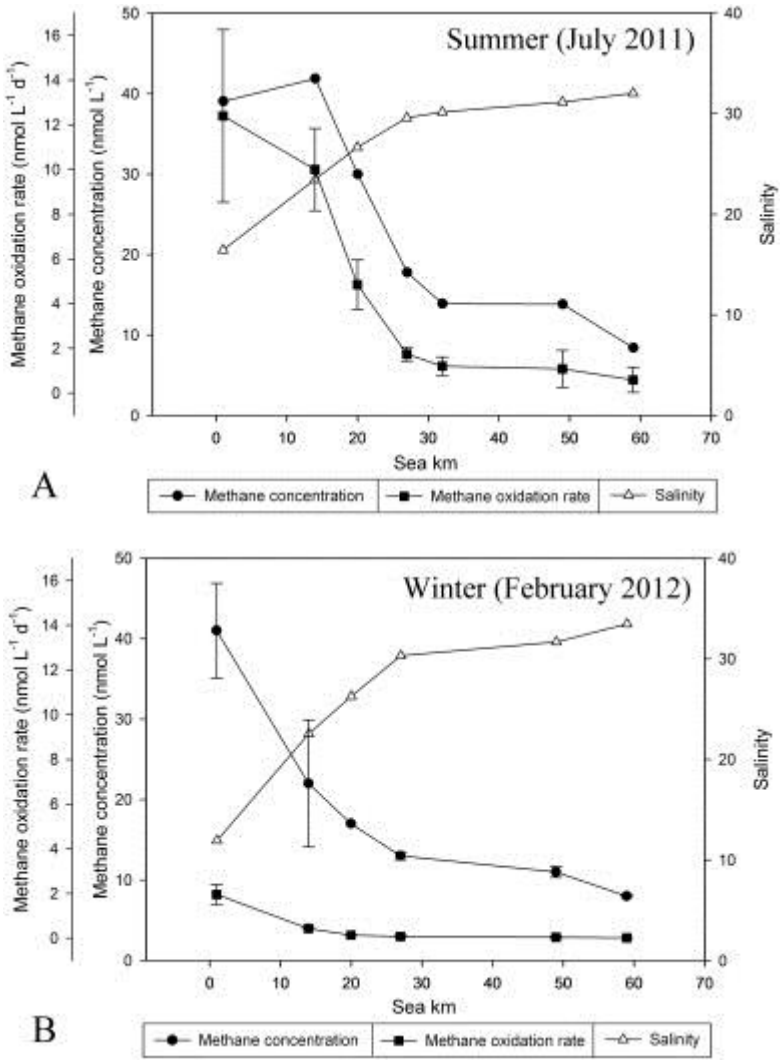

Fig. 2. Distribution of methane concentration, MOX rate, and salinity along the transect in A) summer (July 2011) and B) winter (February 2012). Shown is the average of surface and bottom water.

3.2. Suspended particulate matter, oxygen and inorganic nutrients

Values for SPM ranged from 8 to 167 mg L^{-1}, but neither seasonal nor spatial (along the transect) differences could be detected. Bottom water was always more turbid than corresponding surface water (paired *t*-test, $n = 49$, $p < 0.001$, data not shown).

Oxygen concentrations did not show any spatial differentiation along the transect, nor any seasonal trend. The lowest concentration of oxygen (6.1 mg L^{-1}) was detected in October 2010 at station Sk 59, while the highest concentration (11.4 mg L^{-1}) was detected in January 2012 near station Sk 14. Values near the surface (average value of 8.7 mg L^{-1}) were generally slightly higher than near the bottom (average value of 8.5 mg L^{-1}) (paired *t*-test, $n = 42$, $p = 0.021$).

Overall concentrations of NO_2, NO_3, NH_4, and PO_4 decreased towards the sea and were nearly depleted at a distance of 30 km from the coast. Fig. 3 shows representative results from two

individual sampling campaigns. Phosphate concentrations ranged from 0.3 µmol L^{-1} (May 2011) to 1.8 µmol L^{-1} (December 2010) at station Sk 59, and from 1.2 µmol L^{-1} (May 2011) to 3.3 µmol L^{-1} (January 2012) at station Sk 1. Nitrite concentrations ranged from 0.1 µmol L^{-1} (October 2010) to 1.2 µmol L^{-1} (March 2011) at station Sk 59, and from 0.7 µmol L^{-1} (May 2011) to 1.5 µmol L^{-1} (January 2012) at station Sk 1. Nitrate concentrations ranged from 0.1 µmol L^{-1} (October 2010) to 25.0 µmol L^{-1} (May 2011) at station Sk 59, and from 81.6 µmol L^{-1} (May 2011) to 219.0 µmol L^{-1} (February 2012) at station Sk 1. Ammonium concentrations ranged from 0.1 µmol L^{-1} (May 2011) to 3.8 µmol L^{-1} (July 2011) at station Sk 59, and from 0.5 µmol L^{-1} (May 2011) to 14.6 µmol L^{-1} (February 2012) at station Sk 1. In the summer months, e.g. July 2011, the ammonium concentration varied significantly over the entire transect. From Sk 1 to Sk 49, the concentration decreased, but suddenly rapidly increased again, until it reached a maximum at Sk 59, which is similar to Sk 1. Silicate concentrations ranged from 1.6 to 15.1 µmol L^{-1} at station Sk 59, and from 21.8 to 155.7 µmol L^{-1} at station Sk 1 in May 2011 and February 2012, respectively.

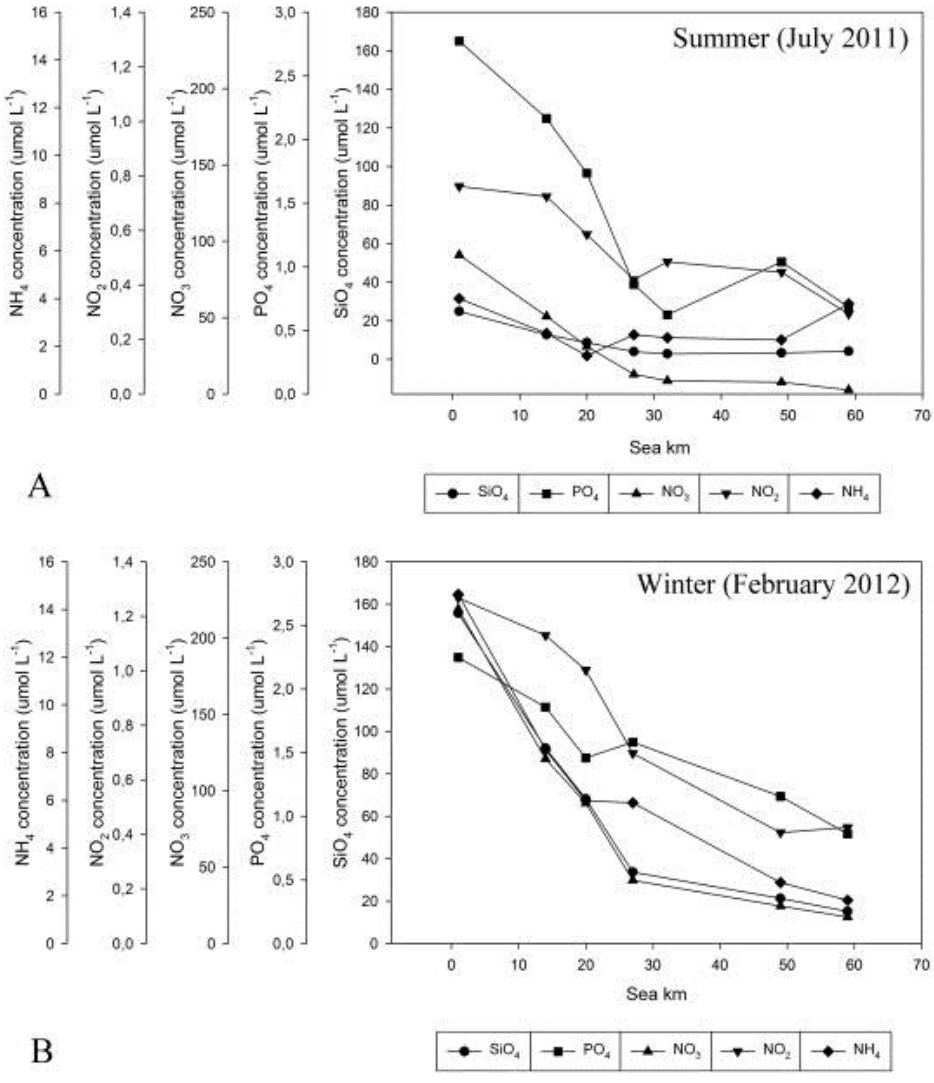

Fig. 3. Distribution of inorganic nutrients in A) summer (July 2011) and B) winter (February 2012). Shown are only data from surface water.

3.3. Methane concentrations

The results of all the measurements are summarized in Fig. 4 and are published in the data library PANGAEA (Bussmann et al., 2014a). No significant difference between surface and bottom values was observed either for the marine (paired *t*-test, $n = 28$, $p = 0.412$), or coastal stations (paired *t*-test, $n = 20$, $p = 0.522$), so the data were pooled. The dissolved equilibrium concentrations varied from 2.9 to 3.1 nmol L^{-1}. Methane concentrations in the water column for both marine and coastal stations were supersaturated. At the coastal stations saturation rate varied from 340 to 1880%, at the marine stations it varied from 170 to 1110%. At the coastal stations, methane concentrations were, in general, higher than at the marine stations, and decreased offshore from station Sk 1 to station Sk 20. The only exception was detected in September 2011, when values were significantly higher than during the rest of the season. These data were the only ones that did not follow the trend, and stood apart from the rest of the observations, so we omitted it from further processing. The three coastal stations had an average methane concentration of 30 ± 13 nmol L^{-1}. The average methane concentration at station Sk 1 was 40.9 ± 9.4 nmol L^{-1}, ranging from 24.0 nmol L^{-1} in May 2011 to 58.3 nmol L^{-1} in March 2012. The average methane concentration at station Sk 20 was 19.8 ± 8.9 nmol L^{-1}, ranging from 10.0 nmol L^{-1} in May 2011 to 36.0 nmol L^{-1} in June 2012. For the marine stations, no spatial variation of methane concentrations was observed, so the data were pooled. The average methane concentration for the marine stations was 14.0 ± 4.8 nmol L^{-1} ($n = 56$), with a minimum of 5 nmol L^{-1} in March 2011 and a maximum of 32 nmol L^{-1} in December 2010.

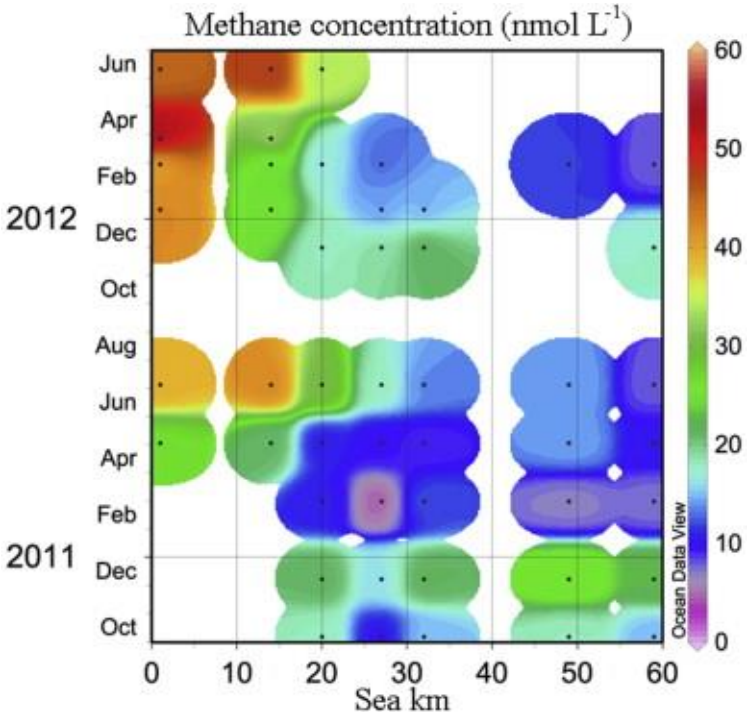

Fig. 4. Methane concentration along the transect during the whole period of investigation (surface and bottom).

To highlight the strong effect of the riverine water and the seasonal trends, two individual sampling campaigns (summer/winter) are shown in Fig. 2. At the coastal stations, methane concentrations were higher in summer (July 2011) than in winter (February 2012). At the marine stations, methane concentrations were approximately the same. Methane concentration decreased offshore, clearly coinciding with the salinity increase in both summer and winter. Regression analysis showed that about 57% of methane variability could be explained by salinity (for all data, n = 93, Fig. 5). On four occasions, we were able to sample all stations on one day. For these dates (May 2011, July 2011, January 2012, and February 2012), the correlation was much stronger and the salinity explained 70–98% of the methane variability. When the regression line (Fig. 5) was extrapolated to a salinity of zero, we obtained a prospective methane concentration of 72 nmol L^{-1} for Elbe waters. The corresponding methane concentrations from the single cruise analysis ranged from 56 to 80 nmol L^{-1}.

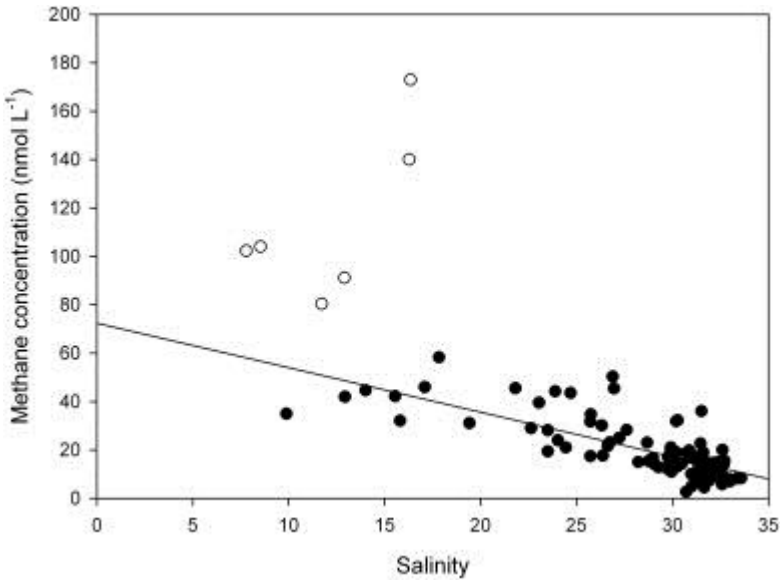

Fig. 5. Linear regression between salinity and methane concentration. Empty circles indicate outliers, which were excluded from regression analysis (measurements from September 2011).

No linear correlation between methane concentration and temperature was observed, however we detected a temperature dependence after rank transformation of the data. At the coastal stations, the highest methane concentrations were found during periods of highest temperatures (r_s = 0.49, n = 36). Since two independent parameters correlated with methane concentration at the coastal stations, we applied multiple linear regressions between methane concentration, salinity, and temperature, and obtained a model with an even higher correlation coefficient (r^2 = 0.74, n = 30) (Fig. 6).

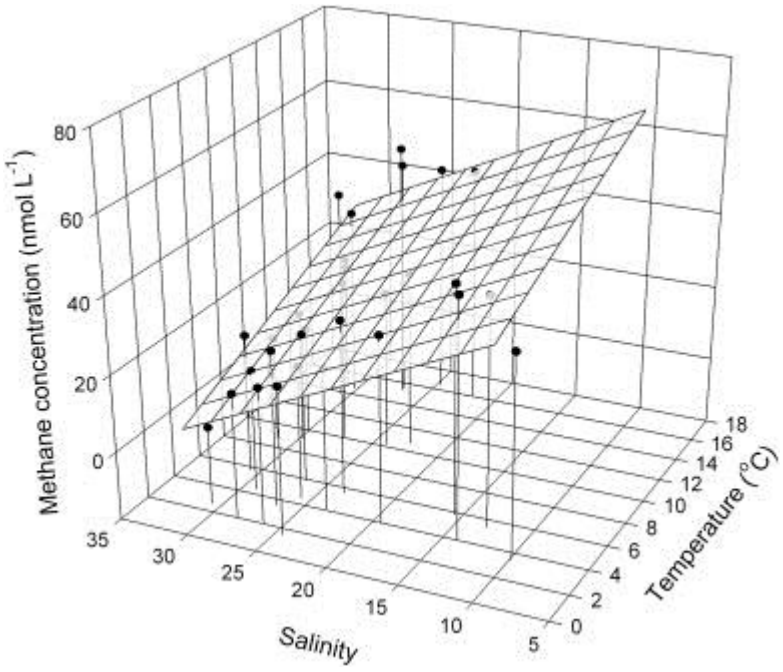

Fig. 6. Methane distribution at the coastal stations according to salinity and temperature. Multiple linear regression: CH_4 = 55.798 + (1.697*Temperature) – (1.709*Salinity); r^2 = 0.737.

No linear correlation, but a weak positive dependence of methane concentration on oxygen, was found along the entire transect (r_s = 0.37, n = 80). We also found a strong correlation between concentrations of methane and inorganic nutrients, except NO_2 (r_s varied from 0.43 to 0.66 depending on the inorganic nutrient). However, we assumed that this was mainly due to the input of nutrient-rich waters from the mouth of the Elbe, as salinity and inorganic nutrient concentrations were also strongly correlated (r^2 for different mineral nutrients varied from 0.46 to 0.87).

No linear correlation between SPM and methane concentrations was found. Moderate negative dependence was indicated after rank transformation of the marine data. Thus, we can state that at the marine stations, the highest methane concentrations were found at the lowest SPM values (r_s = −0.45, n = 54).

3.4. Methane oxidation rate

The results of all the measurements are summarized in Fig. 7 and are published in the data library PANGAEA (Bussmann et al., 2014a). No significant differences between surface and bottom values were observed either for the coastal stations (paired t-test, n = 18, p = 0.154), or for the marine stations (paired t-test, n = 28, p = 0.290), so the data were pooled. At the coastal stations, MOX rates were in general higher than at the marine stations, and decreased offshore from station Sk 1 to station Sk 20. The coastal stations had an average MOX rate of 2.6 ± 2.7 nmol $L^{-1}d^{-1}$. The average MOX rate at station Sk 1 (nearest the coast) was 5.26 ± 4.72 nmol $L^{-1}d^{-1}$, ranging from

0.78 nmol $L^{-1}d^{-1}$ in June 2012 to 16.5 nmol $L^{-1}d^{-1}$ in July 2011. The average MOX rate at station Sk 20 was 0.97 ± 1.85 nmol $L^{-1}d^{-1}$, ranging from 0.04 nmol $L^{-1}d^{-1}$ in May 2011 to 5.81 nmol $L^{-1}d^{-1}$ in July 2011. The average MOX rate for the marine stations was 0.417 ± 0.529 nmol $L^{-1}d^{-1}$, with a minimum of 0.009 nmol $L^{-1}d^{-1}$ in February 2012 and a maximum of 1.96 nmol $L^{-1}d^{-1}$ in July 2011.

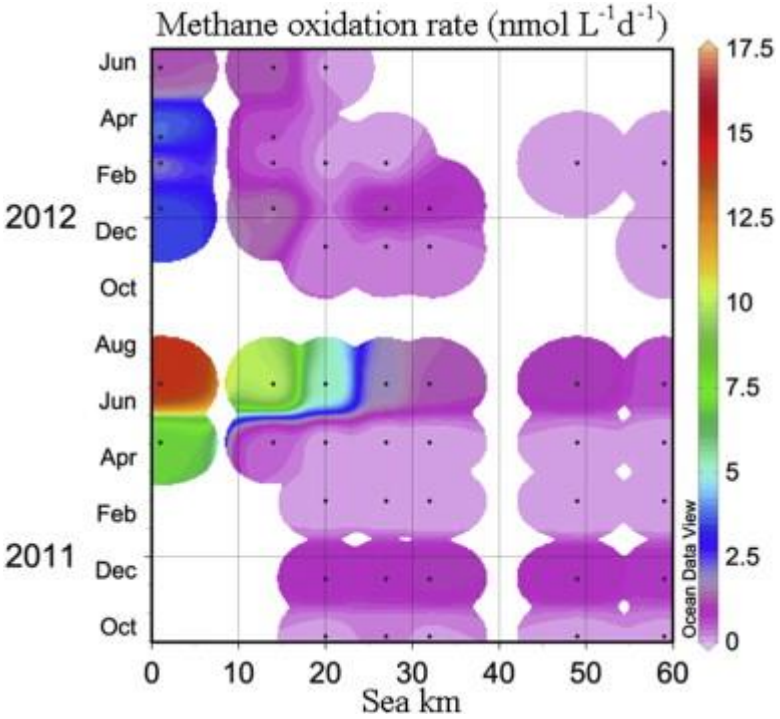

Fig. 7. MOX rates along the transect during the whole period of investigation (surface and bottom).

For the turnover time no significant differences between surface and bottom values were observed either for coastal stations (paired *t*-test, $n = 18$, $p = 0.182$), or marine stations (paired *t*-test, $n = 28$, $p = 0.136$). Thus, the data were pooled. The coastal stations had an average turnover time of 64 ± 75 days. The average turnover time at station Sk 1 was 16 ± 15 days, with a minimum of 3 days in July 2011 and a maximum of 56 days in June 2012. The average turnover time at station Sk 20 was 120 ± 92 days, with a minimum of 5 days in July 2011 and a maximum of 293 days in October 2010. The average turnover time for the marine stations was 196 days, with a minimum of 9 days in July 2011 and a maximum of 1049 days in February 2012. To highlight the strong effect of the riverine water and the seasonal trends, two individual sampling campaigns (summer/winter) are shown in Fig. 2. MOX rates along the transect generally followed a trend similar to the methane concentrations and salinity. However, MOX rates were significantly lower in winter (February 2012) than in summer (July 2011), especially at the coastal stations.

Because of great variability in the turnover times and MOX rates, linear regression analysis did not reveal clear results. Therefore, we rank transformed the data and performed Spearman rank order correlation tests (Table 1). The tests showed that the variability of the turnover time was influenced

by methane concentration (r_s = −0.60, n = 94) in a negative way, i.e. highest turnover times (the slowest rates) were found at lowest methane concentrations. Salinity influenced the variability of the turnover time in a positive way (r_s = 0.56, n = 91), especially in the coastal area (r_s = 0.64, n = 37), i.e. highest turnover times were found at highest salinities. Turnover time was moderately correlated in a negative way with temperature (r_s = −0.46, n = 86), i.e. highest turnover times were found at lowest temperatures. Thus, we found that turnover time was correlated to a greater or lesser extent with three factors: methane concentration, salinity, and temperature.

Table 1. Spearman rank correlation of the turnover time and MOX rates with hydrographic parameters.

Dependent parameter	Independent parameter	Spearman rank order correlation	Comments
Turnover time	Methane concentration	- 0.60	
	Salinity	+ 0.56	Due to co-correlation of salinity with methane, methane data were grouped, then only with methane > 30 nmol L^{-1}, salinity influences turnover time with r_s = 0.39
	Temperature	- 0.46	
MOX rate	Methane Concentration	n. d.	
	Salinity	- 0.66	Due to co-correlation of salinity with methane, methane data were grouped, than only with methane > 30 nmol L^{-1}, salinity influences MOX with r_s = - 0.34
	Temperature	+ 0.43	

n.d. – not determined

Because of the dilution of the methane-rich freshwater, we mostly found low methane concentrations at high salinities. To exclude this interaction, and to check for the 'real' influence of salinity on MOX rate and turnover time, we grouped the methane concentrations, according to their

frequency distribution, to low methane concentrations (<15 nmol L^{-1}, n = 37), medium methane concentrations (15–30 nmol L^{-1}, n = 41), and high methane concentrations (>30 nmol L^{-1}, n = 21, Table 1). Only when methane concentrations were high (>30 nmol L^{-1}), MOX rate and the turnover time (rank transformed data) were correlated with salinity (r_s = 0.39 and 0.34, respectively). At lower methane concentrations, these parameters were independent of salinity. Thus at 'high' methane concentrations, salinity had a negative effect on the turnover time and MOX rate. At lower methane concentrations, the most important factor for the turnover time was simply the methane concentration.

The same tendency was observed for MOX rates (Table 1), which were negatively correlated with salinity (r_s = −0.66, n = 92), but positively correlated with methane concentration (r_s = 0.78, n = 94) and temperature (r_s = 0.43, n = 87), i.e. highest MOX rates were detected at lowest salinities and highest methane concentrations and temperatures. However, the correlation between MOX rate and methane concentration should be viewed with caution, because MOX rate calculations are dependent on methane concentrations.

MOX rates were correlated with phosphate concentrations (r_s = 0.54, n = 42), but phosphate was strongly correlated with salinity. Therefore, to circumvent the co-correlation of phosphate and salinity, we grouped the salinity data into meso-, poly-, and euhaline (5–18, 18–30, and >30; (Caspers, 1959). For each of these salinity groups, no influence of phosphate on turnover time or MOX rate was observed (rank transformed data). No influence of the other inorganic nutrients, SPM, or oxygen on MOX rates or turnover times could be detected by statistical analyses.

4. Discussion

Methane distribution is defined as the balance between methane sources and sinks. Estuaries are one of the main sources of methane in the North Sea. They, in turn, are supplied with methane by riverine input, tidal flats, and marshes (Rehder et al., 1998, Middelburg et al., 2002, Abril and Borges, 2005 and Grunwald et al., 2009). The main methane sinks are represented by the dilution of methane-rich waters with methane-depleted waters, outgassing, and bacterial methane oxidation (Scranton and McShane, 1991).

Methane concentrations were monitored over two years along a transect from the Elbe estuary towards the German Bight. The highest methane concentrations were detected near the coast (the first coastal station, Sk 1). Methane concentrations for the next 20 km offshore, decreased until they reached a plateau, and did not significantly vary any further (20–60 km). Therefore, we can conclude that in terms of methane distribution, the direct impact zone of the Elbe riverine waters is in the range of 20 km from the river mouth in Cuxhaven. The coastal stations (1–20 km from the coast) had

an average methane concentration of 30 ± 13 nmol L^{-1}, comparable with the measurements of Rehder et al. (1998), which were in the range of 10–40 nmol L^{-1}. Methane concentrations at the marine stations were on average 14 ± 6 nmol L^{-1}. These concentrations are slightly higher than those reported by Rehder et al. (1998), but remarkably lower than values reported by Grunwald et al. (2009), which were around 200 nmol L^{-1} near Helgoland. In general, methane concentrations in the Elbe estuary and in the German Bight are comparable with those measured in other estuaries (de Angelis and Scranton, 1993, Abril and Iversen, 2002, Middelburg et al., 2002, Silvennoinen et al., 2008, Zhang et al., 2008 and Grunwald et al., 2009) and open ocean locations (Kelley, 2003 and Mau et al., 2013) (Table 2).

Table 2. Methane concentrations and MOX rates, measured in different estuaries and in the open ocean

Location	Methane concentrations (nmol L^{-1})	MOX rates (nmol $L^{-1}d^{-1}$)	Reference
Estuaries			
Elbe (German Bight)	3–60	0.01–17	This study
Elbe	4–111	n.m.	(Middelburg *et al.*, 2002)
North Sea around Helgoland	200	n.m.	(Grunwald *et al.*, 2009)
Southern Bight (North Sea)	3–22	<<1.3	(Scranton & McShane, 1991)
Ems	91–51	n.m.	(Middelburg *et al.*, 2002)
Thames	5–273	n.m.	(Middelburg *et al.*, 2002)
Rhine	4.1–1437	n.m.	(Middelburg *et al.*, 2002)
Scheldt	20–485	n.m.	(Middelburg *et al.*, 2002)
Loire	16–671	n.m.	(Middelburg *et al.*, 2002)
Gironde	4–559	n.m.	(Middelburg *et al.*, 2002)
Douro	15–128	n.m.	(Middelburg *et al.*, 2002)
Sado	37–40	n.m.	(Middelburg *et al.*, 2002)
Hudson river estuary	48–858	0.1–68	(de Angelis & Scranton, 1993)
Randers Fjord, Denmark	28–420	<0.2–15.2	(Abril & Iversen, 2002)
Bay of Temmesjoki River (Baltic Sea)	62–588	n.m.	(Silvennoinen *et al.*, 2008)
Estuary of the Yangtze River	3–89	n.m.	(Zhang *et al.*, 2008)
Open ocean			
Gulf of Mexico	10–343	0–57	(Kelley, 2003)
Cape Lookout Bight	18–246	0	(Kelley, 2003)
Arctic fjord Storfjorden	5–80	0–3	(Mau *et al.*, 2013)

n.m. – not measured

For all stations and at all times the water was supersaturated with methane (170–1880 %), thus the German Bight acts as a methane source to the atmosphere both at the coastal and at the open sea part.

As was done in previous studies, we extrapolated methane concentration at zero salinity using a linear correlation model. In March and June 2012, we had the opportunity to also sample water from the Elbe River itself. These data are published in the PANGAEA data base (Bussmann et al., 2014b). Thus, we were able to examine the actual riverine input more closely (Fig. 8). At salinities of 10–15, methane concentrations were 65 ± 5 nmol L^{-1} (Bussmann et al., 2014b), which is very close to our interpolated value of 72 nmol L^{-1}. The corresponding stations EC-719 and EC-724 are close to the port of Cuxhaven. In contrast, the real riverine methane concentrations with salinities <5 (river stations EC-679, 699 and 709) were much lower (26 ± 8 nmol L^{-1}).

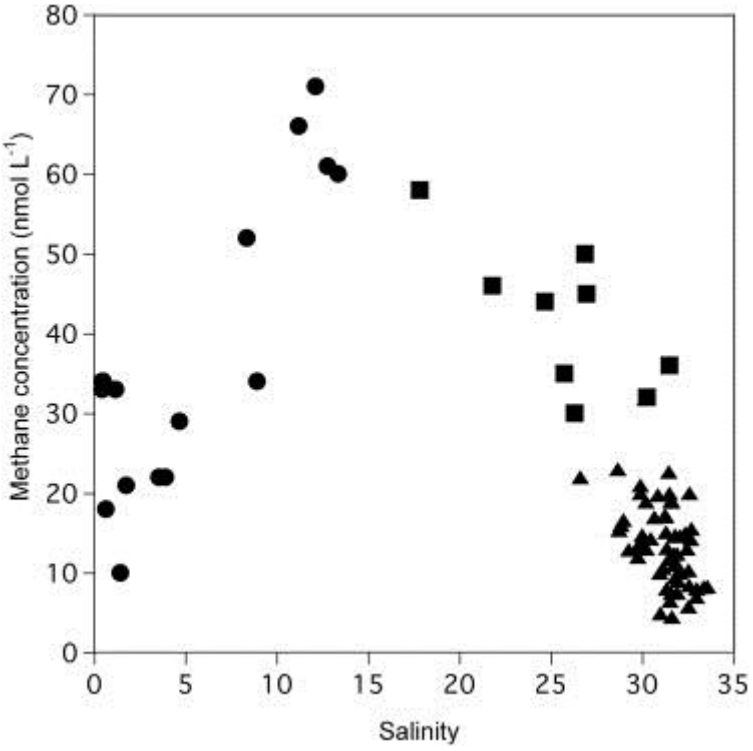

Fig. 8. Methane concentrations with corresponding salinities. Circles indicate river stations (Bussmann et al., 2014b), and squares indicate coastal stations from this study, both for March and June 2012. The triangles represent the values from all marine stations from this study.

This shows that the Elbe is not the main methane source in the estuary, and that the mixing model can only be applied at salinities 10–15. Thus, application of extrapolating approaches as proposed by Rehder et al. (1998) is not possible.

Middelburg et al. (2002) measured a significantly higher methane concentration of 111 nmol L^{-1} at zero salinity in 1997. However, as the water quality in the Elbe has improved over the last 20 years

(Amann et al., 2012), the methane concentration may have decreased. Besides, Middelburg et al. (2002) made measurements during only one sampling campaign in April, and as we have shown, methane concentrations are subject to significant temporal variations (this will be discussed later).

Explanations for the methane increase near Cuxhaven are: a) increased methane production in the underlying sediment, b) lateral input. Additionally, we would expect decreased methane oxidation in the estuary in comparison with the freshwater end-member (discussed later). Methane is mostly produced in anoxic sediment zones, from where it can diffuse into the overlying water column. Our comparison of bottom and surface waters gave no indication of strong methane production in the sediments. The sediment in this area is supposed to be very coarse due to the strong currents, and even though methanogenesis also occurs in oxygenated, organic-rich sediments just several cm under the sediments surface (Deborde et al., 2010), we did not observe a strong direct sedimentary input. This is in agreement with the observation made by Scranton and McShane (1991), who stated that sandy sediments of the North Sea are not a significant methane source.

Tidal flats in the North Sea are known to be active sites of mineralization of organic material, which eventually leads to methane accumulation. Due to advective flow in the tidal areas, which is of special importance in permeable sandy sediments, pore waters enriched in re-mineralized nutrients and methane are actively released from sediments into the overlying water column (Beck and Brumsack, 2012 and Segarra et al., 2013). As Cuxhaven is surrounded by tidal flats, we assume a strong lateral input of methane from these tidal flats.

Other potential methane sources are inputs from other rivers draining into the estuary, and sewage discharge. The Oste, a small river which flows into the North Sea near Cuxhaven, has low water velocities and therefore could have much higher methane concentrations. However, no data were available for this river. A wastewater treatment plant in Cuxhaven, as well as industrial activity, could lead to additional input of organics which might trigger *in situ* methane production both in sediments and in the water column. Input of inorganic nutrients was also detectable in the hydrochemical data; the phosphate and nitrate concentrations were especially high at the nearby station. We can thus conclude that the Elbe River gets enriched with methane at its mouth due to additional methane sources, whereby methanogenesis might also play an important role. Furthermore, water in the estuary gets diluted with methane-depleted water from the North Sea. The last section of the transect represents North Sea water almost exclusively, and methane concentrations there do not vary significantly.

We expected a seasonality for our methane concentration data, with higher methane concentrations in summer and low ones in winter. However, we could not find any clear seasonal pattern, which may be also due to the too large sampling intervals. But as seasonality is also reflected in changing

temperatures, we could find a correlation with water temperature. The effect of temperature on methane production has been shown for many aquatic systems (Pulliam, 1993, Bange et al., 1994, Duc et al., 2010 and Lofton et al., 2014), including river and estuary systems (Fedorov et al., 2003). Enhanced methane production in the warmer months is known for various river and estuary systems, such as the Don River, with the Taganrog Bay in the Sea of Azov, Russia (Fedorov et al., 2003), and the Baltic Sea (Bange et al., 1994). Clear seasonality with increased methane in the summer and autumn was also shown for the Rhine estuary (Middelburg et al., 2002). However, in the Scheldt and Gironde estuaries, seasonality was not pronounced (Middelburg et al., 2002), nor in Humber estuary, where methane concentrations were lowest in the summer (Upstill-Goddard et al., 2000). In our investigation, moderate correlation of methane concentration with temperature was shown, but only for the coastal stations (r_s = 0.49). Absence of the correlation at the marine stations can be explained by insignificant methane production and rather stable temperature regimes in the open sea and sediments.

Further on, we have to consider that a seasonality of methane concentrations could also originate from variation in the Elbe water discharge. As discussed before, methane distribution along the transect was correlated with salinity. Finally, a multiple linear regression combining salinity and temperature as parameters affecting the methane concentration explained 74% of the methane distribution. Water discharge measured at Neu Darchau from September 2010 to June 2012 ranged from 300 to 3500 $m^3 s^{-1}$ (River Basin Community Elbe, http://www.fgg-elbe.de). Indeed, during the entire period of our sampling campaign at station Sk 1, the salinity varied widely from 8 to 25. However, we did not manage to find a strong correlation between water discharge and methane variations. This can be partly explained by the remoteness between Neu Darchau and station Sk1. Additionally, tides are likely to also be a significant factor affecting short-term methane distribution, as shown in previous studies (Grunwald et al., 2009). However, in our investigation, we did not have enough information to correlate methane concentration with the tidal surge.

MOX rates, as well as turnover times, were calculated to assess the role of methane oxidation as a methane sink, and to define its role in methane distribution. The highest MOX rates were found at the coastal stations (2.6 ± 2.7 nmol $L^{-1}d^{-1}$), and the lowest MOX rates were found at the marine stations (0.4 ± 0.5 nmol $L^{-1}d^{-1}$). Despite the importance of methane oxidation processes in the water column, very few measurements have been made in estuaries. MOX rates in the Hudson estuary (in the salt intrusion area) varied from 0.1 to 68 nmol $L^{-1}d^{-1}$ (de Angelis and Scranton, 1993). In the Randers fjord MOX rates reached 15 nmol $L^{-1}d^{-1}$ (Abril and Iversen, 2002). Summarized data on aerobic methane oxidation in ocean waters from different locations show that MOX rates are generally in the range of 0.001–10 nmol $L^{-1}d^{-1}$ (Kelley, 2003 and Mau et al., 2013). MOX rates

measured at different estuaries and in the open ocean are summarized in Table 2. Thus, our measurements along the entire transect are in the same range of MOX rates in other aquatic environments.

For the southeast coast of the North Sea a flushing time of 11 days and for the central North Sea of 40 days is given by Ilyina et al. (2006). Our average turnover times for the coastal stations and marine stations were 64 days and 196 days, respectively. Thus, the water masses are faster exported than MOX could consume the methane. Scranton and McShane (1991), who studied methane distribution in the Southern Bight (North Sea) also came to a conclusion that bacterial methane oxidation was not a significant methane sink. However, a more detailed modelling would be necessary to adequately address the question if methane oxidation is a significant methane sink in the Elbe estuary and adjacent German Bight.

Microbial activities are often controlled by substrate concentration, following the enzyme kinetics as described by Michaelis Menten. In our case this means, that with increasing methane concentration the MOX rate also increases, until (enzyme) saturation is reached and no further increase of MOX can be observed. To describe this phenomenon and make it comparable between different studies, the parameter V_{max} and K_m are used to describe the maximal velocity and the half saturation concentration (Lehninger, 1985). Unfortunately, to our knowledge there are no kinetic studies on marine methanotrophs, which usually endure at low methane concentrations. Recent studies from arctic lakes reveal K_m from 4 to 10 µM (Lofton et al., 2014) and the review from Hanson and Hanson (1996) gives a K_m of 1 µM. In a study on the kinetics of cultured methanotrophic strains under low methane concentration (10–100 ppm), it was shown that these strains, which have a K_m within the above described range, are able to grow under these limiting conditions (Knief and Dunfield, 2005). In our study, natural methane concentrations ranged from 3 to 58 nmol L^{-1}, which are concentrations well below half saturation. Thus we assume that the methanotrophic population of the North Sea is strongly limited by methane concentration and an increase in methane concentration would lead to increased activity. With our data we did not calculate such a relation between methane concentration and MOX rate due to methodological restraints (the MOX rate is calculated by multiplying the ratio of consumed tracer with the methane concentration). But even when setting these restraints apart only a weak correlation was observed.

The effect of salt as a chemical agent inhibiting methane oxidation in freshwater has been shown before (de Angelis and Scranton, 1993). The changing salinity likely causes osmotic stress for freshwater methanotrophic bacteria (Hanson and Hanson, 1996). At the same time, most studies report that microbial methane oxidation is already significantly reduced at salinities <10 (Abril and Borges, 2005), whereas in our investigation, high MOX rates (17 nmol L^{-1} d^{-1}) were detected even at

a salinity of 17. Our results show that salinity, as such, only has a (negative) effect when methane concentrations are >30 nmol L^{-1}. Thus, we conclude that, at the coastal stations, the negative effect of osmotic stress is counteracted by the positive effect of high methane concentrations in the estuary. An explanation might be that microorganisms which are frequently exposed to changing salinity (like the Elbe estuary, due to the significant influence of tides) are adapted to changing salinities. However, it remains unclear as to what extent freshwater or marine methanotrophic bacteria participate in methane oxidation.

Our results show that temperature also has a moderate effect on methane oxidation. Thus, the lowest turnover times and highest MOX rates were detected during the highest temperatures. This is in contrast with observations made by Lofton et al. (2014), who states that temperature can influence methane oxidation only in substrate-saturated environment.

Another factor which can stimulate methane oxidation is turbidity or SPM. It was mentioned before that SPM can serve as a vehicle for methanogens, and the same principle can be applied to methane-oxidizing microorganisms (Middelburg et al., 2002 and Abril et al., 2007). *In vitro* experiments showed that removal of particles smaller than 11 µm can decrease the MOX rate by 50% (de Angelis and Scranton, 1993). In our study, we did not detect any correlation of turnover times/MOX rates with SPM. The easiest explanations would be that stronger factors (such as methane concentration and temperature) simply suppressed the influence of SPM.

Oxygen is another important factor for methane oxidation. Summarized data on oxygen half-saturation constants for aerobic methane oxidation (the concentration at which the growth rate of bacteria reaches the half-maximum) show a wide range, from 0.14 to 58 µM (Guérin and Abril, 2007). Oxygen concentrations measured along the transect in our study were within this range, thus oxygen was never a limiting factor, and no correlation with methane oxidation was detected.

Methanotrophs are regarded as slow growing bacteria, and hence tend to lose out on nutrients to faster growing heterotrophs. Besides, some mineral nutrients, like ammonium, are known to inhibit methane oxidation (Alam and Jia, 2012) while others, like phosphate, increase MOX rates (Boiesen et al., 1993). Also, the availability of nitrogen can become a limiting factor for the growth of methanotrophs in nitrogen-limited environments (Bodelier et al., 2000). In our study, large quantities of inorganic nutrients, were brought to the German Bight from the mouth of the Elbe, thus providing all the inorganic nutrients needed for intensive methane oxidation. However, we did not detect any correlation between MOX rates and any mineral nutrients at the marine stations. Due to low MOX rates at the marine stations, the supply of inorganic nutrients was still sufficient, and thus did not influence the methanotrophy.

5. Conclusion

We observed a wide variation of methane concentration in the water column along a 60 km transect from Cuxhaven to Helgoland. Highest concentrations were detected near the coast, where the water is enriched with methane by river water and lateral sources. Over the next 20 km, in the direction of Helgoland, we observed decrease in methane concentration due to dilution with methane-depleted sea water from the German Bight. The last 40 km of the transect represents seawater almost exclusively, with a consistently low methane concentration. We also discovered that most of the methane in the Elbe estuary does not come from the Elbe River itself, as was thought before, but from an area near Cuxhaven. Thus, the conservative mixing model, which describes methane distribution as a simple dilution of methane-rich freshwater from the river with marine water, is only applicable at salinities >10. Possible methane sources near Cuxhaven are input from small rivers, and methane rich tidal flats.

Though we did not find any clear seasonal pattern, sampling through the year also enabled us to discover that the methane distribution in the Elbe estuary was subject to significant temporal changes. We assume that these changes were controlled by the interaction of Elbe water discharge and methane concentrations in the mouth of the Elbe, which were higher in the warmer seasons. More information on the tidal surge, as well as the current regime would be useful for a better interpretation of the methane variations. However in the present study we could show that salinity explained about 57% of the methane variability.

Methane oxidation measurements were made in this area for the first time during at least the last 10 years. We discovered that methane oxidation was likely not a significant methane sink in most of the Elbe estuary. However, more data on water residence time is needed to make definite conclusions. The main factors affecting methanotrophic activity were methane concentration, salinity, and temperature. However, further kinetic studies would be useful to gain more insight into the influence of methane concentrations on MOX.

Acknowledgements

Many thanks are given to the scientific parties and crews of the research vessels Prandtl and Uthörn. We thank K.W. Klings for excellent technical assistance and the group of Prof. Wiltshire (K. Carstens) for providing hydrographic and chemical data. The work of A.M. was funded by the DAAD, by the Grant Agency of the Czech Republic (Grant no. 13-00243S) and a grant of the Faculty of Science, University of South Bohemia (GAJU 04-145/2013/P).

Manuscript III

Effect of salinity and light on aerobic bacterial methane oxidation in the marine and freshwater

Roman Osudar, Karl-Walter Klings, Julia Warnstedt, Dirk Wagner, Ingeborg Bussmann

Abstract

Salinity is an important environmental control of aerobic methane oxidation (MOX), which reduces emission of portent greenhouse gas methane to the atmosphere. Effect of salinity on MOX is especially meaningful in the river estuaries and adjacent coastal waters which are important sources of methane emission and at the same time are usually characterized by the pronounced salinity gradient. Using MOX rates, calculated following radiotracer technique, as a measure of methanotrophic activity we tested the effect of immediate and gradual salinity change on the methanotrophic bacteria (MOB) isolates and natural marine (North Sea) and freshwater (Elbe River) MOB populations. Additionally we tested the effect of light on MOX considering limited knowledge of the importance of this environmental control. According to our results *Methylomonas* sp. and *Methylosinus trichosporium* are resistant to salinity increase in contrast to *Methylovulum* sp. and *Methylobacter luteus*, which are sensitive to salinity increase. Natural MOB populations from the freshwater are more resistant to salinity increase than those from the marine water to salinity decrease. In both cases, however, response of the natural MOB populations to salinity stress appeared to be heterogeneous, which is likely attributed to variance in MOB community composition. Gradual salinity increase in contrast to immediate one can attenuate salinity effect. Light has a selective inhibitory effect on methanotrophic activity of MOB isolates and communities in natural environments.

1. Introduction

Methane is an important radiatively active trace gas, responsible for approximately 20% of the greenhouse effect (Cicerone & Oremland, 1988, IPCC, 2014). Its atmospheric concentration was steadily increasing over the past 300 years, mostly due to anthropogenic activities (Singh *et al.*, 2010). Sources of the methane emission to the atmosphere can be divided into two categories: anthropogenic (≈ 60 %) and natural (≈ 40 %) (Kirschke *et al.*, 2013). Freshwaters such as lakes and rivers and near-shore marine environments such as shelf areas and estuaries are an important natural methane source (Bange *et al.*, 1994, Bange, 2006).

The main sink of methane in the aerobic aquatic environments is bacterial methane oxidation. It can be responsible for the disposal of up to 80-90 % of the available methane (Reeburgh *et al.*, 1993, Guérin & Abril, 2007). There are several factors, which can affect methane oxidation rates: methane concentration (Gentz *et al.*, 2013, Jakobs *et al.*, 2013, Mau *et al.*, 2013), temperature (Lofton *et al.*,

2014), salinity (de Angelis & Scranton, 1993), oxygen (Guérin & Abril, 2007), suspended particulate matter (Middelburg *et al.*, 2002, Abril *et al.*, 2007), light (Dumestre *et al.*, 1999, Murase & Sugimoto, 2005) etc. However, most of these findings are based on environmental studies and the magnitude of the impact of each individual parameter is hard to assess.

In our study we focused on two environmental factors: salinity and light. Investigation of salinity tolerance of methanotrophic bacteria (MOB) leads us to more basic questions on the salt requirements and physiological responses of bacteria in general. To describe microorganisms according to their behaviour towards salt, different classification schemes have been devised. The most widely used was suggested by Kushner (1978). The three principal groups are: 1) non-halophilic microorganisms (grow best in media containing less than 0.2 M salt); 2) halophilic microorganisms (grow best in media containing 0.2–5.2 M salt); and 3) halotolerant microorganisms (non-halophilic microorganisms, which can tolerate salt). Halophilic microorganisms can be further contingently classified into slight (0.2–0.5 M salt), moderate (0.5–2.5 M salt), borderline extreme (1.5–4.0 M salt) and extreme halophiles (2.5–5.2 M salt) (Kushner, 1978, Oren, 2013). Most freshwater and marine microorganisms belong to non-halophilic and slight halophilic groups respectively. Most known MOB have been isolated from the non-saline environments (soils, sediments and lakes (Hanson & Hanson, 1996, Khmelenina *et al.*, 1999), however there are few examples of MOB isolated from marine (Hirayama *et al.*, 2013, Tavormina *et al.*, 2015) and other hypersaline environments (Trotsenko & Khmelenina, 2002).

So what happens if bacteria encounter a sudden change of salinity, i.e. external osmolarity? When salinity increases the response of most bacteria to hyperosmosis has two phases. The immediate and short-term response to hyperosmotic and high-salinity changes is the accumulation of K^+ in the cell (Naughton *et al.*, 2009). As the Na^+ ions require a lot of water for its hydration, it is transported out of the cell in exchange for K^+ ions (Eitinger *et al.*, 2007). Because high K^+ concentrations are detrimental to most cells, a more long-term strategy to deal with osmotic shock is required. The second strategy, which is more widely used among halophiles and microorganisms, which have to face salinity stress in general, is the synthesis and/or accumulation of organic osmotic solutes (Naughton *et al.*, 2009) and references therein). The so-called compatible solutes, balance the osmotic pressure of the surrounding medium and maintain cell turgor pressure. Compatible solutes are low molecular-weight organic compounds, named so because they do not interact with macromolecules in detrimental ways (Reina-Bueno *et al.*, 2012). In the opposite case the hypoosmotic shock, a sudden downward shift in the external solute concentration is life threatening. Water rushes into the cell and immediately increases turgor pressure and membrane tension, consequently, the cell is faced with rupturing (Morbach & Krämer, 2002). Under these conditions

emergency release valves, so-called mechanosensitive channels, are activated. These channels allow an almost instant adaptation to a lowered external osmolarity. In a second step cytoplasmic solutes are effectively jettisoned into the environment to reduce the force for water entry by lowering internal osmolarity (Morbach & Krämer, 2002). The protection provided by mechanosensitive channels depends strongly on the rate of osmotic change as well as the genetic background (Bialecka-Fornal *et al.*, 2015). The majority of cells "fail" long after (10 to 20 min) the osmotic challenge took place (Bialecka-Fornal *et al.*, 2015). MOB adapted to high salinity and/or pH values are geno- and phenotypically different from the inhabitants of freshwater environments with neutral pH values and have been described as new species (Khmelenina *et al.*, 2010). However, irrespective of their taxonomic affiliation halophilic and halotolerant MOB, synthesize the same spectrum of compatible solutes, mostly the amino acid ectoine (Khmelenina *et al.*, 2010).

Beside the investigation on the ecophysiology of single strains, there are also more recent studies on the gene abundance and expression patterns along a salinity gradient indicating that the adaptation to a salinity change can also occur on a community level (Fortunato & Crump, 2015).

In this study we assessed the dependence of methanotrophic activity of freshwater MOB on an increase of salinity and vice versa the dependence of marine MOB on a decrease of salinity. Our hypothesis was that different MOB species have different salinity resistance, thus experiments were conducted with environmental water samples and also with pure cultures of various MOB. As an alternative to immediate salinity change we also performed experiments where salinity was altered gradually, expecting therefore to attenuate osmotic stress for the bacterial cells.

Light was also shown to have an inhibitory effect on methane oxidation in several studies (Dumestre *et al.*, 1999, Murase & Sugimoto, 2005), however in other studies no influence of light was detected (van der Nat & Middelburg, 1998). In our study we also tested how freshwater and marine water MOB communities as well as pure cultures respond to light influence.

2. Materials and methods

2.1. Sample material

Experiments were conducted with the environmental samples (the Elbe River and the North Sea), and with methanotrophic cultures. The Elbe River water samples were collected near Hamburg at Elbe kilometer EC 659. The North Sea water samples were collected at Helgoland Island (German Bight, North Sea). We sampled from surface waters (1 m below the surface) with an UWITEC water sampler. Samples were stored for maximal 2 days at 4°C in the dark.

Methanotrophic cultures were grown with modified NMS medium (Whittenbury *et al.*, 1970) buffered with 10 mM HEPES and 0.15 mM PO4 under an atmosphere of 50% CH4 and rest air. They

were grown in glass desiccators at 18°C in the dark. Pure cultures of *Methylosinus trichosporium*, *Methylobacter luteus* were obtained from DSMZ and NBRC, the German and Scottish culture collections, respectively. The strains (*Methylovulum* sp., and *Methylomonas* sp.) had been isolated from river water of the Elbe at Elbe kilometer EC 659. The isolate *Methylovulum* sp. has been tentatively described as 97% similar to *Methylovulum miyakonense* and *Methylomonas* sp. was 97% similar to *Methylomonas lenta* (Bussmann et al., (in prep)). For the experiments colonies were scrapped from agar plates, incubated in fluid medium in cell culture bottles (Nunc). To an OD of approximately 0.5 and then transferred into the different experimental set ups. Abbreviated names of all the experiments with dates and short descriptions are summarized in Table 1.

Table 1. Dates and short forms of the performed experiments with numbers of the figures, which illustrate the main results

	Concept of the performed experiment		
	Immediate salinity change	Gradual salinity change	Light impact
Freshwater samples	Dec-2011; IS-FW-1; Fig. 1a May-2012; IS-FW-2; Fig. 1b Feb-2013; IS-FW-3; Fig. 1b Jun-2013; IS-FW-4; Fig. 1a	Feb-2013; GS-FW; Fig. 4c	Jun-2013; L-FW-1; Fig. 5a Nov-2012; L-FW-2; Fig. 5b Feb-2013; L-FW-3; Fig. 5c
Marine water samples	May-2012; IS-MW-1; Fig. 3a May-2012; IS-MW-2; Fig. 3b Feb-2013; IS-MW-3; Fig. 3a Jun-2013; IS-MW-4; Fig. 3b		Jun-2013; L-MW-1; Fig. 6a Oct-2012; L-MW-2; Fig. 6b Sep-2012; L-MW-3; Fig. 6c
Methylovulum sp.	Apr-2013; IS-methylovulum; Fig. 2a	Feb-2013; GS-methylovulum; Fig. 4b	May-2013; L-methylovulum; not shown
Methylomonas sp.	Jan-2013; IS-methylomonas; Fig. 2b		May-2013; L-methylomonas; not shown
Methylobacter luteus	Jan-2013; IS-methylobacter; Fig. 2a	Mar-2013;GS- methylobacter; Fig. 4a	Nov-2012; L-methylobacter-1; not shown Jan-2013; L-methylobacter-2; not shown
Methylosinus trichosporium	Jan-2013; IS-methylosinus; Fig. 2b		Nov-2012; L-methylosinus-1; not shown Jan-2013; L-methylosinus-2; not shown

2.2. Determination of the methane oxidation rate

Samples were filled bubble-free into 120 ml glass serum bottles, capped with black rubber stoppers, and sealed with an aluminium crimp. To eliminate agents that inhibit methane oxidation (such as soap), the glass bottles and the stoppers before being used underwent extensive chemical cleaning

as suggested by Osudar *et al.* (2015). Each experimental set up was performed with 3–10 parallels. As the experimental manipulations reduced the natural methane concentration, we added unlabeled methane to all set ups. Final methane concentration varied from approximately 10–20 (near in situ concentration) to 1000 nmol L^{-1} for marine and freshwater samples and from 0.1–0.2 mmol L^{-1} for cultures.

MOX rates were measured following radiotracer technique using tritiated methane (American Radiolabeled Chemicals, 20 Ci µmol-1, Bussmann *et al.* (2015)). Diluted tracer (0.1 mL) was added to the samples (2 kBq ml^{-1}) vigorously shaken and incubated in the dark near *in situ* temperature. MOB from the Elbe River and the North Sea were incubated for 20-24 hours. Pure cultures were incubated for 5 hours. After incubation methane oxidation was stopped by adding 0.3 mL of 25 % H_2SO_4 (samples with salinity > 10) or 5N NaOH (samples with salinity ≤ 10). Controls were stopped before the addition of tracer.

The MOX rate was determined by relating the radioactivity in the sample (C^*H_4) with the radioactivity of the (tritiated) water ($^*H_2O$) that was produced. This ratio was, multiplied with the ambient methane concentration ($[CH_4]$) corrected for the incubation time (t) (Bussmann *et al.*, 2015). The methane concentration in each bottle was determined by gas chromatography.

In the light effect experiment with the *Methylomonas* sp. isolate we detected big differences between the methane concentrations in the samples. For this experiment only, we calculated the turnover time (tt). The turnover time is the time it would take to oxidize all the methane at a given MOX rate, assuming that methane oxidation is a first-order reaction. This parameter is independent of the ambient methane concentration. The turnover time was calculated as the inverted ratio (r) corrected for the incubation time (t).

To make comparison of the experiments easier we decided to compare the data on the basis of percentages. The initial MOX rate - without any salinity modifications - was set as 100%.

2.3. Immediate change of salinity

There are different definitions of salinity and salt concentration. In oceanography the salinity is refers to the electronic conductivity of seawater, the so called „practical salinity unit = PSU“, which does not have a unit. Seawater is composed of many ions, but in physiological experiments and the discussion of the microbial salt tolerance, this aspect is simplified / restricted to the concentrations of sodium chloride (NaCl). In the course of this study we decided to simplify these aspects to the following conversion scheme: 30 g L^{-1} NaCl = 0.5 mol L^{-1} NaCl = 3% NaCl = 30 ‰ = 30 PSU.

The effect of changing salinity on the MOX rate was determined for Elbe River water, North Sea water and for the methanotrophic cultures. To change the salinity of the samples we either added

NaCl (Sigma, p.a.) to the samples (Experiments IS-FW-1, IS-methylosinus, - methylobacter, -methylovulum and -methylomonas) or mixed marine and freshwater to the requested salinities (Experiments IS-FW-2, -3, -4, IS-MW-1, -2, -3 and -4). Earlier investigations (de Angelis & Scranton, 1993) and our preliminary experiments had shown that there was no difference between these manipulations.

For the mixing experiments, bacteria were separated from riverine and marine samples (3 L) by filtering them onto 5 µm and 0.2 µm filters. Afterwards they were resuspended in 30 mL of the original water. The sterile filtered riverine and marine waters were mixed to the requested salinities (1, 3, 5, 10, 20 and 30 PSU). The bacteria were added to these mixtures to the initial concentration and the mixtures were distributed into triplicate 120 ml glass bottles. In these bottles the MOX-rate was determined as described above. Salinity was measured using Universal Pocket Meter (Multi 340i) with precision of 0.01.

2.4. Gradual change of salinity

In a next step we wanted to test if MOB were able to adapt to a gradual change of salinity. Previous experiments had shown that *Methylobacter luteus* and *Methylovulum* sp. sensitive to changes in salinity. Thus these two cultures were chosen for further experiments (Exp. GS-methylobacter and GS-methylovulum). Additionally, we tested the natural MOB populations of Elbe and North Sea water (Exp. GS-FW and GS-MW).

Triplicate samples (250 ml) of methanotrophic cultures, riverine or marine water were incubated in 600 mL cell culture bottles (Nunc) in a desiccator as described above. Every day an aliquot was withdrawn and distributed into 12 mL ampoules to measure MOX and one subsample to measure salinity. Afterwards we added NaCl directly to three parallels, while to another 3 parallels no salt was added. Thus we had no dilution effect and the cell number in both set-ups should remain similar. The flasks were gently shaken to dilute the salt and then incubated again in the desiccator. Within 8 days the salinity increased from 0.3 to 10 PSU. To marine water samples we added sterile filtered MQ-water, while to another three parallels we added sterile filtered sea water. Thus all the samples were diluted, but both set ups with the same amount of water, so the cell numbers should remain comparable. Within 8 days the salinity decreased from 32 to 22 PSU.

To normalize for the growth (and increasing MOX rate) we calculated the ratio between MOX without salt addition to the MOX with salt addition. Thus, a value around 1 indicates no influence of salinity, values < 1 indicate an inhibiting effect of salinity and values >1 indicate a stimulation through changed salinity.

2.5. Light regime

To test the effect of light on methane oxidation, different samples were exposed to light and compared with controls, incubated in the dark (Table 1). Samples were incubated in 120 ml glass bottles for 5 or 10 hours under a day light lamp as used for growth of planktonic algae (Lumilux L 58W/865, 380–780 nm, Osram), at 15°C. Distance from the light 20–30 cm. Controls were wrapped with aluminum foil. Eight to ten parallels were used for the cultures and environmental samples respectively. The average MOX rate of the dark incubation was set as 100%.

2.6. Statistics

To test the significance of light effect on MOX rates we performed t-test in the case of a normal distribution, and a non-parametric Mann-Whitney Rank Sum Test when a normality test (Shapiro-Wilk Test) failed. In the box plots the bottom and top of the box are the first and third quartiles, and the band inside the box is the second quartile (the median). Whiskers above and below the box indicate the 90^{th} and 10^{th} percentiles. Percentile value (v) is calculated according to Cleveland method:

$v=f*xk+1+(1-f)*xk$.

Where Xn is the highest ranked data point, p is percentile, k is the nearest integer to $N*p/100$, and $f=N*p/100 + .5 - k$

The plots were created using SigmaPlot for Windows Version 11.0.

3. Results

3.1. Immediate change of salinity

In a first step we tested the influence of the immediate increase of salinity on the MOX rate in the Elbe water. In all experiments (IS-FW-1 – IS-WF-4) the immediate salinity increase resulted in a decrease of MOX rates (Fig. 1).

In the experiments IS-FW-1 and IS-FW-4 the methane concentrations were low (20 and 160 nmol L^{-1}), thus also the initial MOX rates was low (approximately 2 nmol L^{-1} h^{-1}, at 0 salinity). The increase of salinity to 1 PSU led to a steep drop of the MOX rate, to 60 and 40% of initial rate (Fig. 1a). At salinities 5–30 PSU MOX rates declined to 25–40% of the initial rate.

In the experiments IS-FW-2 and IS-FW-3 the methane concentrations were higher (190 and 950 nmol L^{-1}), thus also the initial MOX rates was higher (11–13 nmol L^{-1} h^{-1}). Up to a salinity of 5 PSU, MOX rates declined to 64–66% (Fig. 1b). At higher salinities of 10–30 PSU, MOX rates stayed almost stable at 51–76% in experiment IS-FW-2 and at 32–45% in experiment IS-FW-3.

Thus there seemed to be a sensitive and less sensitive response of the freshwater samples to an immediate increase of salinity.

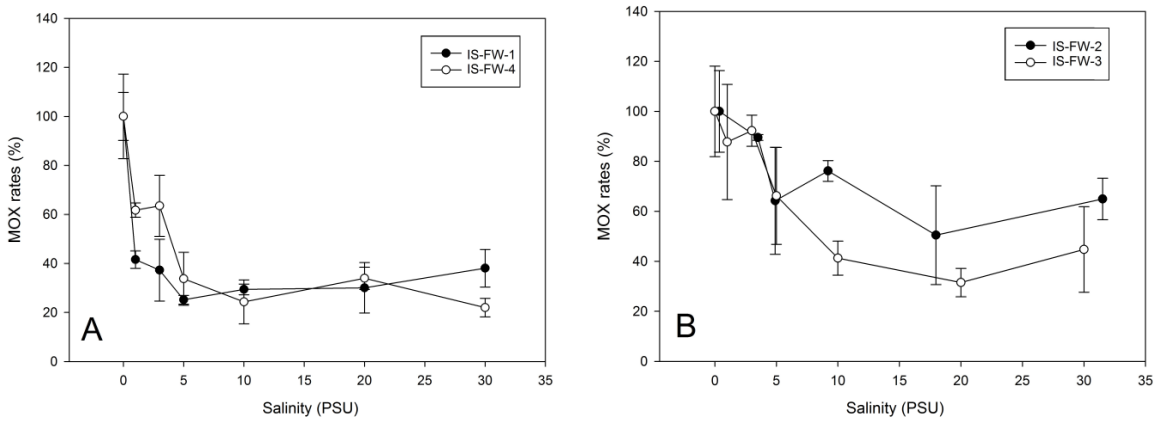

Fig. 1. Effect of immediate salinity increase on the MOX rates in samples from the Elbe River. IS-FW-1 and IS-FW-4 experiments (a) and IS-FW-2 and IS-FW-3 experiments (b). Measurements of methane oxidation rates were performed in triplicate; shown is the mean with the standard deviation.

Salt was also added to different methanotrophic cultures (*Methylosinus trichosporium, Methylobacter luteus, Methylovulum* sp. and *Methylomonas* sp.). In the experiment with *Methylovulum* sp., MOX rates decreased proportionally to salinity and reached 23% at salinity 10 (Exp. IS-methylovulum, Fig. 2a). At salinities from 10 to 30 PSU, MOX rate declined to 8%. In the experiment with *Methylobacter luteus*, MOX rate at salinity 1 PSU dropped to 72% (Exp. IS-methylobacter, Fig. 2a). At salinities from 1 to 20 PSU, MOX rates decreased from 72 to 53%. At salinity 30 PSU, MOX rate abruptly dropped to 8%. In contrast, *Methylosinus trichosporium* (Exp. IS-methylosinus) and *Methylomonas* sp. (Exp. IS-methylomonas) strains showed variable MOX rate fluctuations, including an increase at salinities from 1 to 10 PSU. Only at salinities from 20 to 30 PSU, MOX rate decreased to 64–89%, (Fig. 2b). Thus, the response of methanotrophic cultures to salinity increase differed depending on the culture.

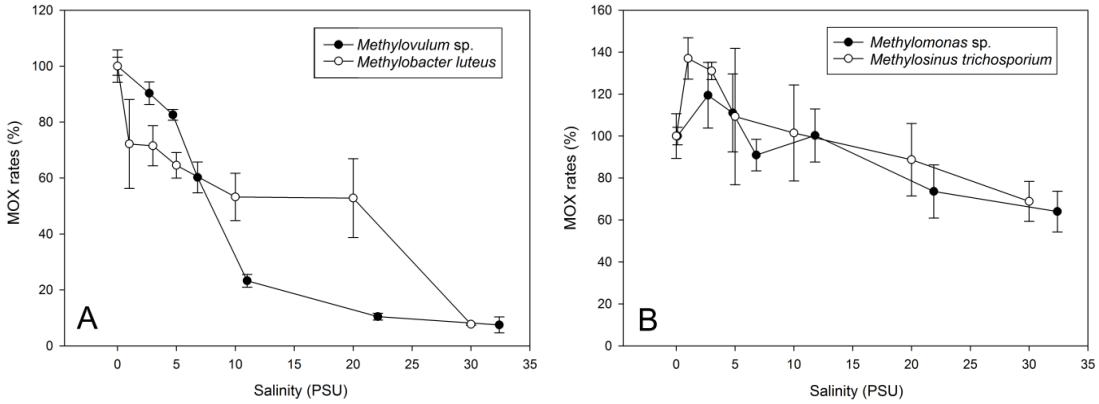

Fig. 2. Effect of immediate salinity increase on the MOX rates of methanotrophic cultures; for *Methylovulum* sp. and *Methylobacter luteus* (a) and *Methylomonas* sp. and *Methylosinus trichosporium* (b). Measurements of methane oxidation rates were performed in triplicate; shown is the mean with the standard deviation.

The influence of decreasing of salinity was tested with marine methanotrophs from North Sea water. In experiments IS-MW-1 and IS-MW-3, the final methane concentrations were 300 and 950 nmol L^{-1} respectively and the corresponding initial MOX rates were relatively high (9–11 nmol L^{-1} h^{-1}). At salinities from 30–20 PSU the MOX rates stayed stable in both experiments (Fig. 3a). At salinities < 15 PSU the MOX rate declined to 10–12%. In experiments IS-MW-2 and IS-MW-4, the final methane concentrations were 360 and 20 nmol L^{-1} respectively and the corresponding initial MOX rates were lower (3 and 0.2 nmol L^{-1} h^{-1} respectively). At the salinity of 20 PSU, MOX rate decreased to 30–35% of the initial (Fig. 3b). At the salinities < 10 PSU, MOX rates declined to 1–17 %. Thus there also seemed to be a sensitive and less sensitive response of the marine samples to an immediate decrease of salinity, like in the freshwater samples.

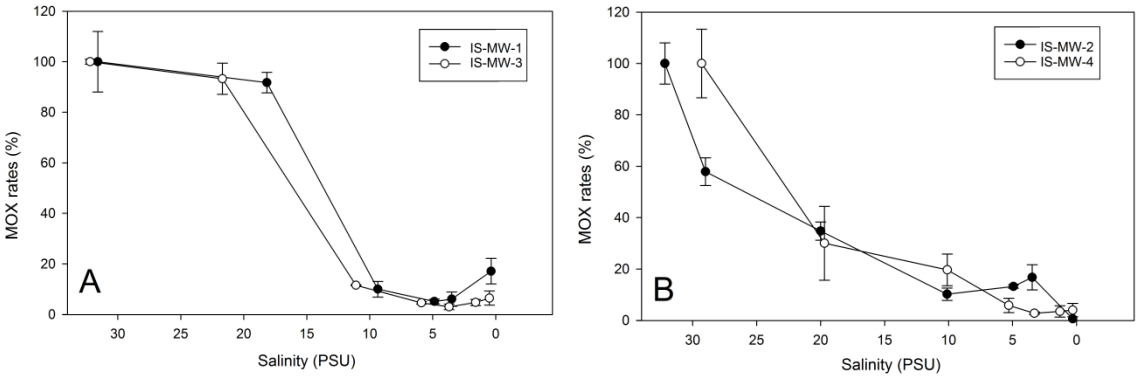

Fig. 3. Effect of immediate salinity decrease on the MOX rates for the marine water samples. The initial MOX rate at a salinity of 30 was set as 100% and for better comparison with Fig. 1, 2 the x-axis is displayed in reverse direction. IS-MW-1 and IS-MW-3 experiments (a) and IS-MW-2 and IS-MW-4 experiments (b). Measurements of methane oxidation rates were performed in triplicate; shown is the mean with the standard deviation.

3.2. Gradual salt addition

In this set of experiments we tested if the observed sensitivity to changes in salinity could be reduced when the in/decrease occurs gradually over 10 days.

As shown in previous experiments *Methylobacter luteus* and *Methylovulum* sp. were sensitive to an increase of salinity from 0 to 10 PSU (Fig. 2a). However, if we gradually increased salinity by 1.25 PSU per day the ratio between MOX rate with and without salt addition (MOX $rate_{+salt}$ / $MOX_{control}$) remained around 1. Thus, *Methylobacter luteus* was able to adapt and its activity remained stable and comparable to the control without salt addition (Exp. GS-methylobacter, Fig. 4a). In contrast, in the experiment with *Methylovulum* sp. the ratio between MOX rates with and without salt addition was stable until a salinity of 3 PSU, but then declined to almost 0. Thus, *Methylovulum* sp. was not able to adapt to this gradual increase of salinity (Exp. GS-methylovulum, Fig. 4b). Natural Elbe River water showed the same pattern as *Methylobacter luteus* and the population adapted to the gradual salinity increase (Exp. GS-FW, Fig. 4c). However, at days 6 and 7 with salinities of 7.7 and 9.2 PSU we observed a strong variability. We also performed experiments in which we gradually decreased the salinity from 32 to 22 PSU for marine water samples. Unfortunately we obtained ambiguous results.

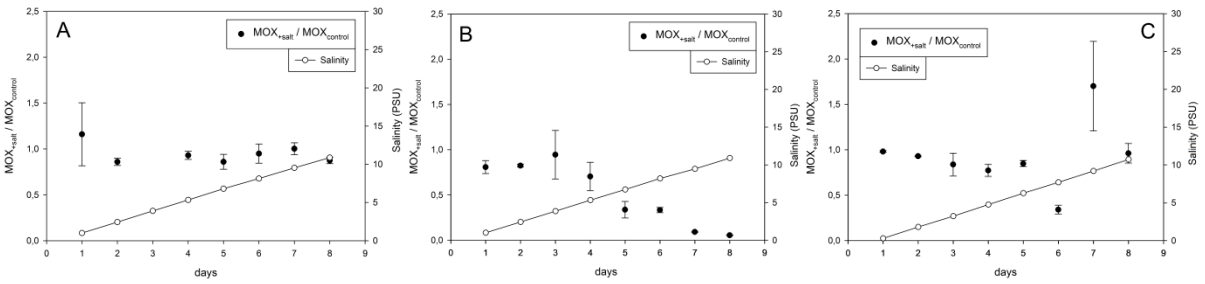

Fig. 4. Effect of gradual salinity change on the MOX rates for the *Methylobacter luteus* culture (a), *Methylovulum* sp. culture (b) and samples from the Elbe River (c). Measurements of methane oxidation rates were performed in triplicate; shown is the mean with the standard deviation.

3.3. Effect of light on MOX rate

Beside the effects of salinity change, also light is supposed to influence methanotrophic activities. Thus we performed several experiments with pure methanotrophic cultures, as well as environmental samples from a freshwater and marine environment.

The effect of light on the MOX rates in the Elbe River water was tested three times. The first experiment showed no difference between dark and light incubations (100 versus 100%, Exp. L-FW-1, Fig. 5a). The other two experiments showed lower average MOX rates in light incubations with 73

and 83% (Exp. L-FW-2 and L-FW-3, Fig. 5b, c). However, only in experiment L-FW-2 the differences was statistically significant (t-test, n=10, P<0.001).

In one of three experiments with the North Sea water we detected no difference between dark and light incubations (100 versus 104%, Exp. L-MW-2, Fig. 6b). The other two experiments showed lower average MOX rates in light incubations with 76 and 43% (Exp. L-MW-1 and L-MW-3, Fig. 6a, c). However, in none of these experiments the difference was statistically significant.

The influence of light on the MOX rate of different cultures was tested in two experiments each. *Methylobacter luteus* showed significantly lower MOX rates when incubated in the light (56 and 61%, t-test, p = 0.005 and 0.01, n = 4, Exp. L-methylobacter-1, -2). Also *Methylomonas* sp. had significantly lower turnover time when grown in the dark (p = 0.03, n = 4, Exp. L-methylomonas). In contrast, *Methylosinus trichosporium* and *Methylovulum* sp. were insensitive to light (Exp. L-methylosinus-1, -2 and L-methylovulum).

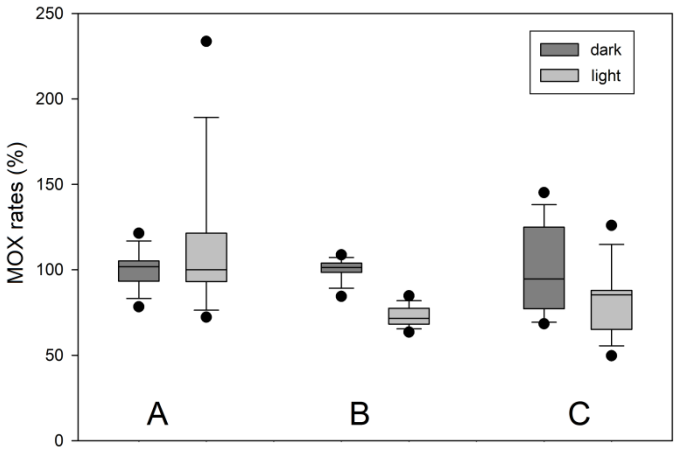

Fig. 5 Effect of light on the MOX rates for the Elbe River samples as shown in three experiments (a) L-FW-1 ,(b) L-FW-2 and (c) L-FW-3 , more details are given in table 1. The boxes show the first, second (the median) and third quartiles.

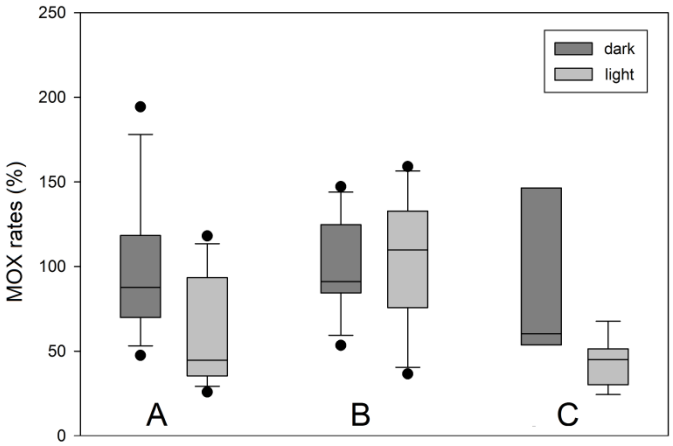

Fig. 6 Effect of light on the MOX rates for the North Sea samples as shown in three experiments (a) L-MW-1 ,(b) L-MW-2 and (c) L-MW-3, more details are given in table 1. The boxes show the first, second (the median) and third quartiles.

4. Discussion

4.1. Response of MOB strains to increasing salinity

In our study we investigated the effect of increasing salinity on methane oxidation on the level of methanotorphic cultures (Exp. IS-methylovulum, -methylomonas, -methylobacter and -methylosinus) as well as on a mixed natural population level (Exp. IS-FW-1, -2, -3 and -4). We also tried to include the temporal aspect, i.e. initial osmolytic shock versus a gradual increase of salinity (GS-FW, GS-methylovulum, GS-methylobacter) to allow for possible production of osmolytes.

Two of the investigated strains (*Methylobacter luteus* and *Methylovulum* sp.) were sensitive to an initial change of salinity (Fig. 2a). At salinities of 10 PSU only 55 and 20% of the initial activity was detected. In contrast *Methylomonas* sp. and *Methylosinus trichosporium* were resistant to the first osmolytic shock. When salinity increased gradually (1.2 PSU / day) the before sensitive *Methylobacter luteus* could adapt (probably producing osmolytes), while *Methylovulum* sp. still could not cope. These findings are supported by the fact that when testing for growth of *Methylovulum* sp. over three weeks, no growth was observed at 5 and 10 PSU (Bussmann *et al.*, in prep). Thus, when methanotrophic bacteria are transported with the river into the marine environment, some species will not be able to stay active and grow. If the mixing process is slow, other methanotrophs will be able to adapt. This hypothesis is supported by Painchaud *et al.* (1995), who observed a strong bacterial mortality in fast mixing estuaries (hours), while no mortality was observed when the mixing occurred within days.

In a recent study Ho *et al.* (2013) linked functional traits and ecological characteristics of methanotrophs to their life strategies. Comparing their classification with our results, we agree that

Methylobacter strains are assigned to be rather not stress-resistant, while *Methylosinus* strains are assigned to be stress-resistant. In contrast, *Methylomonas* strain which we found to be stress-resistant is characterized to be not stress-resistant in the referred study. Not much is known on the ecological characteristics of *Methylovulum* strains yet.

4.2. Response of a river-borne MOB population to increasing salinity

In the Exp. IS-FW-1, -2, -3 and -4 the whole methanotrophic community of river water was exposed to increasing salinities. Here again, we found a similar pattern with a very sensitive community (Exp. IS-FW-1 and -4) and a moderately sensitive one (Exp. IS-FW-2 and -3). When a gradual increase of salinity was allowed, the community seemed to be resistant and no reduction in activity was observed (Exp. GS-FW).

We hypothesized that other environmental stressors, such as methane concentration, could affect the sensitivity of the MOB community. However, we encountered very sensitive and moderately sensitive populations despite the almost similar methane concentrations (160 and 190 nmol L^{-1}). It is remarkable, however, that the MOX rates also varied at the salinity unamended experimental set ups. Furthermore, in the experiments with the initially higher MOX rates MOB population was more salinity resistant. We assumed that the community composition at the start of the experiment influences the sensitivity. Variance in salinity tolerance between different MOB strains is well documented (Khmelenina *et al.*, 2010) and also shown in the present study. Also it seems quite likely that MOB community composition in the water column of the Elbe River mouth is subject to temporal variations. We could have expected to observe more salinity-resistant MOB communities in the water samples collected in the warmer months. It was shown before that optimal temperature can mitigate the effect of salinity stress on freshwater bacteria (McArthur, 2006). However, correspondence between sampling period and salinity tolerance was not observed either. At the same time temperature is not the only potential environmental control of MOB community structure. The Elbe river estuary is a very dynamic aquatic system (Osudar *et al.*, 2015) and fluctuations in bacterial community composition followed by the influence of various factors or dispersion from the other aquatic and terrestrial environments seem quite possible. So, for example, a study on MOB community composition in sediments of the Tyne estuary shows that some of the observed “extremophilic” types originate from various and sometimes remote sites.

Unfortunately we did not allow for a full set of combination of the mentioned factors. So, for example, it would be interesting to observe salinity tolerance of the moderately sensitive communities of MOB at low (*in situ*) methane concentrations (<200 nmol L^{-1}). We can conclude, however, that some MOB communities will not be able to cope with the salinity stress even at high

temperatures typical for the warm months and relatively high methane concentrations (160 nmol L^{-1}).

4.3. Response of marine MOB communities to decreasing salinity

There are only few marine methanotrophs described until now (Hirayama *et al.*, 2013, Hirayama *et al.*, 2014, Tavormina *et al.*, 2015). Not much is known on their ecological capabilities; only that they do not grow at salinities < 1% (approximately 10 PSU). The 10 PSU seem to be a threshold, also displayed in the present study. In all four experiments activity at salinity ≤ 10 PSU was on average 8 ± 6 %. At salinity of approximately 20 PSU moderately sensitive MOB communities stayed rather active (with an average of 93 ± 1 % activity), while the activity of the very sensitive communities substantially decreased (with an average of 32 ± 3 % activity).

In our study we exposed freshwater MOB pure cultures as well as marine and freshwater natural populations to salinity stress. We found stress-resistant strains, as well as more sensitive ones. The reactions of the natural communities could also be divided into stress-resistant and stress-sensitive responses. The responses of the communities did differ between sampling times. We could not assign methane concentration to this variable sensitivity. Thus, we hypothesized that the response on the community level is determined by the community composition, i.e. the ratio of stress-resistant and stress-sensitive strains. Unfortunately we were not able to investigate these effects. However, also the frequency of disturbances as well as the site history are important factors in assessing the resilience of the MOB community to changes in salinity (Ho *et al.*, 2016).

Within an estuary we assume that marine methanotrophs would be active down to a salinity of approximately 10 PSU, but only the moderately sensitive communities. In contrast freshwater MOB seem to be more flexible and should be able to adapt also to marine environments. However, as pointed out by Ho *et al.* (2016), on the long run the indigenous population with more competitive traits will become an active part of a stable MOB population again.

4.4. Response of MOB strains and natural populations to light

Results of the investigations of effect of light on methanotrophy in aquatic environments are contradictory (van der Nat & Middelburg, 1998, Dumestre *et al.*, 1999, Murase & Sugimoto, 2005), which can be possibly explained by the heterogeneity in water optical properties, effect of other environmental controls and heterogeneity in light tolerance of different MOB specious. However, light has a potential to damage bacterial cells or hypothetically inhibit methanotrophic activity directly (Dumestre *et al.*, 1999). In the current study inhibitory effect of light was observed in most of the experiments with both environmental samples and MOB isolates. However, only for one freshwater sample out of three (MOX rate decrease up to 70%) and two MOB isolates out of four

(MOX rate decrease up to 60%) this effect was statistically significant. These results are generally in line with our salinity experiments indicating that environmental samples as well as MOB isolates have different tolerance to environmental stressing factors.

It should be noted that effect of light on MOX rates shown in our experiments might diverge from the effect of sunlight on MOX in nature due to the difference in the light wavelengths. Apart from the visible light, bacterial cells can be harmed by the UV light, not used in our experiments. Additionally, samples, which were wrapped with aluminium foil to avoid light influence, could be exposed to additional heating.

5. Conclusion

In the current study we showed that: (1) MOB isolates as well as marine and freshwater MOB communities substantially differ regarding salinity effect on their methanotrophic activity; (2) marine water MOB communities are generally more sensitive to salinity decrease than freshwater MOB communities are to salinity increase (3) gradual salinity increase can mitigate salinity influence on methanotrophic activity of MOB isolates and freshwater MOB communities; (4) light has a selective inhibitory effect on methanotrophic activity of MOB isolates and MOB communities in natural environments.

The current research has shed some light on the effect of salinity change on methane oxidation in marine and freshwater environments revealing even more questions to be answered in the future investigations and emphasizing the complexity of the studied phenomena. The main questions, still to be answered are: how long salinity-resistant MOB communities and isolates can survive and stay metabolically active at different salinities, can gradual salinity decrease mitigate salinity effect on activity of marine MOB communities and isolates, how salinity controls composition and methanotrophic activity of MOB communities and how sustainable these communities in the changing environment.

III SYNTHESIS

3.1 Discussion

1) What determines methane distribution in the interfaces between aquatic and terrestrial environments?

This study accounts for the field of environmental microbiology. It contributes to our understanding of the interaction between bordering aquatic and terrestrial environments with regard to methane distribution and aerobic methane oxidation. It also helps to assess consequences of global climate change for complex ecosystems and biomes. Arctic water bodies and estuaries, chosen as the study sites, exemplify different aquatic ecosystems, which represent important methane sources and are subject to pronounced influence of the bordering environments.

Arctic permafrost regions are an example of areas with enhanced interactions between aquatic and terrestrial environments which, amongst others, consequences for the methane distribution and cycling. As substantiated by the present research, methane concentrations in Arctic water bodies greatly vary. This is attributed to the high heterogeneity of Arctic soil regarding its organic carbon and nutrient content, permafrost distribution, and the morphological variability of Arctic water bodies.

Methane concentration in five lake-outlet complexes varied within two orders of magnitude from 200 to 24,000 nmol L^{-1}. The lakes themselves did not show high variance except for one lake which was located at the floodplain area and had substantially higher methane concentrations. Floodplains are known to be hot spots of methane emission also from previous investigations (Van Huissteden *et al.*, 2005). It is suggested that enhanced methane production results from higher primary productivity of the floodplain vegetation and the supply of substrate for methanogens by sedimentation of particulate organic matter from flood water (Van Huissteden *et al.*, 2005). Indeed, the uniqueness of the studied floodplain ecosystem was also reflected in its vegetation (Boike *et al.*, 2012). It is remarkable that most of the other lakes are also flooded in the spring with different periodicity. This flooding, however, has a local, sporadic impact, and as can be concluded from the current study is less influential for the methane content.

Methane concentrations in the streams (lake outlets) were generally higher than those in the lakes and also showed higher variance regardless of flooding periodicity. Methane saturation can be attributed to the smaller volume of the streams. The current work corroborates previous, but sparse studies (Striegl *et al.*, 2012, Crawford *et al.*, 2013) showing the importance of high-latitude streams as methane sources and emphasizing the necessity of their further investigation and potential implementation into global methane emission models.

The input of methane-rich water from one of the streams was shown to increase methane concentration of the Lena River near the shore. This observation is in accordance with Bussmann (2013). She showed that creeks draining into the Lena River systems represent hot spots of methane input. Thus, apart from coastal erosion, which leads to organic carbon loading with subsequent enhanced methane production (Vonk *et al.*, 2012, Schuur *et al.*, 2015), lake outlets, which are draining into the rivers, could be considered as an alternative methane and probably organic carbon source, associated with lateral transport from terrestrial environments.

Except for one river site, methane concentrations in the Lena River did not vary substantially, ranging from 150 to 200 nmol L^{-1}. The Lena River, thus, represents a more uniform environment with a weaker terrestrial imprint at least in the scope of the studied area.

Estuaries are another example of the interface between different environments. Estuaries represent intermediate zone where methane-rich river water is mixed with methane-depleted marine water. Methane distribution in the estuary, however, cannot always be described by the conservative mixing model i.e. gradual decrease from the freshwater end-member to the marine water end-member. In some estuaries, additional methane sources were observed in the estuarine plume (Middelburg *et al.*, 2002). In the Elbe estuary, we also detected an additional methane source located in the area close to the city of Cuxhaven. According to our results this additional methane source is attributed to small tributaries and/or to enhanced methane production which originates from tidal flats. Tidal flats in the North Sea are known to be active sites of mineralization of organic material which eventually leads to methane accumulation. Due to advective flow in the tidal areas, which is of special importance in permeable sandy sediments, pore waters enriched in re-mineralized nutrients and methane are actively released from sediments into the overlying water column (Beck & Brumsack, 2012, Segarra *et al.*, 2013). Another potential reason for the enhanced methane production is anthropogenically-induced pollution. A wastewater treatment plant in Cuxhaven could lead to additional input of organics and could thus trigger *in situ* methane production both in sediments and in the water column. Input of inorganic nutrients, for example, was detectable in the hydrochemistry data. Phosphate and nitrate concentrations were especially high at the nearby station. Regardless of the origin of this methane source it is remarkable that it was not reported previously (Rehder *et al.*, 1998, Middelburg *et al.*, 2002). This can be partly explained by the lower spatial resolution of the sampling sites (Rehder *et al.*, 1998) than in the current research. Besides, both mentioned investigations were performed during single sampling campaigns without replication through the year, while our research showed that methane concentrations in the estuary are subject to temporal variations. These temporal variations are presumably controlled by the temperature and water dynamics.

Enhanced methane production in the warmer months is known for various river and estuary systems, such as the Don River, with the Taganrog Bay in the Sea of Azov, Russia (Fedorov *et al.*, 2003), and the Baltic Sea (Bange *et al.*, 1994). Clear seasonality with increased methane in the summer and autumn was also shown for the Rhine estuary (Middelburg *et al.*, 2002). However, in the Scheldt and Gironde estuaries seasonality was not pronounced (Middelburg *et al.*, 2002), nor in Humber estuary where methane concentrations were lowest in the summer (Upstill-Goddard *et al.*, 2000). According to our results, temperature in the Elbe estuary was positively correlated with methane concentration, but only at the coastal stations. At the marine stations we did not detect this dependence which can be explained by insignificant methane production and rather stable temperature regimes in the open sea water column and sediments.

Seasonality of methane concentrations also originated from variation in the Elbe water discharge. Water discharge measured from September 2010 to June 2012 at Neu Darchau gauging station (approximately 150 km from the Elbe mouth) ranged from 300 to 3,500 $m^3 s^{-1}$. Salinity, which was used as an indicator of a ratio between freshwater from the river and marine water from the sea, also showed high variations at the coastal stations and was strongly correlated with methane concentration. Tides are likely to be a significant factor affecting short-term methane distribution, as shown in previous studies (Grunwald *et al.*, 2009). However, in our investigation, we did not have enough information to correlate methane concentration with the tidal surge.

To sum up, our results reveal limitation of extrapolation and interpolation approaches used in previous studies to predict methane distribution in estuaries and proves the necessity to perform research at higher spatial and temporal resolutions.

2) How does the interaction between bordering aquatic and terrestrial environments affect abundance and community composition of MOB and MOX rates?

Our results illustrate that in the studied aquatic systems not only methane distribution but also MOX rates are strongly regulated by the bordering environments. The MOX rates in the Arctic lakes, streams and river sites varied from 0.2 to 480 nmol $L^{-1} h^{-1}$, which is in the range of previously reported studies in high-latitude lakes and rivers (Kling et al., 1992, Repo et al., 2007, Shakhova et al., 2007, Bussmann, 2013, Negandhi et al., 2013, Lofton et al., 2014, Martinez-Cruz et al., 2015). The MOX rates generally coincided with methane concentrations, especially when we compared sites with low and high methane concentrations. Thus, the highest MOX rates were detected at the streams and in the floodplain area. Additionally, MOX rates depended on the abundance of MOB. Finally, our results imply that MOX rates are linked with MOB community composition. Neither methane concentrations nor MOB abundance could fully explain enhanced MOX rates in the lakes

and streams in comparison with the Lena River; therefore, we assume that MOB in these lakes and streams are more efficient in oxidizing methane. Indeed, analysis of the MOB community structure revealed that lakes, outlet streams, and river showed individual patterns in terms of MOB community structure. The river sites were characterized by a rather homogeneous MOB community, with a dominance of three OTUs related to the genus *Methylocystis* and two OTUs related to the freshwater (FWs) cluster. In contrast, the MOB composition of the lake-outlet complexes was more heterogeneous. In addition to the MOB clusters common for all sampling sites most of the lakes and outlets had unique MOB clusters. It should be noted, however, that richness of MOB on the species level was comparable at all the sampling sites. It is interesting that *Methylocystis*-related OTUs differed in the river sites vs lakes and outlets. Remarkably, MOB in the lakes and streams had a strong terrestrial imprint. So, for example, in the lakes and streams MOB clusters typical for organic, upland and rice field soils (OSC, USC-g, RPC clusters) were more relatively abundant than at the river sites. This corroborates the observations of Crump *et al.* (2012) who stated that structure of microbial communities in aquatic environments can be strongly affected by the inoculation of soil bacteria. Bacterial transport between neighboring environments might be important considering the heterogeneity of their indigenous community composition, abundance, and, potentially, methanotrophic activity.

It is also remarkable that MOB community composition in the studied water bodies, as well as in Arctic water bodies from previous studies (Jugnia *et al.*, 2006, He *et al.*, 2012a), was highly diverse at high taxonomic level (with comparable abundance of type I and II MOB) in comparison with both terrestrial permafrost and temperate aquatic environments. Liebner *et al.* (2009) stated that predominance of either type I or type II MOB is usually indicative for environmental extremes while overall MOB community in more moderate environments, such as wetlands, is not restricted to a certain MOB group. It appears, therefore, that Arctic water bodies provide more moderate conditions than the surrounding terrestrial permafrost environments, hypothetically due to less stressful temperature regime. The studied lakes, which were 4 to 6 meters deep, do not get frozen to the bottom in the winter and are most likely underlain by layers of year-round unfrozen ground called taliks (Boike et al., 2015). The same is true for the Lena River (Costard & Gautier, 2007). Furthermore, all the samples were collected in the summer period when the surface water temperature varied between 11 and 15 °C in the lakes and approximately 17 °C in the river. Another explanation would be high heterogeneity of Arctic aquatic environments, with diverse micro-niches, suitable for different MOB. Indeed, not only sediments, but also the water column in relatively shallow Arctic and sub-Arctic ponds were shown to be stratified into different MOB clusters (He *et al.*, 2012a).

It is hard to explain, however, why MOB community composition in Arctic water bodies is more diverse than those in the lakes in the middle and low latitudes. It is tempting to speculate that Arctic aquatic environments represent developing ecosystems which undergo significant transformations and have not established a stable bacterial community yet. Knief (2015) showed that MOB in the upland soils and aquatic environments (investigated mainly in temperate zones) form distinctive and large clusters and are often specialized to a certain type of habitat. In contrast, MOB in relatively young habitats such as rice field soils, landfill cover soils, and wetlands are found in smaller distinct clusters and present also in other habitats. These ecosystems, thus, represent important markers of the future changes and should be further thoroughly investigated regarding their structure and functioning.

To sum up, our results corroborate previous investigations in Arctic and sub-Arctic aquatic environments, which showed relatively high heterogeneity of MOB within and between studied water bodies (Jugnia *et al.*, 2006, He *et al.*, 2012a). This implies that the composition of bacteria in aquatic environments, and presumably their biogeochemical functioning, are regulated by local landscape features (Comte *et al.*, 2015). The identification of these features as well as the mechanisms and potential of MOB inoculation from bordering environments on the one hand and MOB community composition (at high taxonomic resolution) and their functional potential on the other hand should become the goal for future investigations.

With regard to the Elbe estuary, MOX rates along the entire transect varied from 2.6 ± 2.7 near the coast to 0.42 ± 0.53 nmol L^{-1} d^{-1} in the open sea which is in the same range as in other aquatic environments (de Angelis and Scranton, 1993, Abril and Iversen, 2002, Middelburg et al., 2002, Silvennoinen et al., 2008, Zhang et al., 2008, Grunwald et al., 2009). The MOX rates both in the water bodies in the Lena Delta and in the Elbe estuary were positively correlated with methane concentrations. Other factors which were shown to affect MOX rates in the Elbe estuary are temperature and salinity. Though these factors are known to be important regulators of MOX rates the magnitude of their effect is largely uncertain. Lofton *et al.* (2014) stated that MOX responds linearly to increased temperature, but only under substrate saturated conditions (approximately 33 µM). Though we also observed an effect of substrate availability on the correlation between MOX rate and temperature, positive dependence of these variables was detected at much lower methane concentrations (0.04–0.2 µM). The effect of salinity on MOX rates is attributed to osmotic stress for MOB. Previously it was considered that salinity of 10 is critical for the freshwater MOB (Abril & Borges, 2005). We, however, detected high MOX rates at salinity ≤ 17. Further experiments with the Elbe River samples and pure MOB cultures showed that the tolerance to salinity substantially varies between the MOB strains and, therefore, between MOB communities which differ in community

compositions. Gradual salinity increase is likely to attenuate salinity stress for freshwater MOB as it was shown in our study. At the same time, it is not clear if gradual salinity change attenuates osmotic stress for marine MOB, that according to the obtained results are more sensitive to the salinity stress than freshwater MOB.

3.2 Conclusion

The present study focuses on the methane distribution and aerobic methane oxidation in the aquatic ecosystems which are subject to a pronounced interaction with the adjacent aquatic and terrestrial environments. Unlike many other case studies this research provides an integrated approach to understanding functioning of biomes highlighting the importance of investigation of complex ecosystems rather than individual ecosystems. Furthermore, comparison of distinct aquatic ecosystems such as Arctic water bodies and estuaries illustrates the applicability of the defined principles of integrity for different types of aquatic environments. The following conclusions can be drawn from the specific results obtained in this study:

- Methane distribution in bordering aquatic environments is strongly determined by their interaction and by the adjacent terrestrial environments. Arctic freshwater bodies are very heterogeneous regarding distribution of dissolved methane which is regulated by local landscape features (e.g. floodplain areas) and the morphology of the water bodies (lakes, streams, and river). Furthermore, aquatic environments have a great potential to transport methane from methane-rich water bodies, such as streams and floodplain lakes, to aquatic environments relatively poor in methane, such as the Lena River. Methane distribution in the Elbe estuary is determined by the dynamic balance between methane-rich river water and methane-depleted marine water. Additionally, substantial methane input occurs from tidal flats, areas of significant interaction between aquatic and terrestrial environments.
- The main environmental regulator of MOX rate is methane concentration. The highest MOX rates in the Arctic water bodies were detected in the streams and in the floodplain area while in the estuary the highest MOX rates were observed at the coastal stations. However, the interaction between bordering environments affects MOX rate not only via the regulation of methane concentrations. MOX rates in the Arctic lakes were shown to be dependent on abundance and community composition of MOB, which, in turn, were controlled by local landscape features (regardless methane concentrations) and the transport of MOB between neighbouring environments. In the estuary MOX rates are largely affected by the water salinity; however magnitude of this impact also depends on the MOB community composition.

3.3 Final remarks

With the predicted climate change, transformation of the existing ecosystems, with subsequent change in methane cycling, seems quite plausible. Aquatic environments have a high potential to play a significant role in these transformations. Main concerns on the possible consequences of global climate change for the Arctic biomes are connected with further release of the organic carbon, stored in permafrost in large amounts. Given the abundance of aquatic environments and their affiliation with taliks, Arctic water bodies are likely to stay an important methane source in the future. Furthermore, permafrost thawing might lead to formation of new water bodies or water-saturated soils (Vonk *et al.*, 2015), such as wetlands, which are shown to be important sources of methane emission, also due to mineralization of newly-produced organic carbon (Van Huissteden *et al.*, 2005). Finally, aquatic environments play an important role in transport of produced methane, or organic carbon and nutrients, which fuel methane production (Vonk *et al.*, 2015). One of the observed consequences of climate change is alteration in river discharge (Peterson *et al.*, 2002, Wagner *et al.*, 2011) and sea level rise (Rahmstorf, 2007). Input of methane, organic carbon, and nutrients together with the relocation of the estuarine area are likely to affect local coastal ecosystems, such as those in tidal flats, and thus affect methane cycling. Methane emission from the tidal flats at freshwater sites was shown to be two orders of magnitude higher than those in the saltwater sites (Abril *et al.*, 2007 and references therein).

The balance between concentrations of methane diffused in the water and the MOX rates appear to have a certain level of sustainability, which was also shown in the current research. Lofton *et al.* (2014) assumed that increase in methane availability of > 1 order of magnitude would be offset by the increased MOX rates. However, the abundance of the factors controlling methane oxidation, especially in interface areas between different environments makes any predictions largely uncertain. It was shown in previous investigations and in the current research that MOX rates in Arctic water bodies as well as methanotrophic bacterial communities, are quite diverse and cannot be fully explained by the methane concentrations. Temporal variations in MOX are exceptionally poorly investigated. Most research studies in the Arctic regions were performed in spring and summer. Though temperature is not considered as a strong environmental control of MOX, Martinez-Cruz *et al.* (2015) observed higher methane concentrations but lower MOX rates in Arctic lakes in the winter than in the summer. This indicates the importance of temperature and other season-dependent environmental factors affecting MOX. Additionally, more precise estimation of the contribution of ebullition to methane emission, as well as the role of MOX in impeding of this emission pathway, is essential. Relocation of the estuarine areas will lead to the disturbance of established methanotrophic communities, adapted to a certain water salinity. Gradualness of salinity

change can partly mitigate osmotic stress; however, since salinity tolerance substantially varies between different MOB species, more knowledge on salinity impact on natural MOB communities is needed. Furthermore, despite the balance between methane concentrations and MOX rates, input of additional methane in some environments will not necessarily lead to increased MOX rates (Mau *et al.*, 2013). At least, adaptation to increased methane concentrations might require some time. Absence of long-term measurements at river mouths in general and in Arctic in particular (Vonk *et al.*, 2015) leads to gaps in understanding of the impact of global warming on methane cycling in these areas.

Factors which regulate methane sources and sinks, especially in interface areas of different environments, are numerous. Mechanisms of their interaction, which determine functioning of these systems, are complex. Consequences of disturbance of such environments caused by global climate change are, therefore, hard to assess. In this study we focused just on some of them and speculatively discussed the others. Some of the aspects of potential impact of climate change on methane cycling stayed beyond the scope of the current research utterly. Our study, however, clearly illustrates the importance of study of the complex ecosystems and interaction between different environments, rather than individual ecosystems, to better understand functioning of the whole biomes and predict their potential transformations.

IV. REFERENCES

Abell GC, Stralis-Pavese N, Pan Y & Bodrossy L (2014) Analysis of methanotroph community structure using a pmoA-based microarray. *Environmental Microbiology: Methods and Protocols* 111-122.

Abnizova A, Siemens J, Langer M & Boike J (2012) Small ponds with major impact: The relevance of ponds and lakes in permafrost landscapes to carbon dioxide emissions. *Global Biogeochemical Cycles* **26**.

Abril G & Iversen N (2002) Methane dynamics in a shallow non-tidal estuary (Randers Fjord, Denmark). *Marine ecology progress series* **230**: 171-181.

Abril G & Borges A (2005) Carbon Dioxide and Methane Emissions from Estuaries. *Greenhouse Gas Emissions — Fluxes and Processes,*(Tremblay A, Varfalvy L, Roehm C & Garneau M, eds.), p.^pp. 187-207. Springer Berlin Heidelberg.

Abril G, Commarieu M-V & Guérin F (2007) Enhanced methane oxidation in an esturaine turbidity maximum. *Limnol Oceanogr* **52**: 470-475.

Anthony KW, Zimov S, Grosse G, Jones MC, Anthony P, Chapin III F, Finlay J, Mack M, Davydov S & Frenzel P (2014) A shift of thermokarst lakes from carbon sources to sinks during the Holocene epoch. *Nature* **511**: 452-456.

Bange H, Bartell U, Rapsomanikis S & Andreae MO (1994) Methane in the Baltic and North Seas and a reassessment of the marine emissions of methane. *Global Biogeochemical Cycles* **86**: 465-480.

Bange HW (2006) Nitrous oxide and methane in European coastal waters. *Estuarine, Coastal and Shelf Science* **70**: 361-374.

Barbier BA, Dziduch I, Liebner S, Ganzert L, Lantuit H, Pollard W & Wagner D (2012) Methane-cycling communities in a permafrost-affected soil on Herschel Island, Western Canadian Arctic: active layer profiling of mcrA and pmoA genes. *FEMS microbiology ecology* **82**: 287-302.

Bartlett KB, Crill PM, Sebacher DI, Harriss RC, Wilson JO & Melack JM (1988) Methane flux from the central Amazonian floodplain. *Journal of Geophysical Research: Atmospheres (1984–2012)* **93**: 1571-1582.

Bastviken D, Ejlertsson J & Tranvik L (2002) Measurement of methane oxidation in lakes: a comparison of methods. *Environmental science & technology* **36**: 3354-3361.

Bastviken D, Cole J, Pace M & Tranvik L (2004) Methane emissions from lakes: Dependence of lake characteristics, two regional assessments, and a global estimate. *Global biogeochemical cycles* **18**.

Bastviken D, Cole JJ, Pace ML & Van de Bogert MC (2008) Fates of methane from different lake habitats: Connecting whole-lake budgets and CH4 emissions. *Journal of Geophysical Research: Biogeosciences (2005–2012)* **113**.

Bastviken D, Tranvik LJ, Downing JA, Crill PM & Enrich-Prast A (2011) Freshwater methane emissions offset the continental carbon sink. *Science* **331**: 50-50.

Beal EJ, House CH & Orphan VJ (2009) Manganese-and iron-dependent marine methane oxidation. *Science* **325**: 184-187.

Beck M & Brumsack H-J (2012) Biogeochemical cycles in sediment and water column of the Wadden Sea: The example Spiekeroog Island in a regional context. *Ocean & Coastal Management* **68**: 102-113.

Becker G, Dick S & Dippner J (1992) Hydrography of the German Bight. *Marine Ecology Progress Series MESEDT* **91**.

Bergemann M & Gaumert T (2010) Elbebericht 2008. *FGG Elbe, Hamburg*.

Bialecka-Fornal M, Lee HJ & Phillips R (2015) The rate of osmotic downshock determines the survival probability of bacterial mechanosensitive channel mutants. *Journal of bacteriology* **197**: 231-237.

Bissett A, Abell GC, Bodrossy L, Richardson AE & Thrall PH (2012) Methanotrophic communities in Australian woodland soils of varying salinity. *FEMS microbiology ecology* **80**: 685-695.

Boetius A, Ravenschlag K, Schubert CJ, Rickert D, Widdel F, Gieseke A, Amann R, Jørgensen BB, Witte U & Pfannkuche O (2000) A marine microbial consortium apparently mediating anaerobic oxidation of methane. *Nature* **407**: 623-626.

Bogard MJ, Del Giorgio PA, Boutet L, Chaves MCG, Prairie YT, Merante A & Derry AM (2014) Oxic water column methanogenesis as a major component of aquatic CH4 fluxes. *Nature communications* **5**.

Boike J, Wille C & Abnizova A (2008) Climatology and summer energy and water balance of polygonal tundra in the Lena River Delta, Siberia. *Journal of Geophysical Research: Biogeosciences (2005–2012)* **113**.

Boike J, Langer M, Lantuit H, Muster S, Roth K, Sachs T, Overduin P, Westermann S & McGuire AD (2012) Permafrost–physical aspects, carbon cycling, databases and uncertainties. *Recarbonization of the Biosphere,*p.^pp. 159-185. Springer.

Boike J, Kattenstroth B, Abramova K, Bornemann N, Chetverova A, Fedorova I, Fröb K, Grigoriev M, Grüber M & Kutzbach L (2012) Baseline characteristics of climate, permafrost, and land cover from a new permafrost observatory in the Lena River Delta, Siberia (1998− 2011). *Biogeosciences Discussions* **9**: 13627.

Boike J, Georgi C, Kirilin G, Muster S, Abramova K, Fedorova I, Chetverova A, Grigoriev M, Bornemann N & Langer M (2015) Physical processes of thermokarst lakes in the continuous permafrost zone of northern Siberia–observations and modeling (Lena River Delta, Siberia). *Biogeosciences Discussions* **12**: 6637-6688.

Börjesson G, Sundh I & Svensson B (2004) Microbial oxidation of CH4 at different temperatures in landfill cover soils. *FEMS Microbiology Ecology* **48**: 305-312.

Borrel G, Jézéquel D, Biderre-Petit C, Morel-Desrosiers N, Morel J-P, Peyret P, Fonty G & Lehours A-C (2011) Production and consumption of methane in freshwater lake ecosystems. *Research in Microbiology* **162**: 832-847.

Bowman JP, Sly LI, Nichols PD & Hayward A (1993) Revised taxonomy of the methanotrophs: description of Methylobacter gen. nov., emendation of Methylococcus, validation of Methylosinus and Methylocystis species, and a proposal that the family Methylococcaceae includes only the group I methanotrophs. *International Journal of Systematic Bacteriology* **43**: 735-753.

Bussmann I (2013) Distribution of Methane in the Lena Delta and Buor Khaya Bay, Russia. *Biogeosciences* **10**: 4641-4652.

Bussmann I, Rahalkar M & Schink B (2006) Cultivation of methanotrophic bacteria in opposing gradients of methane and oxygen. *FEMS microbiology ecology* **56**: 331-344.

Bussmann I, Pester M, Brune A & Schink B (2004) Preferential cultivation of type II methanotrophic bacteria from littoral sediments (Lake Constance). *FEMS microbiology ecology* **47**: 179-189.

Bussmann I, Matousu A, Osudar R & Mau S (2015) Assessment of the radio 3H-CH4 tracer technique to measure aerobic methane oxidation in the water column. *Limnology and Oceanography: Methods*.

Bussmann I, Klings K, Warnstedt J, Hoppert M & Liebner S (in prep) Methylovulum flocci sp. nov., Methylomonas albis sp. nov., and Methylomonas labe sp. nov. three methanotrophs isolated from river water. *Int J Syst Evol Microbiol*.

Chen Y, Dumont MG, McNamara NP, Chamberlain PM, Bodrossy L, Stralis-Pavese N & Murrell JC (2008) Diversity of the active methanotrophic community in acidic peatlands as assessed by mRNA and SIP-PLFA analyses. *Environmental Microbiology* **10**: 446-459.

Chetverova A, Fedorova I, Potapova T & Boike J (2013) Hydrological and geochemical features of lakes of Samoylov Island of the Lena River Delta. *Proceedings of AARI, 2013* **1(95)**: 97-110.

Chowdhury TR & Dick RP (2013) Ecology of aerobic methanotrophs in controlling methane fluxes from wetlands. *Applied soil ecology* **65**: 8-22.

Cicerone RJ & Oremland RS (1988) Biogeochemical aspects of atmospheric methane. *Global Biogeochemical Cycles* **2**: 299-327.

Cole JJ, Caraco NF & Peierls BL (1992) Can phytoplankton maintain a positive carbon balance in a turbid, freshwater, tidal estuary? *Limnology and Oceanography* **37**: 1608-1617.

Commission O (2000) Quality status report 2000, region II–Greater North Sea. *OSPAR Commission, London* **136**.

Comte J, Lovejoy C, Crevecoeur S & Vincent W (2015) Co-occurrence patterns in aquatic bacterial communities across changing permafrost landscapes. *Biogeosciences Discussions* **12**.

Conrad R (2005) Quantification of methanogenic pathways using stable carbon isotopic signatures: a review and a proposal. *Organic geochemistry* **36**: 739-752.

Conrad R (2009) The global methane cycle: recent advances in understanding the microbial processes involved. *Environmental Microbiology Reports* **1**: 285-292.

Costard F & Gautier E (2007) The Lena River: hydromorphodynamic features in a deep permafrost zone. *Large Rivers: Geomorphology and Management* 225-233.

Costello AM & Lidstrom ME (1999) Molecular characterization of functional and phylogenetic genes from natural populations of methanotrophs in lake sediments. *Applied and Environmental Microbiology* **65**: 5066-5074.

Costello AM, Auman AJ, Macalady JL, Scow KM & Lidstrom ME (2002) Estimation of methanotroph abundance in a freshwater lake sediment. *Environmental microbiology* **4**: 443-450.

Crawford JT, Striegl RG, Wickland KP, Dornblaser MM & Stanley EH (2013) Emissions of carbon dioxide and methane from a headwater stream network of interior Alaska. *Journal of Geophysical Research: Biogeosciences* **118**: 482-494.

Crawford JT, Lottig NR, Stanley EH, Walker JF, Hanson PC, Finlay JC & Striegl RG (2014) CO2 and CH4 emissions from streams in a lake-rich landscape: Patterns, controls, and regional significance. *Global Biogeochemical Cycles* **28**: 197-210.

Crevecoeur S, Vincent WF, Comte J & Lovejoy C (2015) Bacterial community structure across environmental gradients in permafrost thaw ponds: methanotroph-rich ecosystems. *Frontiers in microbiology* **6**.

Crump BC, Amaral-Zettler LA & Kling GW (2012) Microbial diversity in arctic freshwaters is structured by inoculation of microbes from soils. *The ISME journal* **6**: 1629-1639.

Czitrom SPR, Budéus G & Krause G (1988) A tidal mixing front in an area influenced by land runoff. *Continental Shelf Research* **8**: 225-237.

Dai A & Trenberth KE (2002) Estimates of freshwater discharge from continents: Latitudinal and seasonal variations. *Journal of hydrometeorology* **3**: 660-687.

Davidson EA & Janssens IA (2006) Temperature sensitivity of soil carbon decomposition and feedbacks to climate change. *Nature* **440**: 165-173.

de Angelis MA & Scranton MI (1993) Fate of methane in the Hudson River and estuary. *Global biogeochemical cycles* **7**: 509-523.

Dedysh SN, Ricke P & Liesack W (2004) NifH and NifD phylogenies: an evolutionary basis for understanding nitrogen fixation capabilities of methanotrophic bacteria. *Microbiology* **150**: 1301-1313.

Dedysh SN, Liesack W, Khmelenina VN, Suzina NE, Trotsenko YA, Semrau JD, Bares AM, Panikov NS & Tiedje JM (2000) Methylocella palustris gen. nov., sp. nov., a new methane-oxidizing acidophilic bacterium from peat bogs, representing a novel subtype of serine-pathway methanotrophs. *International Journal of Systematic and Evolutionary Microbiology* **50**: 955-969.

Dedysh SN, Belova SE, Bodelier PL, Smirnova KV, Khmelenina VN, Chidthaisong A, Trotsenko YA, Liesack W & Dunfield PF (2007) Methylocystis heyeri sp. nov., a novel type II methanotrophic bacterium possessing 'signature'fatty acids of type I methanotrophs. *International journal of systematic and evolutionary microbiology* **57**: 472-479.

Degelmann DM, Borken W, Drake HL & Kolb S (2010) Different atmospheric methane-oxidizing communities in European beech and Norway spruce soils. *Applied and environmental microbiology* **76**: 3228-3235.

Duc N, Crill P & Bastviken D (2010) Implications of temperature and sediment characteristics on methane formation and oxidation in lake sediments. *Biogeochemistry* **100**: 185-196.

Dumestre J-F, Casamayor EO, Massana R & Pedrós-Alió C (2002) Changes in bacterial and archaeal assemblages in an equatorial river induced by the water eutrophication of Petit Saut dam reservoir (French Guiana). *Aquatic Microbial Ecology* **26**: 209-221.

Dumestre J, Guézennec J, Galy-Lacaux C, Delmas R, Richard S & Labroue L (1999) Influence of light intensity on methanotrophic bacterial activity in Petit Saut Reservoir, French Guiana. *Applied and environmental microbiology* **65**: 534-539.

Dumont MG, Pommerenke B, Casper P & Conrad R (2011) DNA-, rRNA-and mRNA-based stable isotope probing of aerobic methanotrophs in lake sediment. *Environmental Microbiology* **13**: 1153-1167.

Dumont MG, Lüke C, Deng Y & Frenzel P (2014) Classification of pmoA amplicon pyrosequences using BLAST and the lowest common ancestor method in MEGAN. *Frontiers in Microbiology* **5**.

Dunfield PF, Yuryev A, Senin P, Smirnova AV, Stott MB, Hou S, Ly B, Saw JH, Zhou Z & Ren Y (2007) Methane oxidation by an extremely acidophilic bacterium of the phylum Verrucomicrobia. *Nature* **450**: 879-882.

Eitinger T, Fuchs G, Heider J, Kemper B, Kothe E, Schink B, Schneider E & Unden G (2007) *Allgemeine Mikrobiologie*. Georg Thieme Verlag, Stuttgart, New York.

Eller G, Känel L & Krüger M (2005) Cooccurrence of aerobic and anaerobic methane oxidation in the water column of Lake Plußsee. *Applied and environmental microbiology* **71**: 8925-8928.

Ettwig KF, Butler MK, Le Paslier D, Pelletier E, Mangenot S, Kuypers MM, Schreiber F, Dutilh BE, Zedelius J & De Beer D (2010) Nitrite-driven anaerobic methane oxidation by oxygenic bacteria. *Nature* **464**: 543-548.

Fedorov YA, Khoroshevskaya V & Tambieva N (2003) Variations in methane concentrations in the water of the Don River and Taganrog Bay under the effect of natural factors. *Water Resources* **30**: 81-85.

Ferry JG (2010) The chemical biology of methanogenesis. *Planetary and space science* **58**: 1775-1783.

Fortunato CS & Crump BC (2015) Microbial gene abundance and expression patterns across a river to ocean salinity gradient. *PloS one* **10**: e0140578.

Galand P, Fritze H, Conrad R & Yrjälä K (2005) Pathways for methanogenesis and diversity of methanogenic archaea in three boreal peatland ecosystems. *Applied and Environmental Microbiology* **71**: 2195-2198.

Gebert J, Groengroeft A & Miehlich G (2003) Kinetics of microbial landfill methane oxidation in biofilters. *Waste Management* **23**: 609-619.

Gentz T, Damm E, Schneider von Deimling J, Mau S, McGinnis DF & Schlüter M (2013) A water column study of methane around gas flares located at the West Spitsbergen continental margin. *Continental Shelf Research*.

Graef C, Hestnes AG, Svenning MM & Frenzel P (2011) The active methanotrophic community in a wetland from the High Arctic. *Environmental microbiology reports* **3**: 466-472.

Graham DE, Wallenstein MD, Vishnivetskaya TA*, et al.* (2012) Microbes in thawing permafrost: the unknown variable in the climate change equation. *ISME J* **6**: 709-712.

Greene S, Walter Anthony K, Archer D, Sepulveda-Jauregui A & Martinez-Cruz K (2014) Modeling the impediment of methane ebullition bubbles by seasonal lake ice. *Biogeosciences* **11**: 6791-6811.

Grunwald M, Dellwig O, Beck M, Dippner JW, Freund JA, Kohlmeier C, Schnetger B & Brumsack H-J (2009) Methane in the southern North Sea: Sources, spatial distribution and budgets. *Estuarine, Coastal and Shelf Science* **81**: 445-456.

Guérin F & Abril G (2007) Significance of pelagic aerobic methane oxidation in the methane and carbon budget of a tropical reservoir. *Journal of Geophysical Research: Biogeosciences (2005–2012)* **112**.

Hanson RS & Hanson TE (1996) Methanotrophic bacteria. *Microbiological reviews* **60**: 439-471.

Harley J, Carvalho L, Dudley B, Heal K, Rees R & Skiba U (2015) Spatial and seasonal fluxes of the greenhouse gases N 2 O, CO 2 and CH 4 in a UK macrotidal estuary. *Estuarine, Coastal and Shelf Science* **153**: 62-73.

Haroon MF, Hu S, Shi Y, Imelfort M, Keller J, Hugenholtz P, Yuan Z & Tyson GW (2013) Anaerobic oxidation of methane coupled to nitrate reduction in a novel archaeal lineage. *Nature* **500**: 567-570.

He R, Wooller MJ, Pohlman JW, Quensen J, Tiedje JM & Leigh MB (2012a) Diversity of active aerobic methanotrophs along depth profiles of arctic and subarctic lake water column and sediments. *The ISME journal* **6**: 1937-1948.

He R, Wooller MJ, Pohlman JW, Quensen J, Tiedje JM & Leigh MB (2012b) Shifts in identity and activity of methanotrophs in Arctic lake sediments in response to temperature changes. *Applied and environmental microbiology* **78**: 4715-4723.

He R, Wooller MJ, Pohlman JW, Catranis C, Quensen J, Tiedje JM & Leigh MB (2012c) Identification of functionally active aerobic methanotrophs in sediments from an arctic lake using stable isotope probing. *Environmental microbiology* **14**: 1403-1419.

Heeschen KU, Keir RS, Rehder G, Klatt O & Suess E (2004) Methane dynamics in the Weddell Sea determined via stable isotope ratios and CFC-11. *Global biogeochemical cycles* **18**.

Heslop J, Anthony W, Katey M, Sepulveda-Jauregui A, Martinez-Cruz K, Bondurant A, Grosse G & Jones M (2015) Thermokarst lake methanogenesis along a complete talik profile. *Biogeosciences* **12**: 4317-4331.

Hirayama H, Abe M, Miyazaki M, Nunoura T, Furushima Y, Yamamoto H & Takai K (2014) Methylomarinovum caldicuralii gen. nov., sp. nov., a moderately thermophilic methanotroph

isolated from a shallow submarine hydrothermal system, and proposal of the family Methylothermaceae fam. nov. *International journal of systematic and evolutionary microbiology* **64**: 989-999.

Hirayama H, Fuse H, Abe M, Miyazaki M, Nakamura T, Nunoura T, Furushima Y, Yamamoto H & Takai K (2013) Methylomarinum vadi gen. nov., sp. nov., a methanotroph isolated from two distinct marine environments. *International journal of systematic and evolutionary microbiology* **63**: 1073-1082.

Ho A, Brink E, Reim A, Krause SMB & Bodelier PLE (2016) Recurrence and frequency of disturbance have cumulative effect on methanotrophic activity, abundance, and community structure. *Frontiers in Microbiology* **6**.

Ho A, Kerckhof FM, Luke C, Reim A, Krause S, Boon N & Bodelier PL (2013) Conceptualizing functional traits and ecological characteristics of methane-oxidizing bacteria as life strategies. *Environmental microbiology reports* **5**: 335-345.

Ho A, De Roy K, Thas O, De Neve J, Hoefman S, Vandamme P, Heylen K & Boon N (2014) The more, the merrier: heterotroph richness stimulates methanotrophic activity. *The ISME journal* **8**: 1945-1948.

Holmes AJ, Owens NJ & Murrell JC (1996) Molecular analysis of enrichment cultures of marine methane oxidising bacteria. *Journal of experimental marine biology and ecology* **203**: 27-38.

Holmes AJ, Costello A, Lidstrom ME & Murrell JC (1995) Evidence that participate methane monooxygenase and ammonia monooxygenase may be evolutionarily related. *FEMS Microbiology Letters* **132**: 203-208.

Horz H-P, Rich V, Avrahami S & Bohannan BJ (2005) Methane-oxidizing bacteria in a California upland grassland soil: diversity and response to simulated global change. *Applied and Environmental Microbiology* **71**: 2642-2652.

Hubberten H-W, Wagner D, Pfeiffer E-M, Boike J & Gukov AY (2006) The Russian-German research station Samoylov, Lena Delta-A key site for polar research in the Siberian Arctic. *Polarforschung* **73**: 111-116.

Hugelius G, Strauss J, Zubrzycki S, Harden JW, Schuur E, Ping C-L, Schirrmeister L, Grosse G, Michaelson GJ & Koven CD (2014) Estimated stocks of circumpolar permafrost carbon with quantified uncertainty ranges and identified data gaps. *Biogeosciences* **11**: 6573-6593.

ICES (1988) *Report of the Study Group on the Effects of Bottom Trawling*. International Council for the Exploration of the Sea.

IPCC, 2014: Climate Change 2014: Synthesis Report. Contribution of Working Groups I, II and III to the Fifth Assessment Report of the Intergovernmental Panel on Climate Change [Core Writing Team, R.K. Pachauri and L.A. Meyer (eds.)]. IPCC, Geneva, Switzerland, 151 pp. .

Islam T, Jensen S, Reigstad LJ, Larsen Ø & Birkeland N-K (2008) Methane oxidation at 55 C and pH 2 by a thermoacidophilic bacterium belonging to the Verrucomicrobia phylum. *Proceedings of the National Academy of Sciences* **105**: 300-304.

Jakobs G, Rehder G, Jost G, Kießlich K, Labrenz M & Schmale O (2013) Comparative studies of pelagic microbial methane oxidation within two anoxic basins of the central Baltic Sea (Gotland Deep and Landsort Deep). *Biogeosciences Discussions* **10**: 12251-12284.

Jugnia L-B, Roy R, Pacheco-Oliver M, Planas D, Miguez C & Greer C (2006) Potential activity and diversity of methanotrophic bacteria in forest soil, peat, and sediments from a hydroelectric reservoir (Robert-Bourassa) and lakes in the Canadian Taiga. *Soil science* **171**: 127-137.

Kalyuzhnaya M, Lidstrom M & Chistoserdova L (2004) Utility of environmental primers targeting ancient enzymes: methylotroph detection in Lake Washington. *Microbial ecology* **48**: 463-472.

Kelley C (2003) Methane oxidation potential in the water column of two diverse coastal marine sites. *Biogeochemistry* **65**: 105-120.

Kelley CA, Martens CS & Ussler W (1995) Methane dynamics across a tidally flooded riverbank margin. *Limnology and Oceanography* **40**: 1112-1129.

Khadem AF, Pol A, Wieczorek A, Mohammadi SS, Francoijs K-J, Stunnenberg HG, Jetten MS & den Camp HJO (2011) Autotrophic Methanotrophy in Verrucomicrobia: Methylacidiphilum fumariolicumSolV Uses the Calvin-Benson-Bassham Cycle for Carbon Dioxide Fixation. *Journal of bacteriology* **193**: 4438-4446.

Khmelenina V, Shchukin V, Reshetnikov A, Mustakhimov I, Suzina N, Eshinimaev BT & Trotsenko YA (2010) Structural and functional features of methanotrophs from hypersaline and alkaline lakes. *Microbiology* **79**: 472-482.

Khmelenina VN, Kalyuzhnaya MG, Sakharovsky VG, Suzina NE, Trotsenko YA & Gottschalk G (1999) Osmoadaptation in halophilic and alkaliphilic methanotrophs. *Archives of microbiology* **172**: 321-329.

King GM, Roslev P & Skovgaard H (1990) Distribution and rate of methane oxidation in sediments of the Florida Everglades. *Applied and Environmental Microbiology* **56**: 2902-2911.

Kirschke S, Bousquet P, Ciais P, Saunois M, Canadell JG, Dlugokencky EJ, Bergamaschi P, Bergmann D, Blake DR & Bruhwiler L (2013) Three decades of global methane sources and sinks. *Nature Geoscience* **6**: 813-823.

Knief C (2015) Diversity and habitat preferences of cultivated and uncultivated aerobic methanotrophic bacteria evaluated based on pmoA as molecular marker. *Frontiers in microbiology* **6**.

Knief C, Lipski A & Dunfield PF (2003) Diversity and activity of methanotrophic bacteria in different upland soils. *Applied and Environmental Microbiology* **69**: 6703-6714.

Knoblauch C, Beer C, Sosnin A, Wagner D & Pfeiffer EM (2013) Predicting long-term carbon mineralization and trace gas production from thawing permafrost of Northeast Siberia. *Global change biology* **19**: 1160-1172.

Knoblauch C, Spott O, Evgrafova S, Kutzbach L & Pfeiffer EM (2015) Regulation of methane production, oxidation, and emission by vascular plants and bryophytes in ponds of the northeast Siberian polygonal tundra. *Journal of Geophysical Research: Biogeosciences* **120**: 2525-2541.

Kolb S, Knief C, Stubner S & Conrad R (2003) Quantitative detection of methanotrophs in soil by novel pmoA-targeted real-time PCR assays. *Applied and Environmental Microbiology* **69**: 2423-2429.

Krause S, Lüke C & Frenzel P (2012) Methane source strength and energy flow shape methanotrophic communities in oxygen–methane counter-gradients. *Environmental microbiology reports* **4**: 203-208.

Krause S, Niklaus PA, Morcillo SB, Franke MM, Lüke C, Reim A & Bodelier PL (2015) Compositional and functional stability of aerobic methane consuming communities in drained and rewetted peat meadows. *FEMS microbiology ecology* **91**: fiv119.

Kushner DJ (1978) Life in high salt and solute concentrations: halophilic bacteria. *Microbial life in extreme environments* 317-368.

Langer M, Westermann S, Walter Anthony K, Wischnewski K & Boike J (2014) Frozen ponds: production and storage of methane during the Arctic winter in a lowland tundra landscape in northern Siberia, Lena River Delta. *Biogeosciences Discussions* **11**: 11061-11094.

Lau E, Ahmad A, Steudler PA & Cavanaugh CM (2007) Molecular characterization of methanotrophic communities in forest soils that consume atmospheric methane. *FEMS microbiology ecology* **60**: 490-500.

Lee HJ, Jeong SE, Kim PJ, Madsen EL & Jeon CO (2015) High resolution depth distribution of Bacteria, Archaea, methanotrophs, and methanogens in the bulk and rhizosphere soils of a flooded rice paddy. *Frontiers in microbiology* **6**.

Levine UY, Teal TK, Robertson GP & Schmidt TM (2011) Agriculture's impact on microbial diversity and associated fluxes of carbon dioxide and methane. *The ISME journal* **5**: 1683-1691.

Liebner S & Wagner D (2007) Abundance, distribution and potential activity of methane oxidizing bacteria in permafrost soils from the Lena Delta, Siberia. *Environmental Microbiology* **9**: 107-117.

Liebner S, Rublack K, Stuehrmann T & Wagner D (2009) Diversity of aerobic methanotrophic bacteria in a permafrost active layer soil of the Lena Delta, Siberia. *Microbial Ecology* **57**: 25-35.

Liebner S, Zeyer J, Wagner D, Schubert C, Pfeiffer EM & Knoblauch C (2011) Methane oxidation associated with submerged brown mosses reduces methane emissions from Siberian polygonal tundra. *Journal of Ecology* **99**: 914-922.

Lin J-L, Joye SB, Scholten JC, Schäfer H, McDonald IR & Murrell JC (2005) Analysis of methane monooxygenase genes in Mono Lake suggests that increased methane oxidation activity may correlate with a change in methanotroph community structure. *Applied and environmental microbiology* **71**: 6458-6462.

Lofton DD, Whalen SC & Hershey AE (2014) Effect of temperature on methane dynamics and evaluation of methane oxidation kinetics in shallow Arctic Alaskan lakes. *Hydrobiologia* **721**: 209-222.

Martineau C, Whyte LG & Greer CW (2010) Stable isotope probing analysis of the diversity and activity of methanotrophic bacteria in soils from the Canadian high Arctic. *Applied and environmental microbiology* **76**: 5773-5784.

Martineau C, Pan Y, Bodrossy L, Yergeau E, Whyte LG & Greer CW (2014) Atmospheric methane oxidizers are present and active in Canadian high Arctic soils. *FEMS microbiology ecology* **89**: 257-269.

Martinez-Cruz K, Sepulveda-Jauregui A, Walter Anthony K & Thalasso F (2015) Geographic and seasonal variation of dissolved methane and aerobic methane oxidation in Alaskan lakes. *Biogeosciences Discussions* **12**: 4213-4243.

Mau S, Blees J, Helmke E, Niemann H & Damm E (2013) Vertical distribution of methane oxidation and methanotrophic response to elevated methane concentrations in stratified waters of the Arctic fjord Storfjorden (Svalbard, Norway). *Biogeosciences* **10**: 6267-6278.

Maxfield P, Evershed R & Hornibrook E (2008) Physical and biological controls on the in situ kinetic isotope effect associated with oxidation of atmospheric CH4 in mineral soils. *Environmental science & technology* **42**: 7824-7830.

McArthur JV (2006) *Microbial ecology: an evolutionary approach*. Academic press.

McAuliffe C (1971) G.C. determination of solutes by multiple phase equilibrium. *Chem Tech* **46**.

McDonald IR, Bodrossy L, Chen Y & Murrell JC (2008) Molecular ecology techniques for the study of aerobic methanotrophs. *Applied and Environmental Microbiology* **74**: 1305-1315.

Middelburg J, Nieuwenhuize J, Iversen N, Høgh N, de Wilde H, Helder W, Seifert R & Christof O (2002) Methane distribution in European tidal estuaries. *Biogeochemistry* **59**: 95-119.

Minke M, Donner N, Karpov NS, de Klerk P & Joosten H (2007) Distribution, diversity, development and dynamics of polygon mires: examples from Northeast Yakutia (Siberia). *Peatlands International* **1**: 36–40.

Morbach S & Krämer R (2002) Body Shaping under Water Stress: Osmosensing and Osmoregulation of Solute Transport in Bacteria. *ChemBioChem* **3**: 384-397.

Murase J & Sugimoto A (2005) Inhibitory effect of light on methane oxidation in the pelagic water column of a mesotrophic lake (Lake Biwa, Japan). *Limnology and oceanography* **50**: 1339-1343.

Muster S, Langer M, Heim B, Westermann S & Boike J (2012) Subpixel heterogeneity of ice-wedge polygonal tundra: a multi-scale analysis of land cover and evapotranspiration in the Lena River Delta, Siberia. *Tellus B* **64**.

Naughton LM, Blumerman SL, Carlberg M & Boyd EF (2009) Osmoadaptation among Vibrio Species and Unique Genomic Features and Physiological Responses of Vibrio parahaemolyticus. *Appl Environ Microbiol* **75**: 2802-2810.

Nazaries L, Murrell JC, Millard P, Baggs L & Singh BK (2013) Methane, microbes and models: fundamental understanding of the soil methane cycle for future predictions. *Environmental microbiology* **15**: 2395-2417.

Nazaries L, Tate KR, Ross DJ, Singh J, Dando J, Saggar S, Baggs EM, Millard P, Murrell JC & Singh BK (2011) Response of methanotrophic communities to afforestation and reforestation in New Zealand. *ISME J* **5**: 1832-1836.

Neufeld JD, Schäfer H, Cox MJ, Boden R, McDonald IR & Murrell JC (2007) Stable-isotope probing implicates Methylophaga spp and novel Gammaproteobacteria in marine methanol and methylamine metabolism. *The ISME journal* **1**: 480-491.

Nichols PD, Smith GA, Antworth CP, Hanson RS & White DC (1985) Phospholipid and lipopolysaccharide normal and hydroxy fatty acids as potential signatures for methane-oxidizing bacteria. *FEMS Microbiology Ecology* **31**: 327-335.

Oren A (2013) Life at high salt concentrations. *The Prokaryotes,*p.^pp. 421-440. Springer.

Ortega-Retuerta E, Joux F, Jeffrey WH & Ghiglione JF (2013) Spatial variability of particle-attached and free-living bacterial diversity in surface waters from the Mackenzie River to the Beaufort Sea (Canadian Arctic). *Biogeosciences* **10**: 2747-2759.

Osudar R, Matoušů A, Alawi M, Wagner D & Bussmann I (2015) Environmental factors affecting methane distribution and bacterial methane oxidation in the German Bight (North Sea). *Estuarine, Coastal and Shelf Science* **160**: 10-21.

Pack MA, Heintz MB, Reeburgh WS, Trumbore SE, Valentine DL, Xu X & Druffel ER (2011) A method for measuring methane oxidation rates using lowlevels of 14C-labeled methane and accelerator mass spectrometry. *Limnology and Oceanography: Methods* **9**: 245-260.

Painchaud J, Therriault J-C & Legendre L (1995) Assessment of salinity-related mortality of freshwater bacteria in the saint lawrence estuary. *Applied and environmental microbiology* **61**: 205-208.

Peterson BJ, Holmes RM, McClelland JW, Vörösmarty CJ, Lammers RB, Shiklomanov AI, Shiklomanov IA & Rahmstorf S (2002) Increasing river discharge to the Arctic Ocean. *science* **298**: 2171-2173.

Pol A, Heijmans K, Harhangi HR, Tedesco D, Jetten MS & Op den Camp HJ (2007) Methanotrophy below pH 1 by a new Verrucomicrobia species. *Nature* **450**: 874-878.

Pozdnyakov L, Stepanov A & Manucharova N (2011) Anaerobic methane oxidation in soils and water ecosystems. *Moscow University Soil Science Bulletin* **66**: 24-31.

Rahalkar M, Deutzmann J, Schink B & Bussmann I (2009) Abundance and activity of methanotrophic bacteria in littoral and profundal sediments of Lake Constance (Germany). *Applied and environmental microbiology* **75**: 119-126.

Rahmstorf S (2007) A semi-empirical approach to projecting future sea-level rise. *Science* **315**: 368-370.

Ramaswamy V, Boucher O, Haigh J, Hauglustine D, Haywood J, Myhre G, Nakajima T, Shi G & Solomon S (2001) Radiative forcing of climate. *Climate change* 349-416.

Reeburgh W, Whalen S & Alperin M (1993) The role of methylotrophy in the global methane budget. *Microbial growth on C1 compounds* 1-14.

Reeburgh WS (2007) Oceanic methane biogeochemistry. *Chemical Reviews* **107**: 486-513.

Reed AJ, Dorn R, Van Dover CL, Lutz RA & Vetriani C (2009) Phylogenetic diversity of methanogenic, sulfate-reducing and methanotrophic prokaryotes from deep-sea hydrothermal vents and cold seeps. *Deep Sea Research Part II: Topical Studies in Oceanography* **56**: 1665-1674.

Rehder G, Keir RS, Suess E & Pohlmann T (1998) The Multiple Sources and Patterns of Methane inNorth Sea Waters. *Aquatic Geochemistry* **4**: 403-427.

Rehder G, Keir RS, Suess E & Rhein M (1999) Methane in the northern Atlantic controlled by microbial oxidation and atmospheric history. *Geophysical Research Letters* **26**: 587-590.

Reina-Bueno M, Argandoña M, Salvador M, Rodríguez-Moya J, Iglesias-Guerra F, Csonka LN, Nieto JJ & Vargas C (2012) Role of Trehalose in Salinity and Temperature Tolerance in the Model Halophilic Bacterium Chromohalobacter salexigens. *PLoS ONE* **7**: e33587.

Ricão Canelhas M, Denfeld BA, Weyhenmeyer GA, Bastviken D & Bertilsson S (2016) Methane oxidation at the water-ice interface of an ice-covered lake. *Limnology and Oceanography*.

Rockne KJ & Strand SE (2003) Amplification of marine methanotrophic enrichment DNA with 16S rDNA PCR primers for type II α Proteobacteria methanotrophs. *Journal of Environmental Science and Health, Part A* **38**: 1877-1887.

Romanovskii NN & Hubberten HW (2001) Results of permafrost modelling of the lowlands and shelf of the Laptev Sea region, Russia. *Permafrost and Periglacial Processes* **12**: 191-202.

Rossi P-G, Laurion I & Lovejoy C (2013) Distribution and identity of bacteria in subarctic permafrost thaw ponds. *Aquat Microb Ecol* **69**: 231-245.

Sanders IA, Heppell CM, Cotton JA, Wharton G, Hildrew AG, Flowers EJ & Trimmer M (2007) Emission of methane from chalk streams has potential implications for agricultural practices. *Freshwater Biology* **52**: 1176-1186.

Schloss PD, Westcott SL, Ryabin T, Hall JR, Hartmann M, Hollister EB, Lesniewski RA, Oakley BB, Parks DH & Robinson CJ (2009) Introducing mothur: open-source, platform-independent, community-supported software for describing and comparing microbial communities. *Applied and environmental microbiology* **75**: 7537-7541.

Schneider J, Grosse G & Wagner D (2009) Land cover classification of tundra environments in the Arctic Lena Delta based on Landsat 7 ETM+ data and its application for upscaling of methane emissions. *Remote Sensing of Environment* **113**: 380-391.

Schuur E, McGuire A, Schädel C, Grosse G, Harden J, Hayes D, Hugelius G, Koven C, Kuhry P & Lawrence D (2015) Climate change and the permafrost carbon feedback. *Nature* **520**: 171-179.

Scranton MI & McShane K (1991) Methane fluxes in the southern North Sea: the role of European rivers. *Continental Shelf Research* **11**: 37-52.

Segarra K, Samarkin V, King E, Meile C & Joye S (2013) Seasonal variations of methane fluxes from an unvegetated tidal freshwater mudflat (Hammersmith Creek, GA). *Biogeochemistry* **115**: 349-361.

Semiletov I, Pipko I, Shakhova N, Dudarev O, Pugach S, Charkin AN, McRoy C, Kosmach D & Gustafsson Ö (2011) Carbon transport by the Lena River from its headwaters to the Arctic Ocean, with emphasis on fluvial input of terrestrial particulate organic carbon vs. carbon transport by coastal erosion. *Biogeosciences* **8**: 2407-2426.

Shakhova N, Semiletov I & Bel'Cheva N (2007) The great Siberian rivers as a source of methane on the Russian Arctic shelf. Vol. 415 p.^pp. 734. Springer Science & Business Media.

Sharp CE, Smirnova AV, Graham JM, Stott MB, Khadka R, Moore TR, Grasby SE, Strack M & Dunfield PF (2014) Distribution and diversity of Verrucomicrobia methanotrophs in geothermal and acidic environments. *Environmental microbiology* **16**: 1867-1878.

Shiklomanov NI, Streletskiy DA, Nelson FE, Hollister RD, Romanovsky VE, Tweedie CE, Bockheim JG & Brown J (2010) Decadal variations of active-layer thickness in moisture-controlled landscapes, Barrow, Alaska. *Journal of Geophysical Research: Biogeosciences* **115**.

Siljanen HM, Saari A, Krause S, Lensu A, Abell GC, Bodrossy L, Bodelier PL & Martikainen PJ (2011) Hydrology is reflected in the functioning and community composition of methanotrophs in the littoral wetland of a boreal lake. *FEMS microbiology ecology* **75**: 430-445.

Siljanen HMP (2012) Activity and diversity of methanotrophs in a littoral wetland of an eutrophic boreal freshwater lake. *Publication of the University of Eastern Finland, Dissertations in Forestry and Natural Sciences* **63**.

Silvennoinen H, Liikanen A, Rintala J & Martikainen PJ (2008) Greenhouse gas fluxes from the eutrophic Temmesjoki River and its Estuary in the Liminganlahti Bay (the Baltic Sea). *Biogeochemistry* **90**: 193-208.

Simon M (2005) *Die Elbe und ihr Einzugsgebiet: ein geographisch-hydrologischer und wasserwirtschaftlicher Überblick*. Internat. Komm. zum Schutz der Elbe.

Singh BK, Bardgett RD, Smith P & Reay DS (2010) Microorganisms and climate change: terrestrial feedbacks and mitigation options. *Nature Reviews Microbiology* **8**: 779-790.

Singh BK, Tate KR, Kolipaka G, Hedley CB, Macdonald CA, Millard P & Murrell JC (2007) Effect of afforestation and reforestation of pastures on the activity and population dynamics of methanotrophic bacteria. *Applied and environmental microbiology* **73**: 5153-5161.

Steinle L, Graves CA, Treude T, Ferré B, Biastoch A, Bussmann I, Berndt C, Krastel S, James RH & Behrens E (2015) Water column methanotrophy controlled by a rapid oceanographic switch. *Nature Geoscience* **8**: 378-382.

Stocker TF, Dahe Q & Plattner G-K (2013) Climate Change 2013: The Physical Science Basis. *Working Group I Contribution to the Fifth Assessment Report of the Intergovernmental Panel on Climate Change Summary for Policymakers (IPCC, 2013)*.

Striegl RG, Dornblaser M, McDonald C, Rover J & Stets E (2012) Carbon dioxide and methane emissions from the Yukon River system. *Global Biogeochemical Cycles* **26**.

Sturm K, Grinham A, Werner U & Yuan Z (2016) Sources and sinks of methane and nitrous oxide in the subtropical Brisbane River estuary, South East Queensland, Australia. *Estuar Coast Shelf Sci* **168**: 10-21.

Sundh I, Bastviken D & Tranvik LJ (2005) Abundance, activity, and community structure of pelagic methane-oxidizing bacteria in temperate lakes. *Applied and environmental microbiology* **71**: 6746-6752.

Tarnocai C, Canadell J, Schuur E, Kuhry P, Mazhitova G & Zimov S (2009) Soil organic carbon pools in the northern circumpolar permafrost region. *Global biogeochemical cycles* **23**.

Tavormina PL, Ussler W, Joye SB, Harrison BK & Orphan VJ (2010) Distributions of putative aerobic methanotrophs in diverse pelagic marine environments. *The ISME journal* **4**: 700-710.

Tavormina PL, Hatzenpichler R, McGlynn S, Chadwick G, Dawson KS, Connon SA & Orphan VJ (2015) Methyloprofundus sedimenti gen. nov., sp. nov., an obligate methanotroph from ocean sediment belonging to the 'deep sea-1'clade of marine methanotrophs. *International journal of systematic and evolutionary microbiology* **65**: 251-259.

Trotsenko YA & Khmelenina VN (2002) Biology of extremophilic and extremotolerant methanotrophs. *Arch Microbiol* **177**: 123-131.

Tsutsumi M, Iwata T, Kojima H & Fukui M (2011) Spatiotemporal variations in an assemblage of closely related planktonic aerobic methanotrophs. *Freshwater Biology* **56**: 342-351.

Upstill-Goddard RC, Barnes J, Frost T, Punshon S & Owens NJ (2000) Methane in the southern North Sea: Low-salinity inputs, estuarine removal, and atmospheric flux. *Global Biogeochemical Cycles* **14**: 1205-1217.

Valentine DL (2011) Emerging topics in marine methane biogeochemistry. *Annual review of marine science* **3**: 147-171.

Valentine DL, Blanton DC, Reeburgh WS & Kastner M (2001) Water column methane oxidation adjacent to an area of active hydrate dissociation, Eel river Basin. *Geochimica et Cosmochimica Acta* **65**: 2633-2640.

van der Nat F-JW & Middelburg JJ (1998) Seasonal variation in methane oxidation by the rhizosphere of Phragmites australis and Scirpus lacustris. *Aquatic Botany* **61**: 95-110.

Van Huissteden J, Maximov T & Dolman A (2005) High methane flux from an arctic floodplain (Indigirka lowlands, eastern Siberia). *Journal of Geophysical Research: Biogeosciences (2005–2012)* **110**.

Vonk J, Sánchez-García L, Van Dongen B, Alling V, Kosmach D, Charkin A, Semiletov I, Dudarev O, Shakhova N & Roos P (2012) Activation of old carbon by erosion of coastal and subsea permafrost in Arctic Siberia. *Nature* **489**: 137-140.

Vonk JE, Tank SE, Bowden WB, Laurion I, Vincent WF, Alekseychik P, Amyot M, Billett M, Canario J & Cory RM (2015) Reviews and syntheses: Effects of permafrost thaw on Arctic aquatic ecosystems.

Vorobev AV, Baani M, Doronina NV, Brady AL, Liesack W, Dunfield PF & Dedysh SN (2011) Methyloferula stellata gen. nov., sp. nov., an acidophilic, obligately methanotrophic bacterium that possesses only a soluble methane monooxygenase. *International journal of systematic and evolutionary microbiology* **61**: 2456-2463.

Wagner A, Lohmann G & Prange M (2011) Arctic river discharge trends since 7ka BP. *Global and Planetary Change* **79**: 48-60.

Wagner D & Liebner S (2009) Global warming and carbon dynamics in permafrost soils: methane production and oxidation. *Permafrost soils,* p.^pp. 219-236. Springer.

Wagner D, Kobabe S & Liebner S (2009) Bacterial community structure and carbon turnover in permafrost-affected soils of the Lena Delta, northeastern Siberia This article is one of a selection of papers in the Special Issue on Polar and Alpine Microbiology. *Canadian Journal of Microbiology* **55**: 73-83.

Walter KM, Smith LC & Chapin FS (2007) Methane bubbling from northern lakes: present and future contributions to the global methane budget. *Philosophical Transactions of the Royal Society A: Mathematical, Physical and Engineering Sciences* **365**: 1657-1676.

Walter KM, Zimov S, Chanton JP, Verbyla D & Chapin FS (2006) Methane bubbling from Siberian thaw lakes as a positive feedback to climate warming. *Nature* **443**: 71-75.

Wang Q, Quensen JF, Fish JA, Lee TK, Sun Y, Tiedje JM & Cole JR (2013) Ecological patterns of nifH genes in four terrestrial climatic zones explored with targeted metagenomics using FrameBot, a new informatics tool. *MBio* **4**: e00592-00513.

Wartiainen I, Hestnes AG & Svenning MM (2003) Methanotrophic diversity in high arctic wetlands on the islands of Svalbard (Norway)-denaturing gradient gel electrophoresis analysis of soil DNA and enrichment cultures. *Canadian journal of microbiology* **49**: 602-612.

Whittenbury R, Phillips K & Wilkinson J (1970) Enrichment, isolation and some properties of methane-utilizing bacteria. *Journal of General Microbiology* **61**: 205-218.

Wiesenburg DA & Guinasso Jr NL (1979) Equilibrium solubilities of methane, carbon monoxide, and hydrogen in water and sea water. *Journal of Chemical and Engineering Data* **24**: 356-360.

Wik M, Varner RK, Anthony KW, MacIntyre S & Bastviken D (2016) Climate-sensitive northern lakes and ponds are critical components of methane release. *Nature Geoscience*.

Wuebbles DJ & Hayhoe K (2000) Atmospheric methane: trends and impacts. *Non-CO2 Greenhouse Gases: Scientific Understanding, Control and Implementation,*p.^pp. 1-44. Springer.

Yun J, Zhuang G, Ma A, Guo H, Wang Y & Zhang H (2012) Community structure, abundance, and activity of methanotrophs in the Zoige wetland of the Tibetan Plateau. *Microbial ecology* **63**: 835-843.

Zhang G, Zhang J, Ren J, Li J & Liu S (2008) Distributions and sea-to-air fluxes of methane and nitrous oxide in the North East China Sea in summer. *Marine Chemistry* **110**: 42-55.

Zigah PK, Oswald K, Brand A, Dinkel C, Wehrli B & Schubert CJ (2015) Methane oxidation pathways and associated methanotrophic communities in the water column of a tropical lake. *Limnology and Oceanography* **60**: 553-572.

Zimov S, Voropaev YV, Semiletov I, Davidov S, Prosiannikov S, Chapin FS, Chapin M, Trumbore S & Tyler S (1997) North Siberian lakes: a methane source fueled by Pleistocene carbon. *Science* **277**: 800-802.

Zimov SA, Schuur EA & Chapin III FS (2006) Permafrost and the global carbon budget. *Science(Washington)* **312**: 1612-1613.

V. APPENDIX

Additional manuscript I (Published in *Limnology and Oceanography: Methods* 13, 2015, 312–327, DOI: 10.1002/lom3.10027)

Assessment of the radio ^{3}H-CH_4 tracer technique to measure aerobic methane oxidation in the water column

Authors: Ingeborg Bussmann,*[1] Anna Matousu,[2,3] Roman Osudar,[1] Susan Mau[4]

[1]Alfred Wegener Institute, Helmholtz Centre for Polar and Marine Research, 27498 Helgoland, Germany

[2]Faculty of Sciences, University of South Bohemia, Branisovska 1760, 370 05 Ceske Budejovice, Czech Republic

[3]Biology Centre of the Czech Academy of Sciences, Institute of Hydrobiology, Na Sadkach 7,370 05Ceske Budejovice, Czech Republic

[4]MARUM Center for Marine Environmental Sciences and Department of Geosciences, University of Bremen, 28359 Bremen, Germany

Abstract

Microbial methane oxidation rates in ocean and freshwater systems reveal how much of emitted methane from the sediments is oxidized to CO_2 and how much can reach the atmosphere directly. The tracer-method using ^{3}H-CH_4 provides a way to measure methane oxidation rates even in water with low methane concentrations. We assessed this method by implementing several experiments, collecting data from various environments, and including recent literature concerning the method to identify any uncertainties that should be considered. Our assessment reveals some difficulties of the method but also reassures previous assumptions to be correct. Some of the difficulties are hardly to be avoided, such as incubating all samples at the right in situ temperature or limiting the variability of methane oxidation rate measurements in water of low methanotrophic activity. Other details, for example, quickly measuring the total radioactivity after stopping the incubation, are easy to adapt in each laboratory. And yet other details as shaking during incubation and bottle size seem to be irrelevant. With our study, we hope to improve and to encourage future measurements of methane oxidation rates in different environments and to provide a standard procedure of methane oxidation rate measurements to make the data better comparable.

Introduction

Measurements of methane oxidation (MOX) rates are essential to understand why the large input of methane into oceans, lakes, rivers is in opposition to the relatively low flux of the gas to the atmosphere (Reeburgh 2007). Methane (CH_4) is after water vapor and CO_2, the most important greenhouse gas with a global warming potential that exceeds carbon dioxide (CO_2) 34-fold over a 100 yr timescale (IPCC, 2013). Methane is produced in aquatic sediments as well as in the water itself. In sediments, methane is generated by microbial breakdown as the last step of anaerobic degradation of organic matter (biogenic methane) and by thermocatalytic processes by increased temperature and pressure in deeply buried sediments [thermogenic methane (Tissot and Welte 1984)]. In the water column of the ocean, methane production has been linked to methylphosphonic acid (Karl et al. 2008; Metcalf et al. 2012) and dimethylsulfoniopropionate (Damm et al. 2010) as substrates for methanogenesis, as well as to anaerobic microenvironments (Reeburgh 2007). Also in the water column of lakes an until now unknown process of methane production in oxygenated water has been suggested based on incubation experiments and isotope analysis (Tang et al. 2014).

Despite of all these methane sources only little of the gas actually escapes to the atmosphere. About 11 Tg CH_4 yr^{-1} is emitted to the atmosphere from the ocean (Bange et al. 1994) contributing 2% to the $\sim$ 550 Tg CH_4 yr^{-1} from all natural and anthropogenic sources (IPCC, 2013). A similar quantity of 40 Tg yr^{-1} (range 8–73 Tg yr^{-1}) originates from freshwater sources like rivers, lakes, and reservoirs (Bastviken et al. 2011; IPCC, 2013). These limited quantities are thought to be due to microbial oxidation of the gas in the water, which maintains the bulk of the ocean at low nanomolar concentrations (Reeburgh 2007).

Aerobic MOX is realized by methanotrophs, who oxidize methane with oxygen to CO2 and water. Methane oxidizing bacteria are found in oxic sediments and in the water column of most marine and freshwater settings, where oxygen is available (Jensen et al. 1992; Ding and Valentine 2008; Rahalkar et al. 2009; Tsutsumi et al. 2012). Aerobic methanotrophic bacteria have been classified as type I and type II methanotrophs based on their phylogenetic position, carbon assimilation pathways, and the arrangement of intracellular membranes, and they belong to the classes Gammaproteobacteria and Alphaproteobacteria, respectively (Bowman 2006). Reported turnover times of methane range from 100s of years in the open ocean (Jones 1991; Angelis et al. 1993) to several years in the coastal seas (Heintz et al. 2012) and to days in freshwater environments (Abril and Iversen 2002). Besides the aerobic oxidation of methane, it can also be oxidized in the absence of oxygen, that is, in sediments and in anoxic waters. Especially the oxidation in sediments by mostly archaea but also some bacteria plays an important role in reducing the methane flux from the sediment into the water column (Krüger et al. 2005).

Several techniques have been implemented to qualify and quantify the microbial methane consumption. MOX can be measured by the decrease of methane concentration over time (Scranton and Brewer 1978; Abril et al. 2007), the change in isotopic composition (Bastviken et al. 2002) or by a combination of stable isotope and conservative tracer measurements (Rehder et al. 1999; Heeschen et al. 2004). However, adding a radioactive tracer such as $^{3}H\text{-}CH_4$ (Valentine et al. 2001; Mau et al. 2013) or $^{14}C\text{-}CH_4$ (Reeburgh et al. 1992; Pack et al. 2011) makes quantification more sensitive.

Especially the method using $^{3}H\text{-}CH^4$ has become more and more established over the last decade as sample processing requires only a few steps, which can be carried out on board a research vessel, the tracer has become commercially available, and it has several advantages compared to $^{14}C\text{-}CH_4$ (Table 1). $^{3}H\text{-}CH_4$ has a higher specific activity ($3.7–7.4 \times 10^{11}$ Bq $mmol^{-1}$) than $^{14}C\text{-}CH_4$ with $3.7 - 18 \times 10^{7}$ Bq $mmol^{-1}$. Thus, the methane concentration of a water sample is changed by < 3 nmol l^{-1} $^{3}H\text{-}CH_4$ whereas the addition of $^{14}C\text{-}CH_4$ increases methane concentration of a sample by up to 500 nmol l^{-1}. This significantly alters the concentration of the gas especially in samples collected from environments with low in situ methane concentrations. However, recently also a low-level $^{14}C\text{-}CH_4$ method has been proposed, where ^{14}C is measured with accelerator mass spectrometry (Pack et al. 2011). Furthermore, the $^{3}H\text{-}CH_4$ has the advantage of a higher permitted radioactivity (10^{9} Bq) compared to ^{14}C with 10^{7} Bq, which can be transported without special license (German Radiation Protection Ordinance, 2001, and ADR 2.2.7.1.1, Tab. 2.2.7.2.2.1, U.S. DoT, CFR Part 173.436). The working limits seem to differ in each country, thus, we will not give further information here. For transportation with ships, documents according to the IMO are recommended (IMO class 7, UN number 2910). For transportation with airplanes, documents according to the IATA are recommended (IATA DGR 10.3.1, Tab 10.3.A).

Table 1. Comparison of the main characteristics of ^{3}H labeled methane vs. ^{14}C-labeled methane.

	^{3}H-methane	**^{14}C-methane**
Reaction	$^{3}H\text{-}CH_4 + 2O_2 \Rightarrow CO_2 + 2\ ^{3}H\text{-}H_2O$	$^{14}C\text{-}CH_4 + 2O_2 \Rightarrow {}^{14}C\text{-}CO_2 + 2H_2O + {}^{14}C$ -biomass
Specific activity	High (0.37–0.74 TBq $mmol^{-1}$), thus, < 3 nmol L^{-1} methane are added to a water sample	Low (37–185 MBq $mmol^{-1}$), thus, < 500 nmol L^{-1} methane are added to a water sample
Tracer storage	Limited tracer storage due to decomposition of the tracer over time	No problems with tracer storage known to date
Lab-	GC for methane concentrations Liquid	GC for methane concentrations

	^{3}H-methane	^{14}C-methane
equipment	scintillation counter for radioactivities.	Liquid scintillation counter for radioactivities. Tube furnace and shaker for quantification of ^{14}C-CH_4 and ^{14}C-CO_2Filtering devices for biomass determination.
Environment	Applicable to aerobic environments only	Applicable to aerobic and anaerobic environments
Exemption limit	Higher exemption limit	Lower exemption limit
Ionization energy	Low ionization energy (19 keV), thus, possible interference with chemo luminescence	Higher ionization energy (156 keV) less interference with chemo luminescence

Regardless of the radiotracer, more and more often tracer incubations are conducted on board of research vessels, where similar to any laboratory country specific radiation regulations apply. The transport of the radioactive tracer, radioactive samples, and radioactive waste has to be organized according to these safety regulations. Ideally, the handling is done in an isotope van, especially if other parties of a cruise are interested in the natural abundance of ^{3}H or ^{14}C. Areas on deck, where incubations are carried out, should be monitored for potential spills on a regular basis and these areas should be regularly hosed. This is particularly important on small vessels with too little space for an isotope van. Furthermore, sufficient ventilation should be assured by an open window, open door, or working outside if no ventilation hood is provided. Of principle importance are regular wipe tests to screen for any potential contaminations. With sufficient care the radiotracer technique provides a great tool to investigate and quantify microbial methane oxidation.

Although we describe here a rather established method, we felt the need to publish an extensive testing of the method to get the best results for current and future users. The idea arose during the Pergamon workshop in Kiel in 2011 where several parties met to discuss MOX rate measurements. Every user tested the method by implementing different experiments. Here, we summarize the tests to make the method of measuring MOX by adding ^{3}H-CH_4 more comparable between laboratories, to facilitate it for newcomers and also to report on the little tricks and pitfalls hidden in the detail of every method.

Material and methods

To test parts of the MOX rate measurements using $^{3}H\text{-}CH_4$ as tracer, we followed the general method described below. Deviations and verifications of this protocol are indicated in the assessment part.

Methane oxidation rate

Water is sampled directly from Niskin bottles attached to a CTD/rosette. A 10–20 cm long tubing, which fits to the stop-cock of the Niskin bottle and reaches to the bottom of the sampling bottle, is used to collect water from the water-sampling device. Water samples are collected in 12–160 mL glass bottles by filling the bottle from the bottom to the top and flushing the bottle twice to minimize contact of the sampled water with the surrounding air, that is, avoiding changes of the in situ methane and oxygen concentrations. The glass bottles are then closed avoiding air bubbles with rubber stoppers and are crimp sealed. Several water samples have to be collected: two to three bottles for determination of MOX rates, one bottle as killed control, and one to two bottles for analysis of in situ methane concentrations.

After crimp sealing of the water sample, the radioactive tracer is added to the sample and poisoned control bottles. $^{3}H\text{-}CH_4$ (as gas), commercially available from Biotrend (Köln, Germany) or from American Labeled Chemicals (St. Louis) is added by syringe using a second needle to allow for displacement of water. The amount of added $^{3}H\text{-}CH_4$-tracer has to be adapted to the environment, it should be high enough to produce a measurable quantity of $^{3}H\text{-}H_2O$, and as low as possible, to minimize any significant methane concentration changes in the water sample.

The addition of the $^{3}H\text{-}CH_4$ is > 1000 Bq resulting in methane addition in the pico molar range (10^{-12} mol). After injection of the $^{3}H\text{-}CH_4$, all bottles are vigorously shaken for at least 30 s to equilibrate the gaseous tracer with the liquid phase.

The samples are then incubated in the dark at near in situ temperature. After incubation for hours until days, microbial activity is stopped by poisoning or the samples are directly processed.

Then the total radioactivity ($^{3}H\text{-}CH_4$ and $^{3}H\text{-}H_2O$) added to the sample and the product of the oxidation, $^{3}H\text{-}H_2O$, have to be measured in the sample and control bottles (Fig. 1). To determine the total radioactivity of the sample, the sample bottle (or control bottle) is opened and 1–2 mL subsample is pipetted into a seven milliliter scintillation vial. Five milliliter scintillation cocktail is added to the subsample. The scintillation cocktail should be specific for ^{3}H-samples and aqueous solutions (e.g., Ultima Gold LLT from Perkin Elmer). Scintillation cocktail and sample are mixed by shaking the scintillation vial and counted in a liquid scintillation counter. This can be a laboratory-based counter (e.g., from Perkin Elmer) or a small, transportable one (e.g., Triathler from Hidex,

Finland). Decays per minute (dpm) are calculated by the instruments based on the efficiency determined from the internal quench correction and calibration.

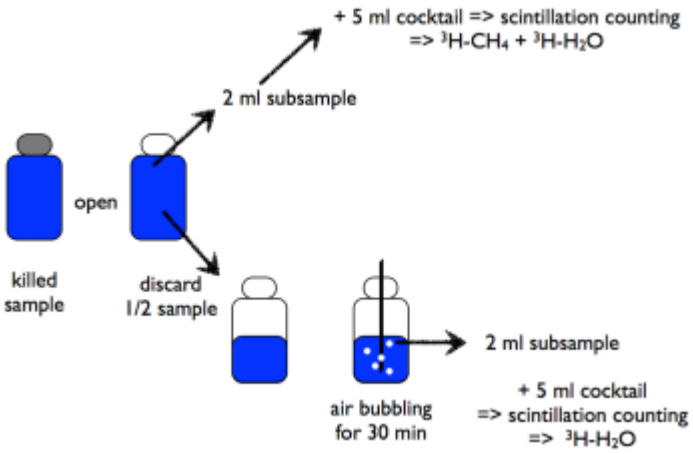

Figure 1. Scheme for analysis of the 3H-radioactivity in the total fraction and in the water fraction of a sample (or control bottle).

After counting the total radioactivity (^{3}H-CH$_4$ and ^{3}H-H$_2$O) of the sample, the ^{3}H-CH$_4$ is removed from the sample and the remaining ^{3}H-H$_2$O counted. For the removal of the ^{3}H-CH$_4$, part of the sample is discarded to prevent overflow when sparging the sample with nitrogen or air. A synthetic air or a nitrogen gas bottle is connected to a sparging device that consists of several long needles or tubes to process more than one sample at a time. During expeditions, we also used an aquarium pump. The needles or tubes should reach nearly to the bottom of the bottle (i.e., be ~ 10-mm long) and the tubes should have a small diameter (~ 1 mm) to leave sufficient space for ventilation at the neck of the bottle. After sparging the sample for at least 30 min, a 1–2 mL subsample is mixed with five milliliter scintillation cocktail in a seven milliliter scintillation vial and counted in a liquid scintillation counter.

Methane concentration

To calculate the MOX rate, the methane concentration of the respective sample has to be known. Commonly, an additional water sample is collected from the same Niskin bottle and poisoned to stop microbial MOX. The sample is then stored cold until methane concentration analysis.

However, if the samples were manipulated by adding different amounts of ^{3}H-CH$_4$ or plain CH$_4$, it is necessary to measure the methane concentration in each sample before measuring its radioactivity (Fig. 2). Therefore, a 10 mL syringe without piston is inserted into the killed sample (120–160 mL sample). With a second syringe 10 mL of nitrogen are injected into the sample bottle while water flows into the syringe without piston assuring atmospheric pressure conditions in the sample bottle. Part of this water is used for measurement of the total radioactivity (^{3}H-CH$_4$ and ^{3}H-H$_2$O; see above).

The sample bottle with headspace is shaken and left standing for at least one day to equilibrate. An aliquot of the headspace is then analyzed with a gas chromatograph (GC) equipped with a flame ionization detector to determine the methane concentration.

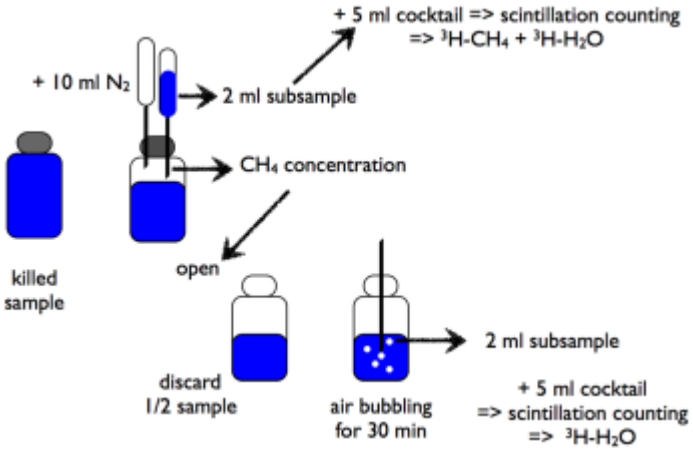

Figure 2. Modified scheme for measuring the methane concentration in the sample bottle, before assessing the radioactive fractions.

Calculation

After measuring methane concentration, the total radioactivity (^{3}H-CH$_4$ and ^{3}H-H$_2$O) and the radioactivity of the produced water (^{3}H-H$_2$O), turnover time (τ in d) and MOX rates (nmol l^{-1} d^{-1}) can be calculated assuming first-order kinetics (Valentine et al. 2001):

$$k' = (^3\text{H-H}_2\text{O}/(^3\text{H-CH}_4 + ^3\text{H-H}_2\text{O}))/t \quad (1)$$

$$\text{MOX} = k' \times [\text{CH}_4]_{\text{in situ}} \quad (2)$$

$$\tau = 1 / k' = [\text{CH}_4] / \text{MOX} \quad (3)$$

where k' is the first-order rate constant calculated as the fraction of ^{3}H-CH$_4$ oxidized per unit time (t) and $[\text{CH}_4]_{\text{in situ}}$ is the ambient methane concentration in nmol L^{-1}. The methane concentration should be measured in separate bottles, without tracer addition. k' was termed the pseudo first-order rate constant for the methane transport into the cells at constant cell population by Button (1991). The turnover time can also been seen as an indication of the relative activity of various water samples as described by Koschel (1980).

The radioactivity of the ^{3}H-H$_2$O fraction in the killed controls is used to check for the amount of not biologically produced water. In case this background value is > 1% the radioactivity of the total fraction, it should be subtracted from the sample value (Jørgensen 1978). In marine waters about 0.1% of the injected tracer was found to be “abiotic water.” In freshwaters the percentage can increase to about 5%.

Statistics

Wilcoxon Rank Sign Tests for nonparametric data were performed with Kaleidagraph 4.1.

Assessment

Number of replicates

Replicates are essential to obtain a good estimate of MOX rates. Commonly, 2–3 replicates are used to quantify MOX rates (Schubert et al. 2010; Mau et al. 2013). To test the quality of data obtained from triplicate measurements, the coefficient of variation (cv = standard deviation × 100/mean) was calculated for data collected during eight cruises in the North Sea and Elbe in 2013. Our results show that the coefficient of variations is rather high (23% ± 11%, n = 58) at low activities (< 10 nmol l−1 d−1) and lower (7% ± 5%, n = 17) at higher activities (> 10 nmol l−1 d−1; Fig. 3). For comparison, when measuring the bacterial production in the water column using the leucine incorporation method, the coefficient of variation ranges from 6% to 10%, with 3–4 replicates (Ducklow et al. 2012; Simon et al. 2012). Hence, if a better precision and discriminatory power is needed, for example, when comparing different experimental setups, more than three replicates are necessary. The precision of replicates describes the total error of MOX rates. This total error consists of the error of each step of the method and the heterogeneity of the methanotrophic population in the water sample. All the tested error causes evaluated below, thus, most likely affect low rate measurements more than high rate measurements.

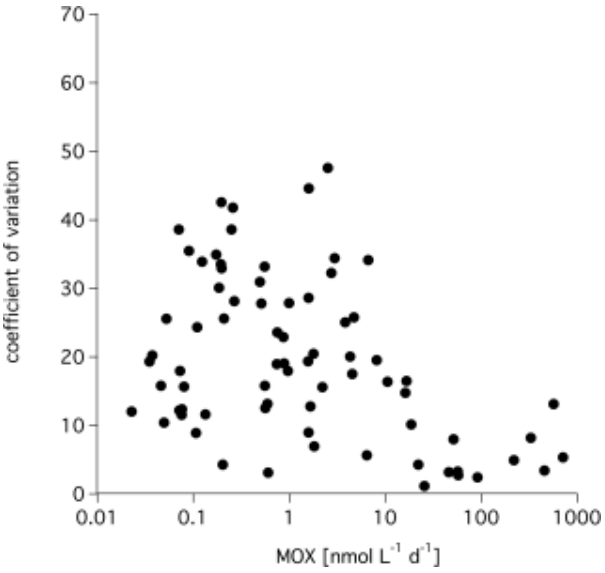

Figure 3. Coefficients of variation of triplicate samples in relation to MOX rates collected during eight research cruises in the North Sea and in the Elbe in 2013.

Bottle size

Glass bottles of different sizes (25–160 mL) are used to measure aerobic MOX rates. While larger samples contain a higher absolute number of bacteria, and thus, might be more representative, small sample vials have laboratory advantages. Less tracer has to be added to smaller samples, less space is needed during incubation, and less radioactive waste is produced. To test if small sample volumes are representative or if the coefficient of variation increases due to the small sample volume, a batch of North Sea water was filled in 12–160 mL glass bottles and incubated as described above. The comparison of incubation of different sample volumes showed no significant differences in turnover times (Wilcoxon Rank Sum Test, $n = 5$). Therefore, small water samples are adequate, at least in waters with a turnover time of less than 20 d.

Stoppers

There are several different rubber stoppers available to firmly close the sample bottles. The stoppers should be gas tight to prevent any losses of methane and at the same time should be "soft" enough to allow easy handling with needles. However, most of the commercially available rubber stoppers leach organic and inorganic contaminants, which can inhibit or limit MOX. An extensive study was conducted by Niemann et al. (2015) recommending halogenated butyl rubber stoppers.

Adding the ^{3}H-CH_4 tracer

The tracer can be added to the sample as a small bubble of concentrated ^{3}H-CH_4 (10 µL) or as a bigger bubble (100 µL) diluted with nitrogen. According to the ratio of surface to volume of a sphere, more gas is diluted from small bubbles than from large ones. Furthermore, large bubbles may result in stripping of methane from the sample into the bubble in case of methane rich waters. However, handling of a 10 µL volume in contrast to a 100 µL volume is rather tricky especially on a moving boat. Furthermore, using diluted tracer has the advantage that the rate of decomposition is decreased. To test the effect of the bubble size, North Sea water was incubated with a 10 µL and a 100 µL bubble containing 131 ± 40 Bq and 190 ± 23 Bq, respectively ($n = 10$ each, 24 h, at ambient methane concentration of 15 nmol l^{-1} at 18°C). The turnover time of the 10 µL samples (5.1 ± 0.4 d) was slightly higher than the turnover time of the 100 µL samples (4.5 ± 0.4 d). The difference is in the range of the error of replicates indicating that the enhanced solubility for the 10 µL sample was negligible.

Incubation time

The incubation time has to be adapted to each environment. The time period should be long enough to produce a measurable amount of $^{3}H\text{-}H_2O$ and as short as possible to minimize incubation artefacts such as decomposition of the $^{3}H\text{-}CH_4$ or isotopic exchange reactions. To test the appropriate incubation time, one or more time series should be conducted. A time series is implemented by taking water samples from one location and incubating duplicate or triplicate samples for 3 h, 6 h, 12 h, 1 d, 2 d, etc. However, during field campaigns such time series may be difficult to perform due to the lack of time, space, or counting instruments. To provide a general idea of appropriate incubation times, we compiled data of time series of freshwater and marine environments. Our compilation suggests incubation times of < 24 h in freshwater and 1–3 d in marine systems (Fig. 4). The time series indicate that $^{3}H\text{-}CH_4$ uptake per time is linearly related as long as the substrate (methane) is not limited. In case of the freshwater sample, the linear relation (first-order kinetics) is given during the first day of incubation and in case of the seawater samples over up to 5 d.

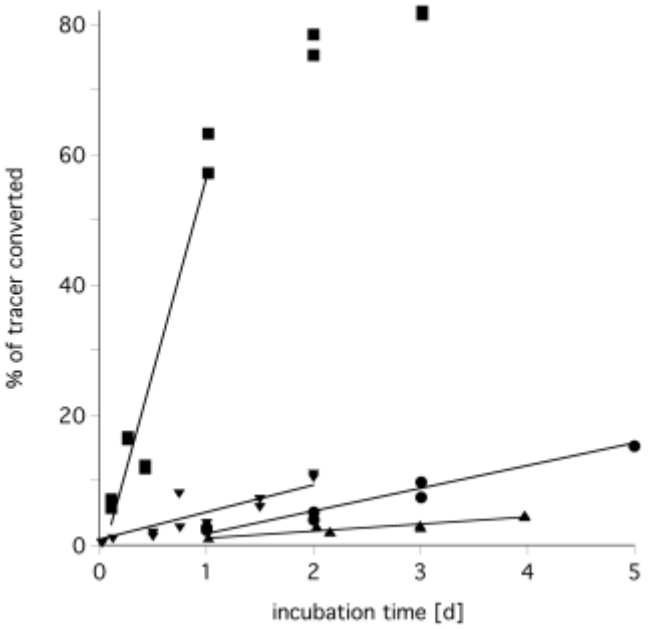

Figure 4. Time series conducted by incubating samples from different environments for 0.1–5 d. Freshwater from the pond of the MPI-Bremen (squares) and seawater from Storfjorden, Svalbard (circles), the North Sea (upward triangle), and the Santa Barbara Basin (downward triangle).

During the incubation

Incubation conditions for rate measurements should mimic the natural environment to determine a rate that resembles as close as possible the in situ rate. Typically, water samples are incubated at near in situ temperature, in the dark, and without motion.

In a set of experiments, we assessed the influence of temperature on the MOX rate. Elbe and North Sea water samples that were incubated at temperatures from 2°C to 25°C show the temperature curve of the MOX reaction (Fig. 5). We determined the Q_{10}-factor, which indicates the temperature dependence of a process: according to Raven and Geider (1988):

$$Q_{10} = \exp(-10 \times m \div T_{is}^2)$$

where T_{is} is the in situ temperature and m the slope of the regression line of the Arrhenius plot (the inverse of the absolute temperature vs. the natural logarithm of the MOX rate). We calculated Q_{10} values to range between 1.52 and 1.75, for Elbe and North Sea water, respectively. These values are in accordance with Q_{10} values between 1.4 and 2.1 determined for MOX rates in northern peatlands by (Dunfield et al. 1993). Also, Q_{10} values of 1–1.84 were reported for ammonia oxidation in a marine setting (Horak et al. 2013). $Q_{10} > 1$ indicates that the reaction rate increases with increasing temperature. Therefore, incubation temperature should be as close as possible to the in situ temperature or should be corrected if one wants to determine the in situ MOX rate.

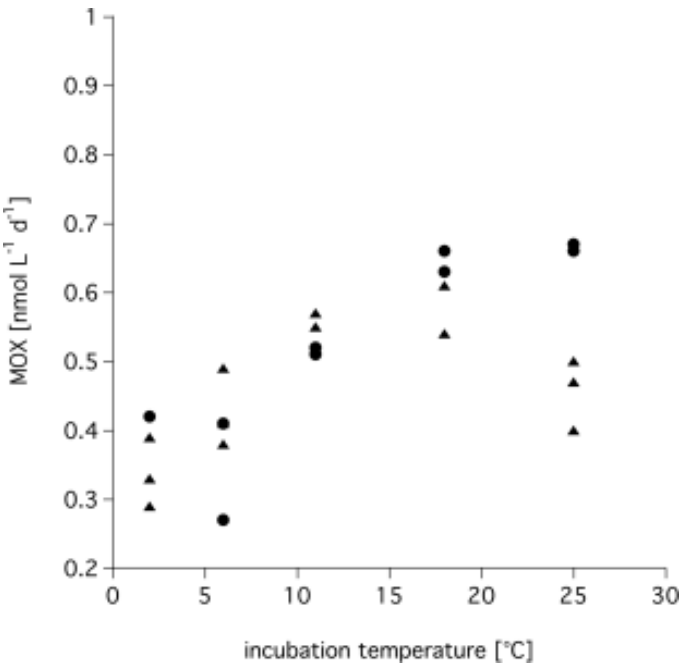

Figure 5. Influence of the incubation temperature on the MOX rate. North Sea water (triangles) and Elbe water (circles) with in situ methane concentrations of 20 nmol L^{-1} and 32 nmol L^{-1}, respectively, were incubated for 24 h at different temperatures. Water samples were collected in January 2011 and had in situ temperatures of 3°C.

Samples are generally incubated in the dark; even though the influence of light on microbial MOX is unknown. Some studies suggest an inhibitory effect of light on methanotrophic growth and activity (Dumestre et al. 1999). Other studies suggest that the inhibitory effect depends on type of methanotrophs (Osudar et al. unpublished data). Unless more knowledge is available, we recommend to incubate the samples in the dark and also to minimize samples processing under high laboratory light.

The influence of motion/shaking of a sample during the incubation was tested. The motion not only increases the solubility of the tracer bubble but also imitates the motion of a research vessel at sea. The 120 mL sample bottles were put on a rocker during incubation to move the tracer bubble along the side of the bottle. No significant difference was found between samples from the rocker and samples incubated without motion ($n = 5$ each). Also, the coefficient of variation was not different. Shaking of the sample is, thus, not necessary during incubation.

Stopping the incubation

If immediate analysis of samples after incubation is impracticable, a "killing" substance to stop microbial activity has to be added to the sample. This can be a toxic substance or a substance that shifts the pH. Strong toxic substances are mercury chloride ($HgCl_2$) and sodium azide (NaN_3), which both require environmental safe disposal. Sulfuric acid (H_2SO_4) or sodium hydroxide solution (NaOH) can be used to shift the pH and to stop microbial activity. We compiled data of the different "killing" substances in Table 2, which shows the amount of ^3H-H_2O in the killed control as percent of the total radioacitivity (^3H-CH_4 and ^3H-H_2O). In seawater samples, we observed 2–15 times as high counts in control samples using NaN_3 in contrast to $HgCl_2$ (Table 2). For $HgCl_2$, it should be noted that some methanotrophs may be able to reduce $HgCl_2$ to elemental Hg, but they need to use most of the energy that they gain from methane metabolism to fuel mercury (II) reduction (Boden et al. 2011). Therefore, especially methanotrophs might not be stopped by adding $HgCl_2$. In seawater both NaOH and H_2SO_4 can be used to poison the samples. The ^3H-H_2O radioactivity of the controls using 10 mol L^{-1} NaOH was 1.0% ± 0.3% ($n = 35$) in North Sea water, while 25% H_2SO_4 had a slightly better performance (Table 2). In freshwater in most cases 5 mol L^{-1} NaOH was superior to 25% H_2SO_4 in stopping the samples (Experiments I and II in Table 2). Field data revealed a low residual activity when stopping with 5 mol L^{-1} NaOH (Elbe river near Hamburg; Lake Constance). However, in some cases (Czech part of the Elbe) NaOH was not sufficient and best results were obtained with concentrated H_2SO_4 (96%; Table 2). Overall H_2SO_4 was the best killing reagent, with a better performance than NaOH, which in turn is advantageous compared to $HgCl_2$ and NaN_3 that are both environmentally hazardous. In the marine environment diluted (25%) H_2SO_4 was sufficient, whereas in freshwater concentrated H_2SO_4 appears to be superior.

Table 2. Field and experimental data on the influence of the stopping reagent on the amount of ^{3}H-H_2O in the killed control as percent of the total radioactivity (^{3}H-CH_4 and ^{3}H-H_2O). Given are the averages ± standard deviation and the number of samples in brackets. The experiments were performed with water from the Elbe near Hamburg and North Sea water near Helgoland. We added 0.2–0.3 mL of base or acid to 120 mL sample bottles, resulting in a pH of < 1.5 or > 10.

	Location/experiment	5M NaOH	10 mol L^{-1} NaOH	25% H_2SO_4	95% H_2SO_4	$HgCl_2$	NaN_3
Seawater	Santa Barbara					0.1±0.0 (6)	0.5±0.2 (6)
Seawater	North Sea		1.0±0.3 (35)	0.1±0.2 (39)			
Freshwater	Elbe near Hamburg	3.8±4.0 (37)					
Freshwater	Elbe near Prague	8.5±2.6 (12)		9.5±4.5 (12)	0.8±1.7 (31)		
Freshwater	Lake Constance	5.2±7.1 (50)					
Freshwater	Exp. I	5.4±1.0 (4)		37.9±0.3 (4)			
Seawater		0.2±0.1 (4)		0.0±0.0 (4)			
Freshwater	Exp. II	0.4±0.1 (3)		28.0±12.6 (3)			

After stopping the incubation, the samples should be analyzed as soon as possible. Experiments with storage time of ^{3}H-CH_4-labeled samples show that within the first week there is a significant loss of ^{3}H-CH_4, while the ^{3}H-H_2O fraction remains stable (Fig. 6a). Presumably the ^{3}H-CH_4 is lost through diffusion through the stoppers. This loss results in an increase of the ratio (^{3}H-H_2O/^{3}H-CH_4 + ^{3}H-H_2O; Fig. 6b). This increase of the ratio will result in an overestimation of the MOX rate by 20–40%.

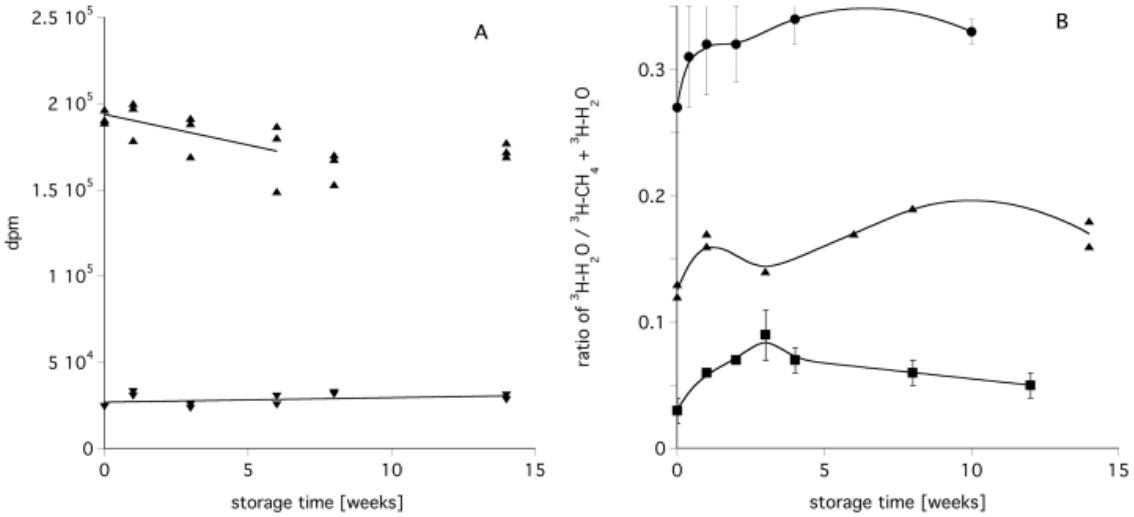

Figure 6. The influence of the storage time on the radioactivity in the different fractions and on their ratio. Incubations of North Sea water were stopped after 24 h with 25% H_2SO_4 and two to four bottles were analyzed immediately. The other samples were stored at 4°C and measured after the indicated time. (A) The radioactivity in dpm in the fraction (^{3}H-CH$_4$ + ^{3}H-H$_2$O) with upward triangles and the radioactivity in the ^{3}H-H$_2$O fraction with downward triangles. (B) The ratio (^{3}H-H$_2$O/^{3}H-CH$_4$ + ^{3}H-H$_2$O) of three experiments, the triangles are from the same experiment shown in figure A.

Thus, samples should be analyzed within 3–4 d, or if this is not possible an overestimation of the MOX rate of approx. 20% has to be accepted.

Total radioactivity (^{3}H-CH$_4$ and ^{3}H-H$_2$O) of the sample

After incubation, the total radioactivity (^{3}H-CH$_4$ and ^{3}H-H$_2$O) that was added to the water sample has to be determined. We determined the total radioactivity in all bottles, samples, and controls. This allowed for a better precision, as we found a high variability (> 10%) between different bottles.

However, as methane has a low solubility, it rapidly equilibrates with the headspace in the scintillation vial and can leak from the scintillation vial. ^{3}H-CH$_4$ in the headspace cannot be counted in a liquid scintillation counter. To measure the total radioactivity (^{3}H-CH$_4$ and ^{3}H-H$_2$O) most accurately, we tested vigorous vs. gently mixing of a sample with scintillation cocktail, how long the mixed sample can be left standing before analysis, and the use of polyethylene vs. glass vials.

Vigorous shaking vs. gentle mixing was tested by adding one milliliter sample to five milliliter scintillation cocktail in each of two scintillation vials. One of the vials was gently turned upside down 3–4 times whereas the other was vigorously shaken by hand. The results show on average 7% less radioactivity in the vigorously shaken samples than in the gentle mixed samples (Supporting Information 1). Vigorous shaking of the samples with the cocktail, thus, leads to a faster equilibration and higher leakage; therefore, mixing should be accomplished gently.

Furthermore, we observed that the total radioactivity rapidly decreases over time after addition of the scintillation cocktail and mixing (Fig. 7). Glass vials were found to have a slightly better performance than polyethylene vials. In glass vials, the total radioactivity decreased by ~ 15% within 60 h, whereas in polyethylene vials radioactivity was reduced by 25% in 60 h. Already in the first hour, 4% of the total radioactivity is lost using polyethylene vials.

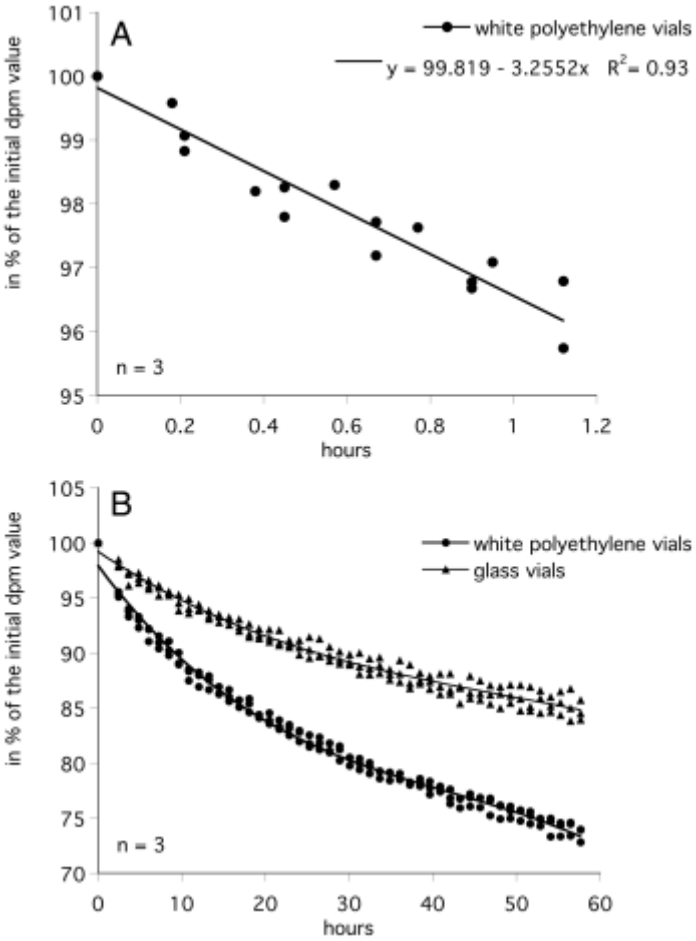

Figure 7. Loss of ^{3}H-CH_4 from the total radioactivity (^{3}H-CH_4 and ^{3}H-H_2O) in a scintillation vial with time. The scintillation vials contained a two milliliter subsample and five milliliter scintillation cocktail. The same vials were counted at different times.

As the loss of radioactivity is due to equilibration between the fluid and the gas phase, the loss depends on the methane concentration in the vial, and might be lower at low methane concentrations. However, the experiments show, that samples should be immediately counted after mixing. Further, we recommend to open and process less than 10 samples at once and set the counting time to 1–3 min as otherwise the total radioactivity of the last sample analyzed is biased due to ^{3}H-CH_4 leakage in the headspace.

Radioactivity of the water fraction (^{3}H-H_2O)

To determine the amount of water that has been produced by the methanotrophic bacteria through the oxidation of methane, the radioactivity of the ^{3}H-H_2O has to be quantified (Table 1). Therefore, the remaining ^{3}H-CH_4 has to be removed from the sample, which can be done by sparging the sample with nitrogen or air. We moistened the air by directing it through a washing flask to prevent evaporation of sample water. However, this effect appears negligible and accounts for < 0.2% of the ^{3}H-H_2O if one assumes an even distribution of the ^{3}H-CH_4 in the sample, an evaporation rate of 200 g water m^{-2} h^{-1} and a sparging time of 30 min.

To test for the appropriate time to remove all of the ^{3}H-CH_4, we sparged samples with a high and low activity for 5–30 min, that is, Elbe water and North Sea water, respectively. In the active samples about 28% of the added ^{3}H-CH_4 was found in the water fraction. In the less active samples, only 2% of the ^{3}H-CH_4 was found in the water fraction. In both cases, a stable counting was reached after 20–30 min of sparging (Fig. 8).

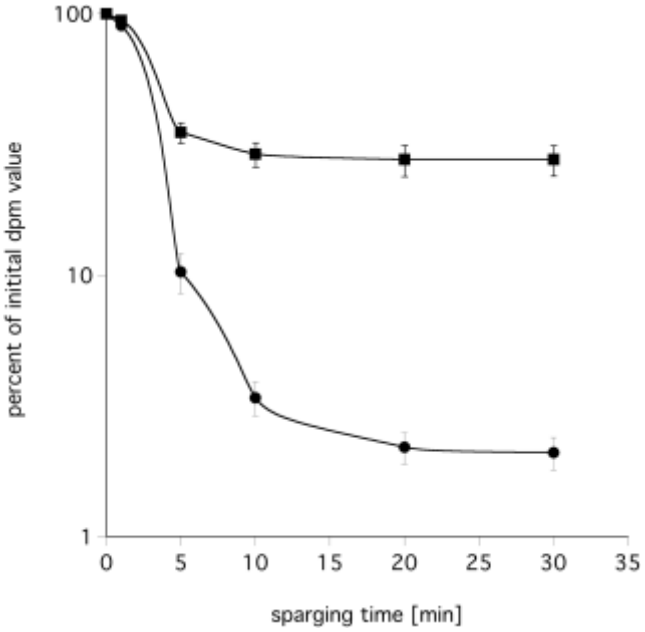

Figure 8. Identification of the necessary sparging time to remove not microbially oxidized ^{3}H-CH_4. Elbe water (squares, *n* = 3) and North Sea water (circles, *n* = 3) samples were incubated for 24 h and stopped by adding a poison. Radioactivity was measured after different times of sparging. Note the logarithmic scale of the y-axis.

In contrast to the total radioactivity (^{3}H-CH_4 and ^{3}H-H_2O), the radioactivity of the ^{3}H-H_2O in the scintillation vial was stable over time (70 h, Supporting Information 2). Therefore, the counting time can be extended to 10 min, to get a better statistical quality of the counts. The 2% sigma value as measured by the liquid scintillation counter for a given counting time decreased from 2% at 1 min to 0.6% at 10 min counting time.

Storage of the ^{3}H-CH_4 tracer

Because ^{3}H-compounds generally have a high specific activity and, thus, a high radioactive decomposition rate, this section provides advice on the optimal conditions for storing the ^{3}H-CH_4 tracer. Decomposition is the interaction of emitted particles with the immediate surroundings and/or with the molecules of the labeled compound causing destruction of the labeled substance. To lessen the decomposition, it is necessary to keep the number of interactions as low as possible. This can be achieved by storing the tracer at low temperatures and by dilution of the tracer. For the ^{3}H-CH_4 tracer dilution from the original ampoule, we recommend to use nitrogen, instead of air. In this way, reactions with OH and other compounds of the air will not occur. If the ^{3}H-CH_4 tracer is to be used over months, it is best to have subsamples in a number of vials. This way, vials to be used later can be kept in the refrigerator to avoid reopening and warming/cooling cycles. Furthermore, ^{3}H-CH_4 tracer is commonly stored on saturated salt solution, which decreases the likelihood of formation of reactive species. The water molecules surround the highly charged Na^+ and Cl^- ions, increasing the structure of water and reducing the number of "free" water molecules, which can form reactive species such as OH^- radicals (Emerson and Hedges 2009).

Background ^{3}H-H_2O

Some of the ^{3}H-H_2O is often suggested not to result from microbial MOX but from isotopic exchange reactions or decomposition of the tracer. Salinity and reactive species (e.g., OH^-, H^+) are assumed to influence these processes (see storage of the tracer). That is, background ^{3}H-H_2O is supposed to be higher in less saline water because more "free" water molecules are around, which are broken by radiation to, for example, $OH^-$and H^+ ions, and react with the tracer forming ^{3}H-H_2O. Similarly, pH modifies water to contain more reactive species. To test the influence of (i) salinity and (ii) pH on the concentration and stability of the background ^{3}H-H_2O, we autoclaved water (deionized water, freshwater, seawater, a saturated salt solution, and freshwaters and seawaters with different pHs) to assure that all microbial activity is stopped. Then, we added the same amount of tracer to all samples. The samples were subsequently incubated in the dark at 10°C for up to 11 d. The results show no significant differences between the different setups, nor a significant change of the background value over time (Fig. 9). Apparently neither the availability of "free" water molecules in low salinity water, nor the increase in H^+ (acidic water) or OH^- ions (basic water) led to elevated concentrations of ^{3}H-H_2O over the 11-d time period. Therefore, the isotopic exchange reaction and decomposition of the ^{3}H-CH_4 tracer is negligible over typical time periods of incubations (hours to 3 d).

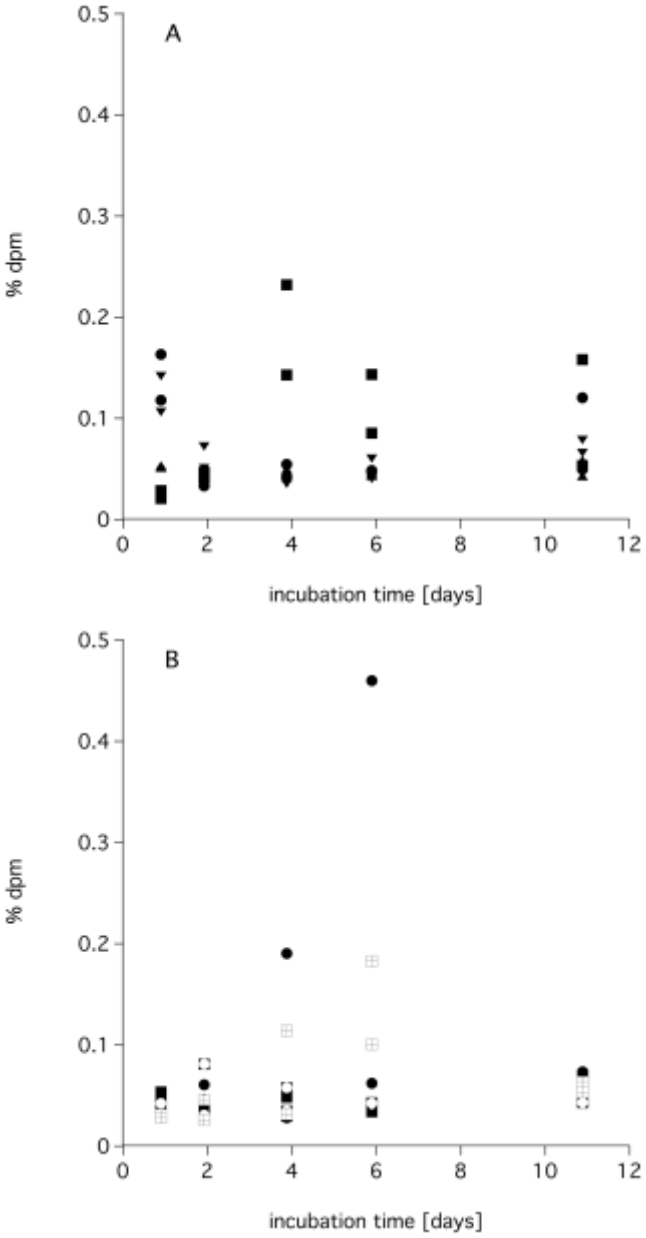

Figure 9. Percent of ^{3}H-tracer remaining in autoclaved water after incubation and sparging for 30 min to remove ^{3}H-CH_4. Samples were stored at 10°C for up to 11 d. (A) Incubations with different salt concentrations: Milli Q (downward triangles), tap water (squares), seawater (circles), and brine (upward triangles). (B) Incubations with different pH: tap water with pH 5 (filled circles) and 9 (engulfed circles), seawater with pH 5 (filled squares) and 9 (crossed squares).

Methane concentrations

The methane concentration is crucial for the calculation of the MOX rate. However, the concentrations can be determined either in separate bottles, in the control bottles or in the sample itself. The first possibility represents the in situ concentrations, while in the other ones, methane concentrations are altered due to the addition of ^{3}H-CH_4. The addition of ^{3}H-CH_4 should not increase the in situ methane concentrations significantly.

In several sets of samples, we determined the methane concentration (i) in separate bottles, (ii) in the killed controls, and (iii) in the sample bottles. Adding a diluted $^{3}H\text{-}CH_4$ (1×10^{11} Bq mol^{-1}) increased the methane concentration in the samples and controls by 3 nmol l^{-1} or to 103% and 135% of the in situ concentration (Fig. 10). Subsequently, the MOX rate calculated with the different methane concentrations also were very similar. However, on a second cruise the $^{3}H\text{-}CH_4$ was more concentrated (5×10^{12} Bq mol^{-1}) and the methane concentrations in the samples and controls increased 1.5–5 times (to 138% and 469% of the in situ concentration). Thus, the MOX rates calculated with the methane concentrations of the control or the sample increased also by 1.5–5 times and were 1.5–5 times faster than the MOX rate calculated with the in situ methane concentration (Fig. 10). The experiment shows that (1) an additional sample for analysis of the in situ concentration is the easiest and most accurate way to calculate MOX rates and (2) the methane concentration of the $^{3}H\text{-}CH_4$-tracer should be adjusted for low methane concentration environments.

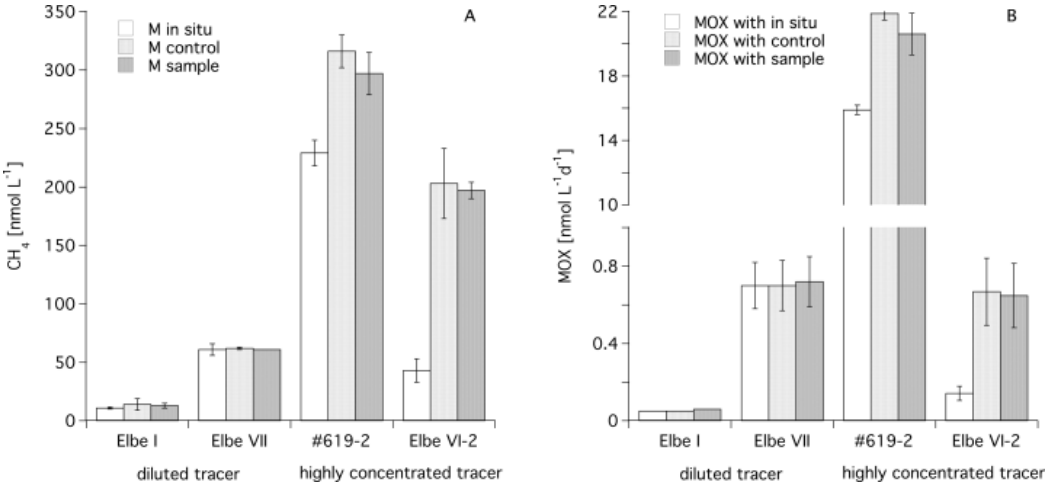

Figure 10. Methane concentrations measured in a separate water samples, in control bottles, and samples bottles, the latter two contain tracer (A). MOX rates calculated with the corresponding in situ methane concentrations, the methane concentrations in the control and sample bottles (B). North Sea and Elbe water was collected for this experiment. Note the break in the *y*-axis.

Using the same dataset, MOX rates were calculated based on the difference in methane concentration between the sample and control bottles. As methane consumption only takes place in the sample but not in the control bottle. In samples with high methanotrophic activity, calculation of the MOX rate with the $^{3}H\text{-}CH_4$-tracer measurement vs. calculation of the difference in concentration were comparable (158 ± 4 nmol L^{-1} d^{-1} vs. 144 ± 31 nmol L^{-1} d^{-1}), however, at low activities the difference in methane concentrations were within the measurement error of the GC (0.8 ± 2.4 nmol L^{-1} d^{-1}) and, thus, not comparable with the radiotracer measurements (0.05 ± 0.01 nmol L^{-1} d^{-1}). The latter comparison illustrates, why tracer experiments are essential in determining aerobic MOX in waters with low methane waters where slow MOX rates are expected. In these waters, the change in methane concentration over time cannot be measured by GC.

MOX rate calculation with time series or single end point measurement

The MOX rate of a specific water sample can be calculated from a time series or as most often is the case from a single end-point measurement. During a time series, consumption of $^{3}H\text{-}CH_4$ is measured after an incubation time of for example 0.5 d, 1 d, 2 d, 3 d, the slope of a linear regression of the fraction of the $^{3}H\text{-}CH_4$ oxidized vs. time is used to calculate k' and then the MOX rate. The rate constant, k', is, thus, determined from a dataset ($n \geq 8$). In contrast, single end-point measurements derive k' from replicate samples ($n \geq 2$). Commonly single end-point measurements are made assuming first-order kinetics, that is, the reaction depends solely on the availability of one substrate, which is methane in this case. Further, it is assumed that the cell population is not growing. To test the reliability of these assumptions, we compared k' derived from (i) a linear regression of time series data, (ii) from the average of the time points of a time series, and (iii) the commonly used 24 h incubation. We used data from marine environments (North Sea and Svalbard), as well as freshwater environments (MPI-pond and Lake Constance), in total 10 datasets. Incubation times ranged from 2 h to 24 h for the freshwater samples and from one day to five days for the marine samples.

As a first step for the time series data, we tested if a linear regression sufficiently describes the data. For all datasets, the average of the residuals was equal to zero (*t*-test for "0"). Also the residuals were normally distributed (Shapiro–Wilk Normality Test with $p = 0.01$, except one dataset). This indicates that the difference from the measured data to the calculated line fit was randomly distributed and showed no systematic deviation. Comparing k' as calculated by (i) a linear regression or by (ii) average of single end points, revealed no significant difference (Wilcoxon Rank Sign Test for paired data, $n = 10$, $p = 0.34$), as also shown in Fig. 11.

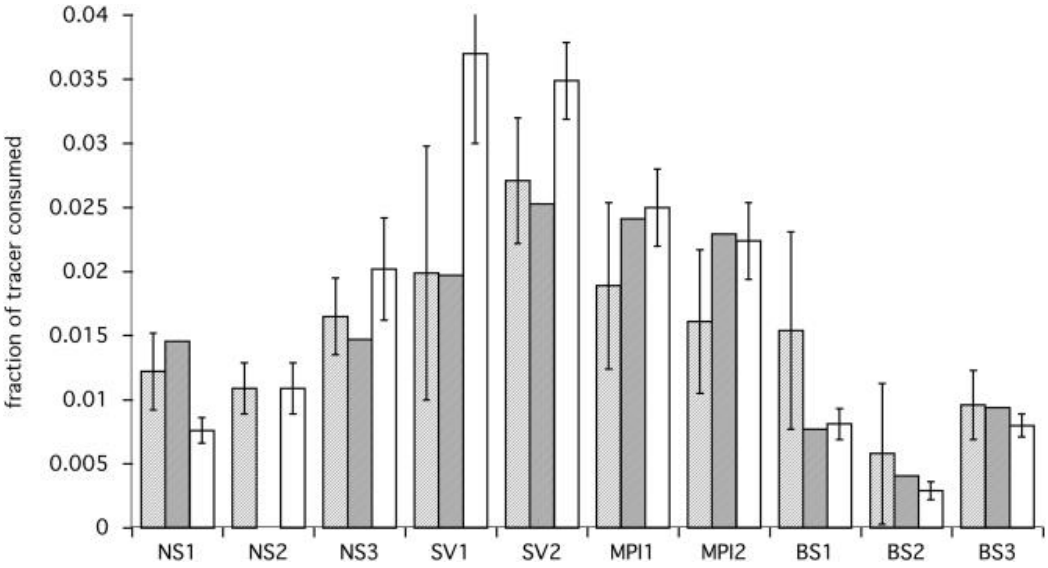

Figure 11. Comparison of the fraction of consumed tracer as calculated either from a linear regression of a time series (white columns), from the average of 3–4 single time points (light shade columns) and from one single end point at 24 h (dark shaded column). Details of the calculation are described in the text. The calculations were applied for three samples from the North Sea (NS1, 2, 3), two samples from off Svalbard (SV1, 2) and for methane rich freshwater settings (MPI1, 2) and Bodensee (BS1, 2, 3).

In general only one single time point (i.e., 24 h) is used for MOX rate calculations. Thus, this one single time point calculation is included among the single time point calculations (*see* also Fig. 4). As shown in Fig. 11 these values range within the values for the linear regression and the single end point calculation and their standard deviations. On average the one single end point calculation was 5% different from the linear regression calculation. Therefore, we assume that the above conclusions are also valid for single time point calculation, as long as this time point lies within the linear range (Fig. 4).

Detection limit

Control samples are frequently taken and are poisoned immediately after the addition of the $^{3}H\text{-}CH_4$ and the "initial ratio" ($^{3}H\text{-}H_2O/^{3}H\text{-}CH_4 + {}^{3}H\text{-}H_2O$) is determined. The mean (x) and the standard deviation (s) of all controls sampled during different cruises in different areas were calculated and the limit of detection (LOD) was set as:

$$LOD = x + 3 \times s$$

All samples with the "initial ratio" below this LOD-value were considered as below the detection limit and had to be set as zero. We applied this strict rule to different datasets of MOX rates (Table 3) with methane concentrations ranging from background concentrations of 1 nmol l^{-1} to high seep concentrations of 1456 nmol l^{-1}. In some cases, 70% of the data were below the detection limit and

had to be set to zero. The lowest detected value was 0.001 nmol L^{-1} d^{-1} based on the datasets of Table 3.

Table 3. LOD calculated for datasets of different areas. The * indicates samples which were measured with a portable Liquid scintillation counter.

Cruise, Year	Area	CH_4 (nmol L^{-1})	LOD MOX (nmol L^{-1} d^{-1})	Data below LOD (%)
HE333, 2010	Svalbard	5–86	0.02	4
PO419, 2011	Svalbard	1–546	0.02*	68
HE406, 2013	North Sea	4–1456	0.02*	70
PS-ANTXXIX, 2013	South Georgia	1–56	0.001	38
HE413, 2014	North Sea	9–686	0.1*	11

The use of laboratory based vs. portable LSD may also influence the LOD. Especially at low activities the counting efficiency of the liquid scintillation counter may be critical. For example, the same samples which were counted with a laboratory-based machine with 760 dpm and 815 dpm, retrieved only 189 dpm and 181 dpm with a portable liquid scintillation counter. While samples with higher counts (47,000 dpm) did not indicate any differences between the two liquid scintillation counters.

Discussion

Although it is known that methane is microbially oxidized in lakes and oceans and that this process reduces the gas flux into the atmosphere, only a small number of MOX data are available. ^{3}H-CH_4 being relatively new commercially available provides a convenient tracer to determine the MOX rate in natural waters. Compared to the ^{14}C-CH_4 method, the ^{3}H-CH_4 method requires minimal sample processing and few specialized equipment. However, as known from the common saying “the devil is in the details,” we checked the method to produce a best practice guide hoping to encourage people to take up the method and indicating the important parameters that can cause large errors. Below, we first discuss the errors found during the method assessment before evaluating existing data.

Error discussion

We compared the different parameters causing uncertainties of the results as outlined in the assessment part by calculating for each tested modification the deviation from the common method in percent. For example, the deviation of the result caused by applying a 10 µL tracer bubble instead of the commonly used 100 µL tracer injection or the deviation caused by storing killed samples for 60 h in contrast to processing samples right after incubation as commonly done (Fig. 12). We also

applied different methane concentrations to calculate the MOX rate, but recommend using the real in situ methane concentration as measured in separate bottles. Otherwise the MOX rates will increase by the same factor as the methane concentrations are increased. However, we did not include this comparison in Fig. 12 as we think this is rather a calculation error than a methodological error.

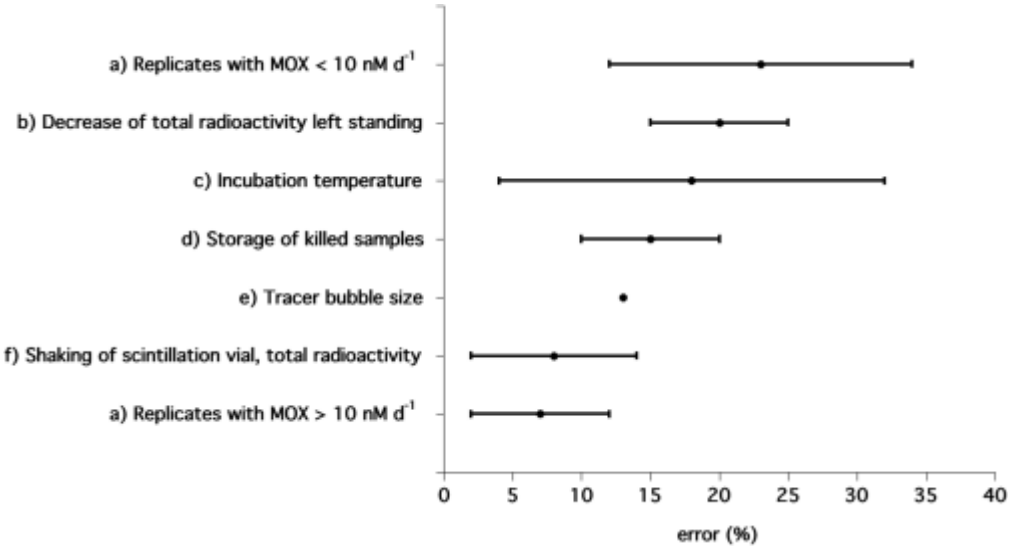

Figure 12. Mean and standard deviation of error associated with different parts of the method: (A) error of replicates indicates the difference from the mean value, (B) decrease of total activity left standing shows the difference between measuring the total activity right after stopping the incubation and measuring after 60 h left standing, (C) incubation temperature illustrates the error of MOX rates if incubation temperatures differ by 1–5°C and Q_{10} ranges between 1.52 and 1.75, (D) storage of killed samples illustrates the error associated with storing a sample instead of rapid post-processing, (E) bubble size indicates the measured difference between a 100 µL bubble and a 10 µL bubble, (F) shaking of scintillation vials indicates the error associated with vigorous shaking of the total activity sample in a scintillation vial.

The largest uncertainty is due to the precision of the MOX rate measurements in waters with low methanotrophic activity (i.e., MOX-rates < 10 mol l^{-1} d^{-1}). By increasing the number of replicates, the precision of the data can be improved, however, at high costs of work effort and material.

This large uncertainty can be viewed as the total error of MOX rates that consists of the error of each step of the method and the heterogeneity of the methanotrophic population in a water sample. This total error is influenced by the following uncertainties which apparently impact low rate measurements more than high rate measurements. The largest impact on the total error is caused by measuring of the total radioactivity (^3H-CH_4 and ^3H-H_2O) not right after opening a sample. The second largest influence is due to incorrect incubation temperature. By incubating samples at temperatures as close as possible to the in situ temperature over- or underestimation of MOX rate can be avoided. The error associated with temperature can also be corrected using published Q_{10} factors. However, as the data base for methanotrophic Q_{10} is very small, we recommend to incubate the samples as

close as possible to the in situ temperature or to determine a Q_{10} for the respective environment. A similarly high error results from the storage of killed samples in comparison to postprocessing the samples right after incubation. The fourth largest error results from the size of the injected $^{3}H\text{-}CH_4$ bubble and minor errors are due to vigorous shaking of the scintillation vial and subsequent counting of the total activity.

Some of these errors are easily avoidable while others can only be limited with more effort. Errors that can be avoided are: (1) measuring the total radioactivity ($^{3}H\text{-}CH_4$ and $^{3}H\text{-}H_2O$) right after opening the sample, (2) not leaving killed samples standing for later analysis, (3) using an appropriate $^{3}H\text{-}CH_4$ bubble volume, and (4) shaking the total radioactivity ($^{3}H\text{-}CH_4$ and $^{3}H\text{-}H_2O$) scintillation mixture gently. The other errors: (1) precision of low activity samples, (2) incubation at in situ temperature or derivation of Q_{10}, and (3) derivation of a more accurate k' by implementing a time series, can also be minimized, but only by processing more samples. It depends on the scientific question and the according precision of the analysis needed, if the additional work and also the additional radioactive waste justify the higher effort.

In contrast to the parameters discussed above, bottle size, background, and produced $^{3}H\text{-}H_2O$, as well as shaking of the samples during incubation cause insignificant MOX rate errors in natural waters. Bottle size insignificantly altered MOX rate measurements; thus, bottle size can be reduced to lessen radioactive waste. Measurements of background $^{3}H\text{-}H_2O$ in microbial inactive waters remained low over 11 d. Therefore, the chemical reaction, that is, self-decomposition and ionic exchange are negligible in the time frame of a typical incubation (< 3 d). If killed controls show a high $^{3}H\text{-}H_2O$ content, microbial metabolism was apparently not efficiently stopped as was shown by Boden and Murrell (2011), who investigated methanotrophic resistivity to $HgCl_2$. Not only the background, but also the produced $^{3}H\text{-}H_2O$ during microbial MOX was found stable over time, thus, these measurements can be delayed, for example, for on-shore analysis. Finally, shaking of the samples during incubation was not found to be relevant and is, thus, not necessary.

Other details of the method investigated resulted in suggestions for best practice to determine MOX rates. Stoppers should consist of halogenated butyl rubber. The tracer is best stored on saturated NaCl-solution, diluted in N_2 and at low temperatures (refrigerator). The incubation time is best determined by conducting a time series and the sparging time should be 30 min. We also recommend to determine the in situ methane concentration used for MOX rate calculations in separate bottles. Thus, one does not need to correct for increased methane concentrations through the addition of $^{3}H\text{-}CH_4$ nor for decreased methane concentrations due to methane consumption by methanotrophs.

Existing data evaluation

MOX rates have been measured using $^{14}C\text{-}CH_4$ and $^{3}H\text{-}CH_4$; data which cannot be readily compared. In the 20st century, water column MOX rates were determined using $^{14}C\text{-}CH_4$ (Scranton and Brewer 1978; Ward et al. 1987) while the $^{3}H\text{-}CH_4$ moved toward becoming commercial accessible in the 21st century. The data are not comparable as 100-fold more methane is added to a sample using $^{14}C\text{-}CH_4$ compared to $^{3}H\text{-}CH_4$ resulting in potential rates at elevated substrate concentration and near in situ rates, respectively. This difference was evaluated in water samples from Storfjorden and discussed in Mau et al. (2013).

For both tracers, the precision of the rate measurement in waters of low methane concentrations and activity appears to be the main uncertainty. In this study, we found the precision of MOX rates in waters of low methanotrophic activity to be the largest error, which might be due to the general higher error associated with low concentration experiments but could also be due to tracer-back-flux as reported for the anaerobic oxidation of methane (Holler et al. 2011). Also Blees et al. (2014) and Jakobs et al. (2013) indicate a great variability in low concentration-samples using $^{14}C\text{-}CH_4$. However, existing publications all include measurements of replicate samples stating the precision. In most studies, duplicate or triplicate sampling is performed. When duplicate samples are used, both data points are shown (Gentz et al. 2013; Mau et al. 2013). Studies with triplicate sampling either show the error bars (Blees et al. 2014) or provide the standard deviation (Jakobs et al. 2013). Hence, the data is of good quality especially when considering rate measurements in the sediment where duplicate or triplicate measurements are not feasible.In contrast to the precision of the measurements, the difference between in situ temperature and incubation temperature was hardly ever corrected, even though we found temperature to cause the second largest influence on error of MOX rates. Most often samples are incubated at a temperature that is close to the in situ temperature, but usually not exactly at in situ temperature. It is normally also not feasible to incubate all samples at in situ temperature, especially in summer when surface ocean temperatures are significantly elevated in comparison to deep water temperatures. Even if two or three incubators are available and set to different temperatures, some water samples are still not incubated at in situ temperatures. Besides, all cooling devices have cooling cycles which might cause temperature variations of up to 5°C (refrigerator). It would be also helpful to monitor more exactly the incubation temperature. Using the Q_{10} correction underestimation or overestimation of the MOX rates can be evaluated, although published Q_{10} values are bulk values and might differ between regions due to the presence of different methanotrophic communities. Certainly, more Q_{10} need to be derived to overcome this insufficient correction of MOX rates.

Another drawback of existing datasets is that no detection limit (LOD) was provided so far. Therefore, very low rates were published, which are most likely below the detection limit. We calculated LOD to be on the order of 0.001 nmol L^{-1} d^{-1} to 0.01 nmol L^{-1} d^{-1} and recommend to use Eq. 5 to derive the detection limit and use only the data that show significant MOX.

Comments and recommendations

Based on the experiments performed for this study, we recommend considering the following aspects when planning MOX rate measurements in an unknown environment. With a time series, the assumption of first-order kinetics can be checked and the appropriate incubation time can be defined. We encountered a rather high variability of the MOX rates, thus, at least three parallel samples are necessary to obtain a sufficient precision. Especially in methane poor environments with low activities the aspect of the detection limit has often been neglected. Therefore, a sufficient number of killed controls have to be setup allowing to distinguish between "real" methane consumption and background noise.

In our study, we investigated some of the important aspects of MOX measurements. However, even when writing the manuscript, we are well aware and realized that more aspects still would be interesting or important to look at. Such aspects could be: Is there a difference when poisoning the controls before or after the tracer addition? What is the influence of different scintillation cocktails and different liquid scintillation counter on the rates? Are there differences between MOX measurements when using gaseous ^{3}H-CH_4 compared to an aqueous tracer solution? The kinetics of MOX in natural waters is still not well-known, as most studies were done with pure cultures of methanotrophs or with soil samples. The priming effect (injection of additional methane and, thus, increasing substrate concentrations) could be tested with nonlabeled methane as well as with labeled methane as was done only by Mau et al. (2013) so far. As with all/many methods an interlaboratory comparison of MOX measurements would be very instructive.

Nevertheless, with our study we hope to improve and to encourage future measurements of MOX rates in different environments. We also hope to develop a standard procedure of MOX rate measurements to make data of MOX better comparable.

References

Abril, G., M.-V. Commarieu, and F. Guérin. 2007. Enhanced methane oxidation in an esturaine turbidity maximum. Limnol. Oceanogr. 52: 470-475,

Abril, G., and N. Iversen. 2002. Methane dynamics in a shallow non-tidal estuary (Randers Fjord, Denmark). Mar. Ecol. Prog. Ser. 230: 171-181,

Angelis, M. a. D., M. D. Liley, E. J. Olson, and J. A. Baross. 1993. Methane oxidation in deep-sea hydrothermal plumes of the Endeavour Segment of the Juan da Fuca Ridge. Deep Sea Research 40: 1169-1186,

Bastviken, D., J. Ejlertsson, I. Sundh, and L. Tranvik. 2002. Measurement of methane oxidation in lakes: a comparison of methods. Environ. Sci. Technol. 36: 3354-3361,

Bastviken, D., L. J. Tranvik, J. A. Downing, P. M. Crill, and A. Enrich-Prast. 2011. Freshwater methane emissions offset the continental carbon sink. Science 331: 50-50, urn:nbn:se:liu:diva-64364.

Blees, J., H. Niemann, C. B. Wenk, J. Zopfi, C. J. Schubert, M. K. Kirf, M. L. Veronesi, C. Hitz, and M. F. Lehmann. 2014. Micro-aerobic bacterial methane oxidation in the chemocline and anoxic water column of deep south-Alpine Lake Lugano (Switzerland). Limnol. Oceanogr. 59: 311-324, DOI: 10.4319/lo.2014.59.2.0311.

Boden, R., M. Cunliffe, J. Scanlan, H. Moussard, K. D. Kits, M. G. Klotz, M. S. M. Jetten, S. Vuilleumier, J. Han, L. Peters, N. Mikhailova, H. Teshima, R. Tapia, N. Kyrpides, N. Ivanova, Ioanna Pagani, A.-F. Cheng, L. Goodwin, C. Han, L. Hauser, M. L. Land, A. Lapidus, S. Lucas, S. Pitluck, T. Woyke, L. Stein, and J. C. Murrell. 2011. Complete Genome Sequence of the Aerobic Marine Methanotroph Methylomonas methanica MC09. J. Bacteriol. 193: 7001, 10.1128/JB.06267-11.

Bowman, J. 2006. The Methanotrophs—The Families Methylococcaceae and Methylocystaceae, p. 266–289. Prokaryotes. Springer.

Button, D. K. 1991. Biochemical basis for whole-cell uptake kinetics: specific affinity, oligotrophic capacity, and the meaning of the Michaelis constant. Appl. Environ. Microbiol. 57: 2033-2038,

Damm, E., E. Helmke, S. Thoms, U. Schauer, E. Nöthig, K. Bakker, and R. P. Kiene. 2010. Methane production in aerobic oligotrophic surface water in the central Arctic Ocean. Biogeosciences 7: 1099-1108,

Ducklow, H. W., O. Schofield, M. Vernet, S. Stammerjohn, and M. Erickson. 2012. Multiscale control of bacterial production by phytoplankton dynamics and sea ice along the western Antarctic Peninsula: A regional and decadal investigation. J. Mar. Syst. 98: 26-39, http://dx.doi.org/10.1016/j.jmarsys.2012.03.003.

Dumestre, J. F., J. Guézennec, C. Gaky.Lacaux, R. Delmas, S. Richard, and L. Labroue. 1999. Influence of light intensity on methanotrophic bacterial activity in Petit Saut Reservoir, French Guiana. Appl. Environ. Microbiol. 65: 534-539,

Dunfield, P., R. Knowles, R. Dumont, and T. R. Moore. 1993. Methane production and consumption in temperate and subarctic peat soils: Response to temperature and pH. Soil Biol. Biochem. 25: 321-326, http://dx.doi.org/10.1016/0038-0717(93)90130-4.

Emerson, S., and J. Hedges. 2009. Chemical Oceanography and the Marine Carbon Cycle. Cambridge University Press,

Gentz, T., E. Damm, J. S. Von Deimling, S. Mau, D. F. Mcginnis, and M. Schlüter. 2013. A water column study of methane around gas flares located at the West Spitsbergen continental margin. Cont. Shelf Res., doi:10.1016/j.csr.2013.07.013.

Heeschen, K. U., R. S. Keir, G. Rehder, O. Klatt, and E. Suess. 2004. Methane dynamics in the Weddell Sea determined via stable isotope ratios and CFC-11. Glob. Biogeochem. Cycl. 18: GB2012 2011-2018,

Heintz, M. B., S. Mau, and D. L. Valentine. 2012. Physical control on methanotrophic potential in waters of the Santa Monica Basin, Southern California. Limnol. Oceanogr. 57: 420-432, 10.4319/lo.2012.57.2.0420.

Holler, T., G. Wegener, H. Niemann, C. Deusner, T. G. Ferdelman, A. Boetius, B. Brunner, and F. Widdel. 2011. Carbon and sulfur back flux during anaerobic microbial oxidation of methane and coupled sulfate reduction. Proceedings of the National Academy of Sciences 108: E1484-E1490,

Horak, R. E. A., W. Qin, A. J. Schauer, E. V. Armbrust, A. E. Ingalls, J. W. Moffett, D. A. Stahl, and A. H. Devol. 2013. Ammonia oxidation kinetics and temperature sensitivity of a natural marine community dominated by Archaea. ISME Journal 7: 2023-2033,

IPCC, P. Ciais, C. Sabine, G. Bala, L. Bopp, V. Brovkin, J. Canadel, A. Chhabra, R. Defries, J. Galloway, M. Heimann, C. Jones, C. L. Quéré, R. B. Myneni, S. Piao, and P. Thornton. 2013. Carbon and Other Biogeochemical Cycles. In T. F. Stocker, D. Qin, G.-K. Plattner, M. Tignor, S. K. Allen, J. Boschung, A. Nauels, Y. Xia, V. Bex and P. M. Midgley [eds.], Climate Change 2013: The Physical Science Basis. Contribution of Working Group I to the Fifth Assessment Report of the Intergovernmental Panel on Climate Change Cambridge University Press.

Jakobs, G., G. Rehder, G. Jost, K. KieVÜlich, M. Labrenz, and O. Schmale. 2013. Comparative studies of pelagic microbial methane oxidation within the redox zones of the Gotland Deep and Landsort Deep (central Baltic Sea). Biogeosciences 10: 7863-7875,

Jones, R. D. 1991. Carbon monoxide and methane distribution and consumption in the photic zone of the Sargasso Sea. Deep Sea Research 38: 625-635,

Jørgensen, B. B. 1978. A comparison of methods for the quantification of bacterial sulfate reduction in coastal marine sediments. I. Measurements with radiotracer techniques. Geomicrobiol. J. 1: 11-64,

Karl, D. M., L. Beversdorf, K. M. Bjoerkman, M. J. Church, A. Martinez, and E. F. Delong. 2008. Aerobic production of methane in the sea. Nat. Geosci. 1: 473-478,

Koschel, R. 1980. Untersuchungen zur Phosphataffinitat des Planktons in der euphotischen Zone von Seen. Limnologica 12: 141-145,

Krüger, M., T. Treude, H. Wolters, K. Nauhaus, and A. Boetius. 2005. Microbial methane turnover in different marine habitats. Palaeogeogr., Palaeoclimatol., Palaeoecol. 227: 6-17,

Mau, S., J. Blees, E. Helmke, H. Niemann, and E. Damm. 2013. Vertical distribution of methane oxidation and methanotrophic response to elevated methane concentrations in stratified waters of the Arctic fjord Storfjorden (Svalbard, Norway). Biogeosciences 10: 6267-6278,

Metcalf, W. W., B. M. Griffin, R. M. Cicchillo, J. Gao, S. C. Janga, H. A. Cooke, B. T. Cir-Cello, B. S. Evans, W. Martens-Habbena, D. A. Stahl, and W. a. V. D. Donk. 2012. Synthesis of methylphosphonic acid by marine microbes: a source for methane in the aerobic ocean. Science 337: 1104–1107,

Niemann, H., L. Steinle, J. Blees, I. Bussmann, T. Treude, S. Krause, M. Elvert, and M. F. Lehmann. 2015. Toxic effects of lab-grade butyl rubber stoppers on aerobic methane oxidation. Limnol. Oceanogr.: Methods 13: 40-52, 10.1002/lom3.10005.

Pack, M. A., M. B. Heintz, W. S. Reeburgh, S. E. Trumbore, D. L. Valentine, X. Xu, and E. R. M. Druffel. 2011. A method for measuring methane oxidation rates using low levels of 14C-labeled methane and accelerator mass spectrometry. Limnol. Oceanogr.: Methods 9: 245-260, 10.4319/lom.2011.9.245.

Raven, J. A., and R. J. Geider. 1988. Temperature and algal growth. New Phytol. 110: 441-461, 10.1111/j.1469-8137.1988.tb00282.x.

Reeburgh, W. 2007. Oceanic methane biogeochemistry. Chemical Reviews 107: 486-513, 10.1021/cr050362v

Reeburgh, W. S., B. B. Ward, S. C. Whalen, K. A. Sandbeck, K. A. Kilpatrick, and L. J. Kerkhof. 1992. Black Sea methane geochemistry. Deep Sea Research 38: 1189-1210,

Rehder, G., R. Keir, E. Suess, and M. Rhein. 1999. Methane in the northern Atlantic controlled by microbial oxidation and atmospheric history. Geophys. Res. Lett. 26: 587-590, DOI: 10.1029/1999GL900049.

Schubert, C. J., F. S. Lucas, E. Durisch-Kaiser, R. Stierli, T. Diem, O. Scheidegger, F. Vazquez, and B. Muller. 2010. Oxidation and emission of methane in a monomictic lake (Rotsee, Switzerland). Aquat. Sci. 72: 455-466, 10.1007/s00027-010-0148-5.

Scranton, M. I., and P. G. Brewer. 1978. Consumption of dissolved methane in the deep ocean. Limnol. Oceanogr. 23: 1207-1213,

Simon, M., S. Billerbeck, D. Kessler, N. Selje, and A. Schlingloff. 2012. Bacterioplankton communities in the Southern Ocean: composition and growth response to various substrate regimes. Aquat. Microb. Ecol. 68: 13-28,

Tang, K. W., D. F. Mcginnis, K. Frindte, V. Brüchert, and H. P. Grossart. 2014. Paradox reconsidered: Methane oversaturation in well-oxygenated lake waters. Limnol. Oceanogr. 59: 275-284,

Tissot, B. P., and D. H. Welte. 1984. Petroleum Formation and Occurrence. . Springer Verlag, Heidelberg,

Valentine, D. L., D. C. Blanton, W. S. Reeburgh, and M. Kastner. 2001. Water column methane oxidation adjacent to an area of active hydrate dissociation, Eel river Basin. Geochim. Cosmochim. Acta 65: 2633-2640,

Ward, B. B., K. A. Kilpatrick, P. C. Novelli, and M. I. Scranton. 1987. Methane oxidation and methane fluxes in the ocean surface layer and deep anoxic waters. Nature 327: 226-229,

Acknowledgments

Many thanks are given to the scientific parties and crews of the research vessels Heincke, Polarstern, Poseidon, Prandtl, and Uthörn. We thank K.W. Klings for excellent technical assistance. We like to thank J. Blees, the laboratory of A. Boetius and D.L. Valentine for their help analyzing samples and providing equipment. We acknowledge the support of the PERGAMON for the initial workshop "Establishing standard protocols for the quantification of microbial methane oxidation rates in sediments and in the water column," Kiel, June 2012. This work was partly funded through the project "Limitations of marine methane oxidation" funded by the DFG (Grant no. MA 3961/2-1). The work of A.M. was funded by the DAAD, by the Grant Agency of the Czech Republic (Grant no. 13-00243S) and a grant of the Faculty of Science, University of South Bohemia (GAJU 04-145/2013/P).

Additional manuscript II (Published in *Aquatic Sciences*, 2016, 1-16, DOI: 10.1007/s00027-016-0509-9)

Methane distribution and methane oxidation in the water column of the Elbe estuary, Germany

Authors: *Matoušů Anna[1,2], Osudar Roman[3], Šimek Karel[1,2] and Bussmann Ingeborg[4]

[1]Faculty of Sciences, University of South Bohemia, České Budějovice, Czech Republic

[2]Biology Centre CAS, v.v.i., Institute of Hydrobiology, České Budějovice, Czech Republic

[3]Alfred Wegener Institut Helmholtz-Zentrum für Polar- und Meeresforschung, Potsdam, Germany

[4]Alfred Wegener Institut Helmholtz-Zentrum für Polar- und Meeresforschung, Helgoland, Germany

*Corresponding author: e-mail anna.matousu@gmail.com; phone number +420 387 775 834

Abstract

The River Elbe, as one of the major waterways of central Europe, is a potential source of high amounts of methane into the North Sea. Twelve sampling cruises from October 2010 until June 2013 were conducted from Hamburg towards the mouth of the Elbe at Cuxhaven. The dynamic of methane concentrations in the water column and its consumption via methane oxidizing bacteria was measured. In addition, physico-chemical parameters were used to estimate their influence on the methanotrophic activity. We observed high methane concentrations at the stations in the area of Hamburg harbour ("upper estuary") and about 10 times lower concentrations in the lower estuary (median of 416 versus 40 nmol L^{-1}, respectively). The methane oxidation rate mirrored the methane distribution with high values in the upper estuary and low values in the lower estuary (median of 161 versus 10 nmol L^{-1} day^{-1}, respectively). Methane concentrations were significantly influenced by the river hydrology (falling water level) and the biological oxygen demand while interestingly, no clear relation to the amount of suspended particulate matter (SPM) was found. Methane oxidation rates were significantly influenced by methane concentration and to a lesser extent by temperature. Methane oxidation accounted for 41 ± 12 % of the total loss of methane in summer/fall periods, but for only 5 ± 3 % of the total loss in the winter/spring periods (total loss = methane oxidation + diffusion into the atmosphere). The average sea-air flux of methane was 33 ± 8 g CH_4 m^{-2} y^{-1}. We applied a box model taking into account the residence times of each water parcel depending on discharge and tidal impact. We observed almost stable methane concentrations in the lower estuary, despite a strong loss of methane through diffusion and oxidation. Thus we postulate that losses in the lower Elbe estuary were balanced by additional inputs of methane, possibly from extensive salt marshes near the river mouth.

Introduction

Estuaries are highly dynamic ecosystems where freshwater meets marine water and diverse biological, physical and chemical parameters constantly change, which makes estuaries to hot-spots of biological production and biodiversity (Bianchi 2007). Due to the physical and chemical mechanisms present in brackish water (e.g. long residence time, low salinity) turbidity zones are produced with high concentrations of suspended particulate matter (SPM). In such zones riverine phytoplankton becomes limited by light and dies, which results in a considerable enhancement of the easily degradable organic matter available to microbes (Cole et al. 1992). This material is subsequently decomposed and re-mineralized by heterotrophic bacteria resulting in elevated levels of carbon dioxide (CO_2) and methane (CH_4) emissions (Frankignoulle et al. 1998; Borges and Abril 2011), being the two most abundant carbon-containing greenhouse gasses in the atmosphere with a considerable impact on global warming. Estuaries present an interface between rivers and oceans, where rivers act as major sources of CH_4 to the atmosphere (Borges et al. 2015a). The role of the ocean as atmospheric methane source (including geological sources) is estimated to be 16 % of natural sources, which is the same range as freshwater (including lakes and rivers) with 12 % of the natural sources (IPCC 2013).

On the contrary to methane production, microbial CH_4 oxidation via specialized microbes, so called methanotrophs (MOB, methane-oxidizing bacteria) represents a biological sink of methane in aquatic environments. Methanotrophy can significantly reduce the amount of CH_4 escaping from the sediments and subsequently from the water column into the atmosphere (Kankaala et al. 2006; Conrad 2009; Bastviken 2009). Methanotrophs are physiologically specialized groups of methylotrophic prokaryotes capable of utilizing single carbon compounds (methane, methanol and few strains can utilize methylamine and a narrow selection of other C1 compounds; Bowman 2006) as an electron donor and source of cell carbon. Aerobic methanotrophs are widely distributed in nature, typically at anoxic–oxic interfaces (Bowman 2006). They can make an important contribution to the biomass entering the food web and can consume up to 50 % of CH_4 diffusing from the sediments in some estuaries (de Angelis and Scranton 1993; Abril and Iversen 2002). However, the conditions influencing the methanotrophic activity in the water column are still largely unknown, making it even more difficult to uncover the major driving forces of the activity of MOB in such a variable ecosystem as an estuary. For instance, temperature may affect enzymatic activity and temperature variations may also lead to changes in the structure of the methanotrophic community (Sundh et al. 2005; Mohanty et al. 2007). It seems likely that methane oxidation (MOx) is mainly controlled by physical processes, i.e. gas-phase diffusion and transport of CH_4 to the cells, rather than by enzymatic reactions (Urmann et al. 2009). Besides CH_4, the limitation of other simple organic

substrates and nutrients may also affect methanotrophic activity (Rudd et al. 1976; Bender and Conrad 1994; Bodelier et al. 2000). King (1990) showed that light strongly controls MOx via photosynthesis by the extension of the oxic zone suitable for methanotrophic activity. On the contrary, the investigations made by Dumestre et al. (1999) in Petit Saut Reservoir and later by Murase and Sugimoto (2005) at mesotrophic Lake Biwa suggested that methane oxidation can be inhibited by visible light. Especially in estuarine habitats, two parameters may strongly affect the MOx—salinity and suspended particulate matter (SPM) content. Whereas salinity has an inhibitory effect on MOx (de Angelis and Scranton 1993; Conrad et al. 1995), SPM shows a positive influence on MOx rate. The MOB may settle on organically rich particles (Zimmermann 1997, 2002) and thus exploit the micro-patchiness with locally enhanced CH_4 concentrations to become available for MOB (Abril et al. 2007).

In an effort to clarify the relationship between MOB and their environment, the aims of this study were: (i) to examine the distribution of CH_4 in the water column of the River Elbe estuary, (ii) to assess the activity of MOB as well as major physical and chemical parameters influencing their activities and (iii) to attempt to budget the different methane related processes along a large estuarine ecosystem.

Material and methods

Study site

The River Elbe rises at an elevation of 1386 m above sea level in the Krkonoše (Giant Mountains) in the northeast of the Czech Republic, flows through the central part of the Czech Republic and central and northern Germany before discharging into the North Sea at Cuxhaven (Fig. 1). The Elbe estuary is a eutrophic ecosystem receiving urban, agricultural and industrial waste. It is an intermediate-turbid, well-mixed estuary with a pronounced estuarine turbidity maximum (ETM; approximately from #659 to #719, see Fig. 1) in the brackish zone of the estuary; note that these station codes are derived from the Elbe-km, which refer to the distance from the Czech-German border (=0 river-km; IKSE 1995). The range of semi-diurnal tides rise from 2 m (at the Geesthacht weir) towards the port of Hamburg where it attains its maximum of 3.5 m. High tidal current velocities (up to 1.8 m s^{-1}; Bergemann and Gaumert 2010) cause a steep horizontal salinity gradient, particularly near Brunsbüttel (#690). The residence time of water varies from 15 to 30 days (Frankignoulle and Middelburg 2002). Based on the different biogeochemical processes and oxygen demands the Elbe estuary can be divided into two sections (according to Amann et al. 2012): (1) the pre-oxygen minimum zone (pre-OMZ; approximately from #585 to #624), and (2) the oxygen minimum zone (OMZ; approximately from #624 to #659), both fall into the tidal freshwater area. The Elbe estuary is

a unique, well monitored system with data on physical and chemical parameter available from www.portal-tideelbe.de and www.fgg-elbe.de. Our sampling stations started in the port of Hamburg at station #619 and were spaced at intervals of 10 and 20 km, terminated at Cuxhaven with #724 (Fig. 1). For the purpose of this study, the sampling sites were divided "upper estuary" and the "lower estuary": the upper estuary includes sampling sites #619 and #629; the lower estuary part covers the sampling sites from #659 till #724; site #639 was designed as the "transition zone".

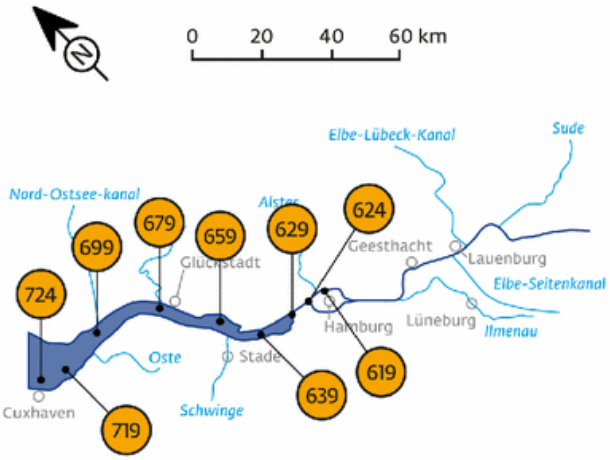

(A)

Station code	Latitude	Longitude
#619 (n=13)	53°31,92 N	10°1,53 E
#624 (n=7)	53°32,59 N	9°57,25 E
#629 (n=10)	53°32,56 N	9°52,77 E
#639 (n=16)	53°33,72 N	9°43,93 E
#659 (n=18)	53°39,99 N	9°30,76 E
#679 (n=18)	53°49,07 N	9°21,50 E
#699 (n=18)	53°52,51 N	9°5,54 E
#719 (n=24)	53°51,10 N	8°47,76 E
#724 (n=20)	53°52,55 N	8°43,94 E

(B)

	Range	Length [km]	Depth [m]	Area [km^2]	Volume [km^3]	Ratio (A / V)
Box 1	#619 - #629	10	8 - 10	3	0.04	97
Box 2	#629 - #639	10	10 - 15	5	0.05	100
Box 3	#639 - #659	20	12 - 15	16	0.13	125
Box 4	#659 - #679	20	12 - 15	25	0.19	134
Box 5	#679 - #699	20	11 - 16	35	0.27	131
Box 6	#699 - #719	20	9 - 16	43	0.34	128
Box 7	#719 - #724	5	9 - 23	23	0.11	204

Fig. 1. Overview of sampling sites in the Elbe River estuary. The station codes are derived from the river-kilometres, which refer to the distance from the Czech-German border (=0 river-km; IKSE 1995). Station coordinates are given in table A. Parameters of used box-model are given in table B

Original map source: https://commons.wikimedia.org/wiki/File:Lauf_der_Elbe.png, modified

Sampling

Twelve sampling campaigns were performed from October 2010 till June 2013. All data are available in the Pangaea data base (www.pangaea.de; Bussmann et al. 2014, Matousu et al. 2015). The water samples were collected in the main channel of the Elbe from the research vessel "Ludwig Prandtl" (Helmholtz-Zentrum Geesthacht, Germany) and were taken from two different depths of the water column: approximately 1 m above the river bed ("bottom") and approximately 1 m below the water surface ("surface"). Samples for CH_4 concentration and CH_4 oxidation rate were transferred directly from a water sampler (Uwitec, Austria) into serum bottles (120 ml). Bottles were overfilled with

approximately two volumes of water, capped with black butyl stoppers (Ochs, Germany), and sealed with an aluminum crimp. Care was taken to exclude air bubbles from capped samples. An additional water sample was taken for analyses of other water properties.

Analytical methods

The duplicate methane concentration samples were killed immediately, by injecting 0.3 ml of 5 M NaOH through the septum into the serum bottle filled with water to stop microbial activity. The samples were analyzed within 1 week in the laboratory by using a headspace technique according to McAuliffe (1971): a 20 ml headspace was created by adding N_2 through a syringe causing displacement of 20 ml of water through another needle in the stopper. Afterwards the samples were vigorously shaken and then stored for 24 h at room temperature to allow equilibration of the gases in the headspace. Subsequently the samples were analyzed with a gas chromatograph equipped with a flame ionization detector (GC 2014 Shimadzu Corp). Calibration was performed with 10 ppm and 100 ppm methane standards (Air Liquide). Precision of the analyses was 2 %; the r^2 of the calibration curve >97 %. Dissolved CH_4 concentrations were calculated with the solubility coefficients of Yamamoto et al. (1976).

The CH_4 oxidation rates were determined as outlined in Bussmann et al. (2015). Water samples were processed in triplicates with one "killed control". Immediately after collecting the samples, 100 µl (10 µCi) of ^3H-CH_4 (American Radiolabeled Chemicals, Inc.) was injected into each sample through the septum. Control samples were killed by injecting 200 µl of 5 M NaOH before the tracer was added. The samples were vigorously shaken for 60 s and incubated in the dark at near in situ temperature. Activities in "live" samples were stopped in the same way as "killed controls", but after approximately 24 h of incubation. Samples were stored in the dark at 4 °C, prior to being analyzed (within 1 week).

In the laboratory, the samples were opened, 2 ml aliquot of each sample was mixed with 5 ml of scintillation cocktail (Ultima Gold™ LLT) and analyzed with a liquid scintillation counter (Tri-Carb® 2910 TR, Perkin Elmer) for estimation of the total radioactivity of the sample, i.e. the labeled CH_4 and labeled produced H_2O (see Eq. 1). Subsequently the samples were sparged with air for 30 min to expel all remaining labeled CH_4. Afterwards, again 2 ml aliquot of each sample was mixed with 5 ml of scintillation cocktail and analyzed with a liquid scintillation counter for estimation of the the microbially produced radioactive water.

The principle of the calculation of the microbial mediated MOx is based on the transformation of added radioactively labeled tracer (^3H-CH_4) into the oxidation product (^3H-H_2O) during incubation:

$$^{*}CH_4 + 2O_2 \rightarrow CO_2 + 2^{*}H_2O \quad (1)$$

In order to calculate the methane oxidation rate (RO_x), first the fraction of methane that was turned over is calculated:

$$F[CH_4] = [H_2O]produced\ /\ [CH_4]injected \quad (2)$$

The fractional turnover rate constant (k) is then determined by dividing it by the incubation time (t):

$$K = F[CH_4] / t \quad (3)$$

Finally the oxidation rate (MO_x) is obtained by multiplication with the in situ methane concentration:

$$MOx = k \times [CH_4] \quad (4)$$

The inverse of the fractional turnover rate (k) is the turnover time (τ):

$$\tau = 1 / k \quad (5)$$

The turnover time is the time which it would take to oxidize the ambient amount of CH_4 dissolved in water with a given methane oxidation rate. The turnover time rate is an effective measure of the methanotrophic potential (Heintz et al. 2012).

The “killed controls” served for estimation of abiotically formed radioactive H_2O, which could lead to an overestimation and these (on average about 3.5 % of total transformation) were subtracted.

During the sampling campaigns along the Elbe River temperature, salinity, and oxygen in the water were measured right after sampling using a Universal Pocket Meter (Multi 340i) with a precision of 0.01 for salinity, 0.1 °C for temperature, and 0.5 % for oxygen.

Depending on the load of suspended particulate matter (SPM) 250 ml of water were filtered through prewashed (with MQ water) and pre-weighed Whatman GF/C filters and dried for 24 h at 60 °C, and weighed for determination of the total SPM content.

For nutrient analysis, water samples were filtered through GF/C filters (Whatman™) immediately after collection. Afterwards the filtrates were transferred into 50 ml Falcon tubes and frozen until further analysis in the laboratory. Samples were analyzed for phosphate, silicate, ammonia, nitrate, and nitrite with an autoanalyzer (AA3 from Seal-Analytical, Germany) and using standardized techniques as detailed in Wiltshire et al. (2010), following techniques described by Grasshoff et al. (1983). The error is estimated to be 10 %.

Additional data for the water level (Ganglinie) were obtained from the "Wasser- und Schifffahrtsverwaltung des Bundes", given through the Bundesanstalt für Gewässerkunde (BfG). We assigned the data from our stations to their locations according to the following: #619 with #623 (St. Pauli), #659 with #660 (Grauerort), #679 with #674 (Glückstadt) and #724 with #724 (Cuxhaven Steubenhöft). We took the original water level of the sampling time and calculated the difference from −10 to +10 min from sampling time and defined this parameter as "delta water level".

Data for the biological oxygen demand in 7 days (BOD-7, in mg O_2 L^{-1}) were obtained from the Elbe data portal (http://www.elbe-datenportal.de). The stations were allocated within 6 km distance to our stations and within 3 days range of our sampling date. Data ranged from 1 to 5.7 mg L^{-1}, n = 24.

Data for the discharge (m^3 s^{-1}) were also obtained from the Elbe data portal (http://www.elbe-datenportal.de). These data were measured at "Pegel Neu Darchau". Data were only allocated to the stations of the upper estuary (#619 and #624), because for the following stations we assume an increasing tidal input. As the water takes about 1 day from Neu Darchau to reach Hamburg, we also took the data from 1 day earlier than the sampling date.

Statistical analysis

To determine the possible dependence of CH_4 concentration and CH_4 oxidation rate on measured physical (water depth, water temperature) and chemical factors (salinity, NH_4^+, NO_3^-, NO_2^-, PO_4^{3-}, SiO_4, O_2, SPM) Spearman rank order correlation analyses were performed. Calculations and graphical representation were performed using SigmaPlot for Windows Version 11.0 software. One way ANOVA, linear correlation after log transformation and Wilcoxon test were performed with Kaleidagraph Version 4.1.3. Redundancy analyses (RDA) were performed using CANOCO program Version 4.5 (Ter Braak and Šmilauer 2002). Environmental parameters were selected using forward selection with 999 Monte Carlo permutations. The results of the RDA were visualized by CanoDraw for Windows. The box plots (Fig. 2) show the median (middle line), the lower and upper quartile (bottom and top of the box) with 25 and 75 % of the data, the minimum and maximum of the data, being the lines extending from the bottom and top of the box. The dots are outliers, whose values are either greater/smaller than 1.5 * upper or lower quartile (Kaleidagraph Version 4.1.3).

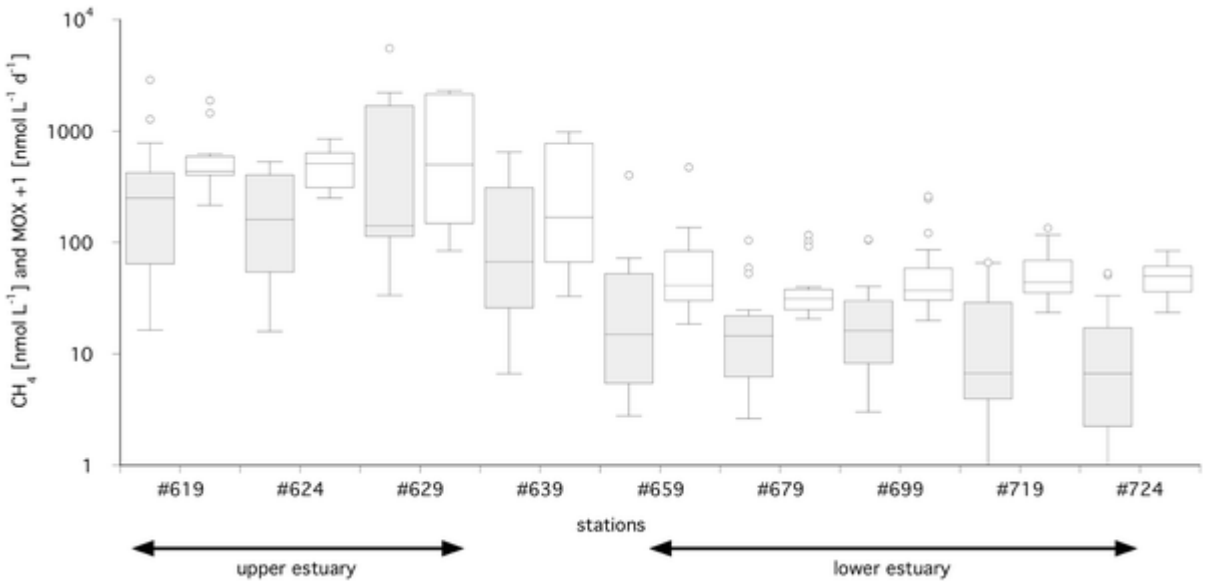

Fig. 2. ***Box plots*** **of the methane concentrations (*grey boxes*) and oxidation rates (*white boxes*) at the river stations in the Elbe estuary during the sampling campaigns from October 2010 to June 2013. We grouped the stations into upper (#619–#629) and lower estuary (#659–#724), with the station #639 as a transition zone. The number of samples ranged from n = 7 at station #624 to n = 24 at station #724. For definition of the *box plot* see "Material and methods".**

Calculations of the sea-air fluxes and the methane budget

To reduce interferences with tidal currents we selected four cruises when the water level was falling during sampling time, i.e. the overall water flow and the ship movement was towards the sea. These cruises were 3. 8. 2011, 12. 4. 2013 and 12. 6. 2013 for stations #619–#679; and 1. 8. 2012 for stations #659–#724. For flux calculation and budgeting we defined boxes between the different stations. With the maps provided by "Wasser- und Schifffahrtsverwaltung des Bundes", given through www.portal-tideelbe.de, we estimated the length and width of the river at each station. The depth of the "navigational channel" was set as 15 m and for the "deep water zone" ranging from 10 to 2 m, an average depth of 6 m was assumed. The boxes were split into different triangles and squares and the respective areas and volumes were calculated (Fig. 1; Supplementary material 1).

Gas exchange across an air–water interface can be described in general by the following function (Wanninkhof et al. 2009):

$$F = k \times (c_m - c_e) \quad (6)$$

where F is the rate of gas flux per unit area, c_m is the methane concentration measured in surface water and c_e is the atmospheric gas equilibrium concentration based on Wiesenburg and Guinasso (1979).

The gas exchange coefficient (k) is a function of water surface agitation. However, in oceans and estuaries k is more determined by wind speed, while in rivers water velocity dominates (Alin et al. 2011). The determination of k is very important for the calculation of the sea–air flux. We decided to calculate k_{600} in the Elbe according to the empirical Eq. 2 from Raymond et al. (2012):

$$k_{600} = 4725 \times (V \times S)^{0.86} \times Q^{-0.14} \times D^{0.66} \quad (7)$$

with V as stream velocity (m s^{-1}), S as slope, Q as discharge (m^3 s^{-1}), and depth (m). Data on stream discharge were obtained from "Pegel Neu Darchau", data on stream velocity were provided by www.portal-tideelbe.de, for the respective stations and dates. The slope of the Elbe estuary at its delta was 0.00005 (tidal range of 5 cm/km for the upper estuary; Vandenbruwaene et al. 2013). For the two lower stations (#719 and #724) we took the empirical model from Borges et al. (2004), which is only wind driven. Wind data were obtained for Cuxhaven from the German Weather Service. Further details are given in Supplementary material 2. The calculated k_{600} (value for CO_2 at 20 °C) was converted to k_{CH4} according to (Striegl et al. 2012):

$$k_{CH4} / k_{600} = (Sc_{CH4} / Sc_{CO2})^{0.69} \quad (8)$$

where Schmidt numbers (Sc) are determined by water temperature and salinity, according to (Wanninkhof 1992).

For each station with its "navigational channel"and its "deep water zone", k_{CH4} was determined as described above. The atmospheric equilibrium concentration and difference to the measured methane concentrations were calculated. With Eq. 6 we calculated the respective sea–air fluxes (mol m^2 day^{-1}). The average of this flux between two neighboring stations was then multiplied with the respective area of the box. Then the sea–air flux for the "navigational channel" and the flux for the "deep water zone" were added, resulting in the total sea–air flux for each box in mol day^{-1}.

For calculation of the total MOx rate, we took the average MOx between two neighboring stations and multiplied it by the total volume of the respective box ($V_{navigational\ channel} + V_{deep\ water}$). This resulted in the total MOx rate of each box in mol day^{-1}.

Results

Physico-chemical parameters of water

The physical parameters of the water samples are shown in Table 1. The values of the chemical parameters fluctuated considerably (Table 1). Phosphate had a clear seasonal trend with the highest values being in winter at #699 and #719. Oxygen also varied seasonally, with the lowest values being in summer. Other nutrients showed no clear seasonal or spatial pattern, in contrast to SPM with the

highest values being in spring at #679 and #699 (i.e., in the estuarine turbidity maximum zone). Salinity increased towards the river mouth with 2.2 ± 1.6 at #699 up to 12.4 ± 6.2 at #724, no clear seasonal pattern was, however, evident.

Table 1. Overview of collected data on physico-chemical parameters in the water column of the River Elbe estuary during all sampling campaigns from October 2010 to June 2013: median and the range of the data (in brackets) are given.

Station code	Salinity [PSU]	Oxygen [mg L^{-1}]	Temperature [°C]	SiO_4 [µmol L^{-1}]	PO_4^{3-} [µmol L^{-1}]	NO_2^- [µmol L^{-1}]	NO_3^- [µmol L^{-1}]	NH_4^+ [µmol L^{-1}]
#619	0.4 ± 0.2	8.1 ± 1.5	14.6 ± 5.2	133.6 (0.0–177.0)	1.5 (0.1–4.8)	1.4 (0.6–2.4)	278.2 (196.5–1451.2)	4.9 (3.6–20.3)
#624	0.3 ± 0.2	9. ± 1.4	15.3 ± 5.7	135.2 (129.5–213.3)	1.3 (1.0–5.9)	2.5 (2.0–2.8)	230.2 (216.4–289.9)	9.6 (8.3–11.4)
#629	0.3 ± 0.2	6.9 ± 2.4	12.7 ± 4.7	133.8 (0.0–135.2)	1.5 (0.3–3.7)	1.3 (0.6–2.6)	290.0 (119.3–1386.7)	5.7 (4.2–12.6)
#639	0. ± 0.2	7.6 ± 2.2	13.9 ± 5.4	130.1 (0.0–175.9)	1.5 (1.2–6.2)	1.5 (0.2–2.9)	273.0 (64.7–1490.1)	4.6 (1.3–12.9)
#659	0.5 ± 0.2	7.7 ± 2.0	14.1 ± 4.8	113.1 (1.7–172.5)	1.4 (0.6–6.5)	1.3 (0.1–2.5)	253.1 (136.1–1523.7)	3.2 (1.5–15.1)
#679	0.7 ± 0.5	8.0 ± 1.7	14.2 ± 4.9	118.3 (12.0–169.8)	1.6 (0.8–8.4)	0.3 (0.0–2.7)	253.0 (116.4–1510.0)	2.9 (0.5–15.7)
#699	2.6 ± 2.1	8.3 ± 1.6	14.2 ± 4.7	116.3 (20.8–184.9)	2.5 (1.6–11.9)	0.4 (0.1–1.6)	237.8 (104.4–1618.6)	3.7 (0.9–9.5)
#719	9.9 ± 6.0	8.2 ± 1.5	13.8 ± 4.8	86.2 (17.1–168.5)	2.3 (1.4–14.1)	0.9 (0.4–2.6)	268.2 (40.2–1659.2)	5.5 (2.8–10.7)
#724	12.2 ± 6.5	8. ± 1.8	12.8 ± 4.8	81.0 (26.4–116.4)	1.7 (1.2–2.6)	1.1 (0.5–2.6)	371.0 (60.1–1659.0)	6.8 (2.8–9.6)

Distribution of methane in the water column

We observed rather high methane concentrations in the upper estuary (#619–#629; median 416 nmol L^{-1}). At stations #659–#724 CH_4 concentrations were about 10 times lower with a median of 40 nmol L^{-1} (Fig. 2). According to this pattern, we grouped our stations into the "upper" and "lower" estuary (one way ANOVA with df = 81, $p < 0.001$, excluding station #639 as a transition zone). This grouping was also valid for most of the nutrients monitored. The site with the highest CH_4 concentration for each cruise moved up- or downstream between #619 and #639. Linear regression analysis (Table 2) and RDA (Fig. 3) revealed no seasonal trend for methane (no CH_4—temperature correlation), for either all stations or for the upper or lower estuary.

Table 2. Linear correlations between methane concentration/methane oxidation rate/methane turnover time and environmental factors, with log transformed data.

	Methane concentration		**Methane oxidation rate**		**Methane turnover time**	
	Upper estuary	**Lower estuary**	**Upper estuary**	**Lower estuary**	**Upper estuary**	**Lower estuary**
	***n* = 30**	***n* = 98**	***n* = 30**	***n* = 95**	***n* = 30**	***n* = 95**
Temperature			0.18/0.06	0.13/0.001	−0.47*/<0.001	−0.11/0.002
Salinity				−0.10/0.001		0.16/<0.001
Oxygen					0.28/0.009	
SPM (all stations)	all stations: −0.36/<0.001					
Delta water level	−0.86**/<0.001 (n = 10)					
BOD7	0.80/0.02 (n = 6)	all stations (n = 24): 0.29/0.007	all stations (n = 24): 0.31/0.005			
PO_4^{3-}						
NO_2^-	−0.27/0.01					
NO_3^-						
NH_4^+	0.15/0.08				−0.18/0.07	
CH_4			0.55/<0.001	0.49/<0.001		

Shown are the regression coefficients (r^2), positive or negative signs indicate a positive or negative correlation, followed by the respective *p* value (r^2/p). Notes: * three very high values were omitted; ** two very high values were omitted; when not indicated otherwise the number of sampling occasions (n) ranged from 19 to 24

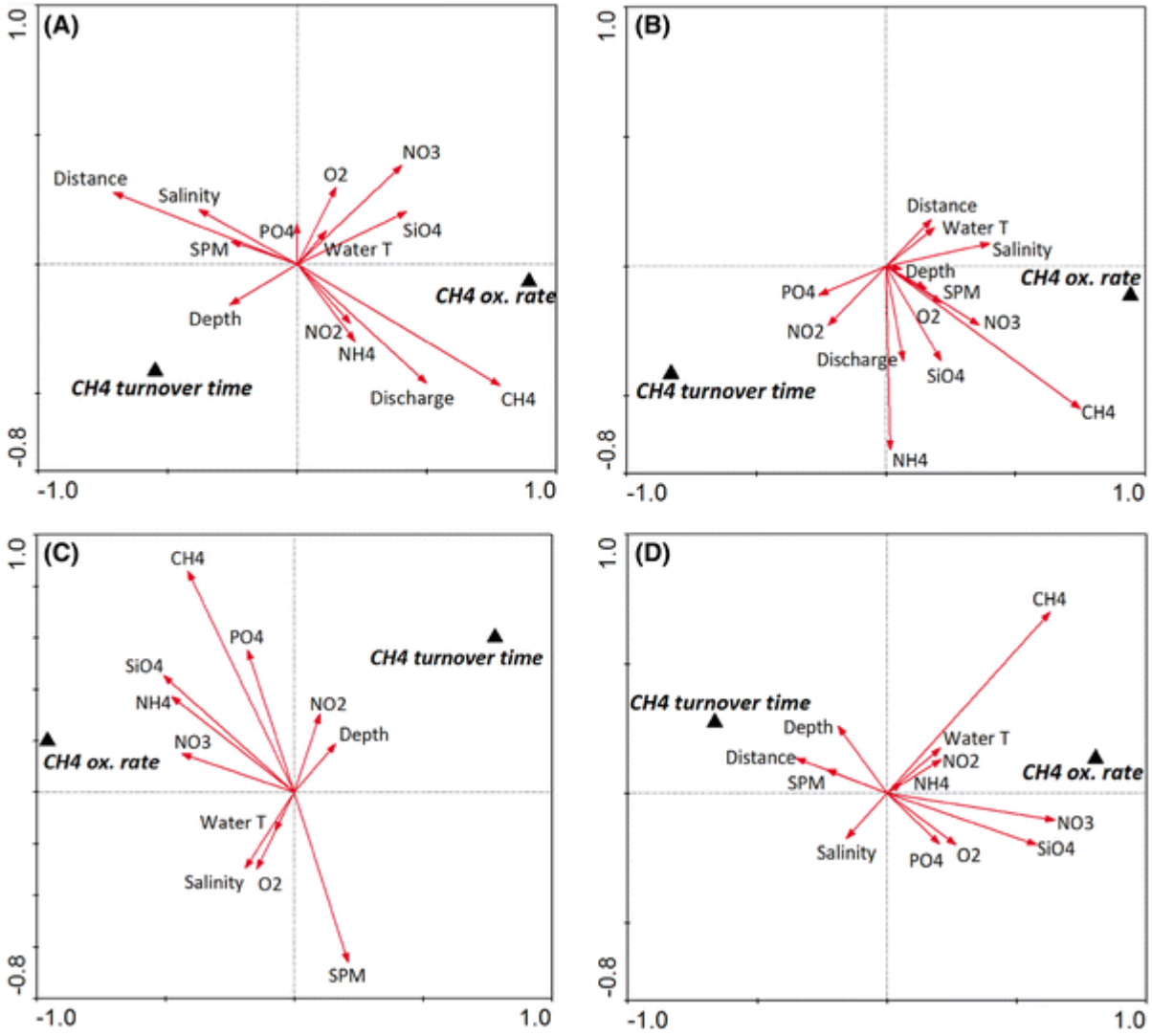

Fig. 3. The ordination diagrams of the *first* and *second axis* of the redundancy analysis (RDA): a **whole estuary;** b **upper estuary;** c **transition zone;** d **lower estuary. Note: CH_4 oxidation rate and CH_4 turnover time (*triangle symbols*) are explained variables; environmental parameters (*arrows*) are explanatory variables. The angle size between variables indicates their interrelationship, while *arrows* pointing in the same direction indicate positive correlations, and *arrows* pointing in opposite directions indicate negative correlations. The length of the *arrows* shows the strength of the environmental variable.**

In the lower estuary, where salinity increases from 5 to 25 PSU towards to the North Sea, CH_4 concentrations remain stable and only a slightly negative yet insignificant influence of salinity (dilution) was detected (Fig. 3d), but with no significant correlation.

We found a clear negative correlation between SPM and CH_4 for all stations ($r^2 = 0.36$, for log transformed data), indicating high methane concentrations at low SPM, i.e. clear water. (Table 2, Fig. 3a). However, when splitting the data into upper and lower estuary, no significant correlation could be found. Using RDA analyses we found a relevant negative correlation only in the case of the

transition zone (Fig. 4c), but a slight indication for all stations and even a positive in the upper estuary (Fig. 3b).

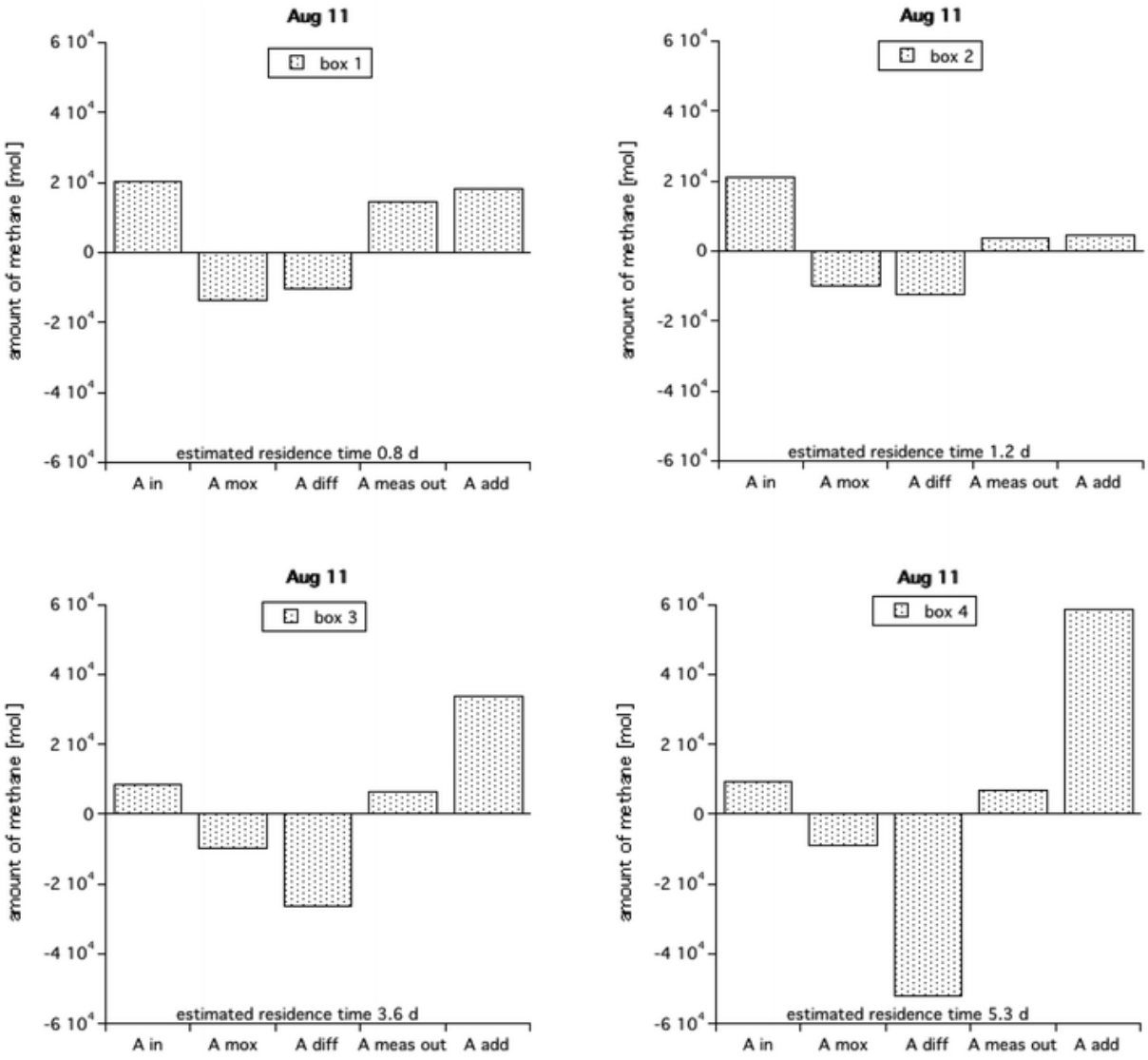

Fig. 4. The amount of methane entering a box (A_{in}) with the methane reducing processes (oxidation A_{Mox} and diffusion into the atmosphere A_{diff}) versus the measured amount of methane "leaving" the box ($A_{meas\ out}$). To obtain equilibrium an additional input (A_{add}) is required. The estimated residence time for each *box* is also given. Data are from 3.8.2011. For details of the calculation see "Results".

The RDA analyses indicated a slight influence of NO_3^- and SiO_4 on the methane dynamics in the upper estuary (Fig. 3b). In the lower estuary, the RDA analysis showed only a minor influence of NO_2^- and water temperature (Fig. 3d). A similar pattern was also evident for the NH_4^+ concentration and we even found a positive correlation between CH_4 and NH_4^+ for the upper estuary (log transformed data, $r^2 = 0.15$), but no correlation for the lower estuary. In the upper estuary, methane concentrations were negatively correlated with nitrite concentrations ($r^2 = 0.27$), but not in the lower estuary.

The water discharge of a river is an important factor in its chemistry. The obtained discharges (see "Materials and methods") can be considered as the total freshwater discharge of the Elbe since the tributary discharges are negligible compared to the discharge of the main channel (factor 100) (Vandenbruwaene et al. 2013). However, no direct correlation between CH_4 concentration and water discharge was detected in the upper estuary.

From the Elbe Daten Portal we obtained data on the BOD-7 and the water level for the respective stations and sampling times. However, these data were not available for all our sampling occasions. When the overall biodegradable material (i.e. BOD-7) in the water was high, we also observed high methane concentrations in the whole estuary ($r^2 = 0.29$, n = 24) and particularly pronounced in the upper estuary ($r^2 = 0.80$, n = 6) but not in the lower estuary. We calculated the difference between the water level 10 min before and 10 min after sampling to get an estimate of tidal influence. We found that when the water level was dropping the higher CH_4 concentrations were observed ($r^2 = 0.86$, n = 10) in the upper estuary, but no correlation was found in the lower estuary.

Methane oxidation and turnover time in the water column

Methane oxidation rates were rather high in the upper estuary (#619–#629) with a median of 161 nmol L^{-1} day^{-1}. In the lower estuary (#659–#724) methane oxidation rates were more than 10 times lower with a median of 10 nmol L^{-1} day^{-1} (Fig. 2). As described for methane concentrations, a one way ANOVA showed that methane oxidation rates and turnover times were significantly different (df = 124, $p < 0.001$) between the upper (#619–#629) and lower estuary (#659–#724).

We found a positive correlation between MOx and temperature in the upper estuary ($r^2 = 0.18$) and a weaker correlation in the lower estuary ($r^2 = 0.13$, $p = 0.06$), as can also be seen in the RDA diagrams (Fig. 3a–d). The MOx rate in the upper and lower estuary were both tightly correlated with CH_4 concentrations ($r^2 = 0.54$ and 0.66, respectively; both with $p < 0.001$). However, as the MOx is calculated by multiplying the fractional turnover rate constant (*k*) with the CH_4 concentration, this correlation has to be regarded with some caution. For the whole estuary MOx also was correlated with the BOD-7 ($r^2 = 0.31$, n = 24, $p = 0.005$). The analysis revealed no further statistically significant correlation. Only a slight indication of a positive correlation between MOx and some nutrients (NH_4^+, NO_3^-) was found in the transition zone (Fig. 3c).

Methane turnover times (τ) were rather short at the upper estuary (#619–#629) with a median of 1.6 days and a range of 1–25 days. In the lower estuary, (#659–#724) τ were about twice as long with a median of 3.7 days, ranging from 1 to 66 days (Supplementary Material 6) being, moreover, significantly different (one way ANOVA, df = 124, $p = 0.01$) from the upper estuary.

In the upper estuary, RDA analyses (Fig. 3b) indicated a slightly negative relationship between τ and water temperature ($r^2 = 0.47$, $p < 0.001$), i.e. a slow turnover at lower temperature, and oxygen ($r^2 = 0.28$, $p = 0.009$), i.e. a fast turnover at higher oxygen concentrations. In the transition zone we found the same correlations between τ and water temperature and additionally a weak negative correlation also with salinity (Fig. 3c). For the lower estuary, we found only a less tight correlation with temperature ($r^2 = 0.11$, $p = 0.002$) and salinity ($r^2 = 0.16$, $p < 0.001$), however, the RDA analyses (Fig. 3d) revealed an influence of the changing nutrient concentrations (NO_3^-, PO_4^{3-}, O_2 and SiO_4).

Calculation of the methane sea–air fluxes and budget

The sea-air flux ranged from 6 up to 115 kmol day^{-1} (Table 3). The higher numbers (>60 kmol day^{-1}) were mainly due to high current velocities (100–130 cm^3 s^{-1}) at the respective stations and dates. The total methane oxidation rate ranged from 2 to 49 kmol day^{-1}. For all cruises the total MOx seemed to be most important in box 1 (#619–#629, Hamburg port) with 57 and 61 % of the total loss assigned to MOx. Generally low MOx rates were observed in April 2013 with rather cold water (6.6 °C) compared to the other dates (18–21 °C), thus obviously the low temperature slowing MOx. However, on average 41 ± 12 % (without the April data) of the total loss can be attributed to microbial methane consumption.

Table 3. The loss of methane (in kmol day^{-1}) via diffusive flux (Diff) into the atmosphere and the microbial methane oxidation (MOx) at the different sampling dates and different boxes (the definition of the boxes is given in Fig. 1). The contribution of MOx to the total loss (diffusion + methane oxidation) is also given.

	03. 08. 2011			01. 08. 2012			12. 04. 2013			12. 06. 2013		
	Diff	MOx	% MOx	Diff	MOx	% MOx	Diff	MOx	% MOx	Diff	MOx	% MOx
Box 1	13	17	57				33	3	9	13	20	61
Box 2	10	8	44				67	4	5	23	24	50
Box 3	7	3	27				115	2	2	68	49	42
Box 4	10	2	15	6	4	44	35	1	2	76	47	38
Box 5				13	8	36						
Box 6				13	11	47						
Box 7				6	4	37						

In a second step we tried to calculate a budget for the boxes, i.e. to estimate the importance of the input and output of methane by the river flow, the methane reducing processes (evasion into the atmosphere and microbial oxidation), and finally—when assuming an equilibrium state and a closed budget—an extra input of methane. The amount of methane transported into or out of a box (A_{in} and A_{out} in mol) was calculated by multiplying the CH_4 concentration at the inflowing and outflowing station of the box with the volume of water entering/leaving this box. The residence time of a water

parcel in the respective box was estimated from the data given in Bergemann et al. (1996) at low, medium, and high discharge (see Supplementary Material 7). No information on the error of his estimate is given, thus we assume an error of at least 10 %. The residence time is determined by the discharge of the river as well as the tidal influence, resulting in short residence times near the port of Hamburg. However, with the stronger tidal effects near the coast, the residence time increases. Also the duration of the CH_4 consuming process within one box is determined by the residence time. Thus we multiplied the rate of the removal process, which results in the amount of CH_4 lost through diffusion (A_{diff}) and the amount lost through CH_4 oxidation (A_{MOx}) in this box. In accordance with Anthony et al. (2012) and Bergemann et al. (1996) we then assume that

$$A_{in} - A_{diff} - A_{MOx} = A_{calc-out} \quad (9)$$

when comparing the calculated amount of CH_4 ($A_{calc\ out}$) with the measured amount of CH_4 ($A_{meas\ out}$) finally gives us the additional input ($A_{additional}$) required to balance the budget for the respective box:

$$A_{calc-out} - A_{meas-out} = A_{additional} \quad (10)$$

In August 2011, the Elbe discharge was moderate (716 $m^3\ s^{-1}$) and the residence times were estimated to range from 0.8 days in box 1 to 5.3 days in box 4. This contrasts to June 2013 with a very high discharge (4041 $m^3\ s^{-1}$) and a residence time ranging from 0.4 days in box 1 to only 2.9 days in box 4. In August 2012 water discharge was low (409 $m^3\ s^{-1}$) and for the boxes in the lower estuary we estimated residence times of 14 days in box 4 and 25 days in box 6. In Fig. 4 we visualize the different processes for the cruise in August 2011. All processes for all cruises are shown in the Supplementary material 7.

In August 2011, in box 1 the amount of methane leaving the box was only slightly lower than the incoming amount (Fig. 4). With a residence time of 0.8 day, the CH_4 consuming process was about half the amount of the input. The measured output was slightly lower than the input, and “adding” the CH_4 reducing process, we estimated an additional input of the same size as the measured input. As the residence times increases downstream, correspondingly we estimated a residence time of 5.3 days in box 4. Thus the CH_4 reducing processes strongly increased, and whereas the measured input and output were almost the same, the CH_4 reducing processes can only be balanced with additional input about six times as high as the input. A similar pattern was observed for the cruises in April and June 2013 (Supplementary material 7).

In August 2012 the discharge was low and the boxes were nearer to the coast, thus the residence time increased to 14–25 days (Supplementary material 7) and consequently the amount of CH_4 reduction also increased. Even though the measured input and output of these boxes was about the

same, the strong loss of CH_4 can only be accounted for by a very strong additional input (22–33 times higher than the input).

Discussion

Methane distribution in the water column of the Elbe estuary

Our exceedingly high values of methane concentration correspond more or less to tropical/warm water systems and large rivers (Zhang et al. 2008; Borges et al. 2015a, b). Middelburg et al. (2002) measured the freshwater end-member for the Elbe River at a concentration of 111 nmol L^{-1} (salinity of approx. 0.4) and the marine end-member at a concentration of 4–6 nmol L^{-1}. This fits our data well, as at salinities between 0.3 and 0.5 we found a median methane concentration of 127 nmol L^{-1}. Wernecke et al. (1994) determined the CH_4 concentrations to be between 60 and 120 nmol L^{-1} in the main stream of the River Elbe, and up to 1200 nmol L^{-1} in the stagnant water (the upper end of the harbor basin), which is in line with our data. Rehder et al. (1998) estimated the average CH_4 input into the North Sea to be 70 nmol L^{-1} compared to our lower estimates with a median of 50 nmol L^{-1} (for our outmost station #724). In contrast to previous studies (Middelburg et al. 2002; Rehder et al. 1998; Osudar et al. 2015) we observed no correlation between CH_4 and salinity (including for the two outmost stations). This indicates that there is no simple two-compartments based mixing of riverine and marine CH_4.

We found significantly higher CH_4 concentrations at falling water levels in the upper estuary. Grunwald et al. (2009) suggested that CH_4 concentrations usually peaked during low tide, probably due to the CH_4-rich freshwater input and that, conversely, low values may be caused by dilution with CH_4-poor marine water and degassing processes. This was revealed and postulated also by others (Koné et al. 2010; Upstill-Goddard and Barnes 2016). However, we did not find a correlation to water gauge/level, like Grunwald, but with the “falling water level”. We assume that our sampling strategy from a moving boat versus fixed stations biased this effect. For the North Sea the tidal flat have been shown to be a methane source (Wu et al. 2015), and we assume that the strong surge at falling water levels results in the release of methane into the river/estuary.

Methane in the whole estuary but more specifically in its upper part is positively correlated with the BOD-7, which represents a measure of the bioavailability of degraded organic matter. The high CH_4 concentrations in the upper part of the Elbe estuary likely result from the high heterotrophic activity related to remineralization processes of high loads of labile organic matter. The organic material originates mainly from phytoplankton biomass (Kerner 2000), which is subject to enhanced mortality in the upper zone of the Elbe Estuary (area of Hamburg Port) due to higher runoff, deeper water

column mixing processes, and high water turbidity (Wolfstein and Kies 1995; Muylaert and Sabbe 1999). No data on waste water input and its influence on the CH_4 concentration in the Elbe were found, however, improvements in wastewater and in industrial inputs led to significant decrease of nitrogen and phosphorus loads since the 1990's (Schlarbaum et al. 2010) and so minor effects are assumed.

Elevated CH_4 concentrations as well as elevated CH_4 oxidation rates are often associated with a high content of SPM or turbidity (Upstill-Goddard et al. 2000; Abril et al. 2007). As most CH_4 is produced in anoxic zones within the sediment, significant CH_4 amounts are also released during particle resuspension (Bussmann 2005). Particle attached bacteria normally show higher activity rates and diversity (Ortega-Retuerta et al. 2013). Additionally, a high variability (from 0 up to 98 %) of the contribution of particle-attached bacteria to total bacterial production is also reported (Garneau et al. 2009). Thus we suggest that MOB may also attach to particles and lead to an elevated particle-attached CH_4 oxidation rate (Abril et al. 2007). However, the described direct relationship does not hold for all rivers and estuaries, as our data do not support these hypotheses, for either CH_4 concentration or MOx. We even observed a negative relationship between CH_4 and SPM for the upper estuary (Fig. 3b). There are also examples in literature where no direct relationship between SPM and methane concentration was found (Grunwald et al. 2009). One possible reason for this inconsistency is that the chemical composition of SPM changes spatially within an estuary (Savoye et al. 2012) and probably also with season. In our data set we observed a great variability of the SPM data, which makes it even more difficult to interpret them. Further, experimental studies would shed light on the relation between SPM and methane, i.e. the composition of the SPM and the status of the particle-attached or free-living MOB being in an active or dormant physiological state (Ho et al. 2013).

Methane oxidation and turnover time in the water column of the Elbe estuary

In our study along the salinity gradient of the Elbe estuary we observed CH_4 oxidation rates from 0.8 nmol L^{-1} day^{-1} to very high about 5542 nmol L^{-1} day^{-1} (at the Hamburg harbour area; Fig. 2). This variability is in line with the literature data from diverse estuaries (Griffiths et al. 1982; Scranton and McShane 1991; de Angelis and Scranton 1993; Abril and Iversen 2002). The turnover time varied between 0 and 66 days. Very few investigations included CH_4 turnover time measurements, e.g. a study from the Ogeechee River estuary with very fast turnover time between 2 h and 1 day (Pulliam 1993).

One important factor in both estuary parts was temperature, i.e. higher MOx rates and a fast turnover rate were observed at higher temperatures. This corroborates the observations made by Osudar et al. (2015) and Lofton et al. (2014) but contradicts the observations of Zaiss et al. (1982) and Utsumi et al. (1998), who revealed only a minor influence of temperature on MOx in situ. Additionally Lofton et al. (2014) suggested a specific substrate-temperature interaction, i.e. only methane saturated MOx was influenced by temperature, at limiting methane concentrations temperature had no influence on MOx. These findings are supported by our data on the turnover time, the influence of temperature was much higher in the upper estuary with its higher CH_4 concentrations. As the oxidation of CH_4 also needs oxygen, the process of CH_4 oxidation is also a part of the BOD-7, as is shown by its correlation; however, this fact does not give any further ecological information.

The availability of CH_4, as a sole source of energy for MOB seems to be the key factor influencing their activity. Similar findings are reported for MOx kinetics in the marine water column (Mau et al. 2015). For riverine, but sediment borne CH_4 concentrations of 2000–4000 nmol L^{-1} were still limiting levels (Shelley et al. 2015). Our observed CH_4 concentrations ranged from 18 to 2306 nmol L^{-1} and support the fact that MOx was mostly limited by CH_4 concentration. Type I MOB responds rapidly to substrate availability and is the predominantly active community in many environments (Ho et al. 2013). In the Elbe Estuary a dominance of type I MOB was also observed, with no type II MOB being detected (Hackbusch 2014).

The influence of nutrients showed no clear pattern found, suggesting limited effects of nutrients for MOx as most parts of this in this system have typically high trophic status (Table 2). Other authors also report a complex influence of nutrients (N and P) on MOx (Veraart et al. 2015). Oxygen also had mostly no influence on the microbial parameters. Thus we assume that the minimal oxygen concentrations of 3.4 mg L^{-1} were still sufficient to permit CH_4 oxidation. This is not surprising as aerobic methanotrophs can be active in microoxic conditions (Deutzmann et al. 2014).

The sea-air fluxes of methane and budget calculations

We calculated the diffusive methane flux along the Elbe estuary for four selected cruises when the overall water movement and the sampling scheme were downstream. For these calculations the values of the gas exchange coefficient (k_{600}) were crucial. They have previously been determined directly via chamber or eddy covariance measurements, or can be alternatively assessed via different models taking into account the stream hydrology. We applied the model from Raymond et al. (2012) and obtained an average k_{600} value of 8.4 m day^{-1} or 35 cm h^{-1}, which is fairly close to the range of 20

and 31 cm h^{-1} previously reported for the Elbe (Abril and Borges 2005; Amann et al. 2015). Thus, we think that our approach is reasonable and our slightly higher values can be related to the rather high water velocities (>100 cm s^{-1}) recorded on some specific occasions.

A direct comparison with flux data from the literature is hindered by the usage of many different units. We calculated an average sea-air flux of CH_4 (for all boxes and all 4 cruises) of 33 ± 8 g CH_4 m^{-2} per year and with a calculated total area of 1.5×10^8 m^{-2} and thus come up with an average CH_4 emission of $5.0 \pm 1.2 \times 10^9$ g per year for the whole Elbe estuary. For the Scottish Tay Estuary 1.02 g C m^{-2} y^{-1} and 5×10^7 g C per year has been calculated (Harley et al. 2015). For both units the flux in the Tay estuary is 30 times and one order of magnitudes lower than in the Elbe, respectively. However, other authors estimated $1.8 - 3 \times 10^{12}$ g CH_4 per year for temperate estuaries, which is much higher than our estimate for the Elbe (Middelburg et al. 2002). For a Baltic estuary CH_4 fluxes were generally below 15 g CH_4 m^2 y^{-1} in the bay (Silvennoinen et al. 2008). For a subtropical estuary CH_4 flux of 0.1–10 g CH_4 m^{-2} y^{-1} is reported (Musenze et al. 2014), which is roughly in line with our estimates. In tropical, African estuaries the flux ranged from 0.1 to 14 g CH_4 m^{-2} y^{-1}, which is less than half of our values (Koné et al. 2010). In a worldwide compilation of CH_4 flux data, the CH_4 flux from estuaries is described as being 539 ± 602 g CH_4 m^{-2} y^{-1} (Ortiz-Llorente and Alvarez-Cobelas 2012), while Borges and Abril estimate the global estuarine CH_4 flux with 6.2 g CH_4 m^{-2} y^{-1} (Borges and Abril 2011). Our data are within the lower range of this data compilation. These examples clearly demonstrate the difficulties of such comparisons. One reason for the variability of the data may be the methods used in calculating the flux, especially the determination of k_{600} (Musenze et al. 2014). Other reasons are certainly the variability of environmental parameters across locations, such as water velocity, tides, river discharge and of course methane contents itself. Also the degree and stability of the stratification, the influence of tidal areas and urban pollution have to be taken into account (Koné et al. 2010; Middelburg et al. 2002; Marwick et al. 2014). Thus the variability of CH_4 emissions is greatest for oceans and estuaries, with no clear seasonal pattern of CH_4 emission found for estuaries (Ortiz-Llorente and Alvarez-Cobelas 2012).

Another process which eliminates CH_4 from estuaries is microbial MOx. For all cruises the total MOx seemed to be most important in box 1 (Hamburg port). This can be attributed to the morphometry of the boxes, as in box 1 the river is deep and narrow i.e. with a low volume ratio: volume ratio, while the river becomes wider and shallower towards the river mouth i.e. high area: volume ratio. Rather low MOx rates were observed in April 2013 at a water temperature of 6.6 °C. The impeding effect of temperature on MOx also becomes obvious through the negative correlation between temperature and MOx (this study) and a Q_{10} of 1.5 for Elbe water (Bussmann et al. 2015). Thus in warm water i.e. in the summer/autumn on average 41 ± 12 % of the total loss can be attributed to microbial CH_4

consumption and this portion of CH_4 is not lost to the atmosphere. In colder water (winter and spring) we estimate that only 5 ± 3 % of the total CH_4 loss is due to MOx.

In previous studies box models were used to estimate the influence of the different CH_4 related processes in a river (de Angelis and Scranton 1993; Anthony et al. 2012). However, in our study area we also have a strong tidal regime, thus the water is not simply moving downstream. Each day a hypothetic water parcel moves four times up- and downstream. Thus, it takes 12 weeks for a water parcel to get from Geesthacht to Cuxhaven (140 km, with a water discharge of 250 $m^3 s^{-1}$) (Bergemann et al. 1996). Therefore any CH_4 reducing or producing processes have ample time to act. So we chose a modified box model taking into account the different residence times, depending on the water discharge of the river and the intensity of the tidal regime (Bergemann et al. 1996). Certainly, numerical modeling would give us a better insight into this dynamic estuarine system (Schroeder 1997; Schöl et al. 2014); however, though this approach may be realized in the future, it was beyond the scope of this study.

When the residence time for a box is low, the importance of the CH_4 consuming processes is also correspondingly low. In several cases we observed almost no difference between the amount of CH_4 entering a box (A_{in}) and the amount leaving a box (A_{out}; Fig. 4, box 1). As the CH_4 consuming processes are active at a low level, a low amount of additional CH_4 is required. Near the coast or at times of low discharge the residence time increases and therefore the amount of consumed CH_4 also increases. To balance out this strong loss of CH_4, the additional input also has to increase (Fig. 4, box 4). So even when the CH_4 concentrations and the amount of CH_4 entering and leaving a box seem to be stable or equal, CH_4 reducing processes are active, and to counterbalance them an additional input of CH_4 is required. In box 1, the ratio of A_{in} to A_{add} was 1–2. In contrast to boxes 4–6 where the ratio was 22–44, indicating a tremendous additional input of methane. As the width of the Elbe increases (from 0.5 km at #629 to almost 7 km at station #724) the bordering tidal marshes could be the source of this additional CH_4 input. For dissolved inorganic carbon (DIC) in the Elbe it is known that marshes contribute up to one-third of the annual DIC excess (Amann et al. 2015). Tidal flats are known to emit CH_4 into the surface water and atmosphere in substantial amounts (Røy et al. 2008; Weston et al. 2014). Due to advective flow, which is of special importance in permeable sandy sediments, pore waters enriched in remineralized nutrients and CH_4 are actively released from sediments into the overlying water column (Beck and Brumsack 2012). Additionally, groundwater also releases CH_4 into estuarine waters (Porubsky et al. 2014).

As the Elbe estuary is surrounded by the tidal flats from the Waden Sea, which are one of the largest sand- and mudflats worldwide (Marencic 2009), we suggest that the influence of these tidal flats is

much stronger than the riverine input into the North Sea. Even though the CH_4 concentrations in the upper estuary are very high, this CH_4 will not reach the North Sea (due to oxidation and diffusion on its way). But it is the lower estuary with its lower CH_4 content which is flowing into the North Sea. This is supported by the fact that we did not see any effect of dilution (correlation between salinity and CH_4) in our data. Only at a greater distance from the coast, the CH_4 of the coastal water, being a mixture of riverine and tidal-flat-originated CH_4, becomes diluted with CH_4 -poor marine water (Osudar et al. 2015). Detailed isotopic studies could help to clarify this hypothesis.

Conclusions and outlook

Estuaries represent a mosaic of habitats changing from freshwater to marine environment, which can be seen also in relation to methane related processes. High methane concentrations were observed in the upper estuary (Hamburg port), which decreased by one order of magnitude towards the lower estuary and the river mouth. Despite active methane oxidation, the microbial filter was estimated to be responsible for 5–41 % of the methane total loss. The other part was attributed to methane diffusion into the atmosphere. We did not observe any dilution of methane-rich river water with methane poor marine water. On the contrary, we assume that marshes bordering the Elbe estuary release a substantial amount of methane into the river and further into the North Sea.

Our study is based on ship-borne measurements, mostly going downstream. However, it would be interesting to relate this approach and our conclusions with methane data from fixed stations along the river, along which the water and its processes are moving by. The other possibility would be measurements within a “water parcel” as it is moving by river discharge and tidal currents. However, in the Elbe estuary, with its high level of ship-traffic, this would be rather difficult for ship-borne measurements. Permanent recording sensors may help to overcome these logistic restrictions.

Acknowledgments

This Project was financially supported by project GAJU 145/2013/D, and by Project GAČR-13-00243S (PI-K. Šimek). I. Bussmann was supported by the Helmholtz society via the program PACES topic 2. A. Matoušů´s stay in the laboratory of the Microbial Ecology group at Helgoland was funded by the German Academic Exchange service (DAAD). Our infinite gratitude belongs to the RV Ludwig Prandtl (Helmholtz-Zentrum Geesthacht, Germany) and its crew; to Kristine Carstens for nutrient analyses; to Karl-Walter Klings for his technician support in the laboratory; to Prof. Hana Šantrůčková and Doc. David Boukal for allowing us to work in the laboratories of the Department of Ecosystem Biology at the Faculty of Science (University of South Bohemia in České Budějovice); and to Matthias Langer for

his patient support during the sampling cruises. At least but not last our infinite gratitude belongs to the reviewers and editor for their improvements of the manuscript.

References

Abril G, Borges AV (2005) Carbon dioxide and methane emissions from estuaries. In: Tremblay A, Varfalvy L, Roehm C, Garneau M (eds) Greenhouse gas emissions—fluxes and processes: hydroelectric reservoirs and natural environments. Springer, Berlin, pp 187–207

Abril G, Iversen N (2002) Methane dynamics in a shallow non-tidal estuary (Randers Fjord, Denmark). Mar Ecol Prog Ser 230:171–181

Abril G, Commarieu MV, Guérin F (2007) Enhanced methane oxidation in an estuarine turbidity maximum. Limnol Oceanogr 52(1):470–475

Alin SR, Rasera MFFL, Salimonn CI, Richey JE, Holtgrieve GW, Krusche AV, Snidvongs A (2011) Physical controls on carbon dioxide transfer velocity and flux in low-gradient river systems and implications for regional carbon budgets. J Geophys Res Biogeosci 116(G1):G01009

Amann T, Weiss A, Hartmann J (2012) Carbon dynamics in the freshwater part of the Elbe estuary, Germany: implications of improving water quality. Estuar Coast Shelf Sci 107:112–121

Amann T, Weiss A, Hartmann J (2015) Inorganic carbon fluxes in the inner Elbe Estuary, Germany. Estuar Coasts 38:192–210

Anthony SE, Prahl FG, Peterson TD (2012) Methane dynamics in the Willamette River, Oregon. Limnol Oceanogr 57(5):1517–1530

Bastviken D (2009) Methane. Encyclopedia of inland waters. Academic Press, Oxford, pp 783–805

Beck M, Brumsack HJ (2012) Biogeochemical cycles in sediment and water column of the Wadden Sea: the example Spiekeroog Island in a regional context. Ocean Coast Manag 68:102–113

Bender M, Conrad R (1994) Methane oxidation activity in various soils and freshwater sediments: occurrence, characteristics, vertical profiles, and distribution on grain size fractions. J Geophys Res 99:16531–16540

Bergemann M, Gaumert T (2010) Elbebericht 2008. Ergebnisse des nationalen Überwachungsprogramms Elbe der Bundesländer über den ökologischen und chemischen Zustand der Elbe nach EG-WRRL sowie der Trendentwicklung von Stoffen und Schadstoffgruppen. FGG Elbe. http://www.fgg-elbe.de/index.php/elbe-datenportal/gewaesserguete.html. Accessed 23 Sept 2016

Bergemann M, Blöcker G, Harms H, Kerner M, Meyer-Nehls R, Petersen W, Schroeder F (1996) Der Sauerstoffhaushalt der Tideelbe. Die Küste 58:200–261

Bianchi TS (2007) Biogeochemistry of estuaries. Oxford University Press, Oxford, p 720

Bodelier PLE, Roslev P, Henckel T, Frenzel P (2000) Stimulation by ammonium-based fertilizers of methane oxidation in soil around rice roots. Nature 403:421–424 PubMed

Borges AV, Abril G (2011) Carbon dioxide and methane dynamics in estuaries. In: Wolanski E, McLusky D (eds) Treatise on estuarine and coastal science—vol 5: biogeochemistry. Academic Press, Waltham, pp 119–161, ISBN 9780080878850, doi:10.1016/B978-0-12-374711-2.00504-0

Borges AV, Delille B, Schiettecatte LS, Gazeau F, Abril G, Frankignoulle M (2004) Gas transfer velocities of CO_2 in three European estuaries (randers fjord, scheldt and thames). Limnol Oceanogr 49(5):1630–1641

Borges AV, Darchambeau F, Teodoru CR, Marwick TR, Tamooh F, Geeraert N, Omengo FO, Guérin F, Lambert T, Morana C, Okuku E, Bouillon S (2015a) Globally significant greenhouse gas emissions from African inland waters. Nat Geosci 8:637–642. doi:10.1038/NGEO2486

Borges AV, Abril G, Darchambeau F, Teodoru CR, Deborde J, Vidal LO, Lambert T, Bouillon S (2015b) Divergent biophysical controls of aquatic CO_2 and CH_4 in the World's two largest rivers. Sci Rep 5:15614. doi:10.1038/srep15614

Bowman J (2006) The Methanotrophs—the families methylococcaceae and methylocystaceae. Prokaryotes 5:266–289

Bussmann I (2005) Methane release through suspension of littoral sediment. Biogeochemistry 74(3):283–302

Bussmann I, Osudar R, Matousu A (2014) Methane concentrations and methane oxidation rates from Oct 2010 to March 2012 in the Elbe Estuary, from Hamburg to Cuxhaven, Germany. doi:10.1594/PANGAEA.833923

Bussmann I, Matousu A, Osudar R, Mau S (2015) Assessment of the radio ^{3}H-CH_4 tracer technique to measure aerobic methane oxidation in the water column. Limnol Oceanogr Methods 13(6):312–327

Cole JJ, Caraco NF, Peierls BL (1992) Can phytoplankton maintain a positive carbon balance in a turbid freshwater, tidal estuary? Limnol Oceanogr 37:1608–1617

Conrad R (2009) The global methane cycle: recent advances in understanding the microbial processes involved. Environ Microbiol Rep 1(5):285–292

Conrad R, Frenzel P, Cohen Y (1995) Methane emission from hypersaline microbial mats: lack of aerobic methane oxidation activity. FEMS Microbiol Ecol 16(4):297–306

de Angelis MA, Scranton MI (1993) Fate of methane in the Hudson River and estuary. Glob Biogeochem Cycles 7:509–523

Deutzmann JS, Stief P, Brandes J, Schink B (2014) Anaerobic methane oxidation coupled to denitrification is the dominant methane sink in a deep lake. Proc Natl Acad Sci 111(51):18273–18278

Dumestre JF, Guézennec J, Lacaux CG, Delmas R, Richard S, Labroue L (1999) Influence of light intensity on methanotrophic bacterial activity in Petit Saut Reservoir, French Guiana. Appl Environ Microbiol 65:534–539

Frankignoulle M, Middelburg JJ (2002) Biogases in tidal European estuaries: the Biogest project. Introductive paper to BIOGEST special issue. Biogeochemistry 59:1–4

Frankignoulle M, Abril G, Borges A, Bourge I, Canon C, Delille B, Libert E, Théate J-M (1998) Carbon dioxide emission from European estuaries. Science 282:434–436

Garneau M-E, Vincent WF, Terrado R, Lovejoy C (2009) Importance of particle-associated bacterial heterotrophy in a coastal Arctic ecosystem. J Mar Syst 75:185–197

Grasshoff K, Ehrhardt M, Kremling K (1983) Methods of seawater analysis. Verlag Chemie, Weinheim

Griffiths RP, Caldwell BA, Cline JD, Broich WA, Morita RJ (1982) Field observations of methane concentrations and oxidation rates in the South-eastern Bering Sea. Appl Environ Microbiol 44:435–446

Grunwald M, Dellwig O, Beck M, Dippner JW, Freund JA, Kohlmeier C, Schnetger B, Brumsack HJ (2009) Methane in the southern North Sea: sources, spatial distribution and budgets. Estuar Coast Shelf Sci 81(4):445–456

Hackbusch S (2014) Abundance and activity of methane oxidizing bacteria in the River Elbe Estuary Master thesis, Friedrich Schiller Universität Jena

Harley JF, Carvalho L, Dudley B, Heal KV, Rees RM, Skiba U (2015) Spatial and seasonal fluxes of the greenhouse gases N2O, CO2 and CH4 in a UK macrotidal estuary. Estuar Coast Shelf Sci 153:62–73

Heintz MB, Mau S, Valentine DL (2012) Physical control on methanotrophic potential in waters of the Santa Monica Basin, Southern California. Limnol Oceanogr 57(2):420–432

Ho A, Kerckhof FM, Luke C, Reim A, Krause S, Boon N, Bodelier PLE (2013) Conceptualizing functional traits and ecological characteristics of methane-oxidizing bacteria as life strategies. Environ Microbiol Rep 5(3):335–345

Internationale Kommission zum Schutz der Elbe (IKSE) (1995) Die Elbe und ihre Nebenflüsse—Belastung, Trends, Bewertung, Perspektiven. In: Prange A, Furrer R, Einax JW, Lochovský P, Kofalk S (eds) ATV-DVWK Forschungsberichte. ISBN 3-933707-63-3

IPCC, Ciais P, Sabine C, Bala G, Bopp L, Brovkin V, Canadel J, Chhabra A, DeFries R, Galloway J, Heimann M, Jones C, Quéré CL, Myneni RB, Piao S, Thornton P (2013) Carbon and other biogeochemical cycles. In: Stocker TF, Qin D, Plattner G-K et al. (eds) Climate change 2013: the physical science basis. Contribution of working group I to the fifth assessment report of the intergovernmental panel on climate change. Cambridge University Press, Cambridge

Kankaala P, Huotari J, Peltomaa E, Saloranta T, Ojala A (2006) Methanotrophic activity in relation to methane efflux and total heterotrophic bacterial production in a stratified, humic, boreal lake. Limnol Oceanogr 51(2):1195–1204

Kerner M (2000) Interactions between local oxygen deficiencies and heterotrophic microbial processes in the Elbe estuary. Limnol Ecol Manag Inland Waters 30(2):137–143

King GM (1990) Regulation by light of methane emissions from a wetland. Nature 345:513–514

Koné YJM, Abril G, Delille B, Borges AV (2010) Seasonal variability of methane in the rivers and lagoons of Ivory Coast (West Africa). Biogeochemistry 100:21–37

Lofton DD, Whalen SC, Hershey AE (2014) Effect of temperature on methane dynamics and evaluation of methane oxidation kinetics in shallow Arctic Alaskan lakes. Hydrobiologia 721(1):209–222

Marencic HE (2009) The Wadden Sea an introduction. Quality Status Report 2009. Wadden Sea Ecosystem No. 25. Common Wadden Sea Secretariat

Marwick TR, Tamooh F, Ogwoka B, Teodoru C, Borges AV, Darchambeau F, Bouillon S (2014) Dynamic seasonal nitrogen cycling in response to anthropogenic N loading in a tropical catchment, Athi-Galana-Sabaki River, Kenya. Biogeosciences 11(2):443–460

Matousu A, Osudar R, Simek K, Bussmann I (2015). Methane concentrations and methane oxidation rates from June 2012 to June 2013 in the Elbe Estuary, from Hamburg to Cuxhaven, Germany. www.pangaea.de, doi:10.1594/PANGAEA.855825

Mau S, Gentz T, Körber JH, Torres ME, Römer M, Sahling H, Wintersteller P, Martinez R, Schlüter M, Helmke E (2015) Seasonal methane accumulation and release from a gas emission site in the central North Sea. Biogeosciences 12:5261–5276.

McAuliffe C (1971) Gas Chromatographic determination of solutes by multiple phase equilibrium. Chem Technol 1:46–51

Middelburg JJ, Nieuwenhuize J, Iversen N, Høgh N, de Wilde W, Helder W, Seifert R, Christof O (2002) Methane distribution in European tidal estuaries. Biogeochemistry 59:95–119

Mohanty SR, Bodelier PLE, Conrad R (2007) Effect of temperature on composition of the methanotrophic community in rice field and forest soil. FEMS Microbiol Ecol 62:24–31

Murase J, Sugimoto A (2005) Inhibitory effect of light on methane oxidation in the pelagic water column of a mesotrophic lake (Lake Biwa, Japan). Limnol Oceanogr 50(4):1339–1343

Musenze RS, Werner U, Grinham A, Udy J, Yuan Z (2014) Methane and nitrous oxide emissions from a subtropical estuary (the Brisbane River estuary, Australia). Sci Total Environ 472:719–729

Muylaert K, Sabbe K (1999) Spring phytoplankton assemblages in an around the maximum turbidity zone of the estuaries of the Elbe (Germany), the Schelde (Belgium/The Netherlands) and the Gironde (France). J Mar Syst 22:133–149

Ortega-Retuerta E, Joux F, Jeffrey WH, Ghiglione JF (2013) Spatial variability of particle-attached and free-living bacterial diversity in surface waters from the Mackenzie River to the Beaufort Sea (Canadian Arctic). Biogeosciences 10(4):2747–2759

Ortiz-Llorente MJ, Alvarez-Cobelas M (2012) Comparison of biogenic methane emissions from unmanaged estuaries, lakes, oceans, rivers and wetlands. Atmos Environ 59:328–337

Osudar R, Matousu A, Alawi M, Wagner D, Bussmann I (2015) Environmental factors affecting methane distribution and bacterial methane oxidation in the German Bight (North Sea). Estuar Coast Shelf Sci.

Porubsky WP, Weston NB, Moore WS, Ruppel C, Joye SB (2014) Dynamics of submarine groundwater discharge and associated fluxes of dissolved nutrients, carbon, and trace gases to the coastal zone (Okatee River estuary, South Carolina). Geochim Cosmochim Acta 131:81–97

Pulliam WM (1993) Carbon dioxide and methane exports from a Southeastern Floodplain Swamp. Ecol Monogr 63(1):29–53

Raymond PA, Zappa CJ, Butman D, Bott TL, Potter J, Mulholland P, Laursen AE, McDowell WH, Newbold D (2012) Scaling the gas transfer velocity and hydraulic geometry in streams and small rivers. Limnol Oceanogr Fluids Environ 2:41–53

Rehder G, Keir RS, Suess E, Pohlmann T (1998) The multiple sources and patterns of methane in North Sea waters. Aquat Geochem 4:403–427

Røy H, Jae SL, Jansen S, De Beer D (2008) Tide-driven deep pore-water flow in intertidal sand flats. Limnol Oceanogr 53(4):1521–1530

Rudd JWM, Furutani A, Flett RJ, Hamilton RD (1976) Factors controlling methane oxidation in Shield lakes: the role of nitrogen fixation and oxygen concentration. Limnol Oceanogr 3(21):357–364

Savoye N, David V, Morisseau F, Etcheber H, Abril G, Billy I, Charlier K, Oggian G, Derriennic H, Sautour B (2012) Origin and composition of particulate organic matter in a macrotidal turbid estuary: the Gironde Estuary, France. Estuar Coast Shelf Sci 108:16–28

Schlarbaum T, Dähnke K, Bahlmann E, Emeis KC (2010) Dissolved organic nitrogen in the Elbe river and estuary: results of nitrogen isotope investigations. Mar Chem 119:1–17

Schöl A, Hein B, Wyrwa J, Kirchesch V (2014) Modelling water quality in the Elbe and its estuary—large scale and long term applications with focus on the oxygen budget of the estuary. Die Küste 81:203–232

Schroeder F (1997) Water quality in the Elbe estuary: significance of different processes for the oxygen deficit at Hamburg. Environ Model Assess 2:73–82

Scranton MI, McShane K (1991) Methane fluxes in the southern North Sea: the role of European rivers. Cont Shelf Res 11(1):37–52

Shelley F, Abdullahi F, Grey J, Trimmer M (2015) Microbial methane cycling in the bed of a chalk river: oxidation has the potential to match methanogenesis enhanced by warming. Freshw Biol 60(1):150–160

Silvennoinen H, Liikanen A, Rintala J, Martikainen P (2008) Greenhouse gas fluxes from the eutrophic Temmesjoki River and its Estuary in the Liminganlahti Bay (the Baltic Sea). Biogeochemistry 90(2):193–208

Striegl RG, Dornblaser MM, McDonald CP, Rover JR, Stets EG (2012) Carbon dioxide and methane emissions from the Yukon River system. Global Biogeochemical Cycles 26 (GB0E05)

Sundh I, Bastviken D, Tranvik LJ (2005) Abundance, activity, and community structure of pelagic methane-oxidizing bacteria in temperate lakes. Appl Environ Microbiol 71(11):6746–6752

Ter Braak JF, Šmilauer P (2002) CANOCO Reference manual and CanoDraw for Windows user's guids: Software for canonical community ordination (version 4.52). Microcomputer Power, Ithaca, New York

Upstill-Goddard R, Barnes J (2016) Methane emissions from UK estuaries: re-evaluating the estuarine source of tropospheric methane from Europe. Mar Chem 180:14–23.

Upstill-Goddard RC, Barnes J, Owens NJP (2000) Methane in the southern North Sea: low-salinity inputs, estuarine removal, and atmospheric flux. Global Biogeochem Cycles 14(4):1205

Urmann K, Lazzaro A, Gandolfi I, Schroth MH, Zeyer J (2009) Response of methanotrophic activity and community structure to temperature changes in a diffusive CH_4/O_2 counter gradient in an unsaturated porous medium. FEMS Microbiol Ecol 69:202–212

Utsumi M, Nojiri Y, Nakamura T, Nozawa T, Otsuki A, Takamura N, Watanabe M, Seki H (1998) Dynamics of dissolved methane and methane oxidation in dimictic Lake Nojiri during winter. Limnol Oceanogr 43:10–17

Vandenbruwaene W, Plancke Y, Verwaest T, Mostaert F (2013) Interestuarine comparison: hydrogeomorphology: hydro- and geomorphodynamics of the TIDE estuaries Scheldt, Elbe, Weser and Humber. Version 4. WL Rapporten, 770_62b. Flanders Hydraulics Research: Antwerp, Belgium

Wanninkhof R (1992) Relationship between wind speed and gas exchange over the ocean. J Geophys Res 97(C5):7373–7382

Wanninkhof R, Asher WE, Ho DT, Sweeney CS, McGillis WR (2009) Advances in quantifying air–sea gas exchange and environmental forcing. Annu Rev Mar Sci 1:213–244

Wernecke G, Flöser G, Korn S, Weitkamp C, Michaelis W (1994) First measurements of the methane concentration in the North Sea with a new in situ device. Bull Geol Soc Den 41:5–11

Weston NB, Neubauer SC, Velinsky DJ, Vile MA (2014) Net ecosystem carbon exchange and the greenhouse gas balance of tidal marshes along an estuarine salinity gradient. Biogeochemistry 120(1–3):163–189

Wiesenburg DA, Guinasso NL (1979) Equilibrium solubilities of methane, carbon monoxide and hydrogen in water and sea water. J Chem Eng Data 24(4):356–360

Wiltshire KH, Kraberg A, Bartsch I, Boersma M, Franke HD, Freund J, Gebühr C, Gerdts G, Stockmann K, Wichels A (2010) Helgoland roads: 45 years of change. Estuar Coasts 33:295–310.

Wolfstein K, Kies L (1995) A case study on the oxygen budget in the freshwater part of the Elbe estuary. 3. Variations in phytoplankton pigments in the Elbe before and during the oxygen minima in 1992 and 1993. Archiv für Hydrobiologie (Supplement) 110:39–54

Wu CS, Røy H, de Beer D (2015) Methanogenesis in sediments of an intertidal sand flat in the Wadden Sea. Estuar Coast Shelf Sci 164:39–45

Yamamoto S, Alcauskas JB, Crozier TE (1976) Solubility of methane in distilled water and seawater. J Chem Eng Data 21:78–80

Zaiss U, Winter P, Kaltwasser H (1982) Microbial methane oxidation in the River Saar. Zeitschrift fur Allgemeine Mikrobiologie 2(22):139–148

Zhang G, Zhang J, Liu S, Ren J, Xu J, Zhang F (2008) Methane in the Changjiang (Yangtze River) Estuary and its adjacent marine area: riverine input, sediment release and atmospheric fluxes. Biogeochemistry 91:71–84

Zimmermann H (1997) The microbial community on aggregates in the Elbe Estuary. Aquat Microb Ecol 13:37–46

Supplementary materials

Supplementary material 1: Morphometric scheme for calculating the areas and volume of the navigational channel and the deep-water zone with increasing width downstream.

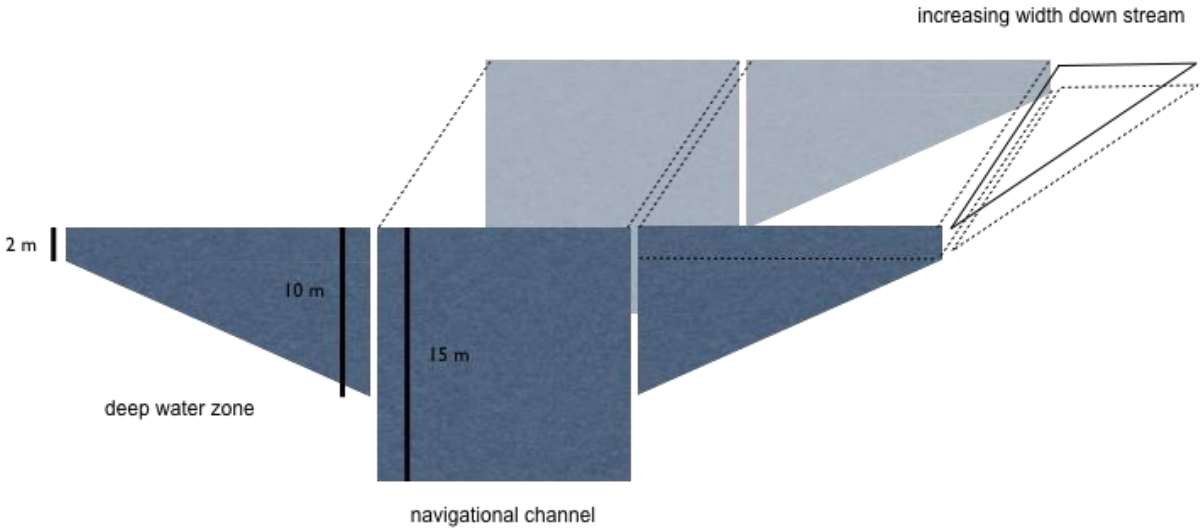

Supplementary material 2: Water velocities provided by www.portal-tideelbe.de, for k calculation.

Station	Date	k determined with
#619	03.8.2011 12.4.2013 12.6.2013	monthly mean of the current velocity in 2008 from #630, Teufelsbrück
#629	03.8.2011 12.4.2013 12.6.2013	monthly mean of the current velocity in 2008 from #630, Teufelsbrück
#639	03.8.2011 12.4.2013 12.6.2013	exact current velocity from #643 Hanskalb
#659	03.8.2011 01.8.2012 12.4.2013 12.6.2013	exact current velocity from #665 Pagensand
#679	03.8.2011 01.8.2012 12.4.2013 12.6.2013	exact current velocity from #676 Rhiplatte
#699	01.8.2012	exact current velocity from #697 Krumdeich
#719	01.8.2012	wind speed in Cuxhaven
#724	01.8.2012	wind speed in Cuxhaven

Supplementary material 3: Box plots of the methane turnover time at the river stations in the Elbe estuary during the sampling campaigns from October 2010 to June 2013. We grouped the stations into inner (#619 - #629) and outer estuary (#659 - #724), with the station #639 as a transition zone. The number of samples ranged from n = 7 at station #624 to n = 24 at station #724. For Definition of the box plot see Material & Methods.

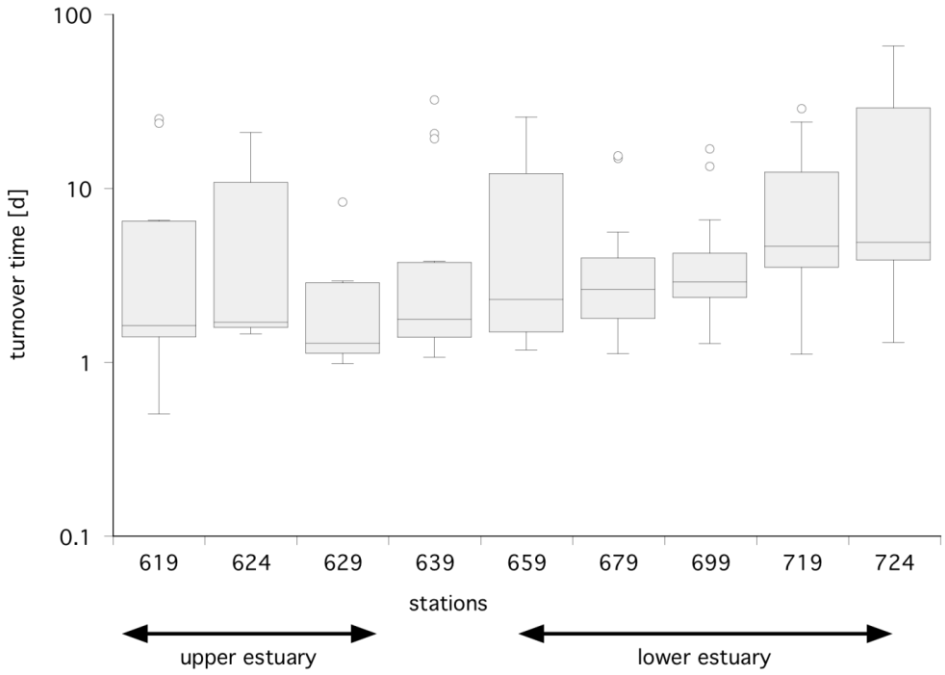

Supplementary material 4: The methane distribution in the whole monitored stretch of the Elbe estuary during the sampling campaigns from October 2010 to June 2013. Note: To achieve a detailed resolution we used logarithmic transformation of the data.

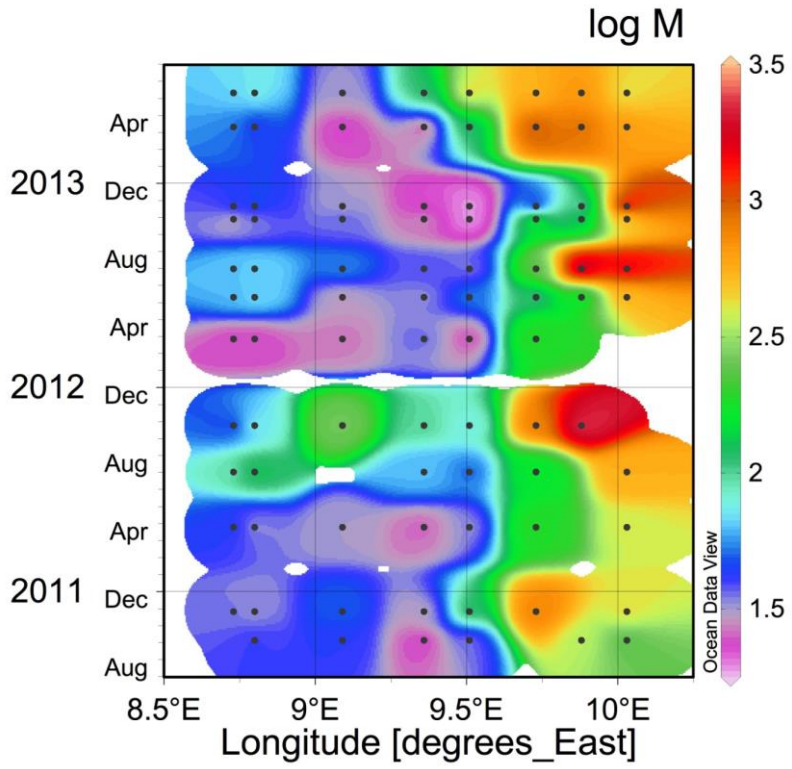

Supplementary material 5: The methane oxidation in the whole monitored stretch of the Elbe estuary during the sampling campaigns from October 2010 to June 2013. Note: To achieve a detailed resolution we used logarithmic transformation of the data.

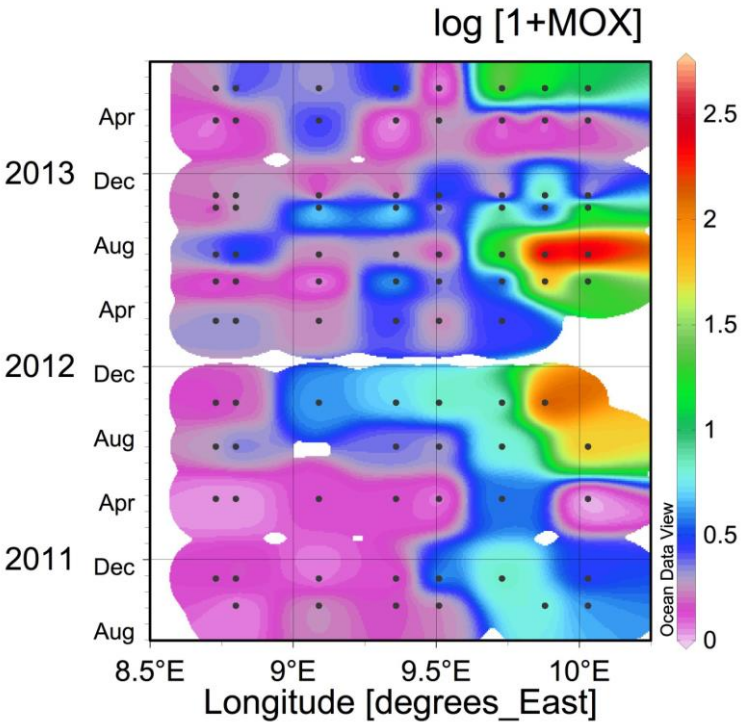

Supplementary material 6: The methane turnover time in the whole monitored stretch of the Elbe estuary during the sampling campaigns from October 2010 to June 2013.

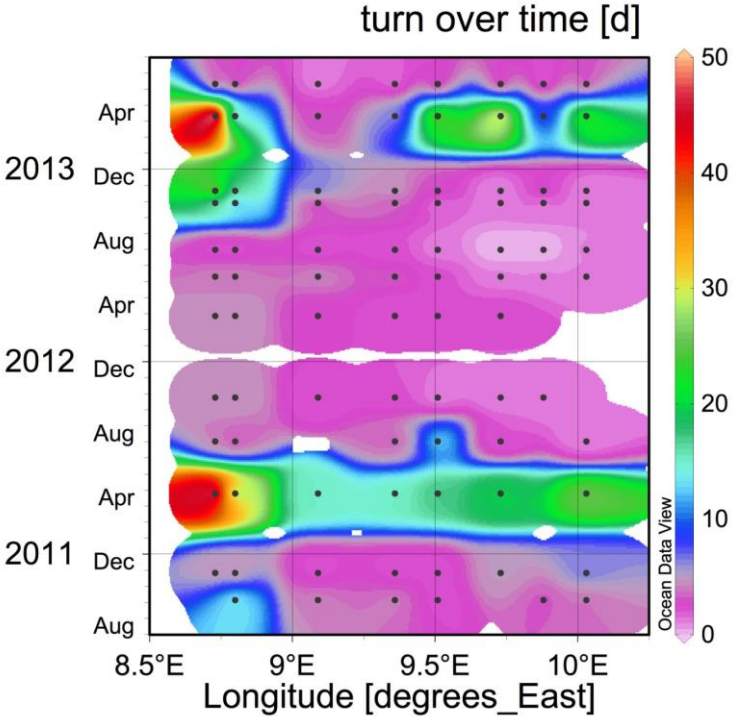

Supplementary material 7: The amount of methane (A_{in} in kmol) entering a box with the amount of methane reduced in this box by methane oxidation and diffusion into the atmosphere (A_{Mox} and A_{diff}). The difference between the calculated amount of methane leaving the box ($A_{calc\ out}$) and the measured amount of methane leaving the box ($A_{meas\ out}$) results in the additional amount of methane (A_{add}). The A_{add} is necessary to counterbalance for the methane consuming processes.

		Box 1	Box 2	Box 3	Box 4	Box 5	Box 6
03.08.2011	residence time (d)	0.8	1.2	3.6	5.3		
	A_{in}	20	21	8	9		
	A_{mox}	14	10	10	9		
	A_{diff}	10	12	26	52		
	$A_{calc\ out}$	-4	-1	-28	-52		
	$A_{meas\ out}$	15	4	6	7		
	A_{add}	18	4	34	59		
	A_{add} / A_{in}	1	0.2	4	6		
12.04.2013	residence time (d)	0.8	1.2	3.6	5.3		
	A_{in}	23	47	124	21		
	A_{mox}	3	4	8	4		
	A_{diff}	26	80	415	185		
	$A_{calc\ out}$	-6	-38	-299	-168		
	$A_{meas\ out}$	32	52	14	4		
	A_{add}	38	90	314	172		
	A_{add} / A_{in}	2	2	3	8		
12.06.2013	residence time (d)	0.4	0.7	2.2	2.9		
	A_{in}	15	35	67	88		
	A_{mox}	8	17	107	136		
	A_{diff}	5	16	150	221		
	$A_{calc\ out}$	2	2	-191	-269		
	$A_{meas\ out}$	24	28	60	22		
	A_{add}	22	26	251	291		
	A_{add} / A_{in}	1	1	4	3		
01.08.2012	residence time (d)				14	21	25
	A_{in}				6	10	18
	A_{mox}				62	160	279
	A_{diff}				80	281	319
	$A_{calc\ out}$				-135	-431	-580
	$A_{meas\ out}$				7	14	22
	A_{add}				142	446	603
	A_{add} / A_{in}				22	44	33